Springer Theses
Recognizing Outstanding Ph.D. Research

Dominic M. Bowman

Amplitude Modulation of Pulsation Modes in Delta Scuti Stars

Springer

Springer Theses

Recognizing Outstanding Ph.D. Research

Aims and Scope

The series "Springer Theses" brings together a selection of the very best Ph.D. theses from around the world and across the physical sciences. Nominated and endorsed by two recognized specialists, each published volume has been selected for its scientific excellence and the high impact of its contents for the pertinent field of research. For greater accessibility to non-specialists, the published versions include an extended introduction, as well as a foreword by the student's supervisor explaining the special relevance of the work for the field. As a whole, the series will provide a valuable resource both for newcomers to the research fields described, and for other scientists seeking detailed background information on special questions. Finally, it provides an accredited documentation of the valuable contributions made by today's younger generation of scientists.

Theses are accepted into the series by invited nomination only and must fulfill all of the following criteria

- They must be written in good English.
- The topic should fall within the confines of Chemistry, Physics, Earth Sciences, Engineering and related interdisciplinary fields such as Materials, Nanoscience, Chemical Engineering, Complex Systems and Biophysics.
- The work reported in the thesis must represent a significant scientific advance.
- If the thesis includes previously published material, permission to reproduce this must be gained from the respective copyright holder.
- They must have been examined and passed during the 12 months prior to nomination.
- Each thesis should include a foreword by the supervisor outlining the significance of its content.
- The theses should have a clearly defined structure including an introduction accessible to scientists not expert in that particular field.

More information about this series at http://www.springer.com/series/8790

Dominic M. Bowman

Amplitude Modulation of Pulsation Modes in Delta Scuti Stars

Doctoral Thesis accepted by
University of Central Lancashire, Preston, UK

Springer

Author
Dr. Dominic M. Bowman
Institute of Astronomy
KU Leuven
Leuven
Belgium

Supervisor
Prof. Don Kurtz
University of Central Lancashire
Preston
UK

ISSN 2190-5053 ISSN 2190-5061 (electronic)
Springer Theses
ISBN 978-3-319-66648-8 ISBN 978-3-319-66649-5 (eBook)
https://doi.org/10.1007/978-3-319-66649-5

Library of Congress Control Number: 2017950281

Printed on acid-free paper

This Springer imprint is published by Springer Nature
The registered company is Springer International Publishing AG
The registered company address is: Gewerbestrasse 11, 6330 Cham, Switzerland

Supervisor's Foreword

The fundamental data of asteroseismology are the frequencies of stellar pulsation modes, which are modelled to give direct measurement of stellar interior physics. To obtain these frequencies, a principal method is analysis of time series data of photometric variations in stellar brightness. For decades, we were limited to observing just one, or at best a few, stars at a time during night-time hours under the best weather conditions at observatories placed in the remote driest regions of Earth. The photometric variations of solar-like oscillators were generally too small to be detected from the ground, and the larger amplitude pulsators needed multi-site campaigns to overcome the confusion that results from gaps in the time series data. The precision in pulsation amplitude that was obtained was of the order of 100 parts per million (ppm).

Then, came the space photometry revolution, with its culmination in the *Kepler* mission. *Kepler* observed nearly 200 000 stars over its four-year lifetime, with precision in the best cases of 1 ppm, and routinely of 10 ppm. Because of its heliocentric orbit, it obtained nearly continuous data. Just as the CCD has made photographic film obsolete as an astronomical detector, the *Kepler* data have made ground-based photometric time series observations for asteroseismology a thing of the past. The *Kepler* mission data are truly revolutionary for asteroseismology, with hundreds of solar-like pulsators and thousands of red giants yielding unprecedented understanding of stellar interiors.

The parameter space for understanding stellar astrophysics is far wider than just the cool stars. In particular, the stars of the upper main sequence have rich potential for asteroseismic inference, yet the *Kepler* mission was designed primarily for the study of cool stars in the quest for eta-Earth. Asteroseismic studies have now been carried out on many hundreds of main sequence solar-like pulsators and more than 10 000 red giants. It is easy to understand why those stochastically driven stars have highly variable amplitudes. Over much of the rest of the HR diagram, stellar pulsations are driven by heat mechanisms, which are much more regular than the stochastic driving in solar-like stars. Yet for decades, amplitude and frequency modulation of pulsation modes have been observed in almost all types of heat-driven pulsating stars. Is this modulation astrophysical, and can we learn more

about the pulsating stars from it? Or is it simply beating of modes with stable amplitudes, unrecognised because of a lack of frequency? This outstanding thesis by Dominic Bowman provides the most thorough investigation of these long-standing questions. He has studied a uniform sample of 983 δ Sct stars—the most common type of main sequence heat engine pulsators—that were observed nearly continuously for 4 years at stunning photometric precision of only a few parts per million by the *Kepler* Space Mission. He has shown that the amplitude and frequency modulation are astrophysical, and he has investigated its implications and prospects, and provided new insight into this, for the δ Sct stars, and for the many other types of heat engine pulsators across the HR diagram. With no mission planned to supersede the *Kepler* four-year data set, this thesis will stand as the definitive study of these questions for many years.

The recognition of the impact of this thesis led to Dominic taking up a prestigious postdoctoral fellowship with Prof. Conny Aerts at the KU Leuven, Belgium, in one of the top asteroseismology groups in the world. He is continuing and expanding his asteroseismology studies to the as-yet-not-understood-low-frequency variations of the most massive stars known, the O-type stars.

This thesis is an outstanding introduction to the study of pulsation in δ Sct stars, and to the *Kepler* data and their analysis. It gives an excellent introduction to, and discussion of, pulsational non-linearity and mode coupling, particularly from the observational viewpoint.

Preston, UK
July 2017

Prof. Don Kurtz

Preface

Context

Astronomy covers numerous aspects of physics and mathematics across many orders of magnitude in size, from the quantum mechanical laws that determine nuclear fusion reactions in the centre of a star, to the dynamics of galaxy clusters over cosmological distances. Astronomy studies the smallest and largest known structures in the universe and the physical laws that govern them. Over the last century, a general description of stellar structure and evolution has been developed. However, the inclusion of physics such as rotation, binarity, pulsation and magnetic fields causes stellar structure and evolution to become more complicated.

Using traditional observational techniques such as photometry and spectroscopy, one barely scratches beneath the visible surface of a star, because these methods are only sensitive to the stellar atmosphere. Until the advent of asteroseismology, astronomy lacked the techniques to validate or invalidate theoretical predictions of the interior conditions of a star through observation and experimentation. This is famously encapsulated by the text *The Internal Constitution of the Stars* published in 1926 by Sir Arthur Stanley Eddington, who asked the following questions:

> " *At first sight it would seem that the deep interior of the Sun and stars is less accessible to scientific investigation than any other region in the universe. Our telescopes may probe farther and farther into the depths of space; but how can we ever obtain certain knowledge of that which is hidden behind substantial barriers? What appliance can pierce through the outer layers of a star and test the conditions within?* "

Asteroseismology is the tool that Eddington sought, which provides direct insight into the interior of a star by studying its oscillations. The pulsations within an oscillating star are governed by the physics of stellar structure, so from observations and analysis of these pulsations the interior properties of a star can be measured. Many different types of pulsator have been discovered, including our nearest stellar neighbour—the Sun. Its proximity has allowed the Sun to be extensively studied since the discovery of its oscillations in the 1960s. Asteroseismology has rapidly expanded in recent years because of improvements in

instrumentation and has been applied to many types of stars across a wide range in stellar mass and for different stages of stellar evolution.

Motivation

This monograph is centred on a group of variable stars called δ Sct stars, which are the most common type of pulsator among the intermediate-mass A and F stars, and have been studied since their discovery in the early twentieth century. Historically, using several hours of ground-based observations, these variable stars were straightforward to classify because they have similar effective temperatures and pulsate with periods of order hours and minutes.

Prior to the twenty-first century, only a handful of δ Sct stars had been extensively studied using ground-based campaigns, which provided intermittent observations with duty cycles typically less than 50 per cent. These investigations were limited by the data coverage and precision of the instrumentation used, but revealed that we lack a complete physical description of these pulsators, primarily because of the diversity of observed pulsations in these stars. A few δ Sct stars were found to exhibit a phenomenon called amplitude modulation—in the time domain this appears as a change in the maxima and minima of the light excursions over time, and in the Fourier domain this appears as variable pulsation mode amplitudes.

Naturally, this causes problems for intermittent observations over a few days if the pulsation mode amplitudes of a variable star change on timescales of order years to decades. From only a few in-depth studies, it was not clear what determines this effect in δ Sct stars, as not all stars exhibited such behaviour. This provides strong motivation to study amplitude modulation in δ Sct stars further. The space-based telescopes CoRoT and *Kepler*, which were launched in 2006 and 2009, respectively, have led to a photometry revolution. The *Kepler* Space Telescope provided a large increase in high-quality observations of hundreds of thousands of stars, including many δ Sct stars, which form the basis of this research text.

Overview

This monograph addresses Eddington's questions by using asteroseismology to expand our understanding of δ Sct stars and studies the incidence of amplitude modulation in approximately 1000 δ Sct stars observed by the *Kepler* Space Telescope. In the original edition of this thesis, the peer-reviewed journal papers by the author were included as they were published, but in this monograph they have been discussed as part of the literature. As a second edition, much of the content is the same, although it has been updated and expanded upon since the original work was published. The general theme of this text is the journey through the discoveries that were made throughout the work.

The pulsations in δ Sct stars are excited by a heat engine driving mechanism caused by increased opacity in their surface layers and have pulsation periods of order a few hours. Observations from the *Kepler* Space Telescope have revealed a diverse range of pulsational behaviour in these stars, which has been investigated using an ensemble of 983 δ Sct stars that were observed continuously for four years at an unprecedented level of photometric precision. A search for amplitude modulation in these stars showed that the majority exhibit amplitude modulation in at least a single pulsation mode. Thus, timescales of years and longer are significant in these stars both observationally and theoretically. The various causes of amplitude modulation include beating, non-linear mode coupling and stellar evolution, each having a characteristic pattern that must be recognised and disentangled to truly understand the physical processes occurring within a star. The observational studies of individual stars in this monograph provide strong evidence that non-linear processes are clearly at work in the many δ Sct stars and provide valuable constraints for future asteroseismic modelling.

Leuven, Belgium Dr. Dominic M. Bowman

The original version of the book has been revised: Book author's family name and givenname have been updated in all the chapters. A correction to this book can be found at https://doi.org/10.1007/978-3-319-66649-5_9

Acknowledgements

First and foremost, I wish to thank my Ph.D. supervisor Prof. Don Kurtz, who has provided me with a wealth of knowledge and experience over the last three years. He is an expert in astronomy, the English language and many other fascinating subjects. I have been fortunate to have Don as a mentor, and I am extremely grateful for all his support. Without his constant inspiration and motivation to push myself throughout my Ph.D., it would not have been possible to write a thesis of the standard required for it to be published as part of the Springer thesis series.

I would also like to thank Dr. Daniel Holdsworth and Dr. Simon Murphy who have been valued collaborators and have been instrumental in many different aspects of my Ph.D. I am grateful to all my collaborators and those who have contributed to the research in my thesis and beyond. I look forward to continued collaborations in the future with all of you.

I would also like to gratefully acknowledge the support from the Jeremiah Horrocks Institute at UCLan, its Director Prof. Derek Ward-Thompson, the UK Science and Technology Facilities Council (STFC) and the Royal Astronomical Society (RAS) for financial support during my studies. I am grateful to my thesis examiners, Prof. Douglas Gough and Dr. Stewart Eyres, who agreed to read my thesis and provide feedback on its content. Fortunately, their feedback was very positive and they made my Ph.D. defence an enjoyable and rewarding experience.

This research has made use of public *Kepler* data via the MAST archive, with funding for the *Kepler* mission provided by the NASA Science Mission Directorate. I appreciate all those who helped make the *Kepler* mission successful and provided the scientific community with exquisite data. I would like to thank Randy Thompson, who provided me with a lot of help in the early days of my Ph.D. when I was learning to use the MAST interface, which resulted in a promise to acknowledge him in my Ph.D. thesis.

My friends and fellow postgraduate students were certainly a source of much needed support over the last three years, especially Dr. Adam Clarke and Samuel Earp. There are too many to name all of you but you know who you are. I will certainly remember all the conferences, and conversations about science, and

particularly the recurring topic of the superiority of python. Some of you may even be pleased to hear that I have now made the permanent switch to python and I do not regret it!

At the time of writing this second edition of my Ph.D. thesis for Springer, I was employed as a Postdoctoral Researcher in the Instituut voor Sterrenkunde at KU Leuven in Belgium. I am grateful to Prof. Conny Aerts for not only hiring me after my Ph.D., but also for giving me the time and freedom to complete this monograph for Springer. I also gratefully acknowledge the European Research Council (ERC) under the European Union's Horizon 2020 research and innovation programme (grant agreement N ^{o} 670519: MAMSIE), from whom my postdoctoral position is funded.

Finally, I would like to thank my parents, to whom I owe a great deal, and all the family that have offered me words, letters, emails of encouragement throughout my studies. Thank you all.

Contents

1 Introduction 1
1.1 Asteroseismology 1
1.1.1 Pulsation Modes 3
1.1.2 What Is Amplitude Modulation? 5
1.2 The Delta Scuti Stars 6
1.2.1 Historical Overview 6
1.2.2 Physical Properties 7
1.2.3 Pulsational Instability: Driving Versus Damping 9
1.2.4 Non-linear Effects 12
1.2.5 Mode Identification 13
1.2.6 HADS Stars 14
1.2.7 SX Phoenicis Stars 15
1.3 The Inhomogeneous A Stars 16
1.3.1 The Incidence of Non-pulsating A Stars 16
1.3.2 Chemically Peculiar A Stars 16
1.3.3 Rotation in A Stars 19
1.4 Pulsations Across the HR Diagram 23
1.4.1 The Gamma Doradus Stars 23
1.4.2 Solar-Type Stars 25
1.4.3 Pulsating B Stars 26
1.4.4 Evolved Stars 28
1.5 4CVn: A Case Study of Amplitude Modulation in a Delta Scuti Star 32
References 35

2 The *Kepler* Space Photometry Revolution 41
2.1 Introductory Remarks 41
2.2 The *Kepler* Space Telescope 42
2.2.1 *Kepler* Instrumentation 42
2.2.2 *Kepler* Data Characteristics 43

2.2.3 The *Kepler* Input Catalogue . . . 45
2.2.4 The Failure of Module 3 . . . 45
2.2.5 K2 . . . 45
2.3 Fourier Analysis of Stellar Time Series . . . 46
2.3.1 The Nyquist Frequency . . . 47
2.3.2 Frequency Resolution . . . 48
2.3.3 Amplitude Visibility Function . . . 50
2.4 *Kepler* Data Catalogues . . . 52
2.4.1 Creating Data Catalogues . . . 52
2.4.2 *Kepler* Data Catalogue Extract . . . 53
2.5 Discussion . . . 56
References . . . 57

3 KIC 7106205—An Archetypal Delta Scuti Star with Amplitude Modulation . . . 59
3.1 Introductory Remarks . . . 59
3.2 Pulsational Frequency and Amplitude Modulation in the δ Sct Star KIC 7106205 . . . 59
3.2.1 *Kepler* Photometry of KIC 7106205 . . . 60
3.2.2 Amplitude and Phase Tracking . . . 65
3.3 Combining WASP and *Kepler* Data: The Case of the δ Sct Star KIC 7106205 . . . 66
3.3.1 The WASP Project . . . 67
3.3.2 Using the HADS Star KIC 9408694 for Calibration . . . 68
3.3.3 Application to the Delta Scuti Star KIC 7106205 . . . 70
3.3.4 Results from Combined WASP and *Kepler* Data . . . 73
3.4 Spectroscopic Analysis of KIC 7106205 . . . 74
3.4.1 Spectral Classification . . . 75
3.5 Discussion . . . 77
References . . . 79

4 *Kepler* Observations of Delta Scuti Stars . . . 81
4.1 Introductory Remarks . . . 81
4.2 Hybrid Stars . . . 82
4.2.1 Are all Hybrid Stars Binaries? . . . 84
4.2.2 Pure Delta Scuti Stars . . . 84
4.3 Low Frequencies in Delta Scuti Stars: The Organ Pipe Stars . . . 85
4.3.1 KIC 10407873 . . . 87
4.4 Hot Gamma Doradus Stars . . . 90
4.4.1 KIC 5130890 . . . 90

4.5 Creating an Ensemble of Delta Scuti Stars 91
4.5.1 Ensemble Limitations 92
4.6 Revisiting the Delta Scuti Instability Strip 93
4.7 Correlations in the Stellar Parameters of Delta Scuti Stars 95
4.7.1 Pulsation and Effective Temperature 97
4.7.2 Pulsation and Surface Gravity 99
4.7.3 Pulsation Across the $T_{\rm eff}$ – log g Diagram 101
4.7.4 Pulsation and Rotation 103
4.8 Discussion 103
References 105

5 Amplitude Modulation in *Kepler* Delta Scuti Stars 107
5.1 Introductory Remarks 107
5.2 Searching for Significant Amplitude Modulation 107
5.2.1 Identifying Pulsation Modes with Variable Amplitudes . . . 108
5.2.2 Defining Significant Amplitude Modulation 108
5.2.3 Phase Adjustment 109
5.3 Amplitude Modulation Catalogue Case Studies 110
5.3.1 Phase Modulation Caused by Super-Nyquist Peaks 110
5.3.2 Constant Amplitudes and Phases: NoMod Stars 112
5.3.3 Amplitude and Phase Modulation Caused by Beating of Close-Frequency Modes 113
5.3.4 Pure Amplitude Modulation with No Phase Variability . . . 113
5.3.5 Phase Modulation Due to Binarity 116
5.4 Statistics from an Ensemble Study of Amplitude Modulation 118
5.5 Amplitude Modulation Catalogue Extract 121
5.6 Ruling Out Rotation as the Ubiquitous Cause of Amplitude Modulation 123
5.7 Differentiating Beating and Pure Amplitude Modulation 124
5.7.1 Modelling Pure Amplitude Modulation 125
5.7.2 Modelling Beating in KIC 4641555 and KIC 8246833 . . . 127
5.8 Investigating the Unresolved Close-Frequency Mode Hypothesis 130
5.8.1 A Bayesian MCMC Approach to Extracting Unresolved Frequencies 132
5.9 Discussion 136
References 138

6 Characterising Pulsational Non-linearity 141
6.1 Introductory Remarks 141
6.2 Coupling Versus Combination Frequencies? 141
6.2.1 Combination Frequencies 142
6.2.2 The Role of Resonances in Pulsating Stars 145

6.2.3 Mode Coupling . . . 146
6.2.4 Resonant Mode Coupling in the Delta Scuti Star KIC 8054146 . . . 148
6.3 Non-linearity in Delta Scuti Stars . . . 151
6.3.1 KIC 4733344 . . . 152
6.3.2 KIC 5857714 . . . 155
6.4 Non-linearity in Gamma Doradus Stars . . . 158
6.4.1 KIC 4731916 . . . 158
6.4.2 KIC 4358571 . . . 163
6.5 Energy Conservation of Pulsation Modes . . . 165
6.5.1 Application to Case Studies of Delta Scuti and Gamma Dor Stars . . . 167
6.6 Discussion . . . 168
References . . . 170

7 Investigating the HADS Stars with *Kepler* Data . . . 173
7.1 Introductory Remarks . . . 173
7.2 Pulsation Period Changes Caused by Stellar Evolution . . . 174
7.2.1 Period Changes in Delta Scuti Stars . . . 175
7.2.2 Period Changes in SX Phe Stars . . . 175
7.3 The ρ Pup Star KIC 3429637 . . . 176
7.3.1 Asteroseismic Analysis of KIC 3429637 . . . 177
7.3.2 Revisiting the Analysis of KIC 3429637 . . . 178
7.4 The Scarcity of HADS Stars Observed by *Kepler* . . . 179
7.5 The Unique HADS Star KIC 5950759 . . . 180
7.5.1 Frequency Analysis . . . 181
7.5.2 Amplitude and Phase Modulation . . . 185
7.6 The HADS Star KIC 9408694 . . . 188
7.7 Discussion . . . 190
References . . . 193

8 Conclusions and Future Work . . . 195
8.1 Conclusions . . . 195
8.2 Future Work . . . 199
8.2.1 Spectroscopic Follow-Up of Delta Scuti Stars . . . 200
8.2.2 Future Missions . . . 201
8.3 Final Remarks . . . 202
References . . . 203

Correction to: Amplitude Modulation of Pulsation Modes in Delta Scuti Stars . . . C1

Chapter 1
Introduction

1.1 Asteroseismology

Almost a century ago, Sir Arthur Stanley Eddington proposed that a star could act as a heat engine and become unstable to pulsation (Eddington 1917, 1926). If the driving from a pulsational excitation mechanism in a star is strong enough to overcome local damping effects, a star will resonate in its natural oscillation modes, which are determined by the physics of stellar structure. Therefore, the observation and modelling of the conditions within stellar interiors, such as density, pressure and temperature, is of paramount importance so that we can understand how and why stars pulsate and the implications for stellar evolution. Asteroseismology, from the Greek meaning *star tremors* or *star quakes*, is the study of stellar structure and evolution from the observation and modelling of stellar pulsation. A thorough text on asteroseismology is given by Aerts et al. (2010).

The requirement of any heat engine is that heat is gained in the compression part of the cycle, with the thermal energy being converted into mechanical work. For Eddington's piston-like driving mechanism inside a star, a source of opacity provides the required instability to drive the heat engine, so it is referred to as the opacity or kappa (κ) mechanism in asteroseismology. The simplest case of driving from the κ mechanism in a star is radial pulsation, with increased levels of opacity in the stellar atmosphere that block the outward flow of radiation. The blocked flux causes a layer of gas to heat up, which increases the internal pressure such that the layer expands to return to equilibrium with its surroundings. Eventually the gas within the layer will become ionised, reducing the local opacity so that the layer is no longer opaque and the radiation flows through again. Having expanded beyond its equilibrium point and no longer being heated, the radial layer cannot support the weight of the overlying stellar atmosphere and contracts once again. The contraction allows the ionised gas to recombine and absorb the stellar flux, regenerating the source of opacity once again. Thus, a piston-like driving mechanism is created with heat being gained upon compression and energy being released upon expansion of a layer of gas in a star's atmosphere.

D.M. Bowman, *Amplitude Modulation of Pulsation Modes in Delta Scuti Stars*,
Springer Theses, DOI 10.1007/978-3-319-66649-5_1

Since the time of Eddington (1917, 1926), pulsations driven by the κ mechanism have been found in variable stars across the Hertzsprung–Russell (HR) diagram, which is shown schematically in Fig. 1.1. The hatched regions in this figure indicate a different type of pulsating star and its location in the HR diagram, with each group labelled by name and coloured approximately by spectral type. The nature of the driving mechanism in the various types of pulsator is specific to the structure of the stars within each group, although the κ mechanism is widespread across the HR diagram. Asteroseismology has been applied to all the types of pulsating star shown

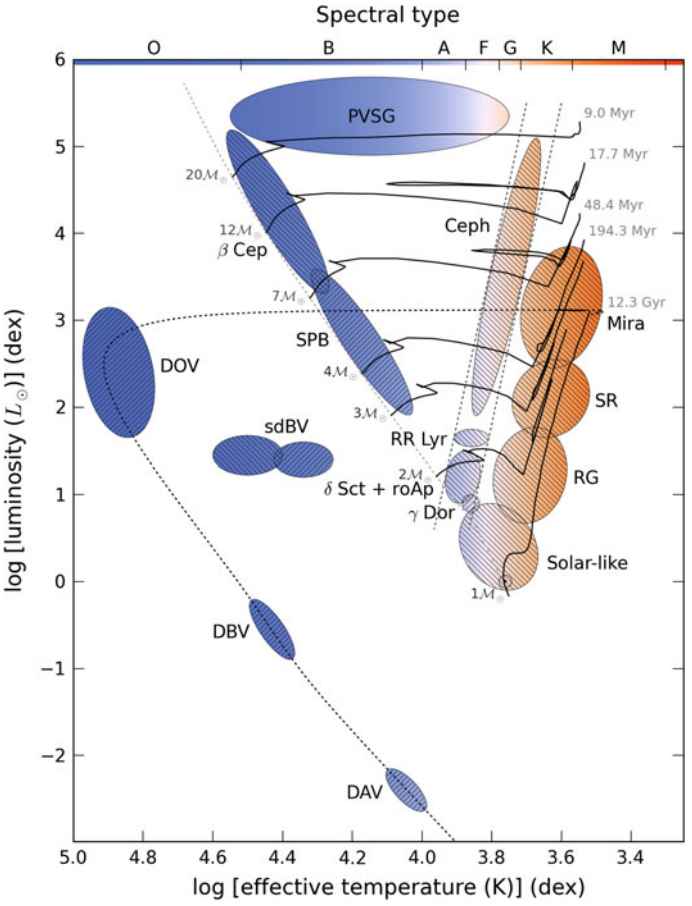

Fig. 1.1 A schematic HR diagram for pulsating stars, demonstrating the various types of stars for which asteroseismology is possible. The main sequence is indicated by a *single dashed light-grey line* and the boundaries of the classical instability strip are indicated by *two parallel dashed grey lines*. Evolutionary tracks for different stellar masses are shown as *solid black lines*, and pulsators are coloured by their approximate spectral type. The direction of that hatching indicates if the dominant pulsations are p modes (\\\) or g modes (///). Figure from Pápics (2013), his Fig. 1.4. Reproduced with kind permission from author

in Fig. 1.1, and has allowed their interiors to be probed to varying levels of success (see e.g., Aerts et al. 2010).

Asteroseismology is a rapidly expanding field within astronomy with far-reaching implications both observationally and theoretically. The success of asteroseismology in recent years has been driven by significant improvements in techniques and instrumentation. This is particularly because of the high quality data produced from space telescopes that have been operating in the last decade. These space telescopes have enabled us to probe further and deeper into the physics that determines whether a star is unstable to pulsation, and have also vastly increased our understanding of stellar structure and evolution.

1.1.1 Pulsation Modes

There are two main types of pulsation modes. The first are acoustic modes, or sound waves, for which pressure is the restoring force and hence are called p modes. These pulsations have vertical gas motions and are most sensitive to the surface conditions within a star. The other main type of pulsation modes are gravity modes, for which buoyancy or gravity is the restoring force and hence are called g modes. The gas motions of g modes can be horizontal and vertical, and are most sensitive to the conditions near the core of a star.[1] All g-mode pulsations are evanescent in a convectively unstable layer as defined by the Schwarzschild criterion, which causes runaway buoyancy and not oscillatory motion. On the other hand, p-mode pulsations can be supported in convectively unstable layers provided that the pulsation driving is stronger than the damping.

The coherent driving of pulsations in a star produces standing waves that are trapped within a pulsation cavity. Stars usually have spherical symmetry, with a displacement node at their centres and the surface acting as an anti-node. The standing waves inside a star are described by spherical harmonics using three quantum indices: n is the radial order or overtone number, ℓ is the angular degree (number of surface nodes), and m is the azimuthal order ($|m|$ is the number of surface nodes that are lines of longitude). The simplest example of a radial p mode is the fundamental radial mode where $\{n, \ell, m\} = 0$. In this mode of pulsation, the entire radius of a star expands and contracts over the pulsation cycle. Thus, the fundamental radial mode is a measure of the average density of a star, because the pulsation wave travels from the stellar surface to the core and back again throughout the pulsation cycle.

Analogous to musical instruments, the next overtone is called the first overtone radial mode where $n = 1$ and $\{\ell, m\} = 0$, which has a displacement node that is a concentric shell within the star. In this mode of pulsation, the layers above and below the nodal shell expand and contract in anti-phase. For higher radial orders, further concentric shells are nodes within a star.

[1] With the exception of pulsating white dwarf stars, in which the g modes are trapped in the surface layers.

There also exist solutions to the equations of motion for a pulsating star where $\ell \geq 1$, which are called non-radial modes. The simplest non-radial mode is an axisymmetric dipole mode with $\ell = 1$ and $m = 0$, for which the equator separating the northern and southern hemispheres is a node. In this mode of pulsation, the northern hemisphere heats and expands whilst the southern hemisphere cools and contracts and vice versa, with no change in cross-sectional area of the star from a distant observer's point of view.[2] For the case of a non-radial p mode, the depth of the pulsation cavity is determined by refraction. Since pulsations are standing waves they are sensitive to the conditions within the star, specifically the local adiabatic sound speed $c(r)$. As a non-radial pulsation wave travels inwards from the stellar surface, it encounters an increasing temperature and density gradient, hence a higher value of $c(r)$. This causes the wave to travel faster and to be continuously refracted. The depth to which a pulsation wave probes is called its turning radius, r_t, which is defined outwards from the core and is proportional to $\sqrt{\ell(\ell+1)}$. Therefore, higher degree modes have larger values of r_t, thus have smaller acoustic cavities and are more sensitive to the stellar surface.

The upper turning point of the pulsation cavity is defined by reflection at the stellar surface, at which a pulsation wave encounters a sharp density gradient. The highest frequency pulsation that can be supported in a star defines an acoustic cut-off frequency, and thus the upper limit of the acoustic cavity. Pulsations with frequencies above the acoustic cut-off are not trapped inside the stellar interior and do not provide a boundary condition for the creation of a standing wave. The various radial and non-radial pulsation cavities for both p and g modes can be interpreted using wave propagation diagrams (see e.g., Fig. 5 from Cunha et al. 2007).

Therefore, for stars that pulsate in g and p modes, the physical conditions throughout the stellar interior can be probed. This has been utilised to determine the surface-to-core rotation profile in main sequence B, A and F stars using asteroseismology (Aerts et al. 2003; Pamyatnykh et al. 2004; Briquet et al. 2007; Kurtz et al. 2014; Saio et al. 2015; Triana et al. 2015; Murphy et al. 2016; Schmid and Aerts 2016). These studies truly demonstrate the power of asteroseismology as an observational science for determining the interior properties of a star.

Mixed Modes

For a star on the zero-age main sequence (ZAMS), there is a clear separation in the pulsation cavities of g and p modes, with the lowest frequency p mode (i.e., the fundamental radial mode) having a larger frequency than the highest frequency g mode. As a star ages and evolves off the ZAMS, the g-mode pulsation cavity extends to higher frequencies as a result of an increasing buoyancy frequency, known as the Brunt–Väisälä frequency (Aerts et al. 2010). It was first discovered by Osaki (1975)

[2] A three-dimensional representation of octupole ($\ell = 3$) pulsation modes with different values of m viewed from different inclination angles, i, is shown in Fig. 1.4 from Aerts et al. (2010), in which red and blue represent the regions on the stellar surface that are moving in (heating) and moving out (cooling), respectively, at a given time.

that this leads to a form of mode interaction called mixed modes, which are pulsations that have g-mode characteristics in the stellar interior and p-mode characteristics in the stellar envelope. The interaction of g and p mode properties takes place through a sequence of avoided crossings, which allow the modes to interact whilst maintaining their independent characters (Osaki 1975).

Therefore, the evolutionary state of a star, specifically if it is near the ZAMS or terminal-age main sequence (TAMS) can influence its pulsational properties and the presence of mixed modes in its amplitude spectrum. Mixed modes are typically found in stars that have evolved off the main sequence and are undergoing hydrogen shell burning, because the large density gradient outside the core couples the g- and p-mode pulsation cavities (Aerts et al. 2010). One of the most remarkable studies of mixed modes in evolved stars was that by Bedding et al. (2011), who were able to distinguish helium core-burning and hydrogen shell-burning red giant stars using asteroseismology.

Asymptotic Pulsation Modes

For high radial order pulsation modes that satisfy $n >> \ell$, p modes become approximately equally spaced in frequency and g modes become approximately equally spaced in period, which is known as the asymptotic regime of pulsation (Tassoul 1980; Gough 1986). Asymptotic pulsation modes create regularities in the amplitude spectrum of a pulsating star, which simplifies mode identification. Deviations from the regular spacings in frequency and period for p and g modes, respectively, have been utilised to study physics within the interiors of intermediate-mass stars, such as chemical mixing (Miglio et al. 2008) and rotation (Bouabid et al. 2013; Van Reeth et al. 2015b, 2016).

1.1.2 What Is Amplitude Modulation?

The oscillations of a star can be detected using two main methods. The first method is to use photometry to measure the periodic changes in surface flux, which are caused by variations in surface temperature, and create a light curve for a star. The second method is to use spectroscopy to measure the displacement variations of the stellar surface and create a time series of radial velocity measurements. The common practice in asteroseismology is to use Fourier analysis to calculate an amplitude (or power) spectrum from a time series and extract the frequencies, amplitudes and phases of the detectable pulsation modes.

Non-continuous observations produce large gaps in a stellar time series and consequently complex window patterns in an amplitude spectrum, which makes it difficult to study pulsating stars. Despite this and the generally high levels of noise in ground-based observations, some δ Sct stars have been shown to oscillate with pulsation modes that varied in amplitude over time spans of months and years (Breger 2000b, 2009, 2016). This raises the question of what physical mechanism is causing the modulation of pulsation mode amplitudes in δ Sct stars. There are few published

examples of δ Sct stars that exhibit amplitude modulation and it is difficult to draw any meaningful conclusions from so few examples. A useful case study of amplitude modulation in a δ Sct star observed from the ground is 4 CVn (Breger 2000b, 2009, 2016), which is discussed further in Sect. 1.5.

A space telescope on the other hand can provide nearly continuous observations with a duty cycle close to 100%, and a high photometric precision. The dawn of space telescopes useful for asteroseismology provides strong motivation for studying δ Sct stars in more detail. In this monograph, the pulsational properties of δ Sct stars are studied using approximately 1000 stars observed by the *Kepler* Space Telescope (Borucki et al. 2010). Furthermore, a search for amplitude modulation in this large ensemble of stars is carried out, with individual case study stars used to demonstrate and distinguish its various physical causes.

1.2 The Delta Scuti Stars

The δ Sct stars are the most common group of pulsators among the A and F stars and have been studied since the discovery of their variability about a century ago (Campbell and Wright 1900; Fath 1935; Colacevich 1935). In this section, a review of δ Sct stars is presented, including a historical overview, a summary of their physical properties and a discussion of the dominant pulsation excitation mechanism. Note that the chemically peculiar stars found in a similar location to the δ Sct stars in the HR diagram are discussed in Sect. 1.3.2, with the current section focusing on the pulsations in δ Sct stars. Reviews of the physical properties of δ Sct stars are also given by Breger (2000a), Aerts et al. (2010) and Murphy (2014).

1.2.1 Historical Overview

The first detection of variability in a δ Sct star was made by Campbell and Wright (1900), who studied nine purported spectroscopic binaries using radial velocity measurements. Campbell and Wright (1900) provided no explanation for the variability, but simply noted it. A few decades later, Fath (1935) and Colacevich (1935) used photometry and radial velocity measurements, respectively, to accurately determine the period of the variability in the star δ Sct itself. They placed it in the variable star group β Canis Majoris, which are today known as β Cep stars (Aerts et al. 2010). The few stars in this group had large photometric amplitudes as ground-based observations were restricted by high noise levels that created a strong selection bias. It was Eggen (1956) who first suggested that a new and separate type of variable star exists, of which δ Sct was the eponymous member. As instrumentation improved, lower levels of noise and an improved duty-cycle allowed more pulsating stars similar to δ Sct to be discovered and added to the group (Baglin et al. 1973; Breger 1979).

The majority of discoveries throughout the early era of δ Sct research were based on studying high-amplitude radial pulsation modes. One of the important conclusions from these studies was made by Breger and Bregman (1975), who calculated pulsation constants (see Sect. 1.2.5) for radial pulsation modes in δ Sct stars and compared them to the predicted values from stellar models created by Cox et al. (1972). From the observations, it was discovered that hotter δ Sct stars typically have higher pulsation mode frequencies (Breger and Bregman 1975).

The focus of δ Sct research expanded to include the study of non-radial pulsation modes, with improved instrumentation allowing dozens, and sometimes hundreds, of low amplitude pulsations to be detected in many δ Sct stars (Baglin et al. 1973; Breger 1979). From a larger number of stars it was demonstrated that most δ Sct stars pulsate in low amplitude non-radial modes in addition to high-amplitude radial modes. Theoretical pulsation models were not limited by instrumentation and predicted a rich spectrum of p, g and mixed modes for δ Sct stars (Dziembowski et al. 1995), but only a few stars were observed to pulsate in high-degree modes ($\ell \leq 20$), for example τ Peg (Kennelly et al. 1998) and 4 CVn (Breger 2000b, 2009).

Today, the δ Sct stars represent a diverse group of stars that host a range of pulsational behaviour. The rich spectrum of pulsation modes excited in these stars offer the potential of probing physics at different depths using asteroseismology, which emphasises that δ Sct stars are useful for studying stellar structure and evolution in a transition region between low- and high-mass stars (Breger 2000a; Aerts et al. 2010).

1.2.2 Physical Properties

The δ Sct stars are Population I stars with spectral types between A2 and F2 (Rodríguez and Breger 2001). This places them within the mass range of $1.5 \leq M \leq 2.5\,\mathrm{M}_{\odot}$ and within the effective temperature range of $6900 \leq T_{\rm eff} \leq 8900\,\mathrm{K}$ whilst on the ZAMS, although more evolved δ Sct stars can be as cool as $T_{\rm eff} \simeq 6300\,\mathrm{K}$ (Uytterhoeven et al. 2011). The δ Sct stars are found at the intersection of the main sequence and the classical instability strip in the HR diagram and are labelled in Fig. 1.1. Using ground-based observations, Rodríguez and Breger (2001) were able to constrain the location of δ Sct stars in the HR diagram by defining observational blue and red edges of the classical instability strip. Calibrated values of absolute visual magnitude $M_{\rm V}$, colour $B-V$, and effective temperature $T_{\rm eff}$ for main sequence dwarfs (i.e., luminosity class V) around spectral type A are given in Table 1.1, which cover the expected range for δ Sct stars.

The δ Sct stars are often referred to as intermediate-mass stars as they lie in a transition region between early- and late-type stars (i.e., high- and low-mass stars), with the separation commonly defined at a spectral type of G0 (Gray and Corbally 2009). This separation is useful because it also corresponds to the lower limit in stellar mass, specifically $M \simeq 1.1\,\mathrm{M}_{\odot}$, for a main sequence star to have a convective core. Therefore, the pulsations in δ Sct stars provide the opportunity to study stellar structure and evolution in the interesting transition region from radiative cores and

Table 1.1 Observed parameters of the main sequence stars similar in spectral type to the δ Sct stars. Values of the absolute visual magnitude, M_V, which are calibrated to spectral type, are from Gray and Corbally (2009), with values of colour, $B - V$, taken from Fitzgerald (1970). Calibrated values of effective temperature, $T_{\rm eff}$, were taken from Bessell (1979) and rounded to the nearest 50 K, with some values interpolated using the colour-temperature relations from Gray (2005)

Spectral type	M_V (mag)	$B - V$ (mag)	$T_{\rm eff}$ (K)	Comment
B8	0.0	−0.11	12 000	
B9	0.7	−0.07	11 000	
A0	1.4	−0.01	10 000	
A1	1.6	0.02	9500	
A2	1.9	0.05	9000	
A3	2.0	0.08	8800	δ Sct blue edge
A4		0.12	8500	
A5	2.1	0.15	8250	
A6	2.2	0.17	8100	
A7	2.3	0.20	7850	γ Dor blue edge
A8	2.4	0.27	7400	
A9	2.5	0.30	7250	
F0	2.6	0.32	7100	
F1	2.8	0.34	7000	δ Sct red edge
F2	3.0	0.35	6950	
F3	3.1	0.41	6650	
F4	3.3	0.42	6600	
F5	3.4	0.45	6500	γ Dor red edge
F6	3.7	0.48	6350	

thick convective envelopes in low-mass stars ($M \lesssim 1\,{\rm M}_\odot$) to large convective cores and radiative envelopes in high-mass stars ($M \gtrsim 2\,{\rm M}_\odot$). Concurrently, the δ Sct stars also represent a transition in luminosity from the high amplitude radial pulsators, such as Cepheid variables, and the non-radial multiperiodic pulsators within the classical instability strip (Breger 2000a). Most δ Sct stars cross the instability strip on approximately horizontal tracks (Breger 2000a), which places them in the core hydrogen or hydrogen shell-burning stage of stellar evolution (Aerts et al. 2010).

Many δ Sct stars are multiperiodic pulsators with numerous radial and non-radial modes with pulsation periods of order a few hours (Uytterhoeven et al. 2011), but can be as short as 15 min (Holdsworth et al. 2014a). However, one of the difficulties encountered when studying δ Sct stars is the issue of mode identification, which is discussed further in Sect. 1.2.5. If pulsation modes can be identified, the rich amplitude spectra of δ Sct stars allow stellar structure to be studied in great detail for both main sequence and post-main sequence stars.

1.2.3 Pulsational Instability: Driving Versus Damping

There are several mechanisms that can drive pulsation in stars across the HR diagram, but pulsational instability is always a balance between the driving and damping processes within a star, which are dependent on stellar structure. The temperature gradient within a star's envelope is a strong function of the effective temperature. As one transitions up the main sequence from late- to early-type stars, the depth of the surface convective envelope rapidly decreases, thus the ratio of the convective flux to total flux also decreases. This transition in stellar structure from low-mass stars with thick envelopes with energy transport dominated by convection to intermediate-mass stars with thin surface convective envelopes is shown in Fig. 1.2. The top panel of Fig. 1.2 shows the temperature range within the stellar envelope that is unstable to convection as a hatched region, as a function of effective temperature. The bottom

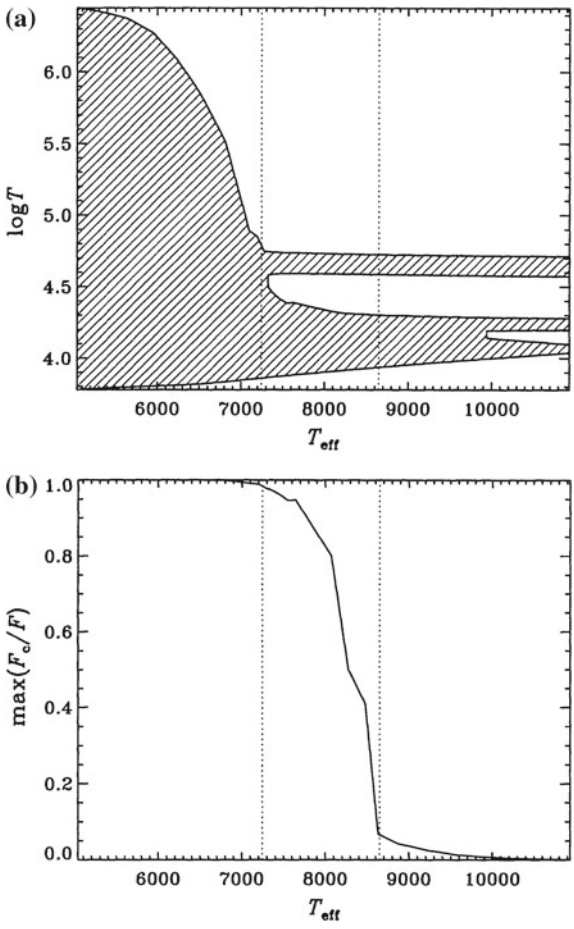

Fig. 1.2 The structure of the stellar envelope in intermediate-mass ZAMS stars. The hatched region in the *upper panel* represents the temperatures within the stellar envelope that are unstable to convection as a function of effective temperature ($T_{\rm eff}$). The *lower panel* shows the fraction of flux that is transported by convection in the envelope as a function of $T_{\rm eff}$. The cool and hot boundaries of the classical instability strip are shown by *vertical dotted lines*, which define a transition region in between. Figure from Christensen-Dalsgaard (2000), his Fig. 3. Reproduced with permission from ASPCS

panel of Fig. 1.2 shows the fraction of the convective flux to the total flux, as a function of effective temperature. Therefore, stars within the temperature range $7000 \leq T_{\rm eff} \leq 9000$ K, i.e., the early-F and late-A stars, represent a transition in stellar structure for which convection goes from being the dominant energy transport mechanism to a negligible contribution to the surface flux, respectively.

This change in stellar structure is the underlying cause of pulsation in the classical instability strip in the HR diagram and has been discussed in detail by Pamyatnykh (1999, 2000), Christensen-Dalsgaard (2000) and Aerts et al. (2010). The boundary between the adiabatic inner region and the non-adiabatic surface of the stellar envelope is defined as the *transition region*, in which the gradient of the flux $\delta L/L$ is not constant (Aerts et al. 2010). If the energy contained within the stellar material is large enough to cause a significant positive or negative perturbation to the flux, i.e., δL, then it can contribute to damping or driving, respectively. The classical instability strip in the HR diagram corresponds to stars within a small range of effective temperature, such that an effective driving mechanism occurs at the same depth as the transition region, which defines hot and cool edges shown as the pair of dotted lines in Fig. 1.2.

Pulsations in δ Sct stars are self-excited by the κ mechanism, resulting in a rich spectrum of predominantly low-overtone radial and non-radial p modes (Breger 2000a). The ionisation layers of H and He I at $T \simeq 15\,000$ K are too close to the surface and are not believed to play an important role, whereas the He II ionisation layer at $T \simeq 48\,000$ K provides increased opacity which is able to block the outward flow of radiation (Cox 1963; Chevalier 1971). Consequently, pulsations in δ Sct stars follow Eddington's heat engine cycle as discussed in Sect. 1.1, with layers of gas in the stellar envelope periodically expanding and contracting about an equilibrium point to allow radiation to reach the stellar surface. The asymptotic relations of Tassoul (1980) are not applicable to the low-overtone p modes observed in δ Sct stars, which make mode identification difficult in these stars. Methods for identifying pulsation modes in δ Sct stars are discussed in Sect. 1.2.5.

Synthetic amplitude spectra generated using theoretical pulsation models of δ Sct stars are only able to reproduce observations in a schematic sense, with models often predicting many more pulsation modes excited than are observed. For example, Dziembowski (1977) calculated that high-degree modes ($\ell \leq 1000$) can be excited for a δ Sct star in the centre of the classical instability strip. However, it is not clear how observations of δ Sct stars with similar effective temperatures, structure and evolutionary state can have significantly different amplitude spectra. What physics determines which pulsation modes are excited, what their amplitudes are and how different pulsation modes interact with each other? A mode selection mechanism is clearly at work within δ Sct stars, as some stars pulsate in only a few radial modes whereas others pulsate in dozens (sometimes hundreds) of radial and non-radial modes (Breger 2000a). Similarly, pulsation mode amplitudes in δ Sct stars can exceed 0.1 mag, whilst others are of the order of a few μmag. There is a diverse range of observed behaviour in δ Sct stars, so it is also possible that multiple mode selection mechanisms occur simultaneously within a star, or different mechanisms are dominant in different regions of the classical instability strip in the HR diagram.

The nature of what causes the diversity of pulsational behaviour in these stars is one of the goals of asteroseismology and motivates the continued study of these stars.

Theoretical models are able to reproduce the observational blue and red edges of the classical instability strip with differing levels of success, and thus if a star is stable or unstable to pulsation (Pamyatnykh 1999; Houdek 2000; Dupret et al. 2004, 2005; Grigahcène et al. 2010). At the blue edge ($T_{\rm eff} \simeq 8800$ K), the effective temperature of a star is too high to support a deep enough driving layer within the star, such that the He II ionisation zone is too shallow where the density of the stellar medium is insufficient to excite pulsation (Pamyatnykh 1999, 2000; Christensen-Dalsgaard 2000; Houdek 2000; Dupret et al. 2004, 2005). Thus, damping wins over driving at the blue edge and a star is returned to stability. Whereas at the red edge ($T_{\rm eff} \simeq 6900$ K), a star is returned to stability as the surface convective envelope is substantial enough such that convection damps the pulsations (Christensen-Dalsgaard 2000; Houdek 2000; Dupret et al. 2004, 2005). At the red edge, the κ mechanism is unable to overcome the damping from convection making the red edge more difficult to determine theoretically than the blue edge (Pamyatnykh 1999; Houdek 2000; Dupret et al. 2004, 2005). The interplay of convection and pulsation is crucial for our understanding of the red edge, with models including time-dependent convection with different treatments of mixing-length theory often needed to accurately match observations (Houdek et al. 1999b; Houdek 2000; Dupret et al. 2005; Grigahcène et al. 2005; Houdek and Dupret 2015).

It is important to note that the structure of a star does change throughout its evolution, including whilst it is on the main sequence (see Fig. 3.6 from Aerts et al. 2010). Most δ Sct stars evolve across the classical instability strip on approximately horizontal tracks, so a star can be unstable to pulsation at the ZAMS and not be unstable to pulsation at the TAMS, and vice versa (Breger 2000a).

Stochastic Excitation of Pulsation Modes

Despite their thin convective envelopes, theoretical models of δ Sct stars predict that stochastically driven pulsations should be excited in these stars (Houdek et al. 1999a; Samadi et al. 2002). These authors used the time-dependent non-local mixing-length formalism for convection from Gough (1977) to study the stability of solar-like oscillations in δ Sct stars near the red edge of the classical instability strip. It was found that turbulence from the surface convection zone was sufficient to excite all the eigenmodes within a frequency range and excite solar-like oscillations to observable amplitudes (Houdek et al. 1999a; Samadi et al. 2002).

A claim of finding stochastically excited p modes in the δ Sct star HD 187547 (KIC 7548479) using data from the *Kepler* Space Telescope was made by Antoci et al. (2011), but a later analysis of the same star with a longer data set revealed that turbulent pressure operating in the H I zone was instead responsible (Antoci et al. 2014). Thus, dedicated observations have been as of yet unsuccessful in detecting solar-like oscillations in δ Sct stars (Antoci et al. 2013, 2014).

In stars with solar-like oscillations, the turbulent motions in the thick convective envelope have random phases and produce stochastic driving (see Sect. 1.4.2). Whereas, turbulent pressure, or the perturbation to the momentum flux associated

with a convectively unstable region (Houdek 2000), is able to produce coherent driving in δ Sct stars. Driving from turbulent pressure in a δ Sct star is able to excite higher radial order ($7 \leq n \leq 10$) pulsation modes (Houdek 2000), and is analogous to driving from the κ mechanism operating in the He II ionisation zone.

For the case of the δ Sct star HD 187547, it was shown using theoretical models how the phase lag between the response of the turbulent pressure to an incoming pulsation wave or density perturbation creates coherent driving of high frequency pulsation modes (Antoci et al. 2014). The study by Antoci et al. (2014) emphasises the importance of the interplay between convection and pulsation in δ Sct stars, especially for those with significant surface convection zones, but also how asteroseismology plays a key role in disentangling the physics at work within these stars.

1.2.4 Non-linear Effects

In any simple oscillatory motion, for example a spring or a swinging pendulum, the amplitude is independent of the oscillation period in the linear regime. Thus we have no prediction of the pulsation amplitudes in variable stars using linear models. The role of non-linearity in classical pulsators has been discussed in the literature for some time (e.g., Stellingwerf 1975a, b). However, the use of non-linear pulsation models to study δ Sct stars led to the problem now known as *The Main Sequence Catastrophe* — models predicted that pulsation amplitudes would grow exponentially and become large enough to cause the outer layers of a star to exceed the escape velocity (Stellingwerf 1980). Therefore, the pulsation mechanism would cause a star's outer layers to overcome the force of gravity and be dispersed from the star. This is similar to the late thermal pulses caused by repeated onsets of helium shell-burning in stars with masses between $2.3 \leq M \leq 9\,\mathrm{M}_{\odot}$ as they ascend the asymptotic giant branch (Aerts et al. 2010). Since observations of δ Sct stars do not have significant mass-loss rates on the main sequence and typically pulsate with amplitudes of order a few mmag, some physics is clearly missing from the non-linear pulsation models.

One solution may lie in introducing stronger damping effects deep within a star, since the interactions between modes and the convection zone itself are not fully understood (Saio and Cox 1980). Alternatively, a non-linear mode selection and/or amplitude saturation mechanism is needed to limit the growth of mode amplitudes and match observations (Dziembowski 1982). The mechanism(s) that determine the amplitudes of pulsation modes are largely unknown (see e.g., Nowakowski 2005), but a mechanism is needed to reproduce observations. This demonstrates the synergy needed between theory and observations and the motivation for further study of these stars.

1.2.5 Mode Identification

A requirement of asteroseismology is to measure the frequency of pulsation modes, and identify modes in terms of their radial order n, angular degree ℓ and azimuthal order m. In the following subsections, different techniques for pulsation mode identification are discussed in the context of δ Sct stars.

Scaling Relations

Mode identification is simplified for stars that pulsate in high-overtone p modes, because the pulsation modes are approximately equally spaced in frequency from being in the asymptotic regime (Tassoul 1980; Gough 1986). The separation in frequency between consecutive overtone radial modes is known as the large separation, and often denoted as $\Delta\nu$. Therefore, if multiple high overtone radial modes are excited then a comb-like pattern of frequencies is observed in the amplitude spectrum.

Pulsation modes in δ Sct stars are typically low radial order, thus are not in the asymptotic regime. This makes it difficult to identify pulsation modes from the lack of obvious patterns in their amplitude spectra. For a few δ Sct stars, however, claims of detecting the large frequency separation have been made (Breger et al. 2009; Paparó et al. 2016a, b). One such star was the δ Sct star FG Vir, which was found to contain regularities in its amplitude spectrum that were conjectured to be caused by the separation between consecutive overtones of radial modes (Breger et al. 2009).

Period Ratios

The period ratios of high-amplitude pulsation modes can be used to identify radial modes in δ Sct stars. The period ratio of the first overtone to fundamental radial mode for δ Sct stars is between $0.756 \leq P_1/P_0 \leq 0.787$, and subsequent ratios are $0.611 \leq P_2/P_0 \leq 0.632$ and $0.500 \leq P_3/P_0 \leq 0.525$ for the second and third radial overtones, respectively (Stellingwerf 1979). Caution is advised when applying this mode identification technique as mode trapping in the stellar envelope (Dziembowski and Krolikowska 1990) or moderate to rapid rotation can lead to ambiguities in stars with a high density of pulsation modes in their amplitude spectra and thus accidental matches (see e.g., Breger and Pamyatnykh 2006).

Pulsation Constants

Pulsation modes can also be identified by calculating pulsation constants using

$$Q = P\sqrt{\frac{\bar{\rho}}{\bar{\rho}_\odot}}\,, \tag{1.1}$$

where Q is the pulsation constant in days, P is the pulsation period in days, and $\bar{\rho}$ is the mean stellar density, which is normalised to the solar value $\bar{\rho}_\odot$. Equation 1.1 can be re-written as

$$\log\ Q = \log\ P + \frac{1}{2}\log\ g + \frac{1}{10}M_{\rm Bol} + \log\ T_{\rm eff} - 6.454\,, \tag{1.2}$$

where $\log g$ is the surface gravity in cgs units, $M_{\rm Bol}$ is the Bolometric absolute magnitude and $T_{\rm eff}$ is the effective temperature in K. A value of $M_{\rm Bol}$ can be calculated using $T_{\rm eff}$ and $\log g$ values in comparison with the main sequence of a cluster (e.g., Pleiades; M45) or, for example, using the calibrations given in Table 1.1.

Typical values of pulsation constants for the fundamental, first and second-overtone radial p modes in δ Sct stars lie between $0.022 \leq Q \leq 0.033$ d (Breger and Bregman 1975). The pulsation constant can be used to identify the overtone number, n, of radial modes (Stellingwerf 1979), but the calculation using Eq. 1.2 is strongly dependent on the stellar parameters used, particularly $\log g$. For example, Breger (1990) quotes fractional uncertainties in Q values as high as 18%, which could cause a first overtone radial mode to be confused for either the fundamental or second overtone radial mode. Therefore, caution is advised when applying this method of mode identification.

1.2.6 HADS Stars

McNamara (2000) defined the subgroup of high amplitude δ Sct (HADS) stars as radial pulsators with asymmetric light curves, large pulsation amplitudes and pulsation periods between 1 and 6 h. The HADS stars are found in a narrow region within the classical instability strip with effective temperatures between $7000 \leq T_{\rm eff} \leq 8000$ K and are typically slow rotators with rotational velocities of $v \sin i \lesssim 40\,{\rm km\,s^{-1}}$ (McNamara 2000; Rodríguez et al. 2000). HADS stars are typically characterised as δ Sct stars with peak-to-peak light amplitudes exceeding 0.3 mag (McNamara 2000), but have similar characteristics to evolved pulsators in the classical instability strip. For example, approximately 40% of HADS stars pulsate in the fundamental and first overtone radial modes (McNamara 2000).

The similarities between HADS stars and evolved pulsators in the classical instability strip resulted in the HADS stars having a long history of being called transitionary objects and being compared to Cepheid variables (see Sect. 1.4.4). Perhaps the most obvious similarity is the non-sinusoidal shape of the light curves, with the changes between maxima and minima light excursions being similar to Cepheid variables and RRab stars (McNamara 2000). Another similarity is that many of the double-mode HADS stars observed in the Large Magellanic Cloud have the same period ratios as Cepheid variables (Poleski et al. 2010), and also follow the same Period-Luminosity relationship (Soszyński et al. 2008). Therefore, it is perhaps not surprising that the HADS stars have been historically thought of as dwarf Cepheids in the literature. For example, Eggen (1976) originally referred to δ Sct stars as ultrashort-period Cepheids (USPC).

It was conjectured by Petersen and Christensen-Dalsgaard (1996), that HADS stars are in a post-main sequence stage of evolution, which creates a physical parameter space that allows HADS stars to pulsate at much higher pulsation amplitudes than main sequence δ Sct stars. Such an evolutionary state would create large changes in stellar structure over a relatively short period of time (Breger 2000a), but

it remains unclear if *all* HADS stars are in a post-main sequence stage of evolution. Alternatively, Breger (2000a) conjectured that slow rotation is a requirement for high-amplitude pulsations for stars within the classical instability strip. It is unclear if the term HADS should be used other than phenomenologically, and if there is a physical distinction in the structure or pulsational excitation mechanism of HADS stars compared to their low-amplitude δ Sct counterparts.

The main advantage of studying HADS stars is the simplification of mode identification through period ratios because of their high amplitude pulsation modes. Statistical studies of intermediate-mass stars have shown that HADS stars are rare, making up less than one per cent of all stars within the classical instability strip (Lee et al. 2008). Clearly the HADS stars are interesting because they are able to pulsate at much higher amplitudes than δ Sct stars, which implies a physical difference in the structure and possibly evolutionary stage of these stars.

1.2.7 SX Phoenicis Stars

SX Phoenicis (SX Phe) stars are Population II variable stars located within the classical instability strip in the HR diagram, but are found below the ZAMS for Population I stars. They have similar pulsation periods to δ Sct stars, but have larger pulsation amplitudes, low metallicities and large spatial motions, and were proposed as a separate class of object by Frolov and Irkaev (1984). The SX Phe stars are mostly found in globular clusters or dwarf galaxies and are considered blue stragglers because they are brighter and bluer than the cluster population. The origin of such objects may be from mass transfer in binary systems or the collision of two stars (Eggen and Iben 1989).

Since their definition, SX Phe stars have been observed to be multiperiodic pulsators with many low-amplitude non-radial modes in addition to high amplitude radial modes (Olech et al. 2005). Therefore, the pulsation mode frequencies and amplitudes are not enough to distinguish δ Sct and SX Phe stars, so confirmation of low metallicity and high spatial motion is often needed (Nemec and Mateo 1990; Balona and Nemec 2012).

A well-studied SX Phe star using data from the *Kepler* Space Telescope is KIC 11754974, which was shown to pulsate with frequencies between $16 \leq \nu \leq 25\,\mathrm{d}^{-1}$, one of which had an amplitude greater than 60 mmag (Murphy et al. 2013). From the frequency analysis, Murphy et al. (2013) demonstrated that KIC 11754974 was in a 343-d binary system and constrained the mass of the SX Phe primary and non-pulsating secondary to 1.53 and $0.63\,\mathrm{M}_{\odot}$, respectively. The authors confirmed KIC 11754974 as a SX Phe star using asteroseismic modelling, and because spectroscopic observations indicated that the star was metal-poor throughout its interior, as opposed to exhibiting only a surface abundance anomaly (Murphy et al. 2013).

1.3 The Inhomogeneous A Stars

The A stars are possibly the most diverse spectral type of all stars in the HR diagram, as the group contains many different aspects of physics including rotation, pulsation, magnetic fields and chemical peculiarities. These properties and the interplay amongst them have been studied to varying levels of success, but they are clearly important for our understanding of stellar structure and evolution. The previous section focussed on discussing pulsations in A stars – i.e., the δ Sct stars – but in this section the diversity of all A stars is discussed for completeness. The incidence of non-pulsating stars in the classical instability strip is discussed in Sect. 1.3.1, the different types of chemically peculiar A stars in Sect. 1.3.2, and rotation among the A stars in the context of *Kepler* data is discussed in Sect. 1.3.3.

1.3.1 The Incidence of Non-pulsating A Stars

The results from statistical studies of a large number of A and F stars by Uytterhoeven et al. (2011) and Balona and Dziembowski (2011) showed that the majority of A stars observed by the *Kepler* Space Telescope are not pulsating above the detection threshold. The lack of pulsation in chemically peculiar stars is not surprising (see Sect. 1.3.2), but the lack of pulsation in a chemically normal star within the classical instability strip is puzzling.

To test the purity of the classical instability strip to pulsation, Murphy et al. (2015a) searched for a non-pulsating chemically normal star within the classical instability strip using high-resolution spectroscopy and photometry from the *Kepler* Space Telescope. The search for such a star resulted in finding only one, specifically KIC 6128236 (HD 184521), which has stellar parameters of $T_{\rm eff} = 7000 \pm 100$ K, $\log g = 3.5 \pm 0.1$ and $v \sin i = 106 \pm 2\,{\rm km\,s^{-1}}$ and a spectral type of F0IV derived from a detailed spectroscopic analysis (Murphy et al. 2015a). It should be noted that the definition of whether a star is pulsating or not is dependent on the choice of detection threshold, with an amplitude threshold of 50 μmag used by Murphy et al. (2015a) in their study. The lack of pulsation in KIC 6128236 remains a challenge to pulsation theory (Murphy et al. 2015a).

On the other hand, it has not been definitively established if *all* of the non-pulsating stars that lie within the classical instability strip are chemically peculiar. Further work is still needed to address this.

1.3.2 Chemically Peculiar A Stars

Chemical peculiarities in A stars come in many flavours, which are characterised by common features in spectroscopic observations. These include the non-magnetic,

metallic-lined Am stars, the magnetic Ap stars, the rapidly oscillating Ap stars and the λ Boo stars. In the following subsections, these chemically peculiar stars are discussed in the context of pulsating A stars.

Am Stars

The first description of Am stars was provided by Titus and Morgan (1940), and later expanded by Conti (1970) and Smith (1971a, b), who characterised Am stars as slow rotators having a difference of at least five spectral subclasses between their Ca K line strength and their metallic line strengths. The Am stars are the most common type of A star, with approximately 50% of A stars at a spectral type of A8 being classified as Am stars (Smith 1973). Marginal Am stars (denoted as Am:) are those that show less than five subclasses between their Ca K line strength and their metallic line strengths (Cowley et al. 1969; Kurtz 1978), but are still significantly different to normal A star abundance patterns. An example of a spectral classification for an Am star is kA3hA9mF1 V, which was taken from Murphy et al. (2015a), lists how the different spectral types of A3, A9 and F1 are obtained for such a star if using the Ca K, Balmer lines, or metal lines, respectively. A thorough review of the classification of Am stars using spectroscopy is given by Gray and Corbally (2009).

Am stars are often found in close binary systems (Abt 1961; Abt and Levy 1985), with at least 60% of all known Am stars in binary systems (Murphy 2014; Smalley et al. 2014), which is significantly higher than the binary fraction of approximately 35% for all A stars (Abt 2009; Duchêne and Kraus 2013; Moe and Di Stefano 2017). The short orbital periods of Am stars are between $1 \leq P_{\rm orb} \leq 10\,{\rm d}$ (Abt 1967), and are sufficient to tidally brake Am stars into being slow rotators. The slow rotation allows gravitational settling and radiative diffusion to occur, with different metallic species rising from radiative levitation or sinking from gravity based on the number of absorption lines (Baglin et al. 1973). Mixing caused by turbulence would prevent the separation of atomic species, but this is negligible in the slowly rotating Am stars (Slettebak 1954, 1955), so transition metals form clouds near the stellar surface and are observed as overabundance anomalies.

It was thought that Am stars cannot pulsate with high mode amplitudes, because atomic diffusion depletes helium from the He II ionisation zone preventing driving by the κ mechanism (Baglin et al. 1973). Observations of Am stars from the ground were in agreement with theoretical predictions of the lack of pulsation in Am stars (Breger 1970). The first classical Am star found to pulsate was HD 1097 by Kurtz (1989), after many attempts to find such a star (e.g., Kurtz 1976). More recently, it has been shown by Smalley et al. (2011) that approximately 14% of all known Am stars pulsate with amplitudes of order 1 mmag, showing that these stars are more complicated than previously thought (Smalley et al. 2017).

An attempt at understanding how Am stars pulsate from the κ mechanism operating in the metal bump (or 'Z bump') in opacity was made by Richer et al. (2000), and by introducing stronger mixing mechanisms by Turcotte et al. (2000) and Théado et al. (2009). Pulsations in marginal Am stars can be understood using diffusion theory because residual helium in the He II ionisation zone is able to excite pulsations through the κ mechanism. Similarly, pulsations in evolved Am stars (known as

ρ Pup stars) can also be understood, as the evolutionary changes to stellar structure in these stars allow the He II ionisation zone to be replenished with helium. A thorough review of pulsations in Am stars is given by Kurtz (2000).

Ap Stars

Chemically peculiar A stars, denoted as Ap stars, are much rarer and constitute only 10% of all A stars (Wolff 1968). The Ap stars have strong dipolar global magnetic fields, which range from 300 G (Aurière et al. 2004) to as large as 34 kG in Babcock's star (HD 215441; Babcock 1960). The magnetic field in an Ap star is misaligned with the rotation axis, with the angle between the magnetic and rotation axes known as the angle of obliquity (Stibbs 1950).

The Ap stars are slow rotators with rotation periods that can be larger than several decades (Mathys 2015), with very few Ap stars known to exist in close binary systems (Abt and Snowden 1973). The slow rotation in Ap stars is believed to be caused be the interaction of the magnetic field with the circumstellar disk during the pre-main sequence contraction phase, which effectively brakes the star (Stępień 2000).

The slow rotation and the presence of a strong magnetic field causes stratification in the atmosphere and often leads to chemical spots on the surface of an Ap star (Stibbs 1950), which can be stable for many decades and thus used to determine the rotation period of the star. These chemical spots are caused by atomic diffusion with the strong magnetic field trapping ions within the stellar atmosphere (see Kochukhov 2011 and references therein). These atmospheric overabundances are rare-earth elements, such as strontium, europium or chromium, and can be as large as 10^6 times solar values.

roAp Stars

The rapidly oscillating Ap (roAp) stars were first discovered by Kurtz (1982), and represent a subgroup of pulsating A stars that contain many complex aspects of physics. They are located within a small region near the main sequence within the classical instability strip (Cunha 2002), and pulsate with periods between 6 and 23 min (Alentiev et al. 2012), with photometric amplitudes as large as 20 mmag in the B band (Kurtz 1990; Holdsworth et al. 2014b). The exact nature of the pulsational driving mechanism is not known in these stars, but it is thought that the κ mechanism operating in the hydrogen ionisation zone is responsible for the high-overtone roAp pulsations, although this may not be true for all roAp stars (Cunha et al. 2013). The roAp stars are rare, with only around 60 confirmed stars known, which is a few per cent of the known Ap stars (Holdsworth et al. 2014b; Smalley et al. 2015). Similarly to the Ap stars, the roAp stars are rarely found in binary or multiple systems (e.g., Schöller et al. 2012).

The most remarkable property of roAp stars is that they provide the opportunity to study pulsations in the presence of a strong magnetic field within a chemically peculiar star. Even though the roAp stars are located within the classical instability strip (Cunha 2002), they do not pulsate in low-overtone p modes, because the dipolar magnetic field is strong enough to suppress low overtone δ Sct pulsation modes (Saio 2005). In a roAp star, the pulsation axis is nearly aligned with the magnetic field axis, which are misaligned with the rotation axis — this is known as the oblique pulsator

model (Kurtz 1982; Bigot and Dziembowski 2002; Bigot and Kurtz 2011), which allows the pulsations to be viewed from different orientations as the star rotates.

The Lambda Boötis Stars

The λ Boo stars are a rare class of Population I stars between late-B and early-F in spectral type which make up a total of approximately 2% of A stars. They are classified by having underabundant iron-peak elements and approximately solar values of lighter elements, for example carbon, nitrogen and oxygen (Gray and Corbally 2009). A study by Paunzen et al. (2002b) revealed that λ Boo stars are found at all stages of stellar evolution, suggesting that the mechanism that causes the underabundant Fe-peak elements occurs continuously throughout an intermediate-mass star's lifetime.

Most λ Boo stars found within the classical instability strip are on the main sequence or pre-main sequence and are observed to pulsate in p modes (Paunzen et al. 2002a). Therefore, there is no clear distinction between δ Sct stars and λ Boo stars from their observed pulsation mode frequencies, but asteroseismology is able to determine if a star is metal-weak throughout its interior or if the underabundances are limited to the star's atmosphere (e.g., Murphy et al. 2013). It has been suggested that the chemically peculiar nature of λ Boo stars is caused by accretion by a star from the interstellar medium (see Murphy et al. 2015b and references therein). A thorough review and updated catalogue of known λ Boo stars is provided by Murphy et al. (2015b).

1.3.3 Rotation in A Stars

Eponymously named after Robert Kraft, the *Kraft Break* divides the main sequence into slowly rotating low-mass stars and fast-rotating high-mass stars (Kraft 1967), with the boundary occurring at approximately spectral type F5 ($M \simeq 1.3\,\mathrm{M}_{\odot}$). The distribution in the rotational velocities of A stars has been described as bimodal (Abt and Morrell 1995) with two populations of A stars: the fast-rotating chemically normal stars and the slowly rotating chemically peculiar stars. If the chemically peculiar stars are excluded, A and F stars generally lie above the Kraft Break and have rotational velocities that typically lie between $100 < v \sin i < 250\,\mathrm{km\,s^{-1}}$ (Zorec and Royer 2012). The distribution of the fast rotating A stars peaks at A5, with stars at this spectral type rotating at approximately two-thirds of their break-up velocity (Royer et al. 2007).

An extensive study of rotation in A stars was carried out by Zorec and Royer (2012), who demonstrated that the distribution is more complex than simple bimodal populations of slowly rotating chemically peculiar stars and fast-rotating chemically normal stars. The probability density distribution for rotational velocities as a function of stellar mass in the range $1.6 \leq M \leq 3.5\,\mathrm{M}_{\odot}$ taken from Zorec and Royer (2012) is shown in Fig. 1.3. Rotation is extremely important in high- and intermediate-mass stars, as it facilitates the mixing of chemical abundances

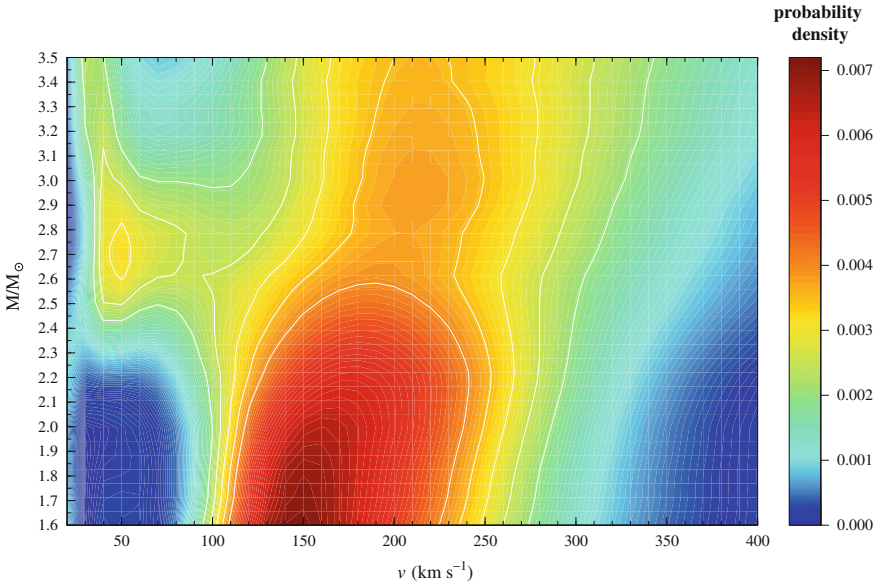

Fig. 1.3 The contour of deprojected rotational velocities of chemically normal A stars excluding binary systems for the stellar mass range of $1.6 \leq M \leq 3.5\,\mathrm{M}_{\odot}$, which corresponds to an approximate spectral type range of F0 to B8, respectively. The fewest stars are found in the *dark blue* regions with a larger number of stars found in the *dark red* regions. Figure from Zorec and Royer (2012), their Fig. 7. © ESO; reproduced with permission from A&A

(Zahn 1992; Talon et al. 1997). The rotational velocities of stars with masses between 1.6 and $2.5\,\mathrm{M}_{\odot}$ – i.e., the A and F stars – only increase by a small amount over their main sequence lifetime (Zorec and Royer 2012). A recent thorough review of rotation among intermediate-mass stars is given by Murphy (2014).

The δ Sct stars are generally considered moderate or fast rotators (Breger 2000a), with rotational velocities that can be as high as $300\,\mathrm{km\,s^{-1}}$ (see e.g., KIC 8054146; Breger et al. 2012). From a high-resolution spectroscopic study of bright *Kepler* A and F stars, Niemczura et al. (2015) determined a mean rotational velocity of $v \sin i \simeq 134\,\mathrm{km\,s^{-1}}$, which supports the view that intermediate-mass stars are generally moderate rotators. However, some δ Sct stars have been confirmed as very slow rotators. For example, the δ Sct star 44 Tau (HD 26322) was determined to have a rotational velocity of $v \sin i = 3 \pm 2\,\mathrm{km\,s^{-1}}$ (Zima et al. 2006), and the δ Sct star KIC 11145123 was determined to have a surface rotation period of approximately 100 d, which can be converted into a rotational velocity of $v_{\mathrm{eq}} \simeq 1\,\mathrm{km\,s^{-1}}$ (Kurtz et al. 2014). Clearly there is a diverse range in rotational velocities among the δ Sct stars, which plays an important role when interpreting their amplitude spectra.

The Effects of Rotation on Pulsation

Discussed by Ledoux (1951) and later by Dziembowski and Goode (1992), Goupil et al. (2000) and Aerts et al. (2010), the rotational splitting of a non-radial mode for the rest frame of an observer is commonly given by

$$\nu_{n\ell m} = \nu_{n\ell 0} + m\,(1 - C_{n\ell})\,\frac{\Omega}{2\pi} + D_{\mathrm{L}}\,\frac{m^2\Omega^2}{2\pi\nu_{n\ell 0}}\,, \tag{1.3}$$

where $\nu_{n\ell m}$ is the observed frequency, $\nu_{n\ell 0}$ is the unperturbed frequency ($m = 0$), Ω is the angular velocity such that $\frac{\Omega}{2\pi}$ is the rotation frequency, $C_{n\ell}$ is the Ledoux constant, and D_{L} is a coefficient that depends on the character of a pulsation mode (Saio 1981; Dziembowski and Goode 1992). The sign convention in Eq. 1.3 follows Aerts et al. (2010), and is chosen such that positive values of m are prograde modes that travel in the direction of rotation, and modes with negative values of m are retrograde modes that travel against the direction of rotation.

Therefore, as shown by Eq. 1.3, rotation lifts the degeneracy of a non-radial pulsation mode into its $2\ell + 1$ components, which are observed as a multiplet in the amplitude spectrum. The splitting among the component frequencies of this multiplet is nearly exact but not perfectly in the cases of moderate and fast rotation because second-order effects act as an additional perturbation to the component frequencies (Goupil et al. 2000; Pamyatnykh 2003). For example, the Coriolis force in a rotating star acts against the direction of rotation and causes predominantly vertical variations to become circular (Aerts et al. 2010). The chosen sign convention in Eq. 1.3 results in prograde modes ($m > 0$) having higher frequencies than the central $m = 0$ component of the multiplet in the rest frame of an observer.

Using the slowly rotating δ Sct star 44 Tau as an example, a rotational splitting of approximately $0.02\,\mathrm{d}^{-1}$ is expected for this star (Breger et al. 2009). For most δ Sct stars, which are moderate and fast rotators, the amplitude spectrum can become forest-like with much larger and asymmetric rotational splittings. This complicates the issue of mode identification and the detection of rotationally split non-radial pulsation modes.

Radial Differential Rotation

In the last two decades, asteroseismology has been used to measure the radial rotation profile of stellar interiors throughout different stages of stellar evolution, from main sequence stars (Aerts et al. 2003; Pamyatnykh et al. 2004; Briquet et al. 2007; Kurtz et al. 2014; Saio et al. 2015; Triana et al. 2015; Murphy et al. 2016; Schmid and Aerts 2016), to subgiant and red giant stars (Beck et al. 2012; Mosser et al. 2012; Deheuvels et al. 2012, 2014, 2015; Di Mauro et al. 2016). The studies of interior rotation in these stars have revealed many interesting and unexpected results. Analyses of the main sequence stars indicate almost uniform rotation, such that they are each rotating approximately as a solid body. Moreover, these main sequence stars are slow rotators for their spectral type, but this is likely a selection effect, as it is easier to identify slowly rotating stars from the smaller rotational splitting in their amplitude spectra.

See Aerts (2015) for a thorough review of interior rotation results obtained using asteroseismology.

Let us take the example of KIC 11145123 studied by Kurtz et al. (2014), which is a hybrid star pulsating in many g- and p-mode frequencies. The amplitude spectrum for KIC 11145123 is shown in Fig. 1.4, which shows a clear distinction in the g- and p-mode frequencies in this star. The authors used Eq. 1.3 to determine a constraint on the core rotation period of $P_{\rm core} \geq 105.13 \pm 0.02$ d using $C_{n\ell} \simeq 0.5$ for the high-overtone g modes, and a constraint on the surface rotation period of $P_{\rm surface} \leq 98.57 \pm 0.02$ d using $C_{n\ell} \simeq 0.03$ for the p modes (Kurtz et al. 2014). Therefore, the surface of this star is rotating slightly, but significantly, faster than the core. To understand a star on the main sequence with only a small gradient in its radial rotation profile, a physical mechanism other than viscosity is required to redistribute angular momentum (Kurtz et al. 2014). What physical mechanism can cause such a rotation profile in a star? Further observations of similar stars are needed to help constrain theoretical models.

The investigation by Blomme et al. (2011) of three O stars observed by the CoRoT mission (Auvergne et al. 2009) found an excess of red noise in their amplitude spectra, which has been recently interpreted in terms of internal gravity waves (IGWs) in these stars (Aerts and Rogers 2015). These IGWs are able to efficiently transport angular momentum throughout a star with a convective core and a radiative envelope (Rogers et al. 2013).

Of the currently known main sequence stars with almost uniform rotation, perhaps the most remarkable is the Slowly Pulsating B (SPB) star KIC 10526294 studied by Triana et al. (2015). The authors studied a series rotationally split dipole modes that were almost equally spaced in period, and asteroseismically modelled the star to determine the radial rotation profile. Their analysis indicated that the stellar envelope was not only rotating slightly faster than the core but was rotating in the opposite direction (Triana et al. 2015). It was shown by Rogers (2015) using numerical models

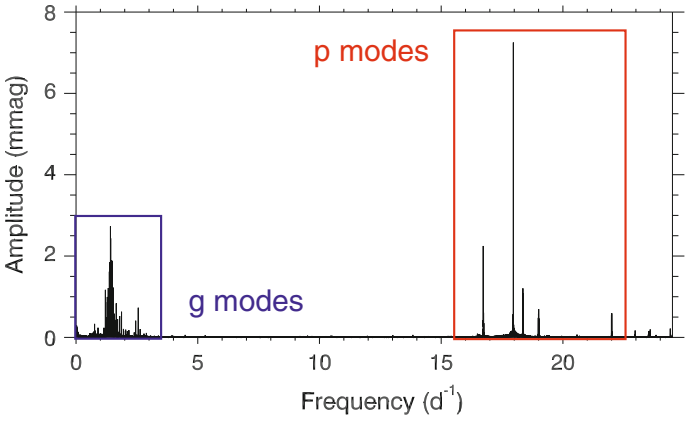

Fig. 1.4 Core-to-surface rotation in KIC 11145123. The distinct g- and p-mode frequency regimes are clearly separated in the amplitude spectrum

that angular momentum transport by convectively-driven IGWs can not only cause uniform rotation in intermediate- and high-mass stars, but also explain counter-rotating cores and envelopes in a star, for example, KIC 10526294 (Triana et al. 2015). The detection, characterisation and interpretation of IGWs in intermediate- and high-mass stars is an exciting prospect for asteroseismology, which is a subject of ongoing research (see e.g., Aerts and Rogers 2015; Aerts et al. 2017).

1.4 Pulsations Across the HR Diagram

As shown by Fig. 1.1, pulsations can occur throughout all stages of stellar evolution, from pre-main sequence to the white dwarf cooling track. However, observations of the pulsation mode frequencies are not enough to fully classify a pulsating star, as other types of pulsators may have similar pulsation periods. Therefore, the fundamental parameters such as mass, effective temperature (or by proxy spectral type or colour) and surface gravity are also needed for a complete definition, so that a star can be placed in the HR diagram. In the current section, a general discussion of different variable stars is provided in the context of amplitude modulation of pulsation modes.

1.4.1 The Gamma Doradus Stars

The gamma Doradus (γ Dor) stars were first considered a unique class of pulsating star about two decades ago (Balona et al. 1994; Kaye et al. 1999). They have similar effective temperatures and luminosities to δ Sct stars and are located on or near the main sequence in the HR diagram (Handler 1999; Uytterhoeven et al. 2011). The γ Dor stars are difficult to study from the ground because their long ($P \simeq 1$ d) pulsation periods are similar to the interval between nightly observations. They also often have a high density of pulsation modes in their amplitude spectra resulting in beat periods of several months to years. Therefore, it is difficult to resolve individual pulsation modes in these stars without long-term continuous observations of order a few years.

With so few γ Dor stars known from ground-based observations, the largest increases in the number of these stars have come from space-based telescopes. For example, Handler (1999) used multicolour Hipparcos photometry to study 70 γ Dor stars, which at the time was an increase in the number of known γ Dor stars by more than a factor of two. Whilst on the ZAMS γ Dor stars lie between $7200 \leq T_{\rm eff} \leq 7700$ K, and between $6900 \leq T_{\rm eff} \leq 7500$ K if they are more evolved (Handler 1999). A more complete sample of pulsating A and F stars was obtained by the *Kepler* Space Telescope, from which Uytterhoeven et al. (2011) found that most γ Dor stars lie between F5 and A7 in spectral type and between $6500 \leq T_{\rm eff} \leq 7800$ K in effective temperature.

Pulsations in γ Dor stars are driven by the flux blocking mechanism, which operates at the base of the surface convection zone (Guzik et al. 2000; Dupret et al. 2004, 2005; Grigahcène et al. 2005). At the boundary between the radiative envelope and the surface convection zone, there is an abrupt change in the dominant mechanism for energy transport. The large opacity gradient at this boundary causes luminosity to be blocked in the radiative zone. The surface convective zone is not able to adapt quickly enough to transport the increased flux causing the luminosity to be periodically blocked (Guzik et al. 2000). The theory of the flux blocking mechanism makes the assumption that fluctuations in convection are negligible throughout the pulsation cycle, because the local convective timescale at the base of the convection zone is similar to, or longer than, the pulsation period (Grigahcène et al. 2005). Thus, only stars with a non-negligible surface convection zone can be unstable from the flux blocking mechanism. Guzik et al. (2000) estimates that the optimum depth of the convection zone as a fraction of the stellar radius should be $\simeq 0.975$, with more substantial convective envelopes creating large enough damping to suppress γ Dor pulsations. Therefore, the flux blocking mechanism is dominant in a narrow transition region between solar-type and δ Sct stars in the HR diagram (Guzik et al. 2000; Dupret et al. 2005).

The buoyancy-driven, high-order non-radial g modes produced by the flux blocking mechanism in γ Dor stars have periods that range between 8 h and 3 d (Kaye et al. 1999; Balona et al. 2011; Uytterhoeven et al. 2011). These high-order g modes follow the asymptotic approximation (Tassoul 1980; Gough 1986), such that g modes of the same degree are equally spaced in period for consecutive radial orders. The observed g modes and the departure from the equal period spacing have allowed the physical conditions deep within the stellar interior, such as chemical mixing (Miglio et al. 2008) and rotation (Bouabid et al. 2013; Van Reeth et al. 2015a, b, 2016), to be probed in many γ Dor stars. Excellent examples of γ Dor stars observed by the *Kepler* Space Telescope to have 'combs' of g modes that are almost equally spaced in period are given by Van Reeth et al. (2015b, 2016). The gradient of the period spacing, ΔP, versus the pulsation period, P, indicates the direction of the pulsation wave relative to the stellar rotation (Bouabid et al. 2011), with the example of KIC 8375138 taken from Van Reeth et al. (2015b) shown in Fig. 1.5. A positive gradient indicates retrograde motion and a negative gradient indicates prograde motion, with the gradient itself indicating the magnitude of the rotation.

On the other hand, many more γ Dor stars do not show regularities in their amplitude spectra consistent with asymptotic g modes that are approximately equally-spaced in period. The γ Dor stars are promising targets to study using asteroseismology with many new and exciting discoveries expected in the near future. Although the focus of this monograph is on amplitude modulation in δ Sct stars, the non-linearity of a selection of γ Dor stars observed by the *Kepler* Space Telescope is discussed in Sect. 6.4.

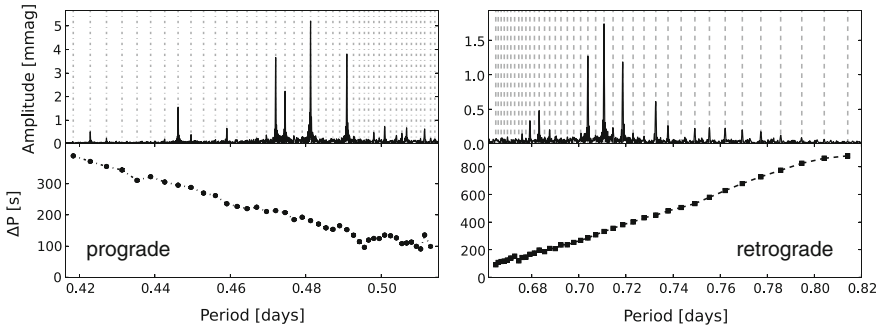

Fig. 1.5 The asymptotic g-mode period spacing patterns in the γ Dor star KIC 8375138. The *top panels* show the amplitude spectrum using 4 yr of LC *Kepler* data. The *bottom-left panel* shows the prograde dipole modes identified as *circles*, and the *bottom-right panel* shows the retrograde dipole modes as *squares*. The *vertical dashed grey lines* are the expected location of the series (or comb) of pulsation mode frequencies. Figure adapted from Van Reeth et al. (2015b), their Fig. 4. © AAS; reproduced with permission from author and AAS

1.4.2 Solar-Type Stars

Helioseismology is the specific application of studying oscillations in our nearest star — the Sun. Pulsations in the Sun are driven by stochastic turbulence in the convective envelope that simultaneously drives and damps the Sun to resonate in its natural oscillation modes (Goldreich and Keeley 1977a, b; Balmforth and Gough 1990), but the κ mechanism has also been shown to play a minor role in mode excitation (Balmforth 1992). Turbulence causes all the eigenmodes within a particular frequency range to be excited, so a roughly Gaussian peak of low-amplitude pulsation modes is observed in the amplitude (power) spectrum. The Gaussian distribution is centred on a particular frequency, which is known as the frequency of maximum amplitude (power) and is denoted $\nu_{\max}$. These stochastically driven oscillations, often called solar-like oscillations, are expected in stars with thick convective envelopes and are predicted to be excited in stars as massive as $1.6\,M_{\odot}$ (Houdek et al. 1999a). In the Sun, the value of $\nu_{\max}$ is approximately 3 mHz ($\simeq 260\,d^{-1}$), with pulsation periods ranging between approximately 3 and 15 min (Aerts et al. 2010).

Since the discovery that the Sun is a pulsating star, helioseismology has been used to study its interior (see e.g., Gough and Toomre 1991 and Christensen-Dalsgaard et al. 1996), including the determination of the depth of the convective envelope to be $0.287 \pm 0.003\,R_{\odot}$ (Christensen-Dalsgaard et al. 1991). Helioseismic inversions of observed pulsation modes in the Sun have also allowed the internal rotation profile for a large fraction of the solar radius to be measured (Schou et al. 1998; Korzennik and Eff-Darwich 2011). The strong rotational shear at the base of the solar convection zone, termed the tachocline by Spiegel and Zahn (1992), is believed to be responsible for the 11-yr Schwabe activity cycle, causing a dynamic solar magnetic field that modulates the frequencies and amplitudes of the solar pulsation modes (Chaplin

et al. 2000, 2011b). Thus, the periodic changes in the frequencies and amplitudes of pulsation modes can be used as a proxy for magnetic activity in the Sun, and possibly other solar-type stars (Chaplin et al. 2011a). This concept has been applied to solar-type stars observed by CoRoT and the *Kepler* Space Telescope (see Régulo et al. 2016).

The p mode pulsations excited from convective turbulence in solar-type stars are high radial order, thus are in the asymptotic regime and are approximately equally spaced in frequency (Tassoul 1980; Gough 1986). The frequency spacing between consecutive radial order modes of the same angular degree, known as the large frequency separation, $\Delta\nu$, creates a comb-like pattern of pulsation modes in the amplitude spectra of stars with solar-like pulsations. Empirical scaling relations from the observables $\Delta\nu$ and $\nu_{\rm max}$ have allowed stellar parameters such as mass and radius to be determined (Kjeldsen and Bedding 1995). The scaling relations have been shown to be very robust with masses and radii of these stars accurate to less than three per cent in the best cases (Chaplin and Miglio 2013). These have been applied to hundreds of solar-type stars (Chaplin et al. 2011b, 2014) and thousands of red giant stars (Stello et al. 2009; Huber et al. 2011), with a thorough review given by Chaplin and Miglio (2013).

1.4.3 Pulsating B Stars

Understanding the physics at work within massive stars ($M \geq 9\,{\rm M}_{\odot}$) is an important goal for asteroseismology as these stars are important in stellar evolution theory. They also play a crucial role in the evolution of galaxies because they are supernovae progenitors that chemically enrich the interstellar medium. It was originally discussed by Maeder and Meynet (2000) how the insight of the internal rotation and possible mixing processes are of vital importance in understanding stellar evolution for high-mass stars. The variety of observed pulsations in massive stars is interesting as the structure of these stars is similar across a wide range of stellar masses and effective temperatures, between the ZAMS and the TAMS (McNamara et al. 2012).

There are two main types of pulsating B star, the β Cep stars that pulsate in p and g modes and the Slowly Pulsating B (SPB) stars that pulsate in g modes (Aerts et al. 2010). The instability regions of these stars overlap in the HR diagram (Miglio et al. 2007; Paxton et al. 2015), thus hybrid stars of both pulsator type are expected and have been observed (e.g., Handler 2009; Degroote et al. 2012). The instability regions for high-mass stars have been investigated using the stellar evolution and

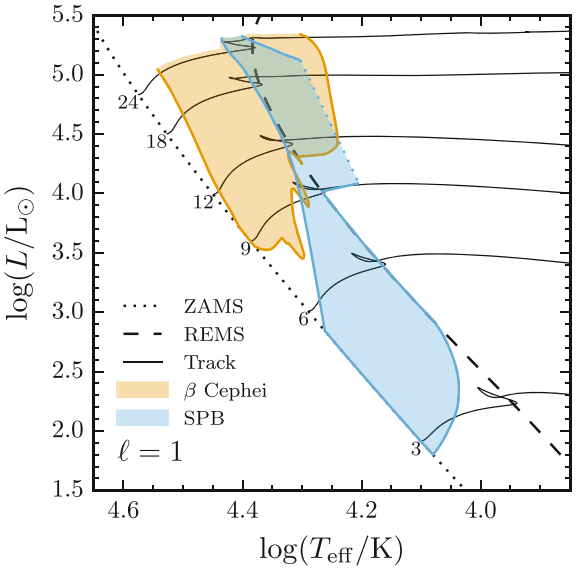

Fig. 1.6 A theoretical HR diagram for the upper main sequence. The instability regions for β Cep and SPB stars calculated using MESA for dipole ($\ell = 1$) modes are shown in *orange* and *blue*, respectively. The zero-age main sequence (ZAMS) and red edge of the main sequence (REMS), are shown as *dotted* and *dashed lines*, respectively, and various evolutionary tracks are shown as *solid black lines* labelled by stellar mass in units of $M_\odot$. Figure from Paxton et al. (2015), their Fig. 11. © AAS; reproduced with permission from author and AAS

modelling code MESA (Paxton et al. 2011, 2013, 2015), and are shown in Fig. 1.6. The MESA models calculated by Paxton et al. (2015) use different opacity tables, OPAL[3] and OP,[4] with the latter shifting the instability regions to higher luminosities, a result also noted by Pamyatnykh (1999) and Miglio et al. (2007). There is also a very clear distinction between the SPB and the δ Sct instability regions, with theoretical models predicting that the κ mechanism is unable to excite pulsations in this gap (Pamyatnykh 1999).

A preliminary analysis of B stars observed by the *Kepler* Space Telescope was conducted by Balona et al. (2011), who found that 15 of 48 B stars were pulsating. A follow-up study was performed by McNamara et al. (2012), who selected all stars observed by *Kepler* with effective temperatures above 10 000 K and within the region on a colour-magnitude diagram that is expected for a B star. This led to a total of 252 B stars, which were classified as β Cep, SPB, or a hybrid (McNamara et al. 2012). There were also subdwarf B and white dwarf stars, and targets that had variability caused by rotation (spots) or binarity included in the sample (McNamara et al. 2012). Further analysis of more than 100 late-B stars observed by *Kepler* was conducted by

[3] Opacity Project at Livermore, for more information see Iglesias and Rogers (1996).

[4] The Opacity Project, for more information see Seaton et al. (1994).

Balona et al. (2015) and extended to early-B stars by Balona (2016), who focussed on the occurrence of low frequency variability in these stars. These low frequencies were often found to be non-periodic and interpreted to be caused by rotational modulation, suggesting that spots generated by magnetic fields can exist in stars with radiative envelopes (Balona et al. 2015; Balona 2016).

Beta Cephei Stars

The β Cep stars are high-mass ($8 \leq M \leq 18\,\mathrm{M}_{\odot}$) Population I stars, pulsating in g and p modes (Stankov and Handler 2005; Aerts et al. 2010). Pulsation modes in β Cep stars are excited by the κ mechanism operating in the Z bump in opacity at $T \simeq 200\,000\,\mathrm{K}$, which causes low-order radial and non-radial p modes with periods between 2 and 8 h to become unstable (Dziembowski and Pamyatnykh 1993). However, this is not a complete explanation of mode excitation in β Cep stars as observations have revealed that these stars also pulsate in g modes with periods of order a few days (Handler et al. 2004; Degroote et al. 2012). To explain the excitation of g modes by the κ mechanism, an overabundance of iron in the driving zone needs to be assumed, which was demonstrated by Pamyatnykh et al. (2004) for the β Cep star ν Eridani, but the exact nature of g-mode excitation in these stars remains unclear.

Slowly Pulsating B Stars

The group of Slowly Pulsating B (SPB) stars was originally defined by Waelkens (1991), with seven Population I B stars with spectral types between B3 and B9. The SPB stars are high-mass stars ($2 \leq M \leq 7\,\mathrm{M}_{\odot}$) with pulsation periods typically between 1 and 3 d, which similarly to γ Dor stars are difficult to study from the ground without long-term multisite observations. It is important to note that without an effective temperature estimate, the time series alone does not distinguish a γ Dor star from a SPB from the similar pulsation mode frequencies.

Pulsations in SPB stars are excited by the κ mechanism operating in the Z bump, which produces high-order low-degree g modes (Dziembowski et al. 1993). A large increase in the number of SPB stars was facilitated by the Hipparcos mission (e.g., Aerts et al. 1999), which allowed pulsation mode properties to be extracted and compared to predictions from theory that these stars pulsate in predominantly dipole g modes (De Cat and Aerts 2002; Townsend 2005; Pápics 2013). More recently, period spacing patterns have been detected and studied in several SPB stars observed by the *Kepler* mission, which has demonstrated that the asymptotic g-mode pulsations in SPB stars can be analysed in a similar way to the γ Dor stars and consequently reveal physical insight of their interiors, such as rotation and mixing (Pápics et al. 2015, 2017).

1.4.4 Evolved Stars

In this section, RR Lyrae stars, Cepheid variables, white dwarfs and sdB stars are discussed in the context of amplitude modulation of their pulsation modes.

RR Lyrae Stars

RR Lyrae (RR Lyr) stars are Population II classical pulsators with masses less than $1\,M_{\odot}$ that are in a post-giant stage of evolution on the horizontal branch (Breger 2000a; Aerts et al. 2010). RR Lyr stars were first classified by Bailey (1902) phenomenologically into subgroups of 'a', 'b' and 'c'. Since then, the 'a' and 'b' subgroups have been consolidated into what are now known as RRab stars, which have non-sinusoidal light curves with the dominant light variations caused by the fundamental radial mode. The 'c' subgroup contains RR Lyr stars which have sinusoidal light curves predominantly caused by the star pulsating in the first-overtone radial mode. The RR Lyr stars have been studied extensively since their discovery (e.g., Preston 1959; Stellingwerf 1975a), with more than 38 000 RR Lyr stars discovered in the bulge of the Milky Way (Soszyński et al. 2014).

RR Lyr stars are not purely periodic and exhibit a quasi-periodic form of amplitude and phase modulation that was first discovered by Blažko (1907), and is today known as the Blazhko effect (TSesevich 1953). The cause of the Blazhko effect in RR Lyr stars remains an unsolved problem but is a well-known example of pulsational non-linearity in asteroseismology. Another characteristic in the pulsation modes in RR Lyr stars is period doubling, which was predicted by Moskalik and Buchler (1990) as half-integer resonances (e.g., 3:2, 9:2) between radial overtones and the fundamental radial mode. In the light curve, period doubling appears as alternating maxima and minima in the brightness of the light excursions, which is shown in the bottom panel of Fig. 1.7. In the amplitude spectrum, period doubling appears as half-integer

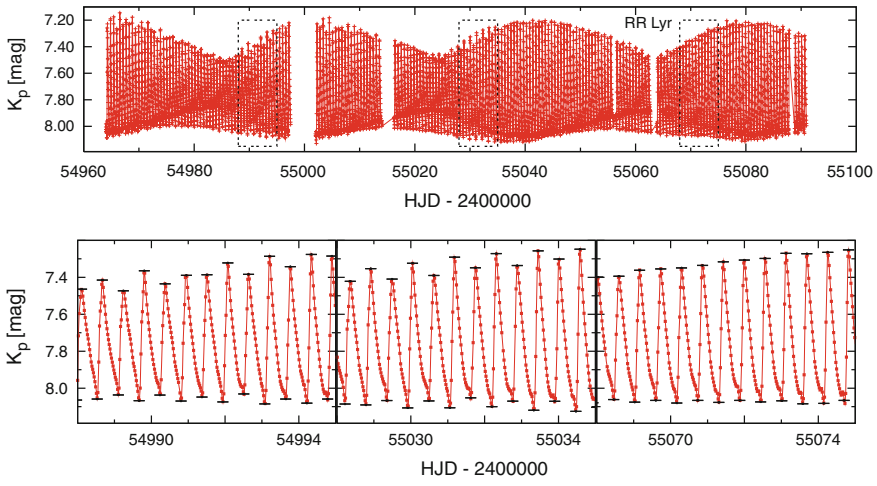

Fig. 1.7 The Blazhko effect and period doubling in RR Lyr (KIC 7198959). The *top panel* shows the long-term quasi-periodic ($P \simeq 40\,\mathrm{d}$) amplitude modulation known as the Blazhko effect in RR Lyr using data from the *Kepler* Space Telescope. The *bottom panel* shows a zoom-in of the three dashed-edge boxes from the panel above, in which the transient period doubling effect can be seen. Figure adapted from Szabó et al. (2010), their Figs. 3 and 4. Reproduced with permission from author and OUP on behalf of MNRAS

frequencies (sub-harmonics) in the form of $f(n + \frac{1}{2})$ where f is the frequency of the period-doubled pulsation mode (Moskalik and Buchler 1990; Kolenberg et al. 2010b; Kolláth et al. 2011). Period doubling is now believed to be ubiquitous in RR Lyr stars, with the first detection made in RR Lyr itself (KIC 7198959) and two other RRab stars observed by the *Kepler* Space Telescope (Kolenberg et al. 2010a; Szabó et al. 2010). A thorough review of period doubling and the Blazhko effect in RR Lyr stars is given by Szabó et al. (2014).

Cepheid Variables

There are two flavours of Cepheid variables, which are referred to as type I and type II Cepheids in the literature. Cepheid variables are stars that are crossing the classical instability strip in the core helium burning stage of stellar evolution, or are stars in a post red giant stage of evolution that are crossing the classical instability strip for a second time (Aerts et al. 2010).

Type I Cepheids are also known as classical Cepheids and are Population I stars, which typically pulsate in the fundamental radial mode and can have amplitudes as large as 1 mag. They are evolved giant or supergiant stars with spectral types between F5 and G5 (Aerts et al. 2010). Typical pulsation periods are between 1 and 50 d, with the longer period Cepheids located in the top-right part of the classical instability strip. Similarly to RRab stars, the light curves of type I Cepheids are non-sinusoidal caused by their high-amplitude and non-linear pulsations, with maximum brightness occurring approximately at the epoch of minimum radial velocity of the stellar surface. Some Cepheids pulsate in the first or second radial overtone in addition to the fundamental radial mode and are known as double-mode Cepheids, so further properties of these star such as mass and radius can be determined from the period ratio of the observed modes (Petersen 1973).

Type II Cepheids are Population II stars, which are crossing the classical instability strip as they transition from the horizontal branch to the asymptotic giant branch. They typically pulsate in the fundamental or first overtone radial mode, with excitation from the κ mechanism operating in the hydrogen and helium ionisation zones (see e.g., Bono et al. 1997). Unlike their type I cousins, type II Cepheids are not a homogenous group of stars, with subgroups defined by the observed pulsation periods: BL Herculis stars pulsate with periods between 1 and 5 d, W Virginis stars pulsate with periods between 10 and 20 d, and RV Tauri stars pulsate with periods longer than 20 d (Aerts et al. 2010). An extensive review of type II Cepheids is given by Wallerstein (2002).

Amplitude modulation has also been observed among Cepheid variables (see e.g., Breger 1981). A study of double-mode Population I Cepheids in the LMC, which pulsate in the first and second overtone radial modes revealed that approximately 19% of these stars exhibited variable pulsation mode amplitudes (Moskalik et al. 2006; Moskalik and Kołaczkowski 2009). This quasi-periodic form of amplitude modulation is similar to the Blazhko effect observed in RR Lyr stars, but typically has a period longer than 700 d. Furthermore, the amplitude modulation of the two radial overtone modes in a Cepheid are always anti-correlated, such that the maxima of one radial mode coincides with the minima of the other (Moskalik and Kołaczkowski 2009). Blazhko models were unable to explain the observations of amplitude modulation in

these double-mode Cepheid variables, and it was proposed that the resonant interaction of radial and non-radial modes may be responsible (Moskalik and Kołaczkowski 2009).

Sub-dwarf B Stars

The subdwarf B (sdB) stars are low luminosity B stars with masses below $0.5\,M_\odot$, effective temperatures between $28\,000 \leq T_{\rm eff} \leq 35\,000$ K and which have weak He I lines in their spectra (Kilkenny 2007; Aerts et al. 2010). The sdB stars are in an unusual stage of stellar evolution having experienced significant mass loss on the red giant branch, which strips the star of its envelope leaving a helium core. The sdB stars are found between the giant branch and the extreme horizontal branch in the HR diagram and they are progenitors of white dwarf stars.

The first sdB star observed to pulsate was EC 14026 with a pulsation period of 144 s and an amplitude of 12 mmag, which was discovered by Kilkenny et al. (1997, 1998). Since their discovery, many variable sdB (sdBV) stars have been observed to pulsate with g, p or mixed modes with periods between 80 and 600 s and amplitudes between 1 and 300 mmag (Kilkenny 2007). The g mode sdBV stars are slightly cooler than the p mode sdBV stars, so these stars are analogous the SPB and β Cep stars, and also the γ Dor and δ Sct stars. Pulsations in sdBV stars are driven by the κ mechanism operating in the Z bump with predominantly low-overtone non-radial p modes of $\ell = 3$ or 4 being excited (Fontaine et al. 2003; Jeffery and Saio 2006a), but g modes of $\ell = 3$ or 4 can also be excited (Jeffery and Saio 2006b). An observational review of variable sdB stars is given by Kilkenny (2007).

Amplitude variations from one observing season to another were first noted for the prototype sdBV star by Kilkenny et al. (1997), and in other sdBV stars since (Kilkenny et al. 2007). Using follow-up observations of a selection of sdBV stars, Kilkenny (2010) re-analysed longer data sets and found that amplitude modulation is common amongst these stars with periods of days to years. However, there were large gaps in the data sets so Kilkenny (2010) cautioned that the observed amplitude variability may be the result of beating of unresolved frequencies and may not have been astrophysical.

White Dwarfs

Practically all stars with masses below $M \lesssim 9\,M_\odot$ will eventually become white dwarf stars, with white dwarf cooling tracks ranging from 200 000 K to cooler than 5000 K. Traditionally, white dwarf stars are categorised spectroscopically into different groups. For example, the DB and DA groups contain white dwarf stars with similar spectral classifications to main sequence B and A stars, respectively — the spectra of DB white dwarfs have few hydrogen lines and are dominated by helium lines, whereas the spectra of DA white dwarfs are dominated by hydrogen lines (Aerts et al. 2010).

The three main groups of white dwarf stars known to pulsate are the variable DO stars (DOV; also known as GW Vir stars), the variable DB stars (DBV; also known as V777 Her stars), and the variable DA stars (DAV; also known as ZZ Cet stars). These groups lie in the effective temperature ranges of $75\,000 \leq T_{\rm eff} \leq 170\,000$ K,

$22\,000 \leq T_{\rm eff} \leq 28\,000$ K and $11\,000 \leq T_{\rm eff} \leq 12\,000$ K, respectively (Fontaine and Brassard 2008). The hottest variable white dwarf stars, the DOV stars, are exclusively low-degree ($\ell < 2$) high-order multiperiodic g mode pulsators; this has allowed asteroseismic studies to constrain rotation periods and inclinations, magnetic field strengths and atmospheric stratification in these stars (Fontaine and Brassard 2008; Winget and Kepler 2008). The pulsations in variable white dwarf stars are thought to be excited from outward radiation being impeded by partial ionisation zones of the main elements contained within the stellar envelope (Fontaine and Brassard 2008; Winget and Kepler 2008), although pulsations in DAV have also sometimes been referred to as convective driving in the literature (Brickhill 1990, 1991a, b). Thorough reviews of pulsating white dwarfs are given by Fontaine and Brassard (2008) and Winget and Kepler (2008).

A fourth and relatively new group of white dwarf stars are the hot DQ stars, which were discovered by Dufour et al. (2007). The hot DQ stars have carbon-dominated atmospheres (Dufour et al. 2007, 2008), with only a few of these stars known to pulsate (Montgomery et al. 2008; Barlow et al. 2008; Dufour et al. 2009). The low-degree g-mode pulsations in variable hot DQ stars (DQV stars) are also thought to be driven by a surface partial-ionisation zone (Fontaine et al. 2008).

Amplitude modulation and non-linearity in the form of harmonics and combination frequencies are well-documented for pulsating white dwarfs (Fontaine and Brassard 2008; Winget and Kepler 2008). For example, combination frequencies in variable white dwarfs were extensively studied by Brickhill (1992) and Wu (2001), who demonstrated mathematically that any variability in parent pulsation modes should be mirrored by similar variability in their combination frequencies. This concept and its application to pulsations in δ Sct and γ Dor stars is discussed further in Chap. 6.

1.5 4 CVn: A Case Study of Amplitude Modulation in a Delta Scuti Star

The variability of the δ Sct star 4 CVn (HD 107904) was first discovered by Jones and Haslam (1966), and the star has been extensively studied since, with 26 independent pulsation mode frequencies and many more combination frequencies discovered (Breger et al. 1990, 1999; Breger 2000b, 2009; Schmid et al. 2014; Breger 2016). This makes it one of the longest-studied δ Sct stars, with observations covering a several decades. Many of the pulsation modes in 4 CVn show frequency and amplitude variations, some of which can be explained by a mode coupling mechanism (Breger 2000b), the beating of two close frequencies (Breger 2009), or have an unknown cause (Breger 2016).

The problems associated with studying amplitude modulation from the ground were epitomised by Breger (2000b) in his study of 4 CVn. Intermittent observations between 1966 and 1997 allowed the amplitudes of pulsation modes to be studied

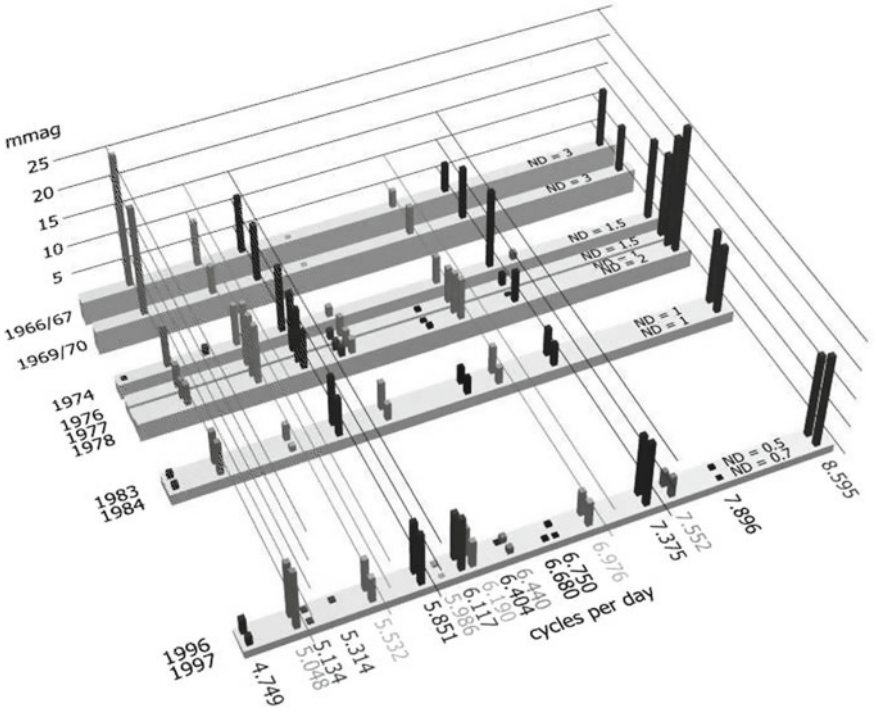

Fig. 1.8 Amplitude modulation in the δ Sct star 4 CVn with observations covering 1966–1997. The noise level of each data set is given by ND in units of mmag, so only peaks with amplitudes above these values are shown. Figure from Breger (2000b), his Fig. 5. Reproduced with permission from author and OUP on behalf of MNRAS

over a long time span, but the large gaps between observation runs and high levels of noise introduced an instrumental bias towards extracting only high amplitude pulsation modes. His results are shown graphically in Fig. 1.8, in which a single p mode at $\nu = 7.375\,\mathrm{d}^{-1}$ decreased in amplitude from 15 mmag in 1974 to 4 mmag in 1976 and to 1 mmag in 1977, after which a phase jump occurred and the mode began increasing in amplitude again (Breger 2000b). Other pulsation modes were found to be coupled to the variable pulsation mode at $\nu = 7.375\,\mathrm{d}^{-1}$, and Breger (2000b) concluded that energy was being transferred between pulsation modes by a mode coupling mechanism. A more exhaustive list of other possible causes of amplitude modulation in the pulsation mode at $\nu = 7.375\,\mathrm{d}^{-1}$ discussed by Breger (2000b) are summarised below.

(i) **Beating**: a simple beating model was indicated by the observed phase change, which suggested that unresolved modes of similar frequency and amplitude were beating against each other. However, the poor quality of the beating model and the lack of a half-cycle phase change, which was required for the beating model, resulted in Breger (2000b) rejecting the beating hypothesis.

(ii) **Mode re-excitation**: multiple pulsation modes, including $\nu = 7.375\,\mathrm{d}^{-1}$, were observed to decay in amplitude and then soon afterwards were re-excited with a random phase. The observed phase change supported the hypothesis of the amplitude modulation being caused by changeable driving or damping in the star (Breger 2000b).

(iii) **Stellar cycle**: the apparent periodic behaviour of the pulsation mode amplitude could be evidence of a stellar activity cycle, as cyclic periodicity in mode amplitude is unlikely to be caused by stellar evolution on time-scales of order a few decades (Breger 2000b).

With more data, Breger (2009) concluded that the observed variability in pulsation mode amplitudes could be fitted with a period of several decades — longer than the current data set for the star. Without observing even a single cycle for this pulsation mode, it was difficult to test the stellar activity cycle hypothesis.

Schmid et al. (2012) obtained spectroscopic data of 4 CVn from the 2.1-m Otto Struve telescope at McDonald observatory in Texas throughout 2010 and 2011. A total of 767 spectra with a signal-to-noise ratio of greater than 200, a resolving power greater than $R = 60\,000$, covering the wavelength range of $4200 < \lambda < 4800$ Å were used to study line profile variations in 4 CVn, with the star discovered to be in a binary system with an orbital period of $P_{\mathrm{orb}} = 124.3$ d (Schmid et al. 2012).

A couple of years later, Schmid et al. (2014) performed a follow-up spectroscopic analysis of 4 CVn, using spectroscopic data collected between 2008 and 2011 from the McDonald observatory. The binarity of 4 CVn was confirmed with the orbital and stellar parameters determined from the spectroscopic analysis by Schmid et al. (2014) given in Table 1.2. The high resolution of the spectroscopy allowed mode identification to be performed, with a resolution of at least $R = 40\,000$ needed to determine the order and degree of a pulsation mode (Aerts et al. 2010). After removing the binary signature, further amplitude and phase variability of order 1 yr remained in pulsation modes (Schmid et al. 2014). A few pulsation modes varied quasi-sinusoidally in amplitude that was explained by the beating of two mode frequencies spaced closer than the frequency resolution (Schmid et al. 2014). However, modes that varied on timescales longer than 1 yr could not be ruled out as single pulsation modes with intrinsic amplitude modulation (Schmid et al. 2014).

Recently, Breger (2016) revisited the analysis of 4 CVn including further photometry taken between 2005–2012, and studied mode coupling in this star. He concluded that the energy associated with variable pulsation modes in 4 CVn was not transferred to any other visible pulsation modes, thus the amplitude modulation in 4 CVn remains an unsolved problem.

Table 1.2 Stellar parameters of the δ Sct 4 CVn from the spectroscopic analysis of Schmid et al. (2014)

P_{orb} (d)	e	T_{eff} (K)	log g (cgs)	[m/H] (dex)	$v_{\mathrm{eq}} \sin i$ (km s^{-1})
124.44 ± 0.03	0.311 ± 0.003	6875 ± 120	3.30 ± 0.35	-0.05 ± 0.15	109 ± 3

4CVn remains one of the longest- and best-studied δ Sct stars from the ground. With the dawn of space telescopes, however, a vast increase in the number and quality of photometric observations of δ Sct stars have allowed amplitude modulation to be investigated in greater detail than is possible from the ground. In this monograph, the results from a statistical study of 983 δ Sct stars that were observed continuously by the *Kepler* Space Telescope for over 4 yr are presented, and specifically the incidence of amplitude modulation in this ensemble of stars (Bowman et al. 2016; Bowman 2016).

References

Abt, H. A. 1961, ApJS, 6, 37
Abt, H. A. 1967, in Magnetic and Related Stars, ed. R. C. Cameron, 173
Abt, H. A. 2009, AJ, 138, 28
Abt, H. A. & Snowden, M. S. 1973, ApJS, 25, 137
Abt, H. A. & Levy, S. G. 1985, ApJS, 59, 229
Abt, H. A. & Morrell, N. I. 1995, ApJS, 99, 135
Aerts, C. 2015, Astronomische Nachrichten, 336, 477
Aerts, C. & Rogers, T. M. 2015, ApJL, 806, L33
Aerts, C., De Cat, P., Peeters, E., et al. 1999, A&A, 343, 872
Aerts, C., Thoul, A., Daszyńska, J., et al. 2003, Science, 300, 1926
Aerts, C., Christensen-Dalsgaard, J., & Kurtz, D. W. 2010, Asteroseismology (Springer)
Aerts, C., Símon-Díaz, S., Bloemen, S., et al. 2017, A&A, 602, A32
Alentiev, D., Kochukhov, O., Ryabchikova, T., et al. 2012, MNRAS, 421, L82
Antoci, V., Handler, G., Campante, T. L., et al. 2011, Nature, 477, 570
Antoci, V., Handler, G., Grundahl, F., et al. 2013, MNRAS, 435, 1563
Antoci, V., Cunha, M., Houdek, G., et al. 2014, ApJ, 796, 118
Aurière, M., Silvester, J., Wade, G. A., et al. 2004, in IAU Symposium, Vol. 224, The A-Star Puzzle, ed. J. Zverko, J. Ziznovsky, S. J. Adelman, & W. W. Weiss, 633–636
Auvergne, M., Bodin, P., Boisnard, L., et al. 2009, A&A, 506, 411
Babcock, H. W. 1960, ApJ, 132, 521
Baglin, A., Breger, M., Chevalier, C., et al. 1973, A&A, 23, 221
Bailey, S. I. 1902, Annals of Harvard College Observatory, 38, 1
Balmforth, N. J. 1992, MNRAS, 255, 603
Balmforth, N. J. & Gough, D. O. 1990, Solar Physics, 128, 161
Balona, L. A. 2016, MNRAS, 457, 3724
Balona, L. A. & Dziembowski, W. A. 2011, MNRAS, 417, 591
Balona, L. A. & Nemec, J. M. 2012, MNRAS, 426, 2413
Balona, L. A., Krisciunas, K., & Cousins, A. W. J. 1994, MNRAS, 270, 905
Balona, L. A., Guzik, J. A., Uytterhoeven, K., et al. 2011, MNRAS, 415, 3531
Balona, L. A., Pigulski, A., Cat, P. D., et al. 2011, MNRAS, 413, 2403
Balona, L. A., Baran, A. S., Daszyńska-Daszkiewicz, J., & De Cat, P. 2015, MNRAS, 451, 1445
Barlow, B. N., Dunlap, B. H., Rosen, R., & Clemens, J. C. 2008, ApJL, 688, L95
Beck, P. G., Montalban, J., Kallinger, T., et al. 2012, Nature, 481, 55
Bedding, T. R., Mosser, B., Huber, D., et al. 2011, Nature, 471, 608
Bessell, M. S. 1979, PASP, 91, 589
Bigot, L. & Dziembowski, W. A. 2002, A&A, 391, 235
Bigot, L. & Kurtz, D. W. 2011, A&A, 536, A73
Blažko, S. 1907, Astronomische Nachrichten, 175, 325

Blomme, R., Mahy, L., Catala, C., et al. 2011, A&A, 533, A4
Bono, G., Caputo, F., & Santolamazza, P. 1997, A&A, 317, 171
Borucki, W. J., Koch, D., Basri, G., et al. 2010, Science, 327, 977
Bouabid, M.-P., Montalbán, J., Miglio, A., et al. 2011, A&A, 531, A145
Bouabid, M.-P., Dupret, M.-A., Salmon, S., et al. 2013, MNRAS, 429, 2500
Bowman, D. M. 2016, PhD thesis, Jeremiah Horrocks Institute, University of Central Lancashire, UK
Bowman, D. M., Kurtz, D. W., Breger, M., Murphy, S. J., & Holdsworth, D. L. 2016, MNRAS, 460, 1970
Breger, M. 1970, ApJ, 162, 597
Breger, M. 1979, PASP, 91, 5
Breger, M. 1981, ApJ, 249, 666
Breger, M. 1990, Delta Scuti Star Newsletter, 2, 13
Breger, M. 2000a, in Astronomical Society of the Pacific Conference Series, Vol. 210, Delta Scuti and Related Stars, ed. M. Breger & M. Montgomery, 3
Breger, M. 2000b, MNRAS, 313, 129
Breger, M. 2009, in American Institute of Physics Conference Series, Vol. 1170, Stellar Pulsation: Challenges for theory and observation, ed. J. A. Guzik & P. A. Bradley (American Institute of Physics Conference Series), 410–414
Breger, M. 2016, A&A, 592, A97
Breger, M. & Bregman, J. N. 1975, ApJ, 200, 343
Breger, M. & Pamyatnykh, A. A. 2006, MNRAS, 368, 571
Breger, M., McNamara, B. J., Kerschbaum, F., et al. 1990, A&A, 231, 56
Breger, M., Handler, G., Garrido, R., et al. 1999, A&A, 349, 225
Breger, M., Lenz, P., & Pamyatnykh, A. A. 2009, MNRAS, 396, 291
Breger, M., Fossati, L., Balona, L., et al. 2012, ApJ, 759, 62
Brickhill, A. J. 1990, MNRAS, 246, 510
Brickhill, A. J. 1991a, MNRAS, 251, 673
Brickhill, A. J. 1991b, MNRAS, 252, 334
Brickhill, A. J. 1992, MNRAS, 259, 519
Briquet, M., Morel, T., Thoul, A., et al. 2007, MNRAS, 381, 1482
Campbell, W. W. & Wright, W. H. 1900, ApJ, 12, 254
Chaplin, W. J. & Miglio, A. 2013, ARA&A, 51, 353
Chaplin, W. J., Elsworth, Y., Isaak, G. R., Miller, B. A., & New, R. 2000, MNRAS, 313, 32
Chaplin, W. J., Elsworth, Y., Miller, B. A., Verner, G. A., & New, R. 2007, ApJ, 659, 1749
Chaplin, W. J., Bedding, T. R., Bonanno, A., et al. 2011a, ApJL, 732, L5
Chaplin, W. J., Kjeldsen, H., Christensen-Dalsgaard, J., et al. 2011b, Science, 332, 213
Chaplin, W. J., Basu, S., Huber, D., et al. 2014, ApJS, 210, 1
Chevalier, C. 1971, A&A, 14, 24
Christensen-Dalsgaard, J. 2000, in Astronomical Society of the Pacific Conference Series, Vol. 210, Delta Scuti and Related Stars, ed. M. Breger & M. Montgomery, 187
Christensen-Dalsgaard, J., Gough, D. O., & Thompson, M. J. 1991, ApJ, 378, 413
Christensen-Dalsgaard, J., Dappen, W., Ajukov, S. V., et al. 1996, Science, 272, 1286
Colacevich, A. 1935, Lick Observatory Bulletin, 17, 171
Conti, P. S. 1970, PASP, 82, 781
Cowley, A., Cowley, C., Jaschek, M., & Jaschek, C. 1969, AJ, 74, 375
Cox, J. P. 1963, ApJ, 138, 487
Cox, J. P., King, D. S., & Stellingwerf, R. F. 1972, ApJ, 171, 93
Cunha, M. S. 2002, MNRAS, 333, 47
Cunha, M. S., Aerts, C., Christensen-Dalsgaard, J., et al. 2007, Astronomy & Astrophysics Reviews, 14, 217
Cunha, M. S., Alentiev, D., Brandão, I. M., & Perraut, K. 2013, MNRAS, 436, 1639
De Cat, P. & Aerts, C. 2002, A&A, 393, 965

Degroote, P., Aerts, C., Michel, E., et al. 2012, A&A, 542, A88
Deheuvels, S., García, R. A., Chaplin, W. J., et al. 2012, ApJ, 756, 19
Deheuvels, S., Doğan, G., Goupil, M. J., et al. 2014, A&A, 564, A27
Deheuvels, S., Ballot, J., Beck, P. G., et al. 2015, A&A, 580, A96
Di Mauro, M. P., Ventura, R., Cardini, D., et al. 2016, ApJ, 817, 65
Duchêne, G. & Kraus, A. 2013, ARA&A, 51, 269
Dufour, P., Liebert, J., Fontaine, G., & Behara, N. 2007, Nature, 450, 522
Dufour, P., Fontaine, G., Liebert, J., Schmidt, G. D., & Behara, N. 2008, ApJ, 683, 978
Dufour, P., Green, E. M., Fontaine, G., et al. 2009, ApJ, 703, 240
Dupret, M. A., Grigahcène, A., Garrido, R., Gabriel, M., & Scuflaire, R. 2004, A&A, 414, L17
Dupret, M. A., Grigahcène, A., Garrido, R., Gabriel, M., & Scuflaire, R. 2005, A&A, 435, 927
Dziembowski, W. 1977, Acta Astronomica, 27, 95
Dziembowski, W. 1982, Acta Astronomica, 32, 147
Dziembowski, W. & Krolikowska, M. 1990, Acta Astronomica, 40, 19
Dziembowski, W. A. & Goode, P. R. 1992, ApJ, 394, 670
Dziembowski, W. A. & Pamyatnykh, A. A. 1993, MNRAS, 262, 204
Dziembowski, W. A., Moskalik, P., & Pamyatnykh, A. A. 1993, MNRAS, 265, 588
Dziembowski, W. A., Goode, P. R., Pamyatnykh, A. A., & Sienkiewicz, R. 1995, in Astronomical Society of the Pacific Conference Series, Vol. 76, GONG 1994. Helio- and Astro-Seismology from the Earth and Space, ed. R. K. Ulrich, E. J. Rhodes, Jr., & W. Dappen, 124
Eddington, A. S. 1917, The Observatory, 40, 290
Eddington, A. S. 1926, The Internal Constitution of the Stars (Cambridge University Press)
Eggen, O. J. 1956, PASP, 68, 238
Eggen, O. J. 1976, PASP, 88, 402
Eggen, O. J. & Iben, Jr., I. 1989, AJ, 97, 431
Fath, E. A. 1935, Lick Observatory Bulletin, 17, 175
Fitzgerald, M. P. 1970, A&A, 4, 234
Fontaine, G. & Brassard, P. 2008, PASP, 120, 1043
Fontaine, G., Brassard, P., Charpinet, S., et al. 2003, ApJ, 597, 518
Fontaine, G., Brassard, P., & Dufour, P. 2008, A&A, 483, L1
Frolov, M. S. & Irkaev, B. N. 1984, Information Bulletin on Variable Stars, 2462
Goldreich, P. & Keeley, D. A. 1977a, ApJ, 211, 934
Goldreich, P. & Keeley, D. A. 1977b, ApJ, 212, 243
Gough, D. & Toomre, J. 1991, ARA&A, 29, 627
Gough, D. O. 1977, ApJ, 214, 196
Gough, D. O. 1986, in Hydrodynamic and Magnetodynamic Problems in the Sun and Stars, ed. Y. Osaki, 117
Goupil, M.-J., Dziembowski, W. A., Pamyatnykh, A. A., & Talon, S. 2000, in Astronomical Society of the Pacific Conference Series, Vol. 210, Delta Scuti and Related Stars, ed. M. Breger & M. Montgomery, 267
Gray, D. F. 2005, The Observation and Analysis of Stellar Photospheres, 3rd edn. (Cambridge University Press)
Gray, R. O. & Corbally, J. C. 2009, Stellar Spectral Classification (Princeton Series in Astrophysics)
Grigahcène, A., Dupret, M.-A., Gabriel, M., Garrido, R., & Scuflaire, R. 2005, A&A, 434, 1055
Grigahcène, A., Antoci, V., Balona, L., et al. 2010, ApJL, 713, L192
Guzik, J. A., Kaye, A. B., Bradley, P. A., Cox, A. N., & Neuforge, C. 2000, ApJL, 542, L57
Handler, G. 1999, MNRAS, 309, L19
Handler, G. 2009, MNRAS, 398, 1339
Handler, G., Shobbrook, R. R., Jerzykiewicz, M., et al. 2004, MNRAS, 347, 454
Holdsworth, D. L., Smalley, B., Gillon, M., et al. 2014a, MNRAS, 439, 2078
Holdsworth, D. L., Smalley, B., Kurtz, D. W., et al. 2014b, MNRAS, 443, 2049
Houdek, G. 2000, in Astronomical Society of the Pacific Conference Series, Vol. 210, Delta Scuti and Related Stars, ed. M. Breger & M. Montgomery, 454

Houdek, G. & Dupret, M.-A. 2015, Living Reviews in Solar Physics, 12
Houdek, G., Balmforth, N. J., Christensen-Dalsgaard, J., & Gough, D. O. 1999a, A&A, 351, 582
Houdek, G., Balmforth, N. J., Christensen-Dalsgaard, J., & Gough, D. O. 1999b, in Astronomical Society of the Pacific Conference Series, Vol. 173, Stellar Structure: Theory and Test of Connective Energy Transport, ed. A. Gimenez, E. F. Guinan, & B. Montesinos, 317
Huber, D., Bedding, T. R., Stello, D., et al. 2011, ApJ, 743, 143
Iglesias, C. A. & Rogers, F. J. 1996, ApJ, 464, 943
Jeffery, C. S. & Saio, H. 2006a, MNRAS, 371, 659
Jeffery, C. S. & Saio, H. 2006b, MNRAS, 372, L48
Jones, D. H. P. & Haslam, C. M. 1966, The Observatory, 86, 34
Kaye, A. B., Handler, G., Krisciunas, K., Poretti, E., & Zerbi, F. M. 1999, PASP, 111, 840
Kennelly, E. J., Brown, T. M., Kotak, R., et al. 1998, ApJ, 495, 440
Kilkenny, D. 2007, Communications in Asteroseismology, 150, 234
Kilkenny, D. 2010, Ap&SS, 329, 175
Kilkenny, D., Koen, C., O'Donoghue, D., & Stobie, R. S. 1997, MNRAS, 285, 640
Kilkenny, D., O'Donoghue, D., Koen, C., Lynas-Gray, A. E., & van Wyk, F. 1998, MNRAS, 296, 329
Kilkenny, D., Copley, C., Zietsman, E., & Worters, H. 2007, MNRAS, 375, 1325
Kjeldsen, H. & Bedding, T. R. 1995, A&A, 293, 87
Kochukhov, O. 2011, in IAU Symposium, Vol. 273, Physics of Sun and Star Spots, ed. D. Prasad Choudhary & K. G. Strassmeier, 249–255
Kolenberg, K., Fossati, L., Shulyak, D., et al. 2010a, A&A, 519, A64
Kolenberg, K., Szabó, R., Kurtz, D. W., et al. 2010b, ApJL, 713, L198
Kolláth, Z., Molnár, L., & Szabó, R. 2011, MNRAS, 414, 1111
Korzennik, S. G. & Eff-Darwich, A. 2011, Journal of Physics Conference Series, 271, 012067
Kraft, R. P. 1967, ApJ, 150, 551
Kurtz, D. W. 1976, ApJS, 32, 651
Kurtz, D. W. 1978, ApJ, 221, 869
Kurtz, D. W. 1982, MNRAS, 200, 807
Kurtz, D. W. 1989, MNRAS, 238, 1077
Kurtz, D. W. 1990, ARA&A, 28, 607
Kurtz, D. W. 2000, in Astronomical Society of the Pacific Conference Series, Vol. 210, Delta Scuti and Related Stars, ed. M. Breger & M. Montgomery, 287
Kurtz, D. W., Saio, H., Takata, M., et al. 2014, MNRAS, 444, 102
Ledoux, P. 1951, ApJ, 114, 373
Lee, Y.-H., Kim, S. S., Shin, J., Lee, J., & Jin, H. 2008, PASJ, 60, 551
Maeder, A. & Meynet, G. 2000, ARA&A, 38, 143
Mathys, G. 2015, in Astronomical Society of the Pacific Conference Series, Vol. 494, Physics and Evolution of Magnetic and Related Stars, ed. Y. Y. Balega, I. I. Romanyuk, & D. O. Kudryavtsev, 3
McNamara, B. J., Jackiewicz, J., & McKeever, J. 2012, AJ, 143, 101
McNamara, D. H. 2000, in Astronomical Society of the Pacific Conference Series, Vol. 210, Delta Scuti and Related Stars, ed. M. Breger & M. Montgomery, 373
Miglio, A., Montalbán, J., & Dupret, M.-A. 2007, MNRAS, 375, L21
Miglio, A., Montalbán, J., Noels, A., & Eggenberger, P. 2008, MNRAS, 386, 1487
Moe, M. & Di Stefano, R. 2017, Mind Your Ps and Qs: The Interrelation between Period (P) and Mass-ratio (Q) Distributions of Binary Stars, APJS, 230, 15
Montgomery, M. H., Williams, K. A., Winget, D. E., et al. 2008, ApJL, 678, L51
Moskalik, P. & Buchler, J. R. 1990, ApJ, 355, 590
Moskalik, P. & Kołaczkowski, Z. 2009, MNRAS, 394, 1649
Moskalik, P., Kołaczkowski, Z., & Mizerski, T. 2006, Memorie della Societ Astronomia Italiana, 77, 563
Mosser, B., Goupil, M. J., Belkacem, K., et al. 2012, A&A, 548, A10

Murphy, S. J. 2014, PhD thesis, Jeremiah Horrocks Institute, University of Central Lancashire, UK
Murphy, S. J., Pigulski, A., Kurtz, D. W., et al. 2013, MNRAS, 432, 2284
Murphy, S. J., Bedding, T. R., Niemczura, E., Kurtz, D. W., & Smalley, B. 2015a, MNRAS, 447, 3948
Murphy, S. J., Corbally, C. J., Gray, R. O., et al. 2015b, PASA, 32, e036
Murphy, S. J., Fossati, L., Bedding, T. R., et al. 2016, MNRAS, 459, 1201
Nemec, J. & Mateo, M. 1990, in Astronomical Society of the Pacific Conference Series, Vol. 11, Confrontation Between Stellar Pulsation and Evolution, ed. C. Cacciari & G. Clementini, 64–84
Niemczura, E., Murphy, S. J., Smalley, B., et al. 2015, MNRAS, 450, 2764
Nowakowski, R. M. 2005, Acta Astronomica, 55, 1
Olech, A., Dziembowski, W. A., Pamyatnykh, A. A., et al. 2005, MNRAS, 363, 40
Osaki, J. 1975, PASJ, 27, 237
Pamyatnykh, A. A. 1999, Acta Astronomica, 49, 119
Pamyatnykh, A. A. 2000, in Astronomical Society of the Pacific Conference Series, Vol. 210, Delta Scuti and Related Stars, ed. M. Breger & M. Montgomery, 215
Pamyatnykh, A. A. 2003, Ap&SS, 284, 97
Pamyatnykh, A. A., Handler, G., & Dziembowski, W. A. 2004, MNRAS, 350, 1022
Paparó, M., Benkő, J. M., Hareter, M., & Guzik, J. A. 2016a, ApJ, 822, 100
Paparó, M., Benkő, J. M., Hareter, M., & Guzik, J. A. 2016b, ApJS, 224, 41
Pápics, P. I. 2013, PhD thesis, Instituut voor Sterrenkunde, KU Leuven, Celestijnenlaan 200D, B-3001 Leuven, Belgium
Pápics, P. I., Tkachenko, A., Aerts, C., et al. 2015, ApJL, 803, L25
Pápics, P. I., Tkachenko, A., Van Reeth, T., et al. 2017, A&A, 598, A74
Paunzen, E., Handler, G., Weiss, W. W., et al. 2002a, A&A, 392, 515
Paunzen, E., Iliev, I. K., Kamp, I., & Barzova, I. S. 2002b, MNRAS, 336, 1030
Paxton, B., Bildsten, L., Dotter, A., et al. 2011, ApJS, 192, 3
Paxton, B., Cantiello, M., Arras, P., et al. 2013, ApJS, 208, 4
Paxton, B., Marchant, P., Schwab, J., et al. 2015, ApJS, 220, 15
Petersen, J. O. 1973, A&A, 27, 89
Petersen, J. O. & Christensen-Dalsgaard, J. 1996, A&A, 312, 463
Poleski, R., Soszyński, I., Udalski, A., et al. 2010, Acta Astronomica, 60, 1
Preston, G. W. 1959, ApJ, 130, 507
Régulo, C., García, R. A., & Ballot, J. 2016, A&A, 589, A103
Richer, J., Michaud, G., & Turcotte, S. 2000, ApJ, 529, 338
Rodríguez, E. & Breger, M. 2001, A&A, 366, 178
Rodríguez, E., López-González, M. J., & López de Coca, P. 2000, A&AS, 144, 469
Rogers, T. M. 2015, ApJL, 815, L30
Rogers, T. M., Lin, D. N. C., McElwaine, J. N., & Lau, H. H. B. 2013, ApJ, 772, 21
Royer, F., Zorec, J., & Gómez, A. E. 2007, A&A, 463, 671
Saio, H. 1981, ApJ, 244, 299
Saio, H. 2005, MNRAS, 360, 1022
Saio, H. & Cox, J. P. 1980, ApJ, 236, 549
Saio, H., Kurtz, D. W., Takata, M., et al. 2015, MNRAS, 447, 3264
Samadi, R., Goupil, M.-J., & Houdek, G. 2002, A&A, 395, 563
Schmid, V. S. & Aerts, C. 2016, A&A, 592, A116
Schmid, V. S., Themessl, N., Breger, M., et al. 2012, Astronomische Nachrichten, 333, 1080
Schmid, V. S., Themeßl, N., Breger, M., et al. 2014, A&A, 570, A33
Schöller, M., Correia, S., Hubrig, S., & Kurtz, D. W. 2012, A&A, 545, A38
Schou, J., Antia, H. M., Basu, S., et al. 1998, ApJ, 505, 390
Seaton, M. J., Yan, Y., Mihalas, D., & Pradhan, A. K. 1994, MNRAS, 266, 805
Slettebak, A. 1954, ApJ, 119, 146
Slettebak, A. 1955, ApJ, 121, 653
Smalley, B., Kurtz, D. W., Smith, A. M. S., et al. 2011, A&A, 535, A3

Smalley, B., Southworth, J., Pintado, O. I., et al. 2014, A&A, 564, A69
Smalley, B., Niemczura, E., Murphy, S. J., et al. 2015, MNRAS, 452, 3334
Smalley, B., Antoci, V., Holdsworth, D. L., et al. 2017, MNRAS, 465, 2662
Smith, M. A. 1971a, A&A, 11, 325
Smith, M. A. 1971b, AJ, 76, 896
Smith, M. A. 1973, ApJS, 25, 277
Soszyński, I., Poleski, R., Udalski, A., et al. 2008, Acta Astronomica, 58, 163
Soszyński, I., Udalski, A., Szymański, M. K., et al. 2014, Acta Astronomica, 64, 177
Spiegel, E. A. & Zahn, J.-P. 1992, A&A, 265, 106
Stankov, A. & Handler, G. 2005, ApJS, 158, 193
Stellingwerf, R. F. 1975a, ApJ, 195, 441
Stellingwerf, R. F. 1975b, ApJ, 199, 705
Stellingwerf, R. F. 1979, ApJ, 227, 935
Stellingwerf, R. F. 1980, in Lecture Notes in Physics, Berlin Springer Verlag, Vol. 125, Nonradial and Nonlinear Stellar Pulsation, ed. H. A. Hill & W. A. Dziembowski, 50–54
Stello, D., Chaplin, W. J., Basu, S., Elsworth, Y., & Bedding, T. R. 2009, MNRAS, 400, L80
Stępień, K. 2000, A&A, 353, 227
Stibbs, D. W. N. 1950, MNRAS, 110, 395
Szabó, R., Kolláth, Z., Molnár, L., et al. 2010, MNRAS, 409, 1244
Szabó, R., Benkő, J. M., Paparó, M., et al. 2014, A&A, 570, A100
Talon, S., Zahn, J.-P., Maeder, A., & Meynet, G. 1997, A&A, 322, 209
Tassoul, M. 1980, ApJS, 43, 469
Théado, S., Vauclair, S., Alecian, G., & LeBlanc, F. 2009, ApJ, 704, 1262
Titus, J. & Morgan, W. W. 1940, ApJ, 92, 256
Townsend, R. H. D. 2005, MNRAS, 360, 465
Triana, S. A., Moravveji, E., Pápics, P. I., et al. 2015, ApJ, 810, 16
TSesevich, V. P. 1953, Trudy Gosudarstvennogo Astronomicheskogo Instituta, 23, 62
Turcotte, S., Richer, J., Michaud, G., & Christensen-Dalsgaard, J. 2000, A&A, 360, 603
Uytterhoeven, K., Moya, A., Grigahcène, A., et al. 2011, A&A, 534, A125
Van Reeth, T., Tkachenko, A., Aerts, C., et al. 2015a, A&A, 574, A17
Van Reeth, T., Tkachenko, A., Aerts, C., et al. 2015b, ApJS, 218, 27
Van Reeth, T., Tkachenko, A., & Aerts, C. 2016, A&A, 593, A120
Waelkens, C. 1991, A&A, 246, 453
Wallerstein, G. 2002, PASP, 114, 689
Winget, D. E. & Kepler, S. O. 2008, ARA&A, 46, 157
Wolff, S. C. 1968, PASP, 80, 281
Wu, Y. 2001, MNRAS, 323, 248
Zahn, J.-P. 1992, A&A, 265, 115
Zima, W., Wright, D., Bentley, J., et al. 2006, A&A, 455, 235
Zorec, J. & Royer, F. 2012, A&A, 537, A120

Chapter 2
The *Kepler* Space Photometry Revolution

2.1 Introductory Remarks

In the last few decades, the field of asteroseismology has rapidly expanded and become a widely-known area within astronomy, primarily because of the launch of space-based telescopes. The MOST (Walker et al. 2003) and CoRoT (Auvergne et al. 2009) missions provided a wealth of data on a variety of pulsating stars and paved the way for the more recent *Kepler*Space Telescope (Borucki et al. 2010). These space missions were overwhelmingly successful for asteroseismology and their data remain of great use to this day. Consequently, the decade between the launch of the MOST telescope and the end of the *Kepler*mission has become known as the start of the *Space Photometry Revolution*.[1] An argument can certainly be made that the biggest advances in asteroseismology have been for stars with solar-like oscillations, especially in red giant stars, with $\sim$14 000 being observed by *Kepler*alone (Chaplin and Miglio 2013). Even though asteroseismology of δ Sct stars was possible from the ground, our understanding of these stars has also undoubtedly improved from high-quality space photometry.

This chapter provides an overview of the *Kepler*Space Telescope and its data in Sect. 2.2, with the specifics of Fourier analysis of stellar time series discussed in Sect. 2.3. Section 2.4 contains an overview of how a series of *Kepler*data catalogues were created, which formed the basis of many research projects within the thesis by Bowman (2016).

[1]This was the title of the CoRoT-3/KASC7 conference held in 2014: http://corot3-kasc7.sciencesconf.org. The conference proceedings for a poster by Bowman and Kurtz (2015) were published in the European Physical Journal Web of Conferences (EPJWC) from this conference.

D.M. Bowman, *Amplitude Modulation of Pulsation Modes in Delta Scuti Stars*,
Springer Theses, DOI 10.1007/978-3-319-66649-5_2

2.2 The *Kepler* Space Telescope

The *Kepler*Space Telescope was launched on 7 March 2009 and positioned into a 372.5-d Earth-trailing orbit (Borucki et al. 2010). The field of view covered approximately 115 deg^2 in the constellations of Cygnus and Lyra, within which *Kepler*observed approximately 200 000 stars at an unprecedented photometric precision of a few μmag (Koch et al. 2010). The field of view was chosen with the CCD array positioned so that the brightest stars were in the gaps between CCD modules, with most stars having apparent magnitudes in the *Kepler*passband between $10 \leq \mathrm{Kp} \leq 14$ mag. The primary goal of *Kepler*was to locate Earth-like planets in the habitable zone of their host star using the transit method (Borucki et al. 2010), but these data have also been extremely useful to asteroseismology.

To date, the *Kepler*mission has obtained transit signals for approximately 4500 candidate exoplanets (Borucki et al. 2011), of which about 3500 have been observed using follow-up spectroscopy and confirmed as exoplanets.[2] On the other hand, an argument can be made that *Kepler*was more successful for stellar astronomy with more discoveries and advances made in asteroseismology than exoplanet science. *Kepler*has validated theoretical predictions and made many new and unexpected discoveries. For example, approximately 2900 eclipsing binary systems[3] were observed by *Kepler*(Prša et al. 2011), which allowed the theoretical prediction of tidally induced pulsations made by Kumar et al. (1995) to be tested. Tidal pulsations were first observed in stars in eccentric binary systems using *Kepler*data, creating a group of stars known colloquially as *'Heartbeat stars'*, because of the characteristic shapes of their light curves resembling an echocardiogram (Thompson et al. 2012; Hambleton et al. 2013; Hambleton 2016).

2.2.1 Kepler Instrumentation

The design of the *Kepler*instrument maximises the search for exoplanets orbiting solar-type stars, hence the wavelength response peaks at ∼6000 Å. The wavelength response function for the *Kepler*telescope is plotted in Fig. 2.1 with Johnson filters from Johnson and Morgan (1953) also plotted for comparison (for an extensive review of standard photometric techniques, see Bessell 2005). Using Wien's law, the peak in the *Kepler*response function corresponds to the λ_{max} for a star with an effective temperature of approximately $T_{\mathrm{eff}} \simeq 5000$ K. Therefore, *Kepler*is optimised for studying F, G and K stars. Consequently, *Kepler*observations of oscillations in A stars are suppressed in amplitude from the instrument's passband, but can be corrected

[2] An up-to-date catalogue is available at: http://exoplanetarchive.ipac.caltech.edu.

[3] An up-to-date catalogue is available at: http://keplerebs.villanova.edu.

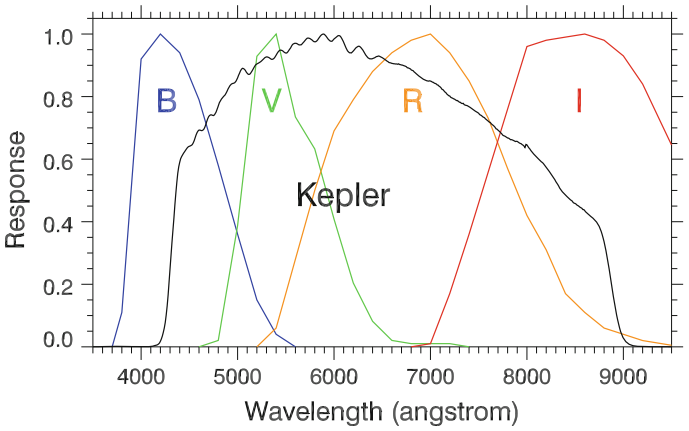

Fig. 2.1 The normalised wavelength response function for the *Kepler*instrument is plotted as the *solid black line* and Johnson B, V, R and I filters taken from Johnson and Morgan (1953) are shown as *coloured solid lines* for comparison

by comparison to other observations (Bowman et al. 2015). This is demonstrated for the δ Sct star KIC 7106205 in Chap. 3.

One of the disadvantages to consider when using broad-band photometry is the restriction of mode visibility. Observations from space telescopes such as *Kepler*are often only sensitive to detecting low-degree ($\ell \leq 2$) pulsation modes, because the amplitudes of high-degree modes are only excited to small amplitudes (Balona and Dziembowski 1999), and because of geometrical cancellation effects (Dziembowski 1977).

2.2.2 *Kepler* Data Characteristics

*Kepler*data are available in long and short cadence (hereafter called LC and SC, respectively), which were created from multiple 6.02-s exposures, each with 0.52-s readout times (Gilliland et al. 2010). The LC data comprised 270 exposures creating a total integration time of 29.45 min, which allowed approximately 170 000 simultaneous observations (Jenkins et al. 2010). The SC data comprised nine exposures creating a total integration time of 58.5 s, which was chosen to increase the temporal resolution, thus increase the number of data points per exoplanet transit of a star. From the limited amount of data storage on board the spacecraft, only 512 stars were observed with SC at any one time (Gilliland et al. 2010). To demonstrate the difference in temporal resolution between LC and SC data, the light curves spanning 1 d of the δ Sct star KIC 71060205 using LC and SC data are shown as blue diamonds and red circles, respectively, in Fig. 2.2.

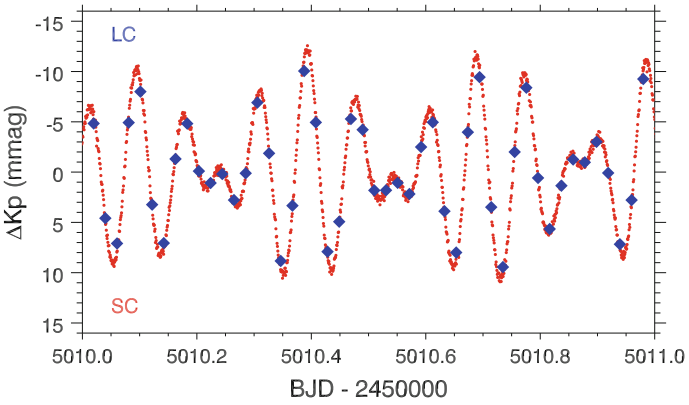

Fig. 2.2 Comparison of LC and SC *Kepler*data spanning 1 d for the δ Sct star KIC 7106205. The SC data have a cadence of 58.5 s and the LC data have a cadence of 29.45 min

To keep its solar panels pointing towards the Sun, the *Kepler*spacecraft had to roll 90 degrees approximately every 93 d — i.e., one quarter of the *Kepler*orbit. The *Kepler*CCD was designed with four-fold symmetry, so a star rotated on the focal plane four times in a *Kepler*year, which is divided into four quarters of LC data. Each quarter was then divided into three months and so SC data are labelled with a quarter and month number. *Kepler*data were stored on board the spacecraft and downloaded to Earth approximately every 31 d. Therefore, *Kepler*data are available as SC months and LC quarters, corresponding to approximately 31 and 93 d, respectively. At the end of the main *Kepler*mission in May 2013, there was a total of 18 LC data quarters each approximately 93 d in length, except for Q0, Q1 and Q17 which were approximately 10, 30 and 30 d, respectively. The length of the complete data set is 1470.5 d, which is just over 4 yr.

Approximately one per cent of all the targets observed by *Kepler*were allocated for asteroseismic research (Gilliland et al. 2010), with a 1-yr proprietary access period given to the *Kepler*Asteroseismic Science Consortium (KASC) via the *Kepler*Asteroseismic Science Operations Center.[4] Today, all *Kepler*light curves in both raw and reduced formats are publicly available from the Mikulski Archive for Space Telescopes (MAST),[5] and are available in two formats. The first type are the raw or unprocessed light curves that are produced using Simple Aperture Photometry (SAP), and the second type are the reduced light curves that are created using a multi-scale Maximum A Prior Pre-Search Data Conditioning (msMAP PDC) pipeline developed by the *Kepler*Science Office — see Smith et al. (2012) and Stumpe et al. (2012) for more details.

The main advantages of using the reduced light curves from the msMAP PDC pipeline over the SAP light curves include: data quarters have been automatically

[4]KASOC website: http://www.kasoc.phys.au.dk.

[5]MAST website: http://archive.stsci.edu/kepler/.

stitched together; the removal of outlying data points; and the removal of systematic sources of instrumental noise. The *Kepler*science pipeline has been developed to optimise the light curves for the detection of exoplanet transit signals and can suppress the amplitudes of long period signals ($P \geq 10$ d). The pipeline does not, however, modify the frequencies of these long-period signals, so the difference for asteroseismology of high-frequency pulsators, such as δ Sct stars, is negligible.

2.2.3 The Kepler Input Catalogue

Approximately 200 000 targets stars were selected to be observed by *Kepler*, with the specific selection criteria discussed by Koch et al. (2010). These targets were characterised with values of $T_{\rm eff}$, log g and [Fe/H] using *griz* and 2MASS *JHK* broad-band photometry prior to the launch of the telescope and were collated into the *Kepler*Input Catalogue (KIC; Brown et al. 2011). Since the end of the nominal *Kepler*mission, Huber et al. (2014) revised the stellar parameters for the ∼200 000 *Kepler*targets and concluded that a colour-dependent offset exists compared to other sources of photometry (e.g., Sloan). This resulted in KIC temperatures for stars hotter than $T_{\rm eff} \gtrsim 6500$ K being, on average, 200 K lower than temperatures obtained from Sloan photometry or the infrared flux method (Pinsonneault et al. 2012). Also, log g values for hot stars were overestimated by up to 0.2 dex. Huber et al. (2014) stress that the $T_{\rm eff}$, log g and [Fe/H] values and their respective uncertainties should not be used for a detailed analysis on a star-by-star basis, as they are only accurate in a statistical sense.

2.2.4 The Failure of Module 3

Approximately 2 yr into the *Kepler*mission, two CCD arrays located on module 3 failed and became inoperative. This resulted in approximately 4/21 of *Kepler*targets not being observed every fourth quarter after this point, because of the rotation of the telescope 90 degrees every ∼93 d. These stars, commonly known as module 3 stars, have a significant gap of ∼90 d in their light curves once per *Kepler*orbit causing more complex window patterns in their amplitude spectra.

2.2.5 K2

In May 2013 the *Kepler*Space Telescope suffered the failure of a second reaction wheel. With only two remaining reaction wheels, the telescope could no longer maintain the necessary level of still-pointing without the significant expenditure of fuel. An ingenious solution was devised by NASA, in which the field of view was

repositioned to point in the direction of the ecliptic, such that torques from the solar radiation pressure were minimised and a smaller amount of fuel was needed to maintain the field of view (Howell et al. 2014). Consequently, the mission parameters have changed and a new mission called K2, *Kepler*'s second light, is underway. K2 data are divided into campaigns, each approximately 80 d in length, with each new campaign observing a variety of targets, including young stars and star-forming regions; supernovae, white dwarfs and the Galactic centre (Howell et al. 2014).

Analysis of K2 data has proved fruitful. Discoveries have included a rare triple-mode RR Lyrae star, EPIC 201585823, with currently only 12 such objects known (Kurtz et al. 2016); an in-depth asteroseismic analysis of O stars for the first time (Buysschaert et al. 2015); and the continued success in finding exoplanets (Vanderburg et al. 2016). The research prospects for asteroseismology using K2 data are good with many more interesting discoveries expected in the next few years. Even though the *Kepler*mission has been redesigned and the telescope is no longer observing the original target stars, the 4 yr of high-quality data will remain a gold mine for scientific discoveries and investigation for many years to come.

2.3 Fourier Analysis of Stellar Time Series

The fundamental data of asteroseismology are the pulsation mode frequencies, which are extracted from time series photometry using Fourier analysis. The Fourier transform (FT) allows one to move from the time domain into the frequency domain by use of

$$F(\nu) = \int_{-\infty}^{+\infty} x(t) e^{2\pi i \nu t} dt \,, \tag{2.1}$$

in which $x(t)$ is a continuous infinite function. The principle of Fourier analysis is that any function can be represented by a summation of sine and cosine functions. In reality, stellar time series are not infinitely long nor are they continuous functions, so the discrete Fourier transform (DFT) described by Deeming (1975) is implemented for finite and discrete data sets. The calculated amplitude spectrum is also convolved with the spectral window of the data set, which is defined by gaps in the data and deviations from a regular cadence (Deeming 1975).

Using the DFT described by Deeming (1975), an amplitude spectrum is calculated using

$$A_i = \left(\frac{2}{N}\right) \sqrt{\left(\sum_{j=0}^{N} x_j(t) \sin(2\pi\nu_i t_j)\right)^2 + \left(\sum_{j=0}^{N} x_j(t) \cos(2\pi\nu_i t_j)\right)^2} \,, \tag{2.2}$$

where A_i is the amplitude at the frequency ν_i calculated from the summation of sine and cosine signals for the discrete time series $x(t)$ with N data points.

2.3.1 The Nyquist Frequency

The Nyquist frequency is the highest frequency that is not undersampled for a given sampling frequency, and is defined as

$$\nu_{\rm Nyq} = \frac{1}{2\Delta t}\,, \tag{2.3}$$

where Δt is the cadence of a discrete data set. For LC *Kepler*data this corresponds to a value of $\nu_{\rm Nyq} = 24.47\ {\rm d}^{-1}$ and for SC data this is $727.35\ {\rm d}^{-1}$. The Nyquist frequency is commonly used as an upper limit in frequency when calculating the amplitude spectrum of a discrete data set because frequencies outside of the range $0 \leq \nu \leq \nu_{\rm Nyq}$ are undersampled and subject to aliasing.

It has been demonstrated that pulsation mode frequencies in δ Sct stars typically lie between $4 \leq \nu \leq 50\ {\rm d}^{-1}$ (Grigahcène et al. 2010; Uytterhoeven et al. 2011; Balona and Dziembowski 2011), thus can exceed the LC *Kepler*Nyquist frequency. Before the advent of the super-Nyquist asteroseismology technique by Murphy et al. (2013), care was needed when extracting frequencies from an amplitude spectrum near or above LC Nyquist frequency because they may be aliases of undersampled frequencies above the Nyquist frequency.

Super-Nyquist Asteroseismology

It was shown by Murphy et al. (2013) using the super-Nyquist asteroseismology (sNa) technique, that real and alias frequencies of pulsation modes can be easily identified in an amplitude spectrum when using *Kepler*data. *Kepler*data were sampled at a regular cadence onboard the spacecraft, but Barycentric time stamp corrections were made to correct for the difference in light arrival time of the photons to the barycentre of the Solar system and to the telescope, respectively, resulting in a non-constant cadence (Murphy et al. 2013). Thus, Nyquist aliases are subject to periodic frequency (phase) modulation with a period equal to the *Kepler*satellite's orbital period of 372.5 d, and consequently have a multiplet structure split by the *Kepler*orbital frequency in an amplitude spectrum (Murphy et al. 2013). The total integrated power is the same for a real peak and its alias multiplet in an amplitude spectrum, but the power of an alias is spread between the central component of the multiplet and its super-Nyquist sidelobes, resulting in a central component with a smaller amplitude when compared to the real peak (Murphy et al. 2013). Therefore, using the sNa technique, real and alias frequencies can often be identified without the need to calculate an amplitude spectrum beyond the LC Nyquist frequency.

To demonstrate the sNa technique described by Murphy et al. (2013), the amplitude spectra for simultaneous LC and SC observations of the HADS star KIC 5950759 have been plotted in the left panel of Fig. 2.3. This HADS star acts as a useful example because of the high S/N of its pulsation modes and because simultaneous LC and SC observations are available. The LC and SC amplitude spectra for KIC 5950759 both show the fundamental radial mode at $\nu_1 = 14.221372\ {\rm d}^{-1}$, and its harmonic $2\nu_{1,{\rm r}} = 28.442744\ {\rm d}^{-1}$ labelled 'r' for real, which lies above the

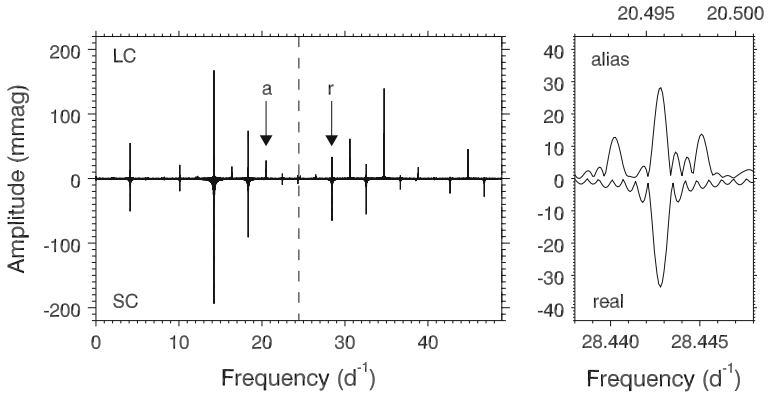

Fig. 2.3 Demonstration of super-Nyquist asteroseismology using the amplitude spectrum of the HADS star KIC 5950759. Real and alias peaks associated with the harmonic of the fundamental radial mode are marked by 'r' and 'a', respectively, in the LC amplitude spectrum in the left panel. The LC Nyquist frequency is indicated by the *vertical dashed line* and the SC amplitude spectrum is shown below for comparison. The *right panel* contains inserts of the LC amplitude spectrum showing the real peak below and the alias peak above. The alias peak is easily identified as its multiplet structure is split by the *Kepler*orbital frequency. Some peaks that exist in the SC amplitude spectrum do not appear in the LC amplitude spectrum as they lie close to the LC sampling frequency and are heavily suppressed in amplitude. Figure from Bowman et al. (2016), their Fig. 2

LC Nyquist frequency indicated by a vertical dashed line in Fig. 2.3. The alias of the harmonic $2\nu_{1,\mathrm{a}} = 20.496203\ \mathrm{d}^{-1}$ can also be seen in the LC amplitude spectrum in Fig. 2.3 and is labelled 'a'. The right panel in Fig. 2.3 shows a zoom-in of the amplitude spectrum using LC data, showing the multiplet structure split by the *Kepler*satellite's orbital frequency of the alias peak in the top panel, compared to the real peak shown below for comparison. Note also, how the amplitude of the alias peak is smaller than the real peak in the LC amplitude spectrum, as predicted by Murphy et al. (2013).

2.3.2 *Frequency Resolution*

It is important to note that SC *Kepler*data does provide a higher temporal resolution, as shown by Fig. 2.2, but does not provide a higher frequency resolution compared to LC observations. The frequency resolution of a data set is given by the Rayleigh resolution criterion of

$$\sigma\left(\nu\right) = \frac{1}{\Delta T}\ , \tag{2.4}$$

where $\sigma\left(\nu\right)$ and ΔT are the frequency resolution and the length of the data set, respectively. A longer time series results in a smaller, and hence improved, frequency resolution, which is represented by the width of the peak in an amplitude spectrum.

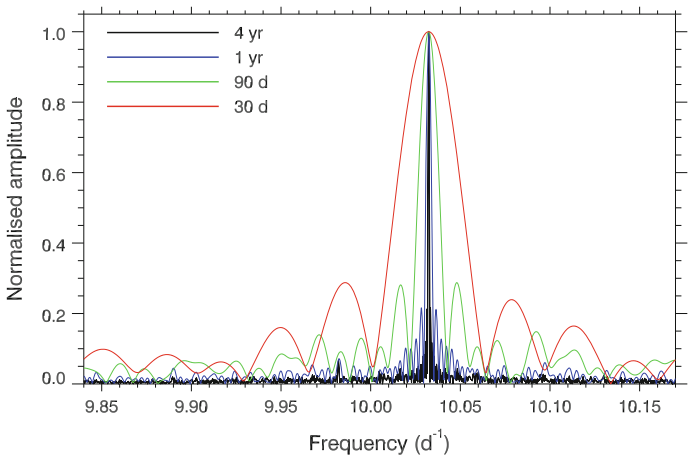

Fig. 2.4 Demonstration of frequency resolution using four different lengths of observations for the pulsation mode frequency at $\nu = 10.0323$ d^{-1} in the δ Sct star KIC 7106205. With a longer time series, a better frequency resolution is obtained, which corresponds to the width of the peak in the amplitude spectrum

This is demonstrated in Fig. 2.4, in which amplitude spectra for time series spanning 30 d, 90 d, 1 yr and 4 yr for a pulsation mode frequency at $\nu = 10.032366$ d^{-1} have been plotted for comparison. As can be seen in Fig. 2.4, the width of the peak is smaller for longer time series following Eq. 2.4. For the 4-yr *Kepler*data set, a frequency resolution of 0.00068 d^{-1} ($\simeq$8 nHz) is obtained.

The relationship in Eq. 2.4 is commonly used in the literature for calculating the frequency resolution of a discrete data set, such as a stellar time series. However, it is not always strictly correct to do so. Loumos and Deeming (1978) analytically derive a frequency resolution of

$$\sigma(\nu) = \frac{3}{2}\,\frac{1}{\Delta T}\,. \tag{2.5}$$

as a more conservative definition of frequency resolution.

Both of the definitions of frequency resolution given in Eqs. 2.4 and 2.5 also only apply for data sets without large gaps. For example, if we take the hypothetical case of two individual time series of a star, each one month in length that are separated by one year, using Eq. 2.4 would yield a frequency resolution of approximately 0.003 d^{-1}, but this is not an appropriate resolution calculation. Mathematically, for data with large gaps, relative to the length of the observations, and also for unequally spaced data, Eq. 2.5 is more appropriate. Loumos and Deeming (1978), show for the hypothetical scenario described here, the frequency resolution of two months of data separated by one year, is no better than the resolution obtained from a single month of observations.

2.3.3 Amplitude Visibility Function

It was discussed in Sect. 2.3.2 how the length of a data set determines the frequency resolution in an amplitude spectrum and is independent of the cadence, such that the width of a peak in an amplitude spectrum is the same for both LC and SC observations of the same length. However, the longer integration times of the LC data reduce the amplitudes of peaks in an amplitude spectrum compared to SC data, which is also a strong function of frequency. The exact functional form of the amplitude suppression caused by integration time is given by the amplitude visibility function in Eq. 2.6. The derivation of this equation is given below and was described by Murphy (2014).

In Fig. 2.5 a periodic flux variation of frequency $\nu = 10.0\,\mathrm{d}^{-1}$ is shown by the solid blue line and the interval between consecutive data points in LC *Kepler*data is shown by the width of the green-hatched rectangle, δ. The height of the rectangle is the area divided by its width, thus for the same frequency signal a shorter sampling would produce a taller and narrower rectangle in Fig. 2.5. Assuming that the $\nu = 10.0\,\mathrm{d}^{-1}$ signal is periodic and has the form $\cos(\omega t)$, then the height of the rectangle, H, is given by:

$$
\begin{aligned}
&= \frac{1}{\delta} \int_{t_0 - \frac{\delta}{2}}^{t_0 + \frac{\delta}{2}} \cos(\omega t) dt \\
&= \frac{1}{\delta} \frac{1}{\omega} \left\{ \sin\left[\omega \left(t_0 + \frac{\delta}{2} \right) \right] - \sin\left[\omega \left(t_0 - \frac{\delta}{2} \right) \right] \right\} .
\end{aligned}
$$

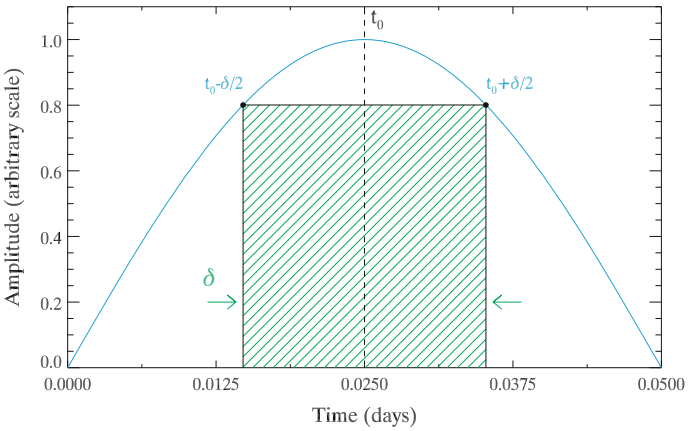

Fig. 2.5 Demonstration of how longer integration times lead to an underestimate in amplitude of a periodic signal. A frequency of $\nu = 10.0\,\mathrm{d}^{-1}$ is shown as the *solid blue line* and the interval between consecutive data points is given by δ, which is symmetric from a reference time, t_0, and has been chosen to emulate the LC *Kepler*sampling frequency. With a shorter integration time, δ, less amplitude suppression occurs as the height of the rectangle increases and approaches the true amplitude of unity in this example. Figure from Murphy (2014), his Fig. 1.4. Reproduced with kind permission from author

This can be re-written using the trigonometric identity $\sin(X+Y) = \sin X \cos Y + \cos X \sin Y$, as:

$$
\begin{aligned}
&= \frac{1}{\delta}\frac{1}{\omega}\left[\sin(\omega t_0)\cos\left(\frac{\omega\delta}{2}\right) + \cos(\omega t_0)\sin\left(\frac{\omega\delta}{2}\right)\right. \\
&\qquad \left. - \sin(\omega t_0)\cos\left(\frac{\omega\delta}{2}\right) + \cos(\omega t_0)\sin\left(\frac{\omega\delta}{2}\right)\right] \\
&= \frac{1}{\omega\delta}\left[2\cos(\omega t_0)\sin\left(\frac{\omega\delta}{2}\right)\right] \\
&= \cos(\omega t_0)\,\mathrm{sinc}\left(\frac{\omega\delta}{2}\right) .
\end{aligned}
$$

Using the relationship between angular frequency and period, $\omega = \frac{2\pi}{P}$, with P being the period of the signal, and that the time interval between consecutive data points is related to the number of data points per cycle, $\delta = \frac{P}{n}$, the above can be rewritten as

$$A = A_0\,\mathrm{sinc}\left(\frac{\pi}{n}\right) = A_0\,\mathrm{sinc}\left(\frac{\pi\nu}{\nu_{\mathrm{samp}}}\right), \tag{2.6}$$

where A is the observed amplitude, A_0 is the true amplitude, n is the number of data points per pulsation cycle, ν is the pulsation mode frequency and ν_{samp} is the instrumental sampling frequency. From the relationship in Eq. 2.6, it can be seen that higher frequency signals are, on average, more heavily suppressed in amplitude, but only exactly integer multiples of the LC sampling frequency, $\nu_{\mathrm{samp}} = 48.9\ \mathrm{d}^{-1}$, are completely suppressed, which is shown graphically in Fig. 2.6. Therefore, from the

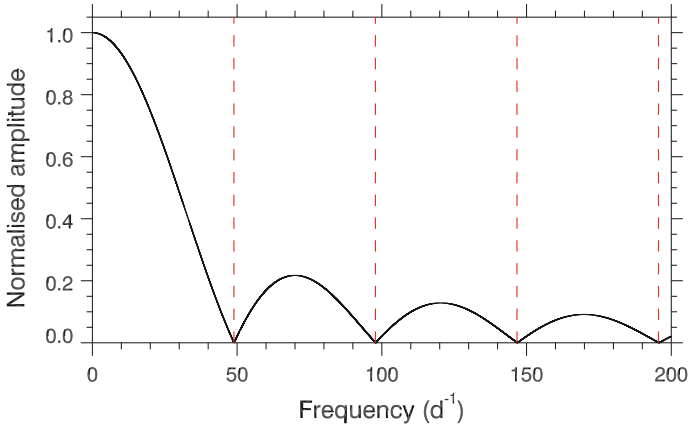

Fig. 2.6 The amplitude visibility function as a function of frequency for LC *Kepler*data. Higher frequencies are suppressed heavily in amplitude because there are fewer data points per pulsation cycle, n, but only frequencies equal to integer multiples of the sampling frequency are completely suppressed. The *vertical red dashed lines* indicate integer multiples of the LC sampling frequency $\nu_{\mathrm{samp}} = 48.9\ \mathrm{d}^{-1}$

shorter integration times, SC data will produce a higher amplitude peak for a given frequency compared to LC data.

2.4 *Kepler* Data Catalogues

One of the first tasks undertaken as part of the thesis by Bowman (2016) was to identify all the pulsating A and F stars, specifically the δ Sct stars, observed by the *Kepler*Space Telescope. Although the *Kepler*instrument is optimised for observing solar-type stars, several thousand A and F stars were included in the 200 000 target stars. In this section, the downloading and processing of light curves for all A and F stars, and the methodology of producing the *Kepler*data catalogues is discussed.

2.4.1 Creating Data Catalogues

To create a statistical ensemble of δ Sct stars, the light curves produced by the msMAP PDC pipeline (Stumpe et al. 2012; Smith et al. 2012) for all *Kepler*targets with effective temperatures between $6400 \leq T_{\rm eff} \leq 10\,000$ K in the KIC were downloaded from MAST. The extracted time series were stored locally in the format of reduced Barycentric Julian Date (BJD $-$ 2 400 000) and stellar magnitudes, which were normalised for each quarter of LC and month of SC data to be zero in the mean. This resulted in approximately 10 400 stars within this $T_{\rm eff}$ range. Examples of the file format for the first LC quarter and first SC month of the fictitious star KIC 1234567 are

```
kic001234567_Q00_LC.txt
kic001234567_Q00_M1_SC.txt
```

The time series were separated into temperature bins for parallelised computing with the number of stars in each temperature bin shown in Table 2.1. The range of the temperature bins is somewhat arbitrary, but was chosen to create bins with similar number of stars and type of pulsator. For example, the overlapping region of the δ Sct and γ Dor instability regions is approximately between $6800 \leq T_{\rm eff} \leq 8000$ K, and so it was important to separate these stars into three groups. Similarly, the hot δ Sct and cool γ Dor stars have separate groups. Thus, considering that typical uncertainties for stars with $T_{\rm eff} \simeq 6500$ K and $T_{\rm eff} \simeq 9000$ K are approximately ± 150 and ± 400 K, respectively, all the stars within a bin can be considered as having the same effective temperature.

An automated pipeline was created to calculate the amplitude spectrum for each LC quarter for each star. The method for calculating the Fourier transform of a discrete data series is described in detail by Deeming (1975), and was optimised for faster computation time by Kurtz (1985). These tools were checked and found to

Table 2.1 The number of stars downloaded from MAST for each temperature bin as listed in the KIC (Brown et al. 2011) is given, indicating fewer hot stars than cool stars

KIC temperature (K)	Number	Spectral type	Comment
$9000 \leq T_{\rm eff} < 10\,000$	329	A1 – A3	
$8000 \leq T_{\rm eff} < 9000$	907	A3 – A6	δ Sct blue edge
$7500 \leq T_{\rm eff} < 8000$	912	A6 – A7	γ Dor blue edge
$7000 \leq T_{\rm eff} < 7500$	1587	A8 – F0	
$6800 \leq T_{\rm eff} < 7000$	1129	F0 – F2	δ Sct red edge
$6600 \leq T_{\rm eff} < 6800$	1752	F3 – F4	
$6500 \leq T_{\rm eff} < 6600$	1754	F4 – F5	γ Dor red edge
$6400 \leq T_{\rm eff} < 6500$	2025	F5 – F6	
Total	10 395		

be consistent with the frequency software package `PERIOD04` (Lenz and Breger 2005).

2.4.2 *Kepler* Data Catalogue Extract

The light curves and amplitude spectra have been collated into a series of PDF catalogues, one for each of the effective temperature bins given in Table 2.1. At the top of each page in a data catalogue, a star's unique *Kepler*ID number starting with the characters KIC (*Kepler*Input Catalogue) and its stellar parameters listed in the KIC (Brown et al. 2011) are given. Next to the KIC ID number, the LC data quarter number is also given. The light curve is shown in the top panel, which have all been set to be zero in the mean and have ordinate units of mmag. The middle panel shows the LC amplitude spectrum calculated out to the Nyquist frequency, and the bottom panel shows a zoom-in of the low-frequency regime in the amplitude spectrum at the same ordinate scale but a smaller abscissa scale. The third panel shows the expected frequency range for g modes, specifically $0 \leq \nu \leq 6\,{\rm d}^{-1}$, and was chosen to show any longer periodicity present in the amplitude spectrum as a separate plot since many δ Sct stars have peaks in the low-frequency regime (see e.g., Grigahcène et al. 2010; Uytterhoeven et al. 2011; Balona 2011). The ordinate scale in every page (i.e., for all LC data quarters) of each star is kept fixed, thus one can see changes in amplitude of the pulsation modes more easily.

The Figs. 2.7 and 2.8 are extracts from the $6800 \leq T_{\rm eff} \leq 7000$ K *Kepler*data catalogue showing Q0 and Q17, respectively, for the δ Sct star KIC 7106205. Scrolling through the *Kepler*data quarters on separate pages of the data catalogues allowed KIC 7106205 to be quickly identified as a δ Sct star with significant amplitude modulation, and motivated the analysis of this star by Bowman and Kurtz (2014), which

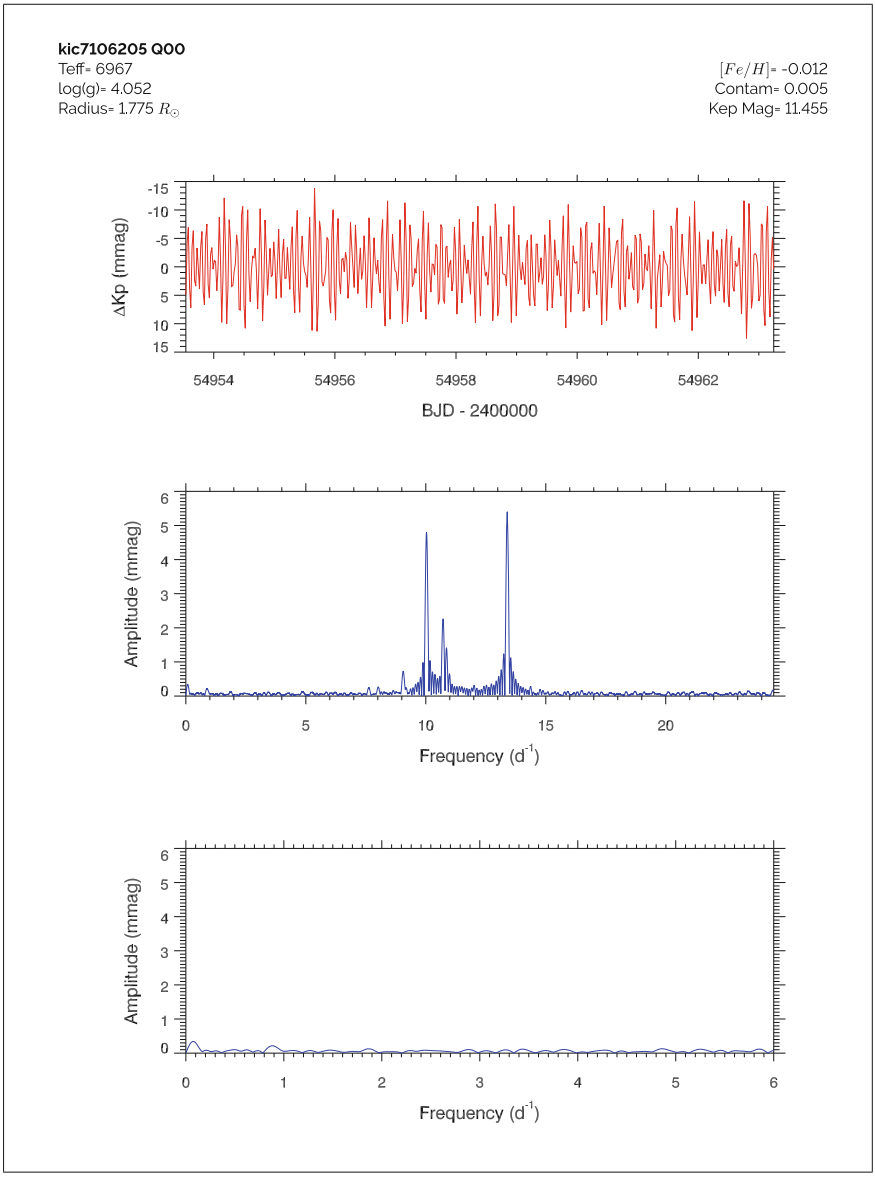

Fig. 2.7 An example page from the *Kepler*data catalogue for Q0 of the δ Sct star KIC 7106205

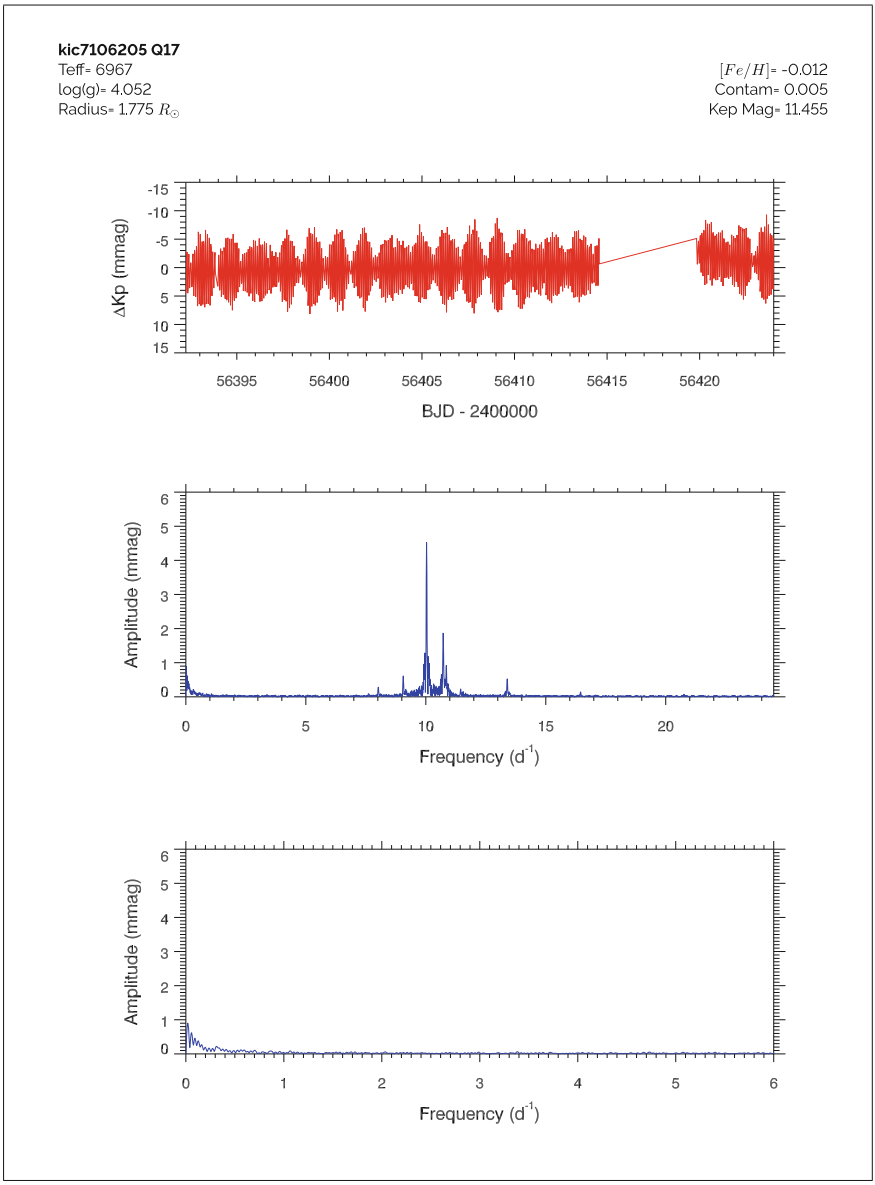

Fig. 2.8 An example page from the *Kepler*data catalogue for Q17 of the δ Sct star KIC 7106205

is discussed in Chap. 3. Specifically, it was the significant decrease in the amplitude of the peak at $\nu \simeq 13.5\ \mathrm{d}^{-1}$ from Q0 to Q17 that is most noticeable.

2.5 Discussion

The advent of space-based telescopes in the last decade such as MOST (Walker et al. 2003), CoRoT (Auvergne et al. 2009) and *Kepler*(Borucki et al. 2010), has become known as the Space Photometry Revolution. The *Kepler*Space Telescope provided high photometric precision, a high duty cycle and data spanning years for 200 000 stars (Koch et al. 2010). Although the mission was designed to find Earth-like exoplanets orbiting solar-type stars using the transit method, these data have also been extremely useful for studying pulsating stars using asteroseismology.

In this chapter, a review of *Kepler*instrumentation has been provided, including a discussion of the main differences in SC and LC data and the implications for asteroseismology. Specifically, the 29.5-min cadence of LC *Kepler*data may have the same frequency resolution for the same length of SC data according to the Rayleigh resolution criterion, but it was shown that the amplitude suppression from the longer integration time is an important factor to consider when interpreting an amplitude spectrum. From the complete 4-yr *Kepler*data set, a frequency resolution of $0.00068\ \mathrm{d}^{-1}$ ($\simeq$8 nHz) and an amplitude precision of order a few μmag is obtained, which are important for studying the changes in the pulsation modes over time – i.e., frequency and amplitude modulation – in pulsating stars such as δ Sct stars.

In this chapter, it was discussed how a total of approximately 10 400 stars with effective temperatures between $6400 \leq T_{\mathrm{eff}} \leq 10\,000$ K observed by *Kepler*were downloaded and processed into *Kepler*data catalogues. These catalogues represent a valuable tool for quickly and efficiently identifying different types of pulsating stars observed by *Kepler*, as one is able to simply search for pulsation modes in the frequency range of interest. The ordinate axis of the amplitude spectra was chosen to be fixed for each LC quarter of each star, such that significant amplitude modulation in δ Sct stars could easily be identified.

The usefulness of these data catalogues was demonstrated for the δ Sct star KIC 7106205 in Sect. 2.4.2, which led to the study of amplitude modulation in this star by Bowman and Kurtz (2014) and Bowman et al. (2015) presented in Chap. 3. The *Kepler*data catalogues discussed in this chapter will remain of great use for years to come, as the 4-yr length of *Kepler*data will not be surpassed in the foreseeable future.

References

Auvergne, M., Bodin, P., Boisnard, L., et al. 2009, A&A, 506, 411
Balona, L. A. 2011, MNRAS, 415, 1691
Balona, L. A. & Dziembowski, W. A. 1999, MNRAS, 309, 221
Balona, L. A. & Dziembowski, W. A. 2011, MNRAS, 417, 591
Bessell, M. S. 2005, ARA&A, 43, 293
Borucki, W. J., Koch, D., Basri, G., et al. 2010, Science, 327, 977
Borucki, W. J., Koch, D. G., Basri, G., et al. 2011, ApJ, 728, 117
Bowman, D. M. 2016, PhD thesis, Jeremiah Horrocks Institute, University of Central Lancashire, UK
Bowman, D. M. & Kurtz, D. W. 2014, MNRAS, 444, 1909
Bowman, D. M. & Kurtz, D. W. 2015, in European Physical Journal Web of Conferences, Vol. 101, European Physical Journal Web of Conferences, 6013
Bowman, D. M., Holdsworth, D. L., & Kurtz, D. W. 2015, MNRAS, 449, 1004
Bowman, D. M., Kurtz, D. W., Breger, M., Murphy, S. J., & Holdsworth, D. L. 2016, MNRAS, 460, 1970
Brown, T. M., Latham, D. W., Everett, M. E., & Esquerdo, G. A. 2011, AJ, 142, 112
Buysschaert, B., Aerts, C., Bloemen, S., et al. 2015, MNRAS, 453, 89
Chaplin, W. J. & Miglio, A. 2013, ARA&A, 51, 353
Deeming, T. J. 1975, Ap&SS, 36, 137
Dziembowski, W. 1977, Acta Astronomica, 27, 203
Gilliland, R. L., Brown, T. M., Christensen-Dalsgaard, J., et al. 2010, PASP, 122, 131
Grigahcène, A., Antoci, V., Balona, L., et al. 2010, ApJL, 713, L192
Hambleton, K. M. 2016, PhD thesis, Jeremiah Horrocks Institute, University of Central Lancashire, UK
Hambleton, K. M., Kurtz, D. W., Prša, A., et al. 2013, MNRAS, 434, 925
Howell, S. B., Sobeck, C., Haas, M., et al. 2014, PASP, 126, 398
Huber, D., Silva Aguirre, V., Matthews, J. M., et al. 2014, ApJS, 211, 2
Jenkins, J. M., Caldwell, D. A., Chandrasekaran, H., et al. 2010, ApJL, 713, L87
Johnson, H. L. & Morgan, W. W. 1953, ApJ, 117, 313
Koch, D. G., Borucki, W. J., Basri, G., et al. 2010, ApJL, 713, L79
Kumar, P., Ao, C. O., & Quataert, E. J. 1995, ApJ, 449, 294
Kurtz, D. W. 1985, MNRAS, 213, 773
Kurtz, D. W., Bowman, D. M., Ebo, S. J., et al. 2016, MNRAS, 455, 1237
Lenz, P. & Breger, M. 2005, Communications in Asteroseismology, 146, 53
Loumos, G. L. & Deeming, T. J. 1978, Ap&SS, 56, 285
Murphy, S. J. 2014, PhD thesis, Jeremiah Horrocks Institute, University of Central Lancashire, UK
Murphy, S. J., Shibahashi, H., & Kurtz, D. W. 2013, MNRAS, 430, 2986
Pinsonneault, M. H., An, D., Molenda-Żakowicz, J., et al. 2012, ApJS, 199, 30
Prša, A., Batalha, N., Slawson, R. W., et al. 2011, AJ, 141, 83
Smith, J. C., Stumpe, M. C., Van Cleve, J. E., et al. 2012, PASP, 124, 1000
Stumpe, M. C., Smith, J. C., Van Cleve, J. E., et al. 2012, PASP, 124, 985
Thompson, S. E., Everett, M., Mullally, F., et al. 2012, ApJ, 753, 86
Uytterhoeven, K., Moya, A., Grigahcène, A., et al. 2011, A&A, 534, A125
Vanderburg, A., Latham, D. W., Buchhave, L. A., et al. 2016, ApJS, 222, 14
Walker, G., Matthews, J., Kuschnig, R., et al. 2003, PASP, 115, 1023

Chapter 3
KIC 7106205 — An Archetypal Delta Scuti Star with Amplitude Modulation

3.1 Introductory Remarks

The δ Sct star KIC 7106205 (TYC 3129-879-1) represents a special case study that allows energy conservation of pulsation modes to be investigated. Only a single pulsation mode exhibits amplitude modulation in KIC 7106205 whilst all other statistically significant modes remain constant in amplitude, such that the visible pulsation energy budget is not conserved over the 4-yr *Kepler* data set (Bowman and Kurtz 2014). Ground-based data from the Wide Angle Search for Planets (WASP; Pollacco et al. 2006) project are used to extend the study of KIC 7106205 and it is shown that the majority of the amplitude modulation in this variable pulsation mode occurred prior to the launch of the *Kepler* Space Telescope (Bowman et al. 2015). It is clear from these studies that time spans of years and decades are important in δ Sct stars, with the 4-yr *Kepler* data set providing only a blink-of-an-eye insight into the physics at work in these stars.

In this chapter, the methods and results from Bowman and Kurtz (2014) and Bowman et al. (2015) are discussed in Sects. 3.2 and 3.3, respectively, with a combined discussion section given in Sect. 3.5.

3.2 Pulsational Frequency and Amplitude Modulation in the δ Sct Star KIC 7106205

Before the space photometry revolution, observations obtained using ground-based telescopes were typically limited to pulsation modes with amplitudes higher than a few mmag. This, coupled with the limitations of instrumental selection effects, aliasing and high levels of noise, made asteroseismology difficult from the ground. However, a handful of δ Sct stars were studied extensively over several decades and discovered to contain pulsation modes with variable amplitudes (Breger 2000). An important case study of amplitude modulation in a δ Sct star is 4 CVn, which was

D.M. Bowman, *Amplitude Modulation of Pulsation Modes in Delta Scuti Stars*,
Springer Theses, DOI 10.1007/978-3-319-66649-5_3

discussed in Sect. 1.5. With the high photometric precision of the 4-yr *Kepler* data set, it is now possible to probe frequency and amplitude modulation of pulsation modes in hundreds of δ Sct stars and, most importantly, gain an improved insight of their physical properties using asteroseismology.

The δ Sct stars represent a good set of candidate stars to study energy conservation between p and g modes, but also between the pulsation modes and driving zones within a star, for both opacity and convective driving. If the pulsational energy budget is conserved within a δ Sct star, then any decrease in mode amplitude in a single or group of modes would result in a corresponding increase in mode amplitude of another mode or group of modes, or vice versa. If, however, a star does not conserve its pulsational energy budget, then no concomitant change in mode amplitudes would be seen and the energy may be transferred to either the convection or ionisation driving zones, or to another damping region. Testing this hypothesis was not thoroughly performed before the *Kepler* Space Telescope since it was the first photometric instrument to have the necessary levels of frequency and amplitude precision.

3.2.1 *Kepler Photometry of KIC 7106205*

The δ Sct star KIC 7106205 is one of almost 1000 δ Sct stars that were observed continuously by the *Kepler* Space Telescope for 4 yr (Bowman et al. 2016). The stellar parameters of KIC 7106025 from the KIC and from Huber et al. (2014), with their respective errors, are given in Table 3.1, which characterise it as an early F-type star. KIC 7106205 demonstrates a conclusion stated in Huber et al. (2014) that stars with $T_{\rm eff} \leq 7000$ K listed in the original KIC have robust values for $T_{\rm eff}$. The revised values of log g and metallicity are sourced from spectroscopy and demonstrate the inconsistencies between spectroscopy and photometry for deriving log g and metallicity values.

The LC *Kepler* light curve of KIC 7106205 is shown in the top panel of Fig. 3.1, which contains 65 308 data points covering 1470.5 d (4 yr). It is easy to see in Fig. 3.1 that the peak-to-peak light amplitude variability decreases throughout the observations. In the time domain, this is a good indicator of amplitude modulation — the light curve is non-periodic and non-sinusoidal.

Table 3.1 Stellar parameters of the δ Sct star KIC 7106205 given in the *Kepler* Input Catalogue (Brown et al. 2011) and the revised values given in Huber et al. (2014)

	$T_{\rm eff}$ (K)	log g (cgs)	[Fe/H] (dex)
KIC (Brown et al. 2011)	6960 ± 150	4.05 ± 0.15	-0.01 ± 0.15
Huber et al. (2014)	6900 ± 140	3.70 ± 0.15	0.32 ± 0.15

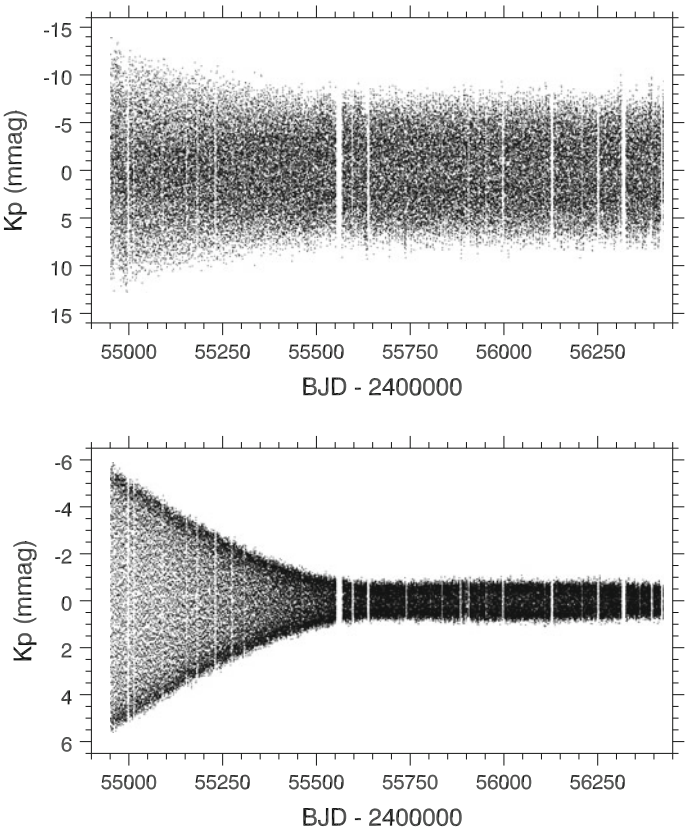

Fig. 3.1 The *top panel* shows the 4-yr *Kepler* light curve of the δ Sct star KIC 7106205. The *bottom panel* shows the residual light curve of KIC 7106205 with all significant peaks in its amplitude spectrum pre-whitened down to 8 μmag except for $\nu_{\rm mod} = 13.3941749\ {\rm d}^{-1}$. Note the difference in the y-axis scale between the panels

In the overview of A- and F-type stars observed by *Kepler*, KIC 7106205 was classified as a pure δ Sct star and also a possible binary system by Uytterhoeven et al. (2011). The tentative suggestion of binarity for this star was only from inspection of DSS and 2MASS images (Uytterhoeven et al. 2011). Bowman and Kurtz (2014) found no evidence of binarity using the frequency modulation (FM) technique (Shibahashi and Kurtz 2012). As for possible contamination, Bowman and Kurtz (2014) also examined the target pixel files available from MAST, and it was found that there was negligible contamination from background sources.

The amplitude spectrum of KIC 7106205 using 4 yr of LC *Kepler* data is shown in Fig. 3.2, in which the sub-plot shows a zoom-in of the low-frequency regime. The p modes are easily visible because of their high mode amplitudes compared to the *Kepler* noise level of order a few μmag. A total of nine significant peaks above $\nu \geq 5\ {\rm d}^{-1}$ with amplitudes above $A \geq 0.1$ mmag were extracted using

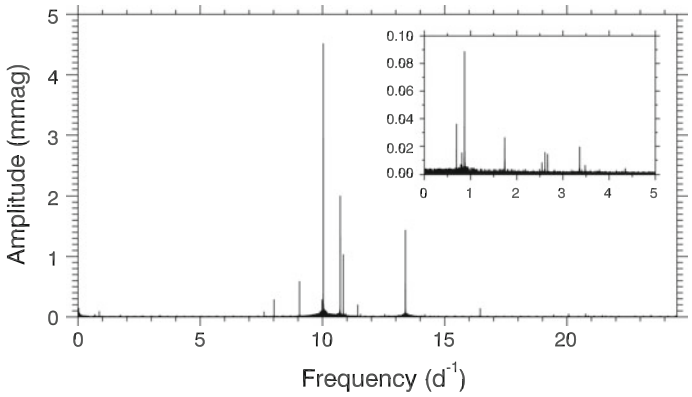

Fig. 3.2 The amplitude spectrum of the 4-yr *Kepler* data set for the δ Sct star KIC 7106205 calculated out to the LC Nyquist frequency. The sub-plot shows the g-mode frequency regime which contains several low-amplitude peaks in KIC 7106205

iterative pre-whitening (Bowman and Kurtz 2014). As commonly found for δ Sct stars, p modes and their spectral window patterns dominate the amplitude spectrum so to study peaks in the g-mode frequency regime, all significant peaks with frequencies above $\nu \geq 5\ \mathrm{d}^{-1}$ were pre-whitened down to an amplitude of 3 μmag, which resulted in eight significant peaks below $\nu < 5\ \mathrm{d}^{-1}$ with amplitudes above $A \geq 0.01$ mmag (Bowman and Kurtz 2014). All peaks extracted and analysed by Bowman and Kurtz (2014) were obtained using a non-linear least-squares fit to the time series and are listed in Table 3.2 along with their pulsation constants calculated using Eq. 1.2 with parameters from Huber et al. (2014). It is stated by Bowman and Kurtz (2014) that the goal of their study was not peak bagging, so peaks were only considered significant if they had relatively high amplitudes for their respective frequency regime, i.e., $A \geq 0.1$ mmag for p modes and $A \geq 0.01$ mmag for g modes.

A preliminary indication of whether a pulsation mode is purely periodic, thus stable in frequency and amplitude, is to pre-whiten it from a time series using the cosinusoidal function, $\Delta m = A_i \cos(2\pi\nu_i(t - t_0) + \phi_i)$, where Δm is the resultant pre-whitened time series, A_i is the amplitude, ν_i is the optimised frequency obtained from the non-linear least-squares fit, ϕ_i is the phase in radians, t is the time, t_0 is the chosen zero-point of the time scale, and the index i refers to a particular mode. The mid-point of the 4-yr time series of KIC 7106205 was chosen by Bowman and Kurtz (2014) as the zero-point of the time scale for calculating pulsation mode phases, specifically $t_0 = 2\,455\,688.770$ BJD. Using this approach, the amplitude spectrum of the residuals of a non-linear least-squares fit can be used to examine what periodicity remained within the light curve after a frequency has been removed.

Bowman and Kurtz (2014) found that all pulsation modes in KIC 7106205 were stable in amplitude to at most 10 μmag, except for a single pulsation mode with a frequency of $13.3941749\ \mathrm{d}^{-1}$, hereafter referred to as ν_{mod}. In the bottom panel of Fig. 3.1, the residual light curve of removing all peaks except ν_{mod} is shown,

Table 3.2 Frequencies with their associated amplitudes, phases and their respective errors extracted for the δ Sct star KIC 7106205 using a non-linear least-squares fit. The phases are all with respect to the time zero-point $t_0 = 2\,455\,688.77$ BJD. Possible combination frequencies are labelled and pulsation constants are calculated using Eq. 1.2 with parameters from Huber et al. (2014). This table only includes the low- and high-frequency peaks which have amplitudes $A \geq 0.01$ mmag and $A \geq 0.1$ mmag, respectively

	Frequency (d^{-1})	Amplitude ± 0.006 (mmag)	Phase (rad)	Q (d)	Comment
g_1	0.6949057 ± 0.0000600	0.038	0.255 ± 0.159	0.3247	$g_1 = g_8 - g_7$
g_2	0.8152912 ± 0.0001757	0.014	3.056 ± 0.466	0.2767	$g_2 = g_8 - g_5$
g_3	0.8696968 ± 0.0000244	0.091	2.997 ± 0.065	0.2594	
g_4	1.7397083 ± 0.0000875	0.026	-3.048 ± 0.232	0.1297	
g_5	2.5463911 ± 0.0002349	0.009	2.082 ± 0.622	0.0886	$g_5 = g_8 - g_2$
g_6	2.6108170 ± 0.0001430	0.015	-2.197 ± 0.379	0.0864	
g_7	2.6668512 ± 0.0001507	0.015	-1.787 ± 0.399	0.0846	$g_7 = g_8 - g_1$
g_8	3.3618307 ± 0.0001037	0.022	0.466 ± 0.275	0.0671	$g_8 = g_7 + g_1$
p_1	8.0193178 ± 0.0000077	0.291	-1.595 ± 0.020	0.0281	
p_2	9.0588126 ± 0.0000038	0.589	-2.957 ± 0.010	0.0249	
p_3	9.9820652 ± 0.0000070	0.321	-3.046 ± 0.018	0.0226	
p_4	10.0323662 ± 0.0000005	4.530	1.602 ± 0.001	0.0225	$p_4 = p_5 - g_1$
p_5	10.7273166 ± 0.0000011	2.004	-2.257 ± 0.003	0.0210	$p_5 = p_4 + g_1$
p_6	10.8477360 ± 0.0000022	1.027	0.038 ± 0.006	0.0208	$p_6 = p_4 + g_2$
p_7	11.4421233 ± 0.0000108	0.206	-1.025 ± 0.029	0.0197	
p_8	16.4530392 ± 0.0000157	0.142	0.393 ± 0.042	0.0137	
ν_{mod}	13.3941749 ± 0.0000015	1.444	-1.016 ± 0.004	0.0168	$\nu_{mod} = p_4 + g_8$
					$\nu_{mod} = p_5 + g_7$
					$\nu_{mod} = p_6 + g_5$

demonstrating that the reducing peak-to-peak light amplitude variability over 4 yr is being caused solely by the ν_{mod} pulsation mode. The calculated pulsation constant of $Q = 0.0168$ d for ν_{mod} suggests that it is a third or fourth radial overtone mode (Bowman and Kurtz 2014). Since none of the p modes have pulsation constants greater than the expected value for the radial fundamental mode, $Q = 0.033$ d, there is no evidence of any mixed modes in KIC 7106205 (Bowman and Kurtz 2014).

The highest amplitude pulsation mode in KIC 7106205, which is labelled p_4 in Table 3.2, has a frequency of 10.0323662 ± 0.0000005 d^{-1} and an amplitude of 4.530 ± 0.006 mmag. A zoom-in of the amplitude spectrum showing this pulsation mode is given in the top panel of Fig. 3.3. For comparison, a zoom-in of the peak corresponding to the ν_{mod} pulsation mode is shown in the bottom panel of Fig. 3.3. The upper and lower parts of each panel in Fig. 3.3 show the amplitude spectrum before and after pre-whitening, respectively. Bowman and Kurtz (2014) found that the remaining mode amplitude after pre-whitening the ν_{mod} peak was approximately

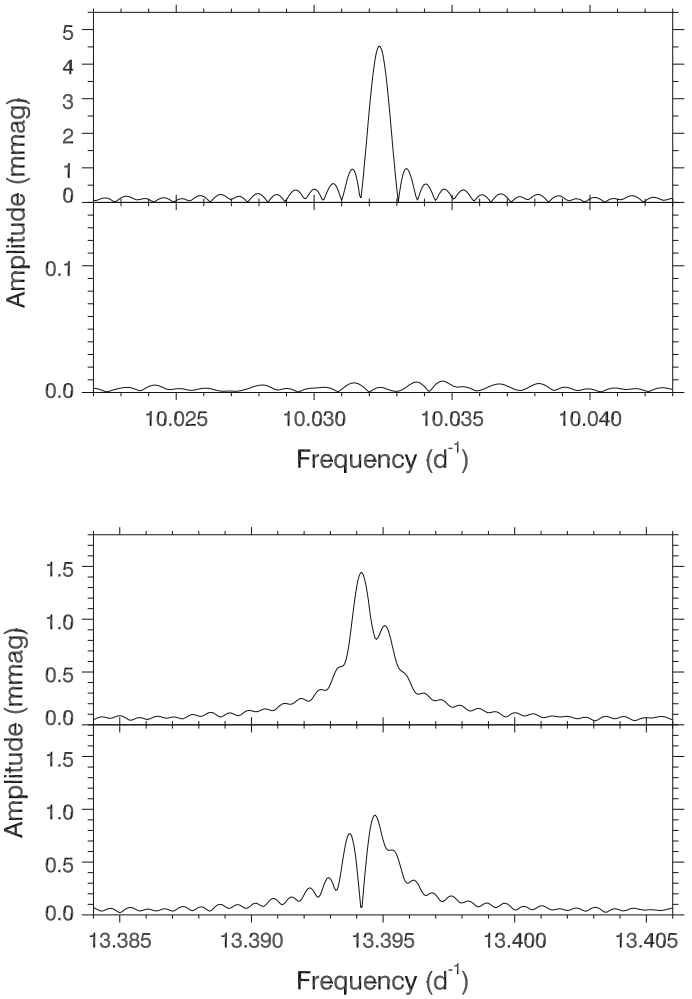

Fig. 3.3 The *top panel* shows a zoom-in of the amplitude spectrum of the highest amplitude pulsation mode at $\nu = 10.0323662\ \mathrm{d}^{-1}$ and the *bottom panel* shows the amplitude spectrum for the modulated pulsation mode at $\nu_{\mathrm{mod}} = 13.3941749\ \mathrm{d}^{-1}$. The *upper* and *lower* parts of each panel show the amplitude spectrum before and after pre-whitening, respectively, for each pulsation mode. Note the difference in the y-axis scale between the panels

1 mmag, which was the result of the peak being unresolved over the length of the 1470 d data set and is a clear result of amplitude modulation. It is important to note that this is the only pulsation mode that showed this behaviour and all others were stable in frequency and amplitude, remarkably stable to a few parts-per-million. Therefore, the analysis of KIC 7106205 by Bowman and Kurtz (2014) established that δ Sct stars can exhibit pulsation modes that are extremely stable in frequency and amplitude over 4 yr.

3.2.2 Amplitude and Phase Tracking

To quantify the observed amplitude modulation in the $\nu_{\rm mod}$ pulsation mode, Bowman and Kurtz (2014) divided the 4-yr data set for KIC 7106205 into 30 bins, each 50 d (except for the last one which was 20 d) in length. The amplitude and phase of each peak given in Table 3.2 were optimised using a linear least-squares fit at fixed frequency in each of the 30 bins (Bowman and Kurtz 2014). This amplitude and phase tracking method was applied to all frequencies listed in Table 3.2, with the results for the highest amplitude pulsation mode and the $\nu_{\rm mod}$ pulsation mode shown in the top and bottom panels of Fig. 3.4, respectively. A bin length of 50 d was chosen for tracking amplitude and phase at fixed frequency as a compromise between temporal and frequency resolution, although using a bin length between 30 and 100 d, with or without an overlap, does not significantly change the results (Bowman and Kurtz 2014).

The amplitude and phase tracking analysis revealed that the $\nu_{\rm mod}$ pulsation mode decreased significantly in amplitude from 5.161 ± 0.031 to 0.528 ± 0.055 mmag with concomitant phase modulation over the length of the data set, whilst all other peaks remained stable in both amplitude and phase (Bowman and Kurtz 2014). This was previously demonstrated using the *Kepler* data catalogues in Sect. 2.4.2, and is also shown graphically in the bottom panel of Fig. 3.4. This behaviour was concluded to be astrophysical and not instrumental, since if it were instrumental, one would expect all modes to decrease (or increase) in amplitude by approximately the same amount over the length of the data set (Bowman and Kurtz 2014).

The modulated pulsation mode $\nu_{\rm mod}$ is related in frequency to low-frequency peaks in the amplitude spectrum, which are given in Table 3.2. However, Bowman and Kurtz (2014) noted that these low-frequency peaks are also not purely periodic, and that the observed fluctuations in amplitudes and phases of these peaks were smaller than the uncertainties in the observed parameters. Furthermore, the low-frequency peaks had only small amplitudes such that it was unlikely that combination effects were the cause of the significant amplitude modulation (Bowman and Kurtz 2014). Since a decrease in amplitude of the $\nu_{\rm mod}$ pulsation mode was observed in KIC 7106205, one would expect the amplitudes of any potentially coupled g modes to significantly increase in amplitude if the visible pulsational energy budget is conserved. Thus, it was concluded that the pulsation mode energy associated with the decrease in amplitude of the $\nu_{\rm mod}$ pulsation mode was not transferred to any visible g modes in KIC 7106205 (Bowman and Kurtz 2014).

Another interesting result from the tracking analysis of KIC 7106205 was the sinusoidal variation in phase of the $\nu_{\rm mod}$ pulsation mode. Similarly to the amplitude modulation, this effect cannot be instrumental in origin, nor can it be caused by KIC 7106205 being in a binary system since this would induce frequency (phase) modulation in all observable pulsation modes (Shibahashi and Kurtz 2012; Murphy et al. 2014), which is clearly not the case.

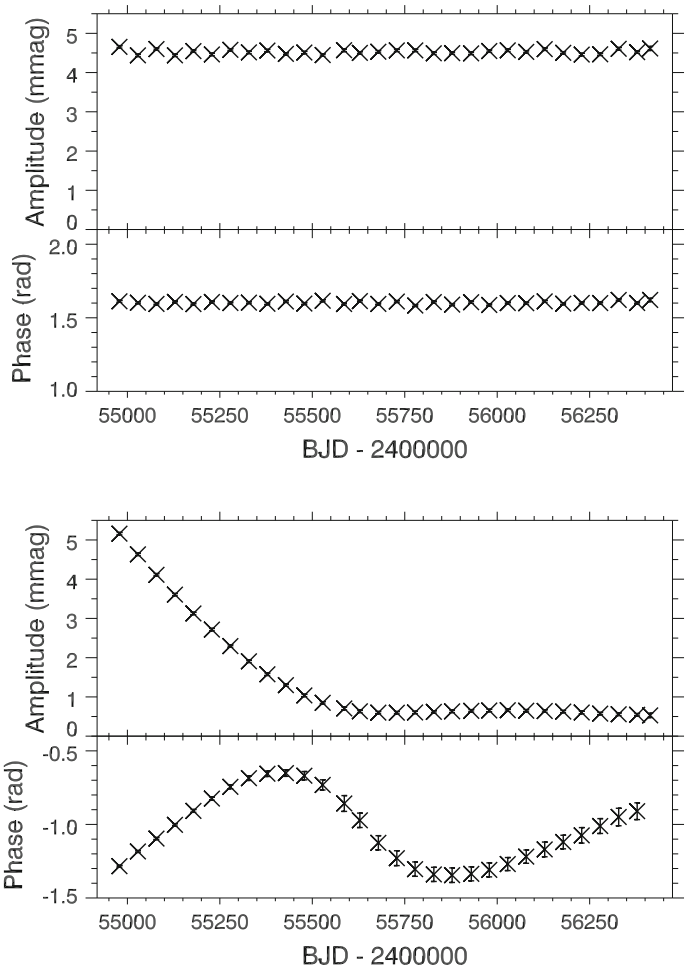

Fig. 3.4 The *top panel* shows the variability in amplitude and phase of the highest amplitude pulsation mode at $\nu = 10.0323662\ \mathrm{d}^{-1}$ over the 4-yr *Kepler* data set. The *bottom panel* shows the variability in amplitude and phase of the highest amplitude pulsation mode at $\nu_{\mathrm{mod}} = 13.3941749\ \mathrm{d}^{-1}$ over the 4-yr *Kepler* data set. Note the y-axis scales have been kept the same for both pulsation modes

3.3 Combining WASP and *Kepler* Data: The Case of the δ Sct Star KIC 7106205

Although space-based photometry offers unprecedented photometric precision and a high duty-cycle, which is useful for asteroseismology, the financial expenditure needed to build, launch and support such missions is large and so these missions often do not last for more than a few years. One of the major advantages of ground-based

telescopes is the relatively small maintenance and support costs, and the accessibility that can extend the lifetime of a telescope if a problem occurs.

For studying variable stars, the pulsation mode frequencies are the main data parameters, so high frequency resolution from long observations is preferable. It was discussed in Sect. 3.2 that 4 yr of *Kepler* data were not long enough to resolve the amplitude modulation in the δ Sct star KIC 7106205 (Bowman and Kurtz 2014), demonstrating that δ Sct stars are not purely periodic. Thus one wonders what happened before the *Kepler* data set started and after the *Kepler* data set ended. Observations from a ground-based telescope are thus extremely useful for extending the observations of a variable star over a longer time span.

In this section, it is discussed how the inclusion of ground-based photometric data, specifically from the Wide Angle Search for Planets (WASP) project, alongside *Kepler* data allowed Bowman et al. (2015) to study the multiperiodic δ Sct star KIC 7106205 (1SWASPJ191157.46+424022.6) over a longer time span than the 4 yr of the *Kepler* data set — a total of 6 yr in this case. Their aim was to investigate the unusual frequency and amplitude modulation in only a single pulsation mode frequency and to test if this behaviour was detectable in the WASP archival data.

3.3.1 The WASP Project

The Wide Angle Search for Planets (WASP) project is a wide-field survey that aims to find transiting exoplanets (Pollacco et al. 2006). The two instruments are located at the Observatorio del Roque de los Muchachos on La Palma and at the Sutherland Station of the South African Astronomical Observatory (SAAO), and achieved first light in 2003 and 2005, respectively. The instruments consist of eight 200-mm, f/1.8 Canon telephoto lenses mounted in a 2×4 configuration, each being backed by an Andor CCD of 2048×2048 pixels, which allows for a pixel size of about 14 arcsec. Observations are made using broad-band filters of 400–700 nm, with the normalised WASP wavelength response function plotted in comparison to the *Kepler* passband in Fig. 3.5. The data are reduced using the SYSREM algorithm (Tamuz et al. 2005), which corrects for extinction, the colour-response of the instrument, the zero-point, and instrumental systematics.

The observing strategy of WASP provides two consecutive 30 s exposures at a given pointing, before moving to the next available field; fields are typically revisited every 10 min. Such an observing strategy produces an extremely high Nyquist frequency, and has enabled the discovery of many types of variable stars, from long-period binary stars (Smalley et al. 2014), to high-frequency pulsating A stars (Holdsworth et al. 2014). For further details of the WASP project and the techniques used for the detection of pulsations, we refer the reader to Pollacco et al. (2006) and Holdsworth (2015), respectively.

The first WASP observations of the δ Sct star KIC 7106205 were in 2007 and provided the opportunity to study the amplitude modulation in this star 2 yr prior to the launch of the *Kepler* Space Telescope. However, the instrumentation differences

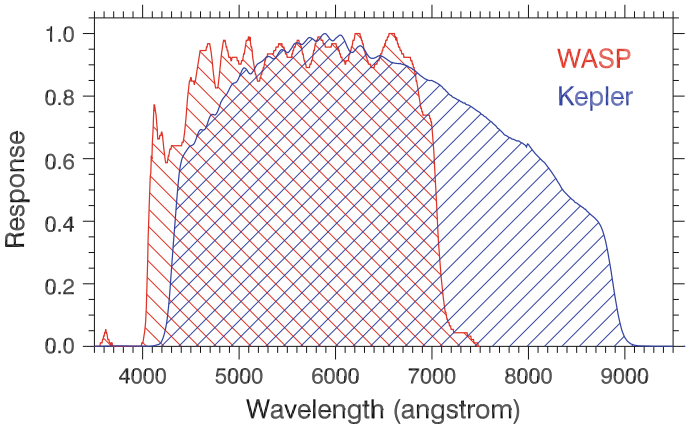

Fig. 3.5 The normalised wavelength response functions for the *Kepler* and WASP instruments are plotted as the *blue* and *red* hatched regions, respectively

between *Kepler* and WASP required Bowman et al. (2015) to calibrate the WASP data before a direct comparison to *Kepler* observations were made. These corrections were as follows:

(i) Amplitude suppression caused by instrument integration time.
(ii) Amplitude difference caused by different instrument passbands.
(iii) Amplitude dilution caused by contaminating neighbouring and/or background objects.

3.3.2 Using the HADS Star KIC 9408694 for Calibration

To calculate each of these correction factors, a star with a periodic, high-amplitude, thus high S/N, pulsation mode was required to have been observed simultaneously by WASP and *Kepler*. The star used by Bowman et al. (2015) was the HADS star KIC 9408694, which has a well-resolved dominant peak at 5.6610572 ± 0.0000005 d^{-1} that satisfied all the necessary requirements. Moreover, this star was studied by Balona et al. (2012) who determined that this peak is the fundamental radial p mode which did not vary in amplitude or frequency over the *Kepler* data set.

Simultaneous WASP and *Kepler* observations of KIC 9408694 were made in 2009 and 2010. A 1-d sample of simultaneous WASP and *Kepler* observations and the amplitude spectra of KIC 9408694 in 2009 and 2010 for both WASP and *Kepler* instruments are shown in Fig. 3.6. The *Kepler* data were truncated to cover the same start and end times as the WASP observations in each season, with each data set analysed to determine the pulsation amplitudes, $A_{0,\mathrm{W}}$ and $A_{0,\mathrm{K}}$ for the fundamental radial mode in KIC 9408694 (Bowman et al. 2015).

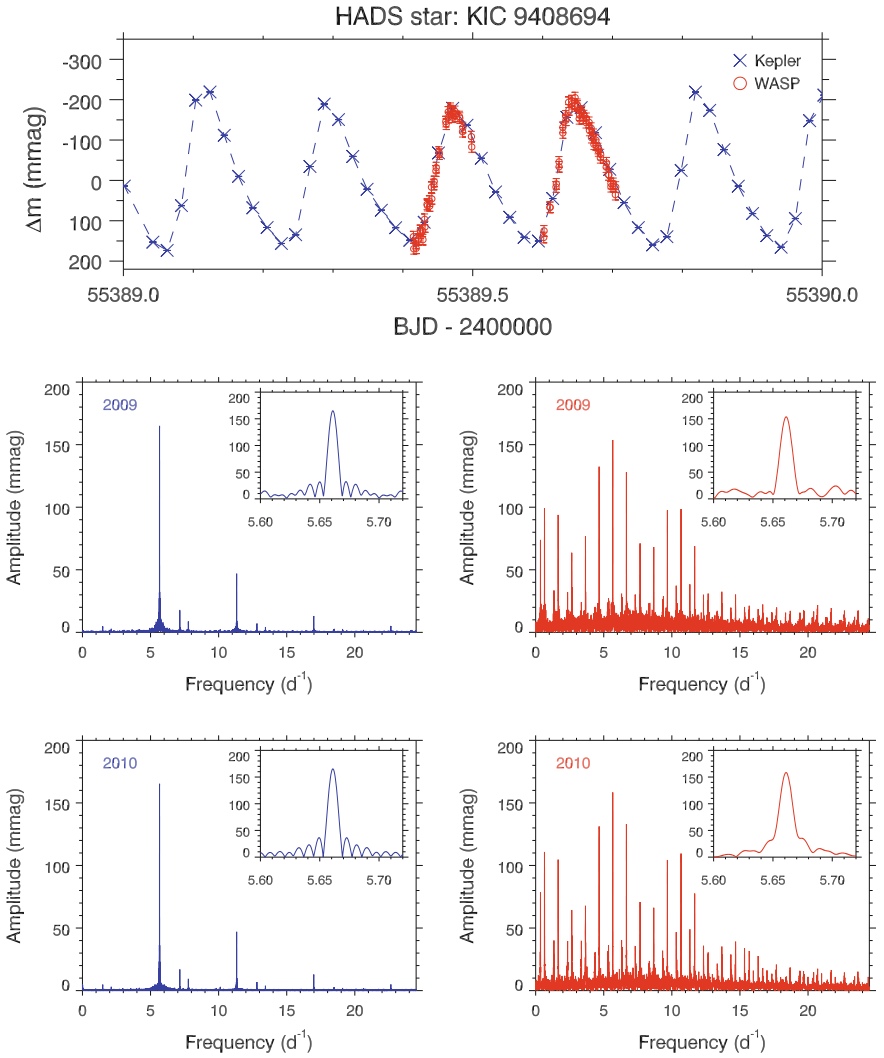

Fig. 3.6 Simultaneous WASP and *Kepler* observations of the HADS star KIC 9408694 covering 1 d are shown in the *top panel*. The *left*- and *right*-hand columns are the amplitude spectra, calculated out to the *Kepler* LC Nyquist frequency, for the *Kepler* (*blue*) and WASP (*red*) time series, respectively, in which 2009 and 2010 are the *top* and *bottom rows*. The sub-plots in each panel show a zoom-in view of the fundamental radial mode at $\nu = 5.6610572\ \mathrm{d}^{-1}$, used for calculating the *Kepler* and WASP passband differences

The first calibration required was to correct for the amplitude suppression in each of the WASP and *Kepler* data sets caused by the respective instrument's integration time. The correction to pulsation mode amplitudes was discussed in Sect. 2.3.3 and was calculated using Eq. 2.6 for KIC 9408694 (Bowman et al. 2015). However, KIC 9408694 is not isolated in the WASP aperture, but the background contaminating objects were approximately 3 mag fainter and only contributed a small amount of flux to the photometry. The dilution suffered by KIC 9408694 star was calculated by comparing the flux of the target star and contaminating stars using

$$\text{Dilution} = \left[1 - \left(\frac{F_\text{T}}{F_\text{T} + F_\text{C}}\right)\right] \times 100\,, \tag{3.1}$$

where F_T is the flux of the target and F_C is the combined flux of the contaminating stars (Holdsworth 2015). The dilution for the HADS star KIC 9408694 was calculated to be 14% — i.e., the observed amplitude of the fundamental radial mode was reduced by 1.1400 in the WASP observations (Bowman et al. 2015).

Therefore, the difference in the calculated pulsation mode amplitudes between WASP and *Kepler* observations (after optimising using linear least squares, correcting for dilution in the WASP data and integration time effects in both data sets) was solely a result of the difference in the instrument passbands and the ratio allows one data set to be scaled for comparison to the other (Bowman et al. 2015). The average of the ratio $\left(A_{0,\text{K}}/A_{0,\text{W}}\right)$ for each of the simultaneous observations in 2009 and 2010 was 0.9242 — i.e., the *Kepler* pulsation mode amplitude was 7.58 per cent smaller than that of the WASP observations solely from the passband differences, which is an expected result for an A star given the filter responses (Bowman et al. 2015).

3.3.3 Application to the Delta Scuti Star KIC 7106205

The WASP project observed the δ Sct star KIC 7106205 for three seasons, 2007, 2009, and 2010. The relatively large pixel size of the WASP instrument means that KIC 7106205 suffers from contamination from background sources (see Figs. 3.7 and 3.8). Therefore, after calibrating the WASP to the *Kepler* observations using the correction factors determined from the analysis of the HADS star KIC 9408694, another correction factor was needed to correct for the WASP aperture dilution before a comparison to *Kepler* data was performed (Bowman et al. 2015).

A 1-d sample of simultaneous WASP and *Kepler* observations and the amplitude spectra of KIC 7106205 in 2009 and 2010 for both WASP and *Kepler* instruments are shown in Fig. 3.7. Simultaneous observations by WASP and *Kepler* of KIC 7106205 in 2009 show the ν_mod peak, as seen in Fig. 3.7. To determine the WASP dilution correction factor, the simultaneous *Kepler* observations were truncated to the same length as the WASP observations, and the ν_mod peak was extracted from both data sets, optimised by linear least squares and then corrected for the different instrument integration times. The corrected amplitudes of the ν_mod peak in the WASP and

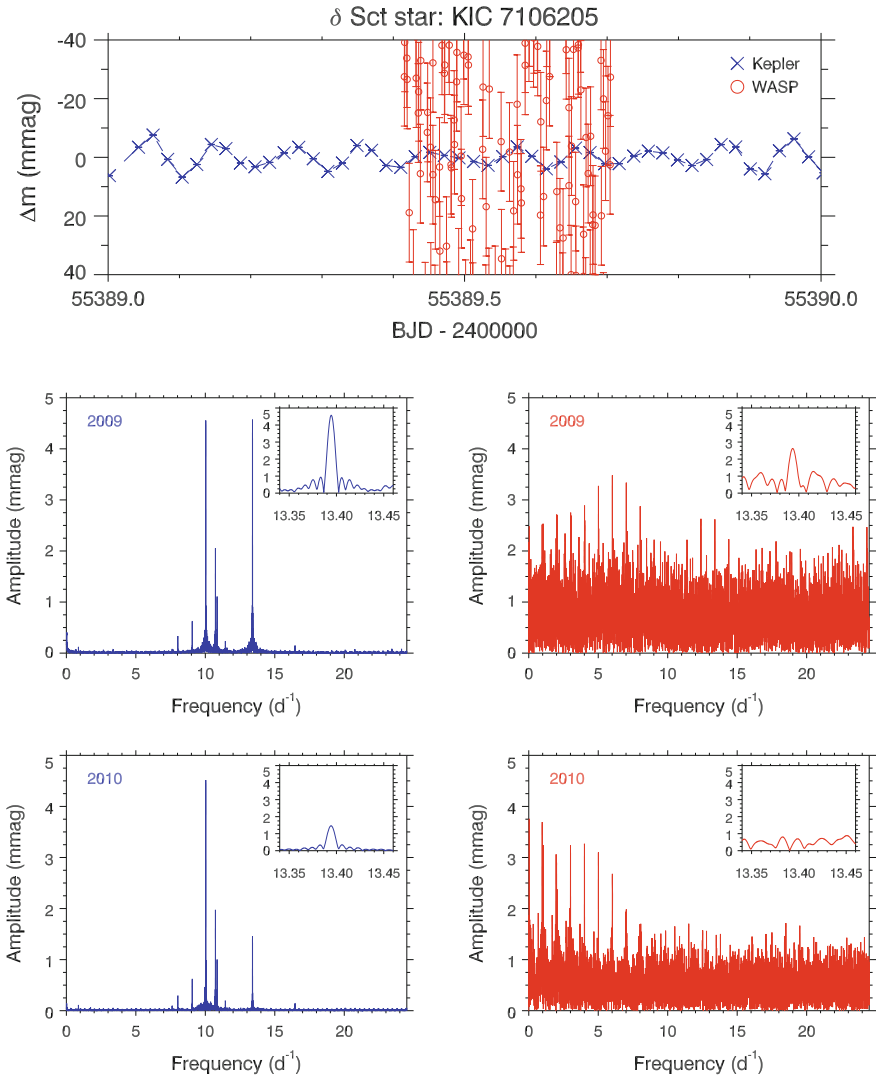

Fig. 3.7 Simultaneous WASP and *Kepler* observations of the δ Sct star KIC 7106205 covering 1 d are shown in the *top panel* with the larger scatter of WASP observations arising from a higher point noise. The *left*- and *right*-hand columns are the amplitude spectra, calculated out to the *Kepler* LC Nyquist frequency, for the *Kepler* (*blue*) and WASP (*red*) time series, respectively, in which 2009 and 2010 are the *top* and *bottom rows*. The sub-plots in each panel show a zoom-in of the modulated mode $\nu_{\rm mod} = 13.3941749\ {\rm d}^{-1}$

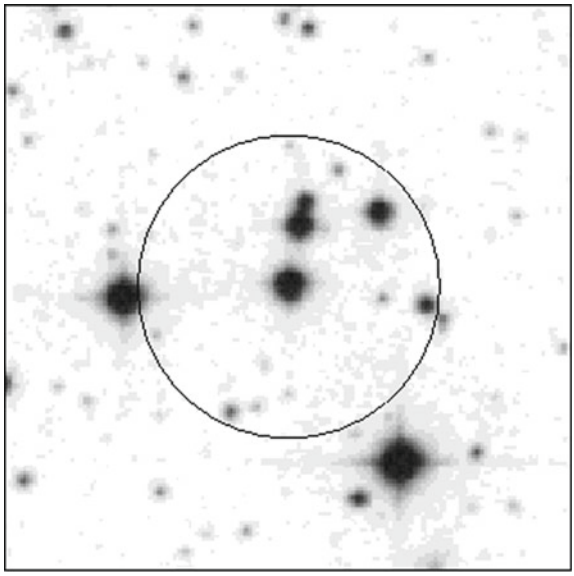

Fig. 3.8 The photometric aperture (*dark circle*) for KIC 7106205 in the WASP data showing multiple sources of contamination. The aperture is 48 arcsec (3.5 WASP pixels) in radius. Image from Digitized Sky Survey (DSS)

Kepler observations were $A_{0,\mathrm{W}} = 2.77 \pm 0.50$ mmag and $A_{0,\mathrm{K}} = 5.18 \pm 0.10$ mmag, respectively (Bowman et al. 2015).

To calculate the WASP dilution effect in KIC 7106205, the *Kepler* peak was transformed into the WASP passband, giving the expected WASP amplitude if no dilution occurred, A_{exp}. Therefore, the ratio between A_{exp} and $A_{0,\mathrm{W}}$ was solely a result of the dilution of other stars in the WASP aperture; this was calculated to be 2.0212 (Bowman et al. 2015). An alternative method used by Bowman et al. (2015) to calculate the WASP dilution correction factor was to use Eq. 3.1, which yielded a dilution factor of 1.7098. The difference in this value and the direct comparison of the two data sets is possibly from the bleeding of light from other nearby bright stars into the extracted WASP pixels. Therefore, Bowman et al. (2015) concluded that the most reliable method was to directly compare the observable pulsation mode amplitudes in each data set, as this also included correcting for any possibly unaccounted effects when correcting for the WASP dilution.

Unfortunately, the WASP observations obtained in 2010 did not show the ν_{mod} peak, which can be seen in the bottom-right panel in Fig. 3.7. The amplitude of the ν_{mod} peak in the 2010 *Kepler* observations was 1.46 ± 0.07 mmag, which after having been corrected for the *Kepler* integration time gives $A_{0,\mathrm{K}} = 1.66 \pm 0.08$ mmag (Bowman et al. 2015). The passband differences between WASP and *Kepler*, the WASP dilution factor for KIC 7106205 of 2.0212, and the WASP integration time correction predicted an amplitude of 0.87 ± 0.50 mmag for the ν_{mod} peak in the 2010 WASP observations. Despite being above the nominal detection limit of 0.5 mmag (Holdsworth et al. 2014), ν_{mod} was not observed in the 2010 WASP data due to higher photometric noise and large uncertainty (Bowman and Kurtz 2015).

3.3.4 Results from Combined WASP and Kepler Data

The direct calibration method employed by Bowman et al. (2015) enabled WASP observations obtained prior to the launch of the *Kepler* Space Telescope to be accurately and reliably compared to *Kepler* observations. The 2007 WASP data set for KIC 7106205 was 66.1 d in length and consisted of 3322 data points. Figure 3.9 shows the amplitude spectrum of the 2007 WASP data, from which the amplitude of the $\nu_{\rm mod}$ peak was extracted, optimised by linear least squares at a fixed frequency of 13.3941749 d^{-1} and then corrected using the methodology described previously. Using the same frequency from Bowman and Kurtz (2014) and the same zero-point of the time scale ($t_0 = 2\,455\,688.77$ BJD), ensured a realistic comparison between the two data sets. Due to the higher levels of noise present in WASP data compared to *Kepler* data, it was not possible to track amplitudes and phases of all pulsation modes in KIC 7106205 listed in Table 3.2.

A corrected amplitude of 11.70 ± 0.05 mmag was obtained for the $\nu_{\rm mod}$ pulsation mode in 2007 and the resulting amplitude modulation is shown graphically in Fig. 3.10. The inclusion of the WASP data alongside the *Kepler* data clearly illustrates that the amplitude of the $\nu_{\rm mod}$ pulsation mode has been steadily decreasing since at least 2007.

It should be noted that when a non-linear least-squares fit of the 2007 WASP data of KIC 7106205 was performed by Bowman et al. (2015), a frequency of 13.3924 ± 0.0001 d^{-1} and a corrected amplitude of 11.88 ± 0.06 mmag were obtained, which has a difference in amplitude of 0.18 mmag. Therefore, the $\nu_{\rm mod}$ pulsation mode has also possibly been exhibiting frequency and amplitude modulation since 2007 (Bowman et al. 2015). The result of the non-linear least-squares fit of the 2009 WASP data is within the uncertainty of the frequency obtained using 4 yr of *Kepler* observations. The difference of approximately 0.0018 d^{-1} between the frequencies obtained from

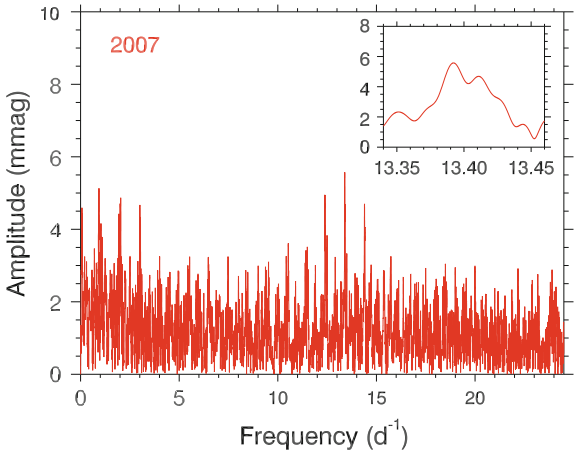

Fig. 3.9 The amplitude spectrum of the 2007 WASP data for KIC 7106205, calculated out to the *Kepler* LC Nyquist frequency. The sub-plot shows a zoom-in of $\nu_{\rm mod}$. Note the difference in y-axis scale compared to the amplitude spectra given in Fig. 3.7, illustrating the large decrease in the amplitude of $\nu_{\rm mod}$ between 2007 and 2009

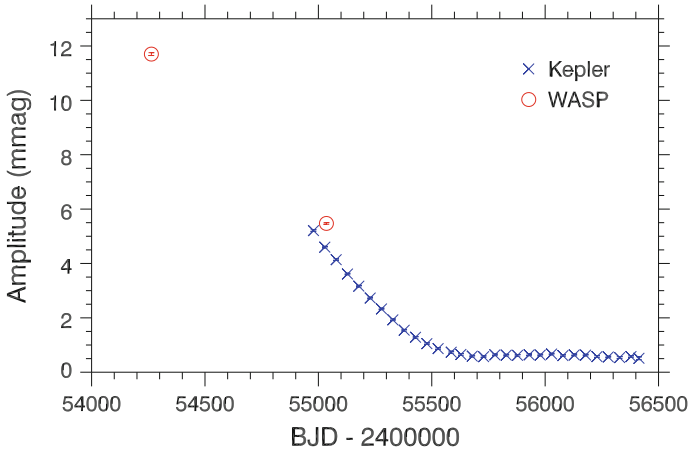

Fig. 3.10 Corrected and calibrated values of amplitude modulation in the pulsation mode $\nu_{\rm mod} = 13.3941749\,{\rm d}^{-1}$ in KIC 7106205 for *Kepler* (in 50-d bins) and WASP (single 66.1-d bin) data, shown as *blue* crosses ($\times$) and *red circles* ($\circ$), respectively. 1σ errors are calculated from the least-squares fit at fixed frequency, but are generally smaller than the data points

the linear and non-linear fits of the 2007 WASP data is smaller than the WASP frequency resolution, so Bowman et al. (2015) concluded that the linear least-squares fit was the more appropriate approach.

3.4 Spectroscopic Analysis of KIC 7106205

To support the photometric analysis of the δ Sct star KIC 7106205, spectroscopic follow-up observations were made with the Intermediate dispersion Spectrograph and Imaging System (ISIS) on the William Herschel Telescope (WHT). This telescope is part of the Isaac Newton Group (ING)[1] and is located at the Spanish Observatorio del Roque de los Muchachos of the Instituto de Astrofísica de Canarias on the island of La Palma. The spectral resolution of ISIS/WHT at 4000 Å using a 1 arcsec slit is approximately $R = \frac{\lambda}{\Delta\lambda} \simeq 2000$, which is sufficient to classify the spectral type of A and F stars and determine an approximate value for the effective temperature, and constrain surface gravity and rotational velocity by comparing the observed spectrum to synthetic spectra or standard stars.

A total of 23 δ Sct stars, which included KIC 7106205, were observed using ISIS/WHT between 30 March 2016 and 24 May 2016, with the right ascension, declination, apparent visual magnitude, SIMBAD classification and date of observations given in Table 3.3.

[1] ING website: http://www.ing.iac.es.

Table 3.3 Parameters of the 23 δ Sct stars observed using ISIS/WHT at epoch J2000.0 with a classification taken from the SIMBAD[†] data base if available

KIC ID	RA	Dec	m_V	Classification	Date observed
3429637	19:08:38.04	+38:30:31.96	7.72	δ Sct	30/03/2016
5964173	19:32:12.82	+41:16:23.68	12.04	δ Sct	20/05/2016
6357702	19:18:46.72	+41:44:21.34	11.27		20/05/2016
6590403	19:05:53.36	+42:02:14.50	10.55	δ Sct	30/03/2016
6848661	19:07:53.77	+42:21:41.98	11.55		30/03/2016
7106205	19:11:57.46	+42:40:22.89	11.38		30/03/2016
7217483	19:45:57.87	+42:45:23.17	10.54		21/05/2016
7533694	19:34:12.91	+43:07:03.54	10.29	δ Sct	24/05/2016
7830684	19:38:14.07	+43:34:10.67	12.07	δ Sct	20/05/2016
8177748	19:43:13.01	+44:05:53.81	11.76	rot var	20/05/2016
8196840	20:03:12.94	+44:04:03.99	11.81	δ Sct	21/05/2016
8246833	19:45:18.48	+44:08:03.85	11.98		21/05/2016
8386122	19:52:56.59	+44:23:24.84	10.45		21/05/2016
9156808	19:30:53.18	+45:33:12.75	11.29	δ Sct	20/05/2016
9353572	19:43:58.62	+45:53:54.74	10.51	δ Sct	21/05/2016
9408694	19:34:45.59	+45:54:16.32	11.48	δ Sct	20/05/2016
9642894	19:16:18.08	+46:21:16.03	11.27	δ Sct	30/03/2016
9700322	19:07:50.71	+46:29:11.93	12.61	δ Sct	30/03/2016
9773094	19:31:35.93	+46:35:19.48	11.37		30/03/2016
10273384	19:26:19.52	+47:23:36.72	11.68	δ Sct	20/05/2016
11513155	19:38:32.33	+49:26:40.09	11.19	star	20/05/2016
11661993	19:27:55.76	+49:45:43.37	9.33	δ Sct	24/05/2016
12117689	19:40:37.23	+50:38:31.47	11.74	star	20/05/2016

[†]http://simbad.u-strasbg.fr/simbad/

3.4.1 *Spectral Classification*

The ISIS/WHT spectrum for KIC 7106205 was reduced using `STARLINK` software,[2] which included cleaning of cosmic rays, de-biasing and flat-fielding. The normalised spectrum for the wavelength range $3800 \leq \lambda \leq 4600$ Å for the δ Sct star KIC 7106205 is shown in Fig. 3.11, along with MK standard F0 V and F2 V stars above and below, respectively, for comparison. The spectral classification of KIC 7106205 closely followed the prescription of Gray and Corbally (2009).

It was discussed in Sect. 1.3.2 how a significant fraction of A stars are Am stars, which are defined as having a difference of at least five spectral subclasses between the Ca K line strength and the metallic line strengths (Conti 1970; Smith 1971a, b). It does not take more than a cursory study of the spectrum of KIC 7106205 in Fig. 3.11

[2] `STARLINK` website: http://starlink.eao.hawaii.edu/starlink/.

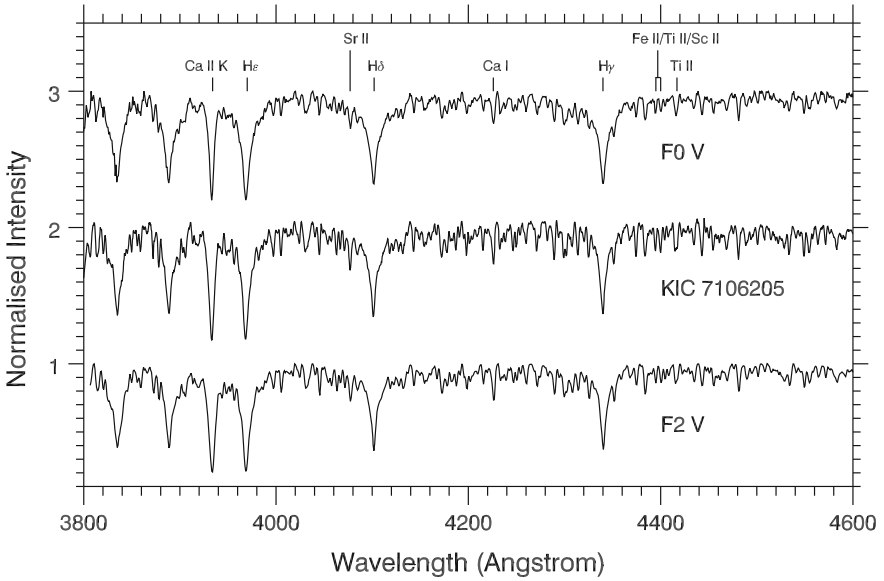

Fig. 3.11 Normalised spectrum of the δ Sct star KIC 7106205, in the wavelength range $3800 \leq \lambda \leq 4600$ Å. The spectra above and below are F0 V and F2 V MK standard stars, respectively, taken from Gray and Corbally (2009)

to note the similar line strengths of the Ca II K and hydrogen lines (Hϵ, Hδ and Hγ), indicating that the Ca II K line strength is normal for a star of spectral type F0 V. On the other hand, the Sr II and Ca I lines in KIC 7106025 appear stronger than in the chemically-normal standard stars shown above and below in Fig. 3.11. Thus KIC 7106205 does have small, yet significant, differences between its Ca II K and metal line strengths and can be classified as a marginal Am star (i.e., Am:). This is not surprising considering the large fraction of A stars that are Am and Am: stars (Conti 1970; Smith 1971a, b).

The low-to-medium resolution of the ISIS/WHT spectrum for KIC 7106205 means that the spectral type of F0 V determined from its hydrogen line strengths is consistent with the effective temperature of $T_{\rm eff} = 6900 \pm 150$ K listed in the KIC for this star. However, the resolution of the spectrum was insufficient to determine precise values of the rotational velocity and surface gravity of KIC 7106205, but these were constrained to $v \sin i \leq 100\ {\rm km\,s^{-1}}$ and $\log g \simeq 4$ (cgs), respectively. Therefore, the spectroscopic analysis of KIC 7106205 indicates that this star is likely a moderate rotator for its spectral type and confirms it is near the red edge of the classical instability strip in the HR diagram.

The spectroscopic analysis of KIC 7106205 indicates that this δ Sct star is not a classical Am star, because it does not have a difference of at least five spectral subclasses between its Ca II K and metal lines. It does have a few relatively strong metal lines for a F0 V star and so can be considered an Am: star, although it should be noted that the spectrum of KIC 7106205 is noisier than the standard stars given in

Fig. 3.11, because a relatively lower signal-to-noise ratio of $S/N \simeq 100$. It appears that chemical peculiarity does not offer a solution to why the δ Sct star KIC 7106205 exhibits amplitude modulation, but further work is needed to address this (Bowman 2016).

A larger and more statistically significant analysis of δ Sct stars is needed, including the remaining stars given in Table 3.3, to establish if chemical peculiarities in A stars are related to amplitude modulation of pulsation modes in δ Sct stars. This is especially since it is only a recent discovery that a significant fraction of Am stars have been observed to pulsate (Smalley et al. 2011, 2017).

3.5 Discussion

Only a single pulsation mode was observed to exhibit amplitude modulation in KIC 7106205 whilst all other statistically significant modes remained constant in amplitude, such that the visible pulsation energy budget was not conserved over the 4-yr *Kepler* data set (Bowman and Kurtz 2014). Ground-based data from the Wide Angle Search for Planets (WASP; Pollacco et al. 2006) were used to extend the study of KIC 7106205 with the majority of the amplitude modulation in this variable pulsation mode occurring prior to the launch of the *Kepler* Space Telescope (Bowman et al. 2015). It is clear from these studies that time spans of years and decades are important in δ Sct stars with the 4-yr *Kepler* data set providing only a blink-of-an-eye insight into the physics at work in these stars.

The analysis of the δ Sct star KIC 7106205 revealed that a single p mode with a frequency of $\nu_{\rm mod} = 13.3941749\ {\rm d}^{-1}$ decreased in amplitude by more than a factor of 20 over 6 yr (Bowman and Kurtz 2014; Bowman et al. 2015). WASP data for KIC 7106205 were calibrated to *Kepler* observations by correcting for the difference in instrument integration times, passband differences and dilution effects and included alongside *Kepler* observations. This allowed the amplitude and frequency modulation of the $\nu_{\rm mod}$ pulsation mode to be extended back to 2007, 2 yr prior to the launch of the *Kepler* Space Telescope (Bowman et al. 2015). The amplitude and phase tracking routine used to study the variability of this mode showed that its amplitude changed from 11.70 ± 0.05 mmag in 2007, to 5.87 ± 0.03 mmag in 2009, and to 0.58 ± 0.06 mmag in 2013 (Bowman et al. 2015).

There are various possible explanations for the lost mode energy: resonant mode-coupling, beating of multiple unresolved pulsation modes, or loss of mode energy to the convection zone and/or the pulsational p mode driving He II ionisation zone. Beating from unresolved close-frequency pulsation modes can produce amplitude modulation, but a multifrequency (more than two) model is required because of the non-sinusoidal amplitude modulation observed (Breger and Bischof 2002; Bowman and Kurtz 2014; Bowman et al. 2016). Furthermore, these multiple frequencies would need to be closer than the *Kepler* resolution limit of $0.00068\ {\rm d}^{-1}$ such that they are unresolved, which is unlikely for a δ Sct star with such low mode density in its amplitude spectrum.

Non-linearity in the form of a parametric resonance instability is predicted in δ Sct stars, in which the instability of a linearly driven mode at ν_1 causes the growth of two modes at ν_2 and ν_3 such that $\nu_1 \simeq \nu_2 + \nu_3$, satisfying a resonance condition (Dziembowski 1982). The most likely scenario is the decay of a high-amplitude p mode into two g modes (Dziembowski 1982). This mechanism of amplitude modulation was investigated for KIC 7106205 by Bowman and Kurtz (2014) but without success because mode coupling to high-degree modes that are not visible in broad-band photometry could not be ruled out. The application of studying non-linearity and mode coupling in δ Sct stars is discussed in detail in Chap. 6.

Another possible mechanism for amplitude modulation are the structural changes to a star caused by stellar evolution. Murphy et al. (2012) analysed the ρ Pup star KIC 3429637 (HD 178875), in which two p modes slowly increased in amplitude over the first 2 yr of *Kepler* observations. They speculated that the observed amplitude modulation may be caused by structural changes in the star which consequently alter the properties of the He II driving zone. Thus, it may be possible to observe stellar evolution in real time, a concept which is the discussed further in Chap. 7. Amplitude modulation caused by stellar evolution is unlikely in KIC 7106205 since the $\nu_{\rm mod}$ pulsation mode was not the highest overtone p mode observed in the star. The pulsation mode at 16.4530392 d^{-1}, labelled p_8 in Table 3.2, was observed to be stable in amplitude, which would be more strongly affected by structural changes since it is more sensitive to the physical conditions near the stellar surface (Bowman and Kurtz 2014).

A spectroscopic analysis of KIC 7106205 using a classification-resolution spectrum obtained from ISIS/WHT revealed that KIC 7106205 does not show the necessary difference of at least five spectral subclasses between its Ca II K and metal line strengths to be defined as a classical Am star. KIC 7106205, however, does have relatively strong Sr II and Ca I metal lines for a F0 V star so can be considered an Am: star. The lack of strong chemical peculiarities in this star implies that this is unrelated to the observed amplitude modulation. The spectroscopic analysis of KIC 7106205 also showed that this star is likely a slow-to-moderate rotator near the red edge of the classical instability strip in the HR diagram. The spectroscopic classification of F0 V determined from comparison of the hydrogen line strengths of KIC 7106205 to standard stars from Gray and Corbally (2009) is consistent with the KIC and Huber et al. (2014) values for KIC 7106205 of $T_{\rm eff} \simeq 6900 \pm 150$ K.

In summary, mode coupling to high-degree modes or internal g modes, beating of multiple unresolved close-frequency pulsation modes and energy being lost to a damping region are all possible explanations of the amplitude modulation observed in KIC 7106205 (Bowman and Kurtz 2014; Bowman et al. 2016). The analyses discussed in this chapter do not distinguish which of these possibilities is physically most or least likely, only that the mode energy lost from the $\nu_{\rm mod}$ pulsation mode was not transferred to any other observed pulsation modes. In reality, all of these mechanisms could be operating in congruence, as they are all feasible solutions to the observed amplitude modulation, which complicates the issue of testing the hypothesis of energy conservation amongst pulsation modes in a δ Sct star. It naturally followed from these studies of amplitude modulation to investigate the effects of beating,

mode-coupling and energy conservation in other δ Sct stars, which are discussed in Chaps. 5 and 6, respectively.

The majority of the significant decrease in mode amplitude of a single pulsation frequency in KIC 7106205 occurred prior to the launch of the *Kepler* mission. Therefore, it is important to remember that the *Kepler* observations provide an extremely high quality, yet small snapshot of 4 yr of data, which is a mere blink-of-an-eye insight into the stellar physics at work within this star. Time spans of the order of a decade may be more significant in δ Sct stars than was previously thought and analyses of these so-called coherent pulsators should take this into account. KIC 7106205 is a special case study – an archetypal example of amplitude modulation in a δ Sct star – that provides strong motivation to study amplitude modulation and energy conservation of pulsation modes in a large number of δ Sct stars, which is discussed in Chap. 5.

References

Balona, L. A., Lenz, P., Antoci, V., et al. 2012, MNRAS, 419, 3028
Bowman, D. M. 2016, PhD thesis, Jeremiah Horrocks Institute, University of Central Lancashire, UK
Bowman, D. M. & Kurtz, D. W. 2014, MNRAS, 444, 1909
Bowman, D. M. & Kurtz, D. W. 2015, in European Physical Journal Web of Conferences, Vol. 101, European Physical Journal Web of Conferences, 6013
Bowman, D. M., Holdsworth, D. L., & Kurtz, D. W. 2015, MNRAS, 449, 1004
Bowman, D. M., Kurtz, D. W., Breger, M., Murphy, S. J., & Holdsworth, D. L. 2016, MNRAS, 460, 1970
Breger, M. 2000, MNRAS, 313, 129
Breger, M. & Bischof, K. M. 2002, A&A, 385, 537
Brown, T. M., Latham, D. W., Everett, M. E., & Esquerdo, G. A. 2011, AJ, 142, 112
Conti, P. S. 1970, PASP, 82, 781
Dziembowski, W. 1982, Acta Astronomica, 32, 147
Gray, R. O. & Corbally, J., C. 2009, Stellar Spectral Classification(Princeton Series in Astrophysics)
Holdsworth, D. L. 2015, PhD thesis, Keele University, UK
Holdsworth, D. L., Smalley, B., Gillon, M., et al. 2014, MNRAS, 439, 2078
Huber, D., Silva Aguirre, V., Matthews, J. M., et al. 2014, ApJS, 211, 2
Murphy, S. J., Grigahcène, A., Niemczura, E., Kurtz, D. W., & Uytterhoeven, K. 2012, MNRAS, 427, 1418
Murphy, S. J., Bedding, T. R., Shibahashi, H., Kurtz, D. W., & Kjeldsen, H. 2014, MNRAS, 441, 2515
Pollacco, D. L., Skillen, I., Collier Cameron, A., et al. 2006, PASP, 118, 1407
Shibahashi, H. & Kurtz, D. W. 2012, MNRAS, 422, 738
Smalley, B., Kurtz, D. W., Smith, A. M. S., et al. 2011, A&A, 535, A3
Smalley, B., Southworth, J., Pintado, O. I., et al. 2014, A&A, 564, A69
Smalley, B., Antoci, V., Holdsworth, D. L., et al. 2017, MNRAS, 465, 2662
Smith, M. A. 1971a, A&A, 11, 325
Smith, M. A. 1971b, AJ, 76, 896
Tamuz, O., Mazeh, T., & Zucker, S. 2005, MNRAS, 356, 1466
Uytterhoeven, K., Moya, A., Grigahcène, A., et al. 2011, A&A, 534, A125

Chapter 4
Kepler Observations of Delta Scuti Stars

4.1 Introductory Remarks

This chapter focusses on the statistical properties of an ensemble of δ Sct stars observed by the *Kepler* Space Telescope. It was previously discussed in Sect. 1.2.2 how the δ Sct stars are the most common type of pulsator among main sequence A and F stars, and are found in a transition region between low- and high-mass stars in the HR diagram. Before the advent of space telescopes, the δ Sct stars were well defined by the observational blue and red edges of the classical instability strip (Rodríguez and Breger 2001), although with improved instrumentation yielding more precise observations, this may no longer be the case. These multiperiodic pulsators are interesting to study using asteroseismology, as the various pulsation modes are sensitive to different depths within a star, thus physical properties can be determined throughout the interior.

In this chapter, the somewhat unexpected discovery of many δ Sct/γ Dor hybrid stars amongst the A and F stars observed by *Kepler* is discussed in Sect. 4.2. In Sect. 4.3, the so-called 'organ pipe' stars are discussed in the context of the incidence of low-frequency peaks in the amplitude spectra of δ Sct stars. In Sect. 4.4, an example of a star pulsating in g modes that lies in the no-man's land between the hot edge of the γ Dor instability region and the cool edge of the SPB instability region is provided. These stars have been termed 'hot γ Dor stars' in the literature (e.g., Balona 2014) and are a challenge to pulsation theory. In Sect. 4.5, it is discussed how an ensemble of 983 δ Sct stars that were observed continuously by *Kepler* for 4 yr was created, which was large enough to characterise statistical properties of the δ Sct stars, including an evaluation of the observational blue and red edges of the classical instability strip. Section 4.7 discusses the correlations between the dominant pulsation mode frequency and stellar parameters using the ensemble of 983 δ Sct stars.

D.M. Bowman, *Amplitude Modulation of Pulsation Modes in Delta Scuti Stars*,
Springer Theses, DOI 10.1007/978-3-319-66649-5_4

4.2 Hybrid Stars

The theoretical instability regions of the δ Sct and γ Dor stars have been shown to overlap in the HR diagram (Dupret et al. 2004). Hybrid pulsators from the δ Sct and γ Dor pulsational excitation mechanisms occurring simultaneously within a star were first predicted by Dupret et al. (2005), but only expected to comprise a small minority of A and F stars. Prior to the recent space photometry revolution, very few hybrid δ Sct/γ Dor stars were known (see e.g., Handler 2009). One of the first confirmed hybrid pulsators was HD 209295, which was studied by Handler and Shobbrook (2002b). Although the g- and p-mode frequencies in HD 209295 were confirmed to be from the same star, it was later shown that the g modes were tidally excited from the star being in an eccentric binary (Handler et al. 2002).

The *Kepler* mission data revealed that many δ Sct stars are in fact hybrid pulsators (Grigahcène et al. 2010a; Uytterhoeven et al. 2011; Balona 2011), exhibiting both p modes ($\nu \geq 5\,\mathrm{d}^{-1}$) and g modes ($\nu < 4\,\mathrm{d}^{-1}$). Attempts have been made to catalogue the different types of hybrid behaviour observed; for example, it has been suggested that δ Sct/γ Dor hybrids and γ Dor/δ Sct hybrids are two distinct groups (Grigahcène et al. 2010a, b). These definitions were used to distinguish hybrid stars that have dominant pulsation modes in the δ Sct and γ Dor frequency regimes, respectively (Grigahcène et al. 2010a). Classifying hybrid stars into these subgroups using these definitions is some what of a pedantic exercise as it often requires visual inspection of the light curves and amplitude spectra of many stars, which can be a lengthy and subjective process. Currently it is not established whether there are any significant physical differences for why a hybrid star should exhibit higher amplitude pulsation modes in one frequency regime compared to the other. It is not clear whether the definitions of Grigahcène et al. (2010a) are distinct groups and so all hybrid stars in this monograph and in the literature are considered a single pulsator type.

A statistical analysis of 750 A and F stars was carried out by Uytterhoeven et al. (2011) using 1 yr (Q0 – Q4) of LC *Kepler* data from the start of the mission. The authors discovered that 475 of these stars were pulsating in either g or p modes, with 171 stars (23%) being classified as hybrid pulsators. The distributions of δ Sct, γ Dor and hybrid stars on a $T_{\mathrm{eff}} - \log g$ diagram from Uytterhoeven et al. (2011) are given in Fig. 4.1, which are shown as red squares, blue stars and black circles, respectively. The top panel in Fig. 4.1 shows the δ Sct, γ Dor and hybrid stars studied using ground-based observations and the bottom panel shows the stars studied by Uytterhoeven et al. (2011) using *Kepler* data for comparison. Using the high-quality *Kepler* data, Uytterhoeven et al. (2011) demonstrated that a significant fraction of A and F stars exhibit at least some form of hybrid behaviour and that the hybrid stars are not restricted to where the δ Sct and γ Dor instability regions overlap in the HR diagram.

The hybrid fraction from Uytterhoeven et al. (2011) can be considered a conservative estimate of the hybrid fraction amongst all δ Sct stars observed by *Kepler*. With the complete 4-yr data set, and subsequently improved frequency resolution and amplitude precision, many more δ Sct stars are observed to have low-frequency

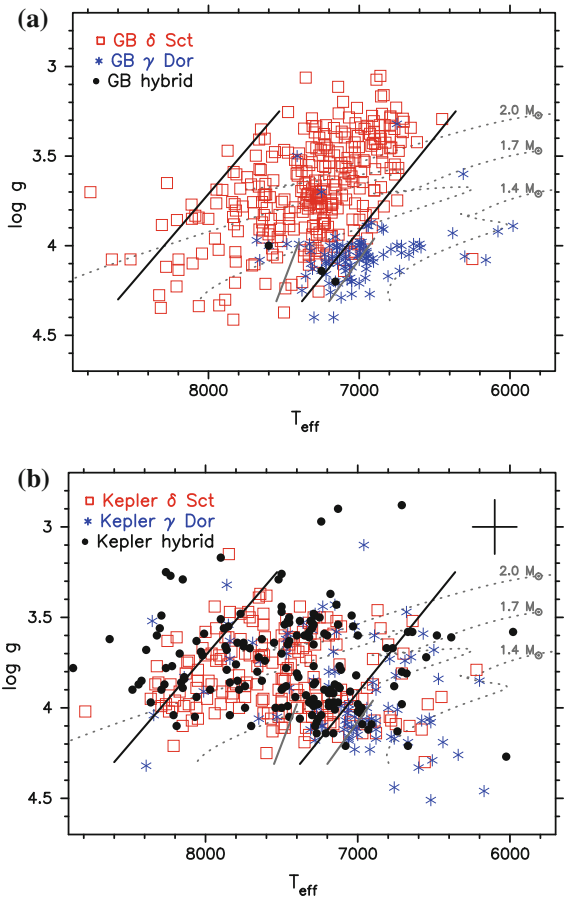

Fig. 4.1 $T_{\rm eff}$ – log g diagrams for intermediate-mass pulsators. The *top panel* shows the known δ Sct stars (shown as *red squares*), γ Dor stars (shown as *blue stars*) and hybrid stars (shown as *filled black circles*) observed using ground-based data. The *bottom panels* shows the same classifications of stars using the first 1 yr of *Kepler* data. The *black* and *grey solid lines* indicate the observational edges of the δ Sct and γ Dor instability regions taken from Rodríguez and Breger (2001) and Handler and Shobbrook (2002a), respectively, and the *dotted lines* represent evolutionary tracks. Figure from Uytterhoeven et al. (2011), their Fig. 10. © ESO; reproduced with permission from A&A

peaks in their amplitude spectra, but it is not established if these are always caused by pulsation (Balona 2011; Balona and Dziembowski 2011; Balona 2014).

The hybrid stars offer the opportunity to study stellar structure throughout a star's interior, because the g modes excited from the flux blocking mechanism are sensitive to conditions near the core and the p modes excited by the κ mechanism are sensitive to conditions near the surface (Aerts et al. 2010). Understanding the multiperiodic hybrid stars is an exciting prospect for asteroseismology as one can make measurements of the radial rotation profile in main sequence A and F stars (Kurtz et al. 2014; Saio et al. 2015; Keen et al. 2015; Triana et al. 2015; Murphy et al. 2016; Schmid and Aerts 2016).

Ideally, the hybrid stars could be used to study the pulsation excitation mechanisms directly, particularly the possible exchange of energy between pulsation modes excited by the different mechanisms. This idea was explored by Chapellier et al. (2012), who studied the interaction between 180 g-mode and 59 p-mode

independent pulsation mode frequencies in the CoRoT hybrid star ID 105733033. The authors demonstrated that the p- and g-mode frequencies originated in the same star and that a coupling mechanism must exist to explain the observed mode interaction between the g- and p-mode frequency regimes (Chapellier et al. 2012).

4.2.1 Are all Hybrid Stars Binaries?

Binarity may appear to be a simple solution to the discovery that the amplitude spectra of many δ Sct stars contain g-mode frequencies, which are associated with a pulsating companion star. The binary fraction of A stars is approximately 35% (Abt 2009; Duchêne and Kraus 2013; Moe and Di Stefano 2017), so to first order this means that a non-negligible fraction of δ Sct stars are in binary systems. However, for most δ Sct stars in binary systems the companion is likely to have a mass too small to be a g-mode pulsator such as a SPB or γ Dor star. Binarity cannot explain all hybrid stars discovered by *Kepler*, because the binary fraction of δ Sct stars is similar to that of all A stars and of the order 30% (S. Murphy, *private communication*). Therefore, the majority of δ Sct stars are in single star systems.

It has been demonstrated by Chapellier et al. (2012), Kurtz et al. (2014) and Van Reeth et al. (2015) (and others) that not all hybrid stars are the result of binary systems with a δ Sct primary and γ Dor secondary, or vice versa. Hybrid stars have been confirmed as members of both single and multiple systems, with p mode frequencies from the κ mechanism and g mode frequencies from the flux blocking mechanism as predicted by Dupret et al. (2005), but in greater numbers in the *Kepler* data set than were originally anticipated.

4.2.2 Pure Delta Scuti Stars

Although there are many hybrid stars in the *Kepler* data set, there are also pure δ Sct stars that show no significant low-frequency peaks in their amplitude spectra. Balona (2014) investigated the incidence of peaks in the γ Dor frequency regime using approximately 1800 δ Sct stars observed by *Kepler* for 1061 d (i.e., Q0 – Q12). He suggested that the majority of, if not all, δ Sct stars have low-frequency peaks in their amplitude spectra and the term hybrid should no longer be used as all δ Sct stars are hybrid stars (Balona 2014; Balona et al. 2015). Whilst it is true that many δ Sct stars have low-frequency peaks in their amplitude spectra, it is not true that they all do. Furthermore, it is not established if the low-frequency peaks are always caused by g-mode pulsations in δ Sct stars.

An example of a δ Sct star with no g modes is KIC 5617488, with its amplitude spectrum given in Fig. 4.2. The sub-plot in the top-left corner of Fig. 4.2 contains a zoom-in of the low-frequency regime for this star, which shows a distinct lack of significant peaks in the typical g-mode frequency range of $0.3 \leq \nu \leq 4$ d^{-1}. A commonly used criterion for whether a peak in an amplitude spectrum is statistically

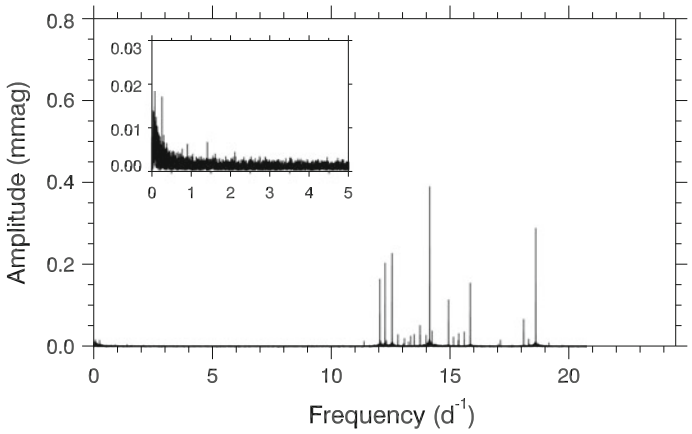

Fig. 4.2 The amplitude spectrum of the pure δ Sct star KIC 5617488 with no statistically significant low-frequency peaks in its amplitude spectrum that can be confirmed as g-mode pulsation frequencies. Note that the peaks between $10 \leq \nu \leq 20$ d^{-1} are mostly sNa frequencies. The rise in noise at low frequencies ($\nu \leq 0.5$ d^{-1}) is common when using msMAP PDC *Kepler* data (see Sect. 2.2.2)

significant is if it has a signal-to-noise ratio in amplitude of $S/N \geq 4$ (Breger et al. 1993). The few peaks in the g-mode frequency regime for KIC 5617488 in Fig. 4.2 have amplitudes of order a few μmag, thus do not satisfy the statistical significance criterion from Breger et al. (1993). The low-frequency peaks in KIC 5617488 cannot be claimed to be statistically significant, let alone represent g-mode pulsation frequencies. Although they are uncommon, this is also demonstrably true for other δ Sct stars, thus pure δ Sct stars pulsating only in p modes do exist, which is contrary to the claim made by Balona (2014) and Balona et al. (2015) that all δ Sct stars are hybrid stars.

Therefore, various studies of hybrid stars across a range of effective temperatures have shown that the majority of δ Sct stars have g-mode pulsation frequencies, but not all do (Grigahcène et al. 2010a; Uytterhoeven et al. 2011; Balona 2011). Further work is needed to study the interplay between the flux blocking mechanism and the κ mechanism in A and F stars, with a focus on understanding the observed minority of δ Sct stars pulsating in purely p modes.

4.3 Low Frequencies in Delta Scuti Stars: The Organ Pipe Stars

Many δ Sct stars in the *Kepler* data set have low-frequency peaks in their amplitude spectra (Balona and Dziembowski 2011; Balona 2014), but it is not established whether these frequencies are always caused by pulsation or the effects of rotation as claimed by Balona (2011, 2013), or have some other cause. For δ Sct stars that have

high effective temperatures, $T_{\rm eff} \geq 8000\,{\rm K}$, such that they are not found within the overlap of the δ Sct and γ Dor instability regions, these low frequencies are difficult to explain as g modes because these stars do not have a thick enough convective envelope to support the convective flux blocking excitation mechanism (Guzik et al. 2000; Dupret et al. 2004, 2005).

Balona et al. (2015) investigated if increased sources of opacity within pulsation models of δ Sct stars were able to explain the low frequencies in terms of pulsation modes excited from the κ mechanism. Increasing the opacity at $T \simeq 115\,000\,{\rm K}$ within the models by a factor of two caused low-degree modes at low frequency to be excited, but also decreased the range of pulsation mode frequencies such that the models were no longer consistent with observations (Balona et al. 2015). It was suggested by Balona et al. (2015) that non-linearity may be, at least in part, responsible for the incidence of low frequencies and the diversity in pulsational behaviour among δ Sct stars. This provides strong motivation for studying pulsations in δ Sct stars as a single population, but also individual stars so that insight of the excitation mechanisms, specifically non-linearity, can be gained.

In this section, a subgroup of δ Sct stars that have been called 'organ pipe' stars is discussed. The organ pipe stars have a series of low-frequency peaks in their amplitude spectra, which are often highly variable in amplitude and phase in a chaotic manner. This coined the term organ pipe as the peaks appear and disappear in an amplitude spectrum throughout the *Kepler* data set, analogous to the various harmonics from an organ in a piece of music. Many δ Sct stars have these low frequencies, but since they often have low amplitudes they are not discovered until the high-amplitude pulsation modes and their window patterns are removed by pre-whitening. In this section, a case study using the organ pipe δ Sct star KIC 10407873 is used to demonstrate that these low-frequency peaks are not necessarily always caused by rotation.

Consider a simple model of a typical δ Sct star with a mass of $M = 1.8\,{\rm M}_{\odot}$ and a radius of $R = 2\,{\rm R}_{\odot}$. To first order, a slow rotator with $v \sin i \simeq 50\,{\rm km\,s^{-1}}$ would produce a rotational splitting of approximately $0.5\ {\rm d}^{-1}$, a moderate rotator with $v \sin i \simeq 100\,{\rm km\,s^{-1}}$ would produce a rotational splitting of approximately $1.0\ {\rm d}^{-1}$, and a fast rotator with $v \sin i \simeq 200\,{\rm km\,s^{-1}}$ would produce a rotational splitting of approximately $2.0\ {\rm d}^{-1}$. Therefore, rotation can easily create complex amplitude spectra with only a few non-radial modes. Now let us consider a hypothetical δ Sct star which has two important properties:

(i) The δ Sct star pulsates in non-radial pulsation modes and is a moderate rotator, with the rotation splitting non-radial pulsation modes into their $2\ell + 1$ components. As discussed in Sect. 1.3.3, the Ledoux constant is very small for p modes (e.g., $C_{n\,\ell} \simeq 0.03$; Kurtz et al. 2014); therefore, to first order, the surface rotation period can be directly inferred as the inverse of the frequency splitting of p modes in a δ Sct star.

(ii) The δ Sct star has surface features, let us call them starspots, which are co-rotating with the star's rotation period. If the modulation of the stellar flux by these starspots is large enough, then the frequencies associated with these co-rotating features will be present in the light curve and amplitude spectrum of our hypothetical δ Sct star.

Thus, from the above two criteria, if a δ Sct star pulsates with a non-radial mode in the presence of rotation and has starspots on its surface, the rotation periods must agree to within some tolerance. KIC 10407873 is an ideal example of an organ pipe star, which is used to demonstrate that the low-frequency peaks in this star are not caused by rotation, as they are not consistent with the surface velocity obtained from a rotationally split non-radial mode.

4.3.1 KIC 10407873

The only significant p-mode frequencies in the amplitude spectrum of KIC 10407873 are a mixed mode triplet split by rotation. The KIC and Huber et al. (2014) stellar parameters for KIC 10407873 are given in Table 4.1, and its amplitude spectrum is shown in the top panel of Fig. 4.3. The triplet consists of three pulsation mode frequencies, 13.077173 d^{-1}, 13.805580 d^{-1} and 14.520178 d^{-1}, which have separations of 0.714598 d^{-1} and 0.728407 d^{-1}. This means that the component frequencies of the triplet are not exactly equally split, as predicted for a rotationally split non-radial mode. A series of low amplitude peaks is also present at low frequency, specifically 0.977732 d^{-1}, 1.954641 d^{-1} and 2.933393 d^{-1}, which are not resolved sinc functions. The almost chaotic variability in the low-frequency peaks is shown graphically using a series of amplitude spectra in Fig. 4.4.

The amplitude and phase variability of the low frequency peaks and the triplet were tracked through the 4-yr *Kepler* data set using a similar method employed by Bowman and Kurtz (2014) to study amplitude modulation in the δ Sct star KIC 7106205 discussed in Chap. 3. The results of the amplitude and phase tracking for the low frequency peaks and triplet of frequencies in KIC 10407873 are given in the bottom-left and bottom-right panels of Fig. 4.3, respectively. Clearly, the pulsation modes in the triplet are constant in amplitude and phase over time, but the low frequency peaks are not.

None of the frequencies in the triplet can be understood in terms of combination frequencies, because the splitting of the triplet is asymmetric and combination frequencies must be exactly equally-split as they are mathematical representations of non-linearity (see e.g., Kurtz et al. 2015). Moreover, the low-frequency peaks cannot be understood as combination frequencies of the triplet, because of the significant difference in frequency values. Therefore, the logical inference is that the triplet

Table 4.1 Stellar parameters of the case study of the δ Sct star KIC 10407873 with low-frequency peaks called organ pipes in its amplitude spectrum

	$T_{\rm eff}$ (K)	log g (cgs)	[Fe/H] (dex)
KIC (Brown et al. 2011)	7270 ± 250	3.42 ± 0.25	0.11 ± 0.25
Huber et al. (2014)	7510 ± 270	3.42 ± 0.28	0.07 ± 0.26

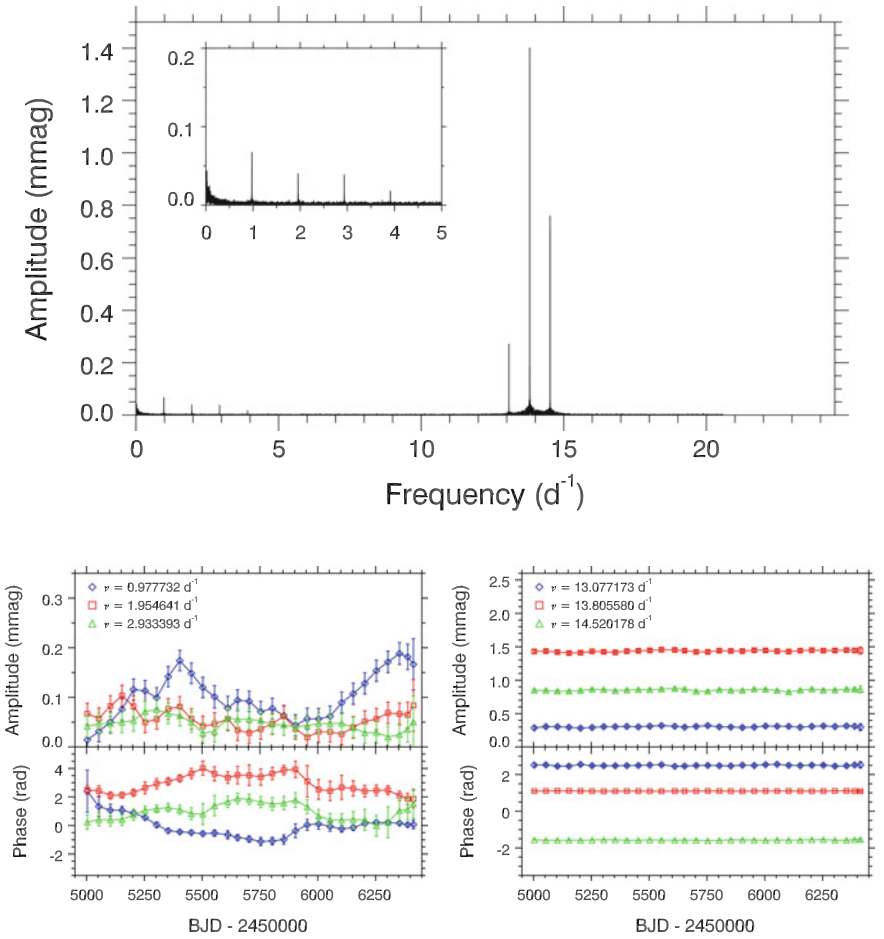

Fig. 4.3 The amplitude spectrum of the δ Sct star KIC 10407873 is given in the *top panel*, which contains a triplet of p mode frequencies interpreted as a rotationally split dipole mode, and a series of peaks at low frequency that are unrelated to the rotation in this star. The *bottom row* shows the amplitude and phase variability of the low frequency peaks and the triplet of frequencies in the *left* and *right panels*, respectively

is likely a rotationally split dipole mode. From theoretical modelling, the central frequency of the triplet was matched to a mixed mode using a model of a 1.8-$M_\odot$ δ Sct star, but the asymmetry of the triplet was smaller than expected for the inferred rotation of this star (H. Saio, *private communication*). Using the model of a δ Sct star with a mass of 1.8 $M_\odot$, a radius of $R \simeq 2\ R_\odot$, and the average of the rotational splitting in the triplet, 0.7215025 d^{-1}, a surface rotation velocity of $v_{eq} \simeq 70\ km\,s^{-1}$ is indicated.

On the other hand, if the low-frequency peaks are assumed to represent harmonics of the star's rotation frequency caused by spot modulation, the rotational velocity

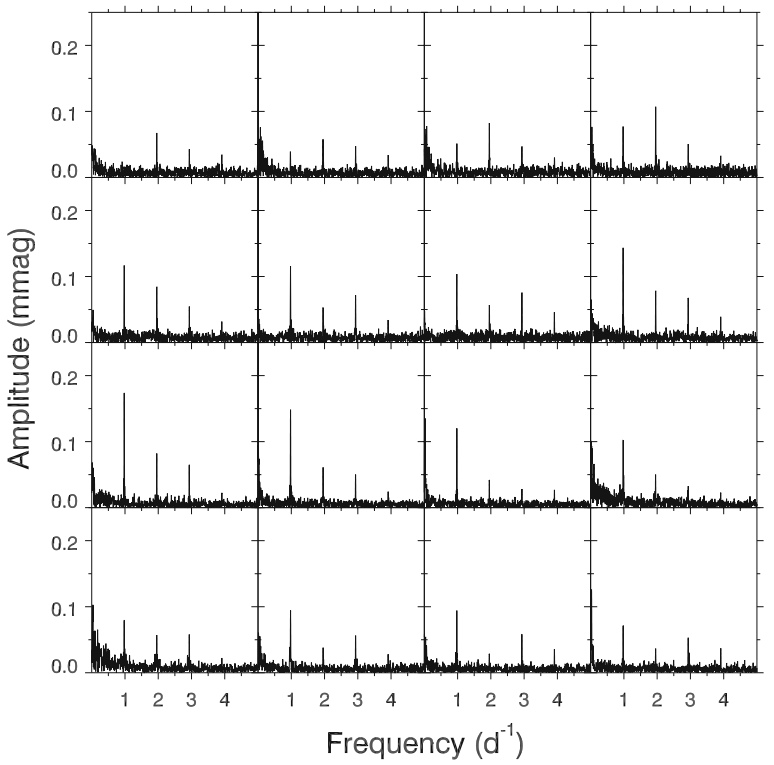

Fig. 4.4 A series of amplitude spectra of the low-frequency peaks for the organ pipe star KIC 10407873 using 100-d bins with a 50-d overlap, which are ordered in time from *left* to *right*, row by row. Only the first 16 time bins are shown, which corresponds to the first 800 d of the *Kepler* data set. From one spectra to the next, the amplitudes of the low-frequency peaks change in a chaotic manner, hence coined the name organ pipes

calculated from the lowest-frequency is $v_{\rm eq} \simeq 100\ {\rm km\,s^{-1}}$, which implies that the triplet cannot be caused by rotation. These hypotheses are inherently mutually exclusive, unless spots on the surface of this star have significantly different rotational velocities than the value calculated from the rotationally split dipole modes. For the low frequencies and the triplet to both be explained by rotation, a significant latitudinal differential rotation is needed in this star, which is physically unlikely.

The organ pipe star KIC 10407873 remains a useful case study for studying rotation and low frequency peaks in the amplitude spectra of δ Sct stars observed by the *Kepler* Space Telescope. Follow-up spectroscopy of KIC 10407873 and other organ pipe stars that have low-frequency peaks in their amplitude spectra is needed to determine a true surface rotational velocity and test if the low frequency peaks are caused by, or are unrelated to, the rotation of the star.

4.4 Hot Gamma Doradus Stars

In this section, stars that pulsate with only g-mode frequencies and lie between the cool edge of the SPB and the hot edge of the γ Dor instability regions are discussed. Balona (2014) identified a dozen of these stars in the *Kepler* data set, which have effective temperatures between $8100 \leq T_{\rm eff} \leq 9200$ K and were pulsating purely in g modes. He termed these stars 'hot γ Dor stars' as they are located in a region of the HR diagram where neither the κ mechanism (Pamyatnykh 1999, 2000) or the flux blocking mechanism (Dupret et al. 2004, 2005) is predicted to excite g modes.

4.4.1 KIC 5130890

One such hot γ Dor star is KIC 5130890, which has an effective temperature and surface gravity that places it beyond the ZAMS blue edge of the classical instability strip, with the KIC and Huber et al. (2014) stellar parameters for KIC 5130890 given in Table 4.2. The amplitude spectrum of KIC 5130890 is shown in the bottom panel of Fig. 4.5, in which the only significant pulsation mode frequencies are below $\nu < 5$ d^{-1} and were interpreted as g modes by Balona (2014).

The simplest interpretation is that KIC 5130890 and other hot γ Dor stars have incorrect $T_{\rm eff}$ values in the KIC and Huber et al. (2014) catalogues, which could be caused by the flux from the target star being contaminated from a background star. If, for example, the target star is a SPB star with $T_{\rm eff} \simeq 11\,000$ K, then a cool contaminant star could dilute the target temperature to the observed $T_{\rm eff}$ value. A spectroscopic study of these hot γ Dor stars is needed for the determination of accurate effective temperatures.

On the other hand, if the effective temperature of KIC 5130890 and other hot γ Dor stars are accurate, and these stars are located outside of the SPB and γ Dor instability regions, then it is interesting how these stars can pulsate purely in g modes in a region in the HR diagram where g modes are not predicted to be excited (Pamyatnykh 1999, 2000; Dupret et al. 2004, 2005). Even though these hot γ Dor stars are rare, the discovery of pure g mode pulsators in the classical instability strip implies that our understanding of the interaction between the δ Sct and γ Dor excitation mechanisms is far from complete.

Table 4.2 Stellar parameters of KIC 5130890 which is too hot to be within the γ Dor instability region and too cool to be within the SPB instability region

	$T_{\rm eff}$ (K)	log g (cgs)	[Fe/H] (dex)
KIC (Brown et al. 2011)	9020 ± 350	4.03 ± 0.25	0.04 ± 0.25
Huber et al. (2014)	9250 ± 340	4.01 ± 0.24	0.07 ± 0.36

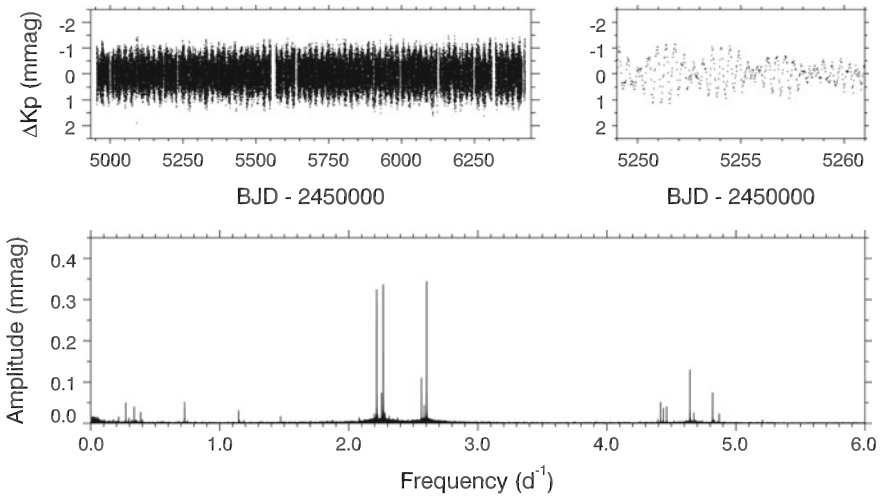

Fig. 4.5 KIC 5130890 is a g mode pulsator characterised by an effective temperature that is too hot to place the star within the γ Dor instability region and too cool to place the star within the SPB instability strip. The 4-yr LC *Kepler* light curve is shown in the *top-left panel* and a 12-d insert of the LC light curve is shown in the *top-right panel*. The *bottom panel* is the LC amplitude spectrum between $0 \leq \nu \leq 6$ d^{-1}, which contains many g-mode frequencies

4.5 Creating an Ensemble of Delta Scuti Stars

Using the *Kepler* data catalogues of ∼10 400 stars that were discussed in Sect. 2.4.1, an ensemble of δ Sct stars was created of the stars that met *all* of the following criteria:

1. Characterised by $6400 \leq T_{\rm eff} \leq 10\,000$ K in the KIC;
2. Observed continuously in LC from Q0 (or Q1) to Q17;
3. Contain peaks in the amplitude spectrum in the sub-Nyquist p-mode frequency regime ($4 \leq \nu \leq 24.5$ d^{-1}) with amplitudes greater than 0.10 mmag.

These criteria produced a statistically significant ensemble of 983 δ Sct and hybrid stars, which was created for two purposes. First of all, a large ensemble of δ Sct stars allowed the statistical properties of these stars to be investigated, which is discussed in the remaining sections of this chapter. Second, this ensemble facilitated a search for amplitude modulation in δ Sct stars, which is discussed in Chap. 5. The following paragraphs justify the motivation for each of the selection criteria.

The lower temperature limit of $T_{\rm eff} \geq 6400$ K was chosen because this is the observational red edge of the classical instability strip for δ Sct stars from Rodríguez and Breger (2001). The ZAMS red edge was calculated to be approximately 6900 K by Dupret et al. (2004), but cooler high-luminosity δ Sct stars are found below 6900 K and so the lower limit of 6400 K was chosen to include these targets. Few δ Sct stars are found between $6400 \leq T_{\rm eff} \leq 6500$ K, supporting this as the observational red

edge defined by Rodríguez and Breger (2001). An upper limit of $T_{\rm eff} \leq 10\,000$ K was chosen to exclude pulsators that do not lie within the classical instability strip, such as SPB and β Cep stars (e.g., see Balona et al. 2011 and McNamara et al. 2012).

The use of LC data gives the largest number of stars that were observed over the longest possible time span of 4 yr. Only a small fraction of intermediate (and high) mass stars were observed in SC and even fewer for many consecutive SC months. Using LC data is motivated by previously studied δ Sct stars that exhibit amplitude modulation over time-scales of order years and decades (e.g., 4 CVn was observed to exhibit amplitude and frequency variability of order a few decades by Breger 2000b, 2016), and so complete data coverage over the maximum of 4 yr is most useful. It was also decided to exclude the stars that fall on module 3 of the *Kepler* CCD, because of the complicated window patterns in these stars.

The stars that contain pulsation mode frequencies within $4 \leq \nu \leq 24.5$ d^{-1} were selected because the LC Nyquist frequency is $\nu_{\rm Nyq} = 24.5$ d^{-1}. Although δ Sct stars can pulsate with frequencies higher than $\nu_{\rm Nyq}$ (e.g., Holdsworth et al. 2014), Nyquist alias peaks are subject to frequency (phase) variations and amplitude suppression (Murphy et al. 2013), thus real and alias frequency peaks can be identified without the need to calculate an amplitude spectrum beyond the Nyquist frequency.

It should be noted that this ensemble of 983 δ Sct stars includes many hybrid stars, but does not include any pure γ Dor stars because these stars do not pulsate in p modes with frequencies $\nu \geq 4$ d^{-1}. Thus, when referring to this ensemble of 983 δ Sct stars, the terms δ Sct and hybrid can be used interchangeably, as the criteria given above selected stars that pulsate in p modes.

4.5.1 Ensemble Limitations

It was discussed in Sect. 2.3.3 and shown graphically in Fig. 2.6 how pulsation mode amplitudes are heavily suppressed for higher frequency signals and completely suppressed at integer multiples of the LC sampling frequency in *Kepler* data. Therefore, it is important to note that this ensemble of δ Sct stars is biased towards low-frequency pulsation modes, hence more evolved and/or cooler δ Sct stars. This is explored in more detail in Sect. 4.7.

An example of a δ Sct star that was not included in the ensemble is KIC 10977859, which has an effective temperature of $T_{\rm eff} = 8180 \pm 170$ K (Huber et al. 2014) and pulsates with high frequency pulsation modes between $50 \leq \nu \leq 60$ d^{-1}. KIC 10977859 was observed continuously by *Kepler* for 4 yr in LC and between Q8 – Q17 in SC, with the amplitude spectra for approximately 90 d of simultaneous LC and SC observations shown in the top and bottom panels of Fig. 4.6, respectively. The amplitude visibility function has resulted in significant amplitude suppression of this star's pulsation mode amplitudes from $A \simeq 1$ mmag in the SC amplitude spectrum to $A \simeq 0.2$ mmag in the LC amplitude spectrum.

To study the δ Sct star KIC 10977859, and other high frequency pulsators in the *Kepler* data set, it is necessary to use SC observations because the amplitude visibility function suppresses mode amplitudes at high frequency in LC data. Furthermore,

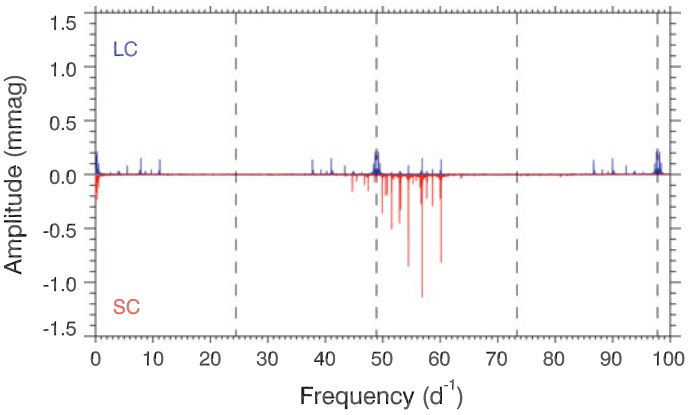

Fig. 4.6 The LC and SC amplitude spectra for the δ Sct star KIC 10977859, calculated out to 100 d^{-1}, are shown in the *top* and *bottom panels*, respectively. Integer multiples of the LC Nyquist frequency are shown as *vertical dashed lines*. The pulsation mode frequencies between $50 \leq \nu \leq 60$ d^{-1} are clearly visible in the SC amplitude spectrum, but are heavily suppressed in the LC amplitude spectrum because of the longer integration time. Nyquist aliases of the pulsation mode frequencies can also be seen throughout the LC amplitude spectrum

amplitudes at integer multiples of the Nyquist frequency are completely suppressed when using LC data. Very few δ Sct stars were observed by *Kepler* in SC for more than a couple of consecutive months. As discussed previously, it was important to maximise both the number of stars in the ensemble and the length of observations to obtain the highest possible frequency resolution.

4.6 Revisiting the Delta Scuti Instability Strip

The δ Sct stars are a diverse group of pulsators, with no obvious consistency in the number of excited pulsation modes, their amplitudes or range in observed frequencies. Balona and Dziembowski (2011) used a subset of 418 d of *Kepler* data (i.e., Q0–Q5) to study 1568 δ Sct stars, particularly the occurrence of pulsation within the classical instability strip in the HR diagram. They concluded that no more than 50% of stars between $7000 \leq T_{\rm eff} \leq 8000$ K in the *Kepler* data set were δ Sct stars. The lack of pulsation in chemically peculiar stars such as Am and Ap stars is not surprising, which explains why many A stars are not observed to pulsate; this was discussed in Sect. 1.3.2.

In this section, the observed boundaries of the classical instability strip are revisited using the ensemble of 983 δ Sct stars that were observed continuously by *Kepler* for over 4 yr. The distribution of these stars in a $T_{\rm eff}$ – log g diagram using values from the KIC is shown in Fig. 4.7. In this figure, the location of each star is shown by a black cross, with stellar evolutionary tracks calculated from the ZAMS for 1.4,

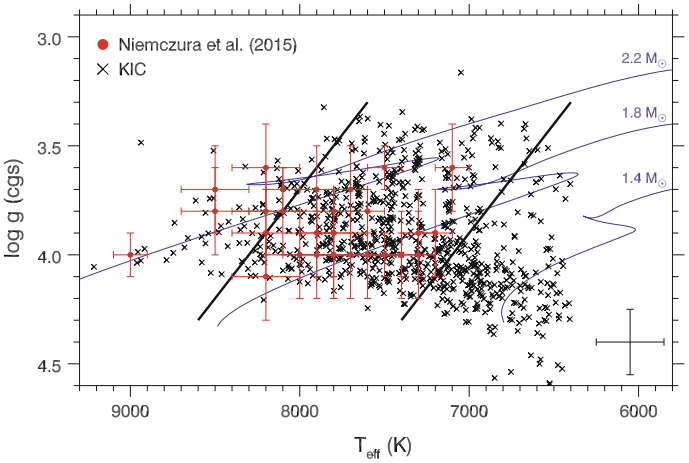

Fig. 4.7 $T_{\rm eff}$ – log g diagram for the ensemble of 983 δ Sct stars. The distribution of KIC parameters for the ensemble of 983 δ Sct stars is shown as *black crosses*, with the typical point uncertainties shown by the *error bars* in the *bottom right*. The observational hot and cool borders of the classical instability strip are taken from Rodríguez and Breger (2001) and are shown as *solid black lines*. Stellar evolutionary tracks calculated using time-dependent convection (TDC) models, courtesy of S. Murphy (*private communication*), are shown as *solid purple lines*. A subgroup of δ Sct stars for which accurate spectroscopic values of $T_{\rm eff}$ and log g from Niemczura et al. (2015) are plotted as *filled red circles*

1.8 and 2.2 $M_\odot$ stars shown as solid purple lines. The stellar evolutionary tracks were calculated using time-dependent convection (TDC) models and are courtesy of S. Murphy (*private communication*). The solid black lines in Fig. 4.7 indicate the observed blue and red edges of the classical instability strip from Rodríguez and Breger (2001), and the typical uncertainty for each star is shown by the error bars in the bottom-right corner of the plot.

A study by Niemczura et al. (2015) using high-resolution spectroscopic data from the HERMES[1] spectrograph on the Mercator Telescope (Raskin et al. 2011), characterised 117 bright ($V \leq 10$ mag) A and F stars observed by the *Kepler* Space Telescope. Accurate values for fundamental stellar parameters including $T_{\rm eff}$, log g, rotational and micro-turbulent velocities and their respective uncertainties were determined for each star (Niemczura et al. 2015). The stars studied by Niemczura et al. (2015) that are included in the ensemble are shown as filled red circles in Fig. 4.7. Therefore, these stars represent a subsample of all the δ Sct stars observed by *Kepler* for which accurate spectroscopic values of $T_{\rm eff}$ and log g are known, with uncertainties for individual stars that range between $100 \leq \sigma\,(T_{\rm eff}) \leq 200$ K and $0.1 \leq \sigma\,(\log\, g) \leq 0.2$ (cgs), respectively.

The majority of δ Sct stars in Fig. 4.7 are cooler than the blue edge of the classical instability strip, especially if the uncertainties in effective temperature are taken into

[1] HERMES website: http://www.mercator.iac.es/instruments/hermes/.

account. In Sect. 2.2.3, it was discussed how the effective temperatures listed in the KIC are accurate in a statistical sense, but are underestimated by approximately 200 K (Pinsonneault et al. 2012; Huber et al. 2014). This was also noted by Niemczura et al. (2015) in their study, and explains the systematic shift to higher temperatures for the stars in the Niemczura et al. (2015) subsample compared to the ensemble of 983 δ Sct stars. If this systematic error is included, then the majority of δ Sct stars in Fig. 4.7 are within 1σ of being within the classical instability strip. What is clear from the distribution of stars in Fig. 4.7 is that almost all δ Sct stars lie within the observational edges of the classical instability strip taken from Rodríguez and Breger (2001) if 3σ uncertainties in $T_{\rm eff}$ and $\log g$ are taken into account. For stars within the classical instability strip, it is not surprising that they are observed to pulsate for the reasons discussed in Sect. 1.2.3.

On the other hand, a minority of δ Sct stars in the ensemble have effective temperatures that are hotter than the blue edge or cooler than the red edge of the classical instability strip by more than 3σ, so further investigation is needed to study these stars. There is also a high density of stars near the red edge in Fig. 4.7 indicating there is not an abrupt transition in temperature for whether a star is stable or unstable to pulsation by the κ mechanism. The edges of the instability strip from Rodríguez and Breger (2001) shown in Fig. 4.7 are purely observational, so could be moved to take into account the outlying δ Sct stars in the *Kepler* data set.

The majority of the δ Sct stars in Fig. 4.7 have surface gravities between $3.5 \leq \log g \leq 4.0$ with few stars around $\log g \simeq 4.4$, thus the TAMS is better sampled than the ZAMS for δ Sct stars observed by the *Kepler* Space Telescope. This result was also found for the subsample of bright A and F stars studied by Niemczura et al. (2015) using spectroscopy.

In summary, it can be concluded that the observed blue and red edges from Rodríguez and Breger (2001) remain a reasonable indicator for the location of δ Sct stars observed by the *Kepler* Space Telescope. However, a few δ Sct stars lie beyond the blue edge of the classical instability strip, some of which have been studied spectroscopically by Niemczura et al. (2015) and have accurate effective temperatures and surface gravities. The outlying δ Sct stars will be interesting to study further, as they lie in a region where the excitation of p modes by the κ mechanism is not expected to occur (Pamyatnykh 1999, 2000; Dupret et al. 2005). Also, a significant fraction of δ Sct stars are located near the red edge of the classical instability strip and so the observed boundaries may need to be moved to take these stars into account.

4.7 Correlations in the Stellar Parameters of Delta Scuti Stars

In this section, correlations between pulsation and different stellar parameters are investigated using the ensemble of 983 δ Sct stars. The amplitude spectrum for each star in the ensemble was calculated to 98 d^{-1}, which is four times the LC Nyquist

frequency, or twice the sampling frequency. The highest amplitude peak in the p mode frequency regime ($4 \leq \nu \leq 98\,\mathrm{d}^{-1}$) was extracted and values of frequency, amplitude and phase were optimised using non-linear least-squares.

In this analysis, only a single frequency is extracted per star to ensure that it is a pulsation mode frequency and not an Nyquist alias peak, as real pulsation mode frequencies have higher amplitudes than their Nyquist aliases (Murphy et al. 2013). It was discussed in Sect. 2.3.1 and demonstrated in Fig. 2.3 how the Barycentric time stamp corrections made to *Kepler* data produce a non-constant cadence, which causes Nyquist aliases to experience a periodic frequency modulation and amplitude suppression (Murphy et al. 2013). Therefore, the frequency of the highest amplitude peak (i.e., the frequency of $A_{\max}$) in the amplitude spectrum cannot be an alias of a pulsation mode frequency, as a real frequency has a larger amplitude (Murphy et al. 2013).

The amplitude spectrum for each star is not corrected for the amplitude visibility function given in Eq. 2.6, because it would then be possible for Nyquist aliases to have higher amplitudes than pulsation mode frequencies. This is demonstrated graphically in Fig. 4.8 using the LC amplitude spectrum of the δ Sct star KIC 7106205. In this figure, integer multiples of the LC Nyquist frequency are shown as dashed lines and the amplitude visibility function is shown as a red line. The highest amplitude peak, which corresponds to a pulsation mode at $\nu = 10.0323\,\mathrm{d}^{-1}$ is labelled 'r' for real, and its Nyquist aliases are labelled a_1, a_2 and a_3. If the amplitude spectrum is corrected for the amplitude visibility function, then the alias frequencies would have larger amplitudes than the real pulsation mode.

By not correcting the amplitude spectra of 983 δ Sct stars for the amplitude visibility function, it is ensured that the extracted frequency is a pulsation mode

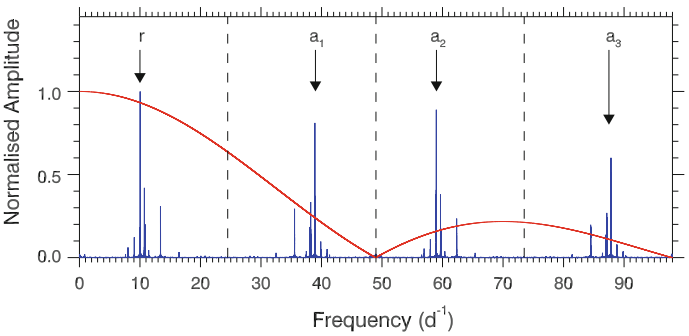

Fig. 4.8 Application of amplitude visibility function using the δ Sct star KIC 7106205. The normalised amplitude spectrum using LC *Kepler* data has been calculated to four times the Nyquist frequency, with integer multiples of ν_{Nyq} shown as *dashed lines*. The highest amplitude peak, which corresponds to a pulsation mode at $\nu = 10.0323\,\mathrm{d}^{-1}$ is labelled 'r' for real, and its Nyquist aliases are labelled with a_i. The normalised amplitude visibility is shown as a *red solid line*. If the amplitude spectrum was corrected for the amplitude visibility function, then the alias peaks, a_1, a_2 and a_3 would have higher amplitudes than the real peak, thus justifying why frequencies are extracted without correcting for the *Kepler* integration time

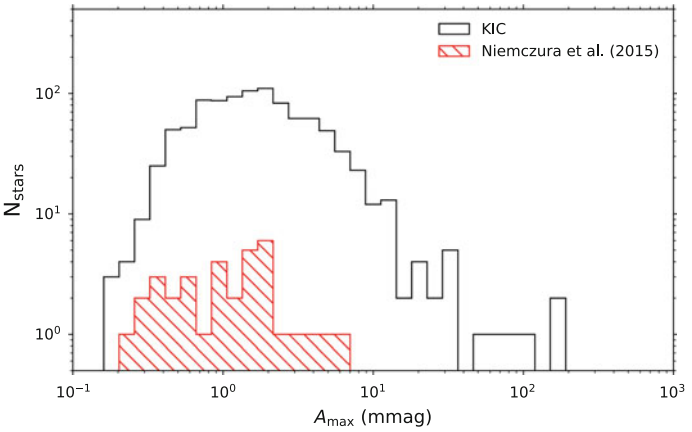

Fig. 4.9 The distribution of the highest amplitude pulsation mode (A_{max}) for the ensemble of 983 δ Sct stars. The maximum amplitude is extracted from the frequency range of $4 \leq \nu \leq 98$ d^{-1}, and is optimised using non-linear least-squares fit to the data set for each star. The subgroup of bright A and F stars studied by Niemczura et al. (2015) is also plotted in *red* for comparison

frequency and not a Nyquist alias frequency. The disadvantage of this approach is that the distribution of frequencies will be biased towards, on average, lower values, but this is a compromise that yields the most meaningful results. Restricting this search to the p-mode frequency regime also ensures that variability from longer period phenomena such as rotation is excluded.

The distribution of the highest amplitude pulsation mode (A_{max}) is shown by the black region in Fig. 4.9, which demonstrates that the dominant pulsation mode has an amplitude that typically lies between 0.2 and 12.0 mmag for most δ Sct stars. There is an extended tail towards very high pulsation mode amplitudes in the logarithmic distribution shown in Fig. 4.9, which is caused by the high-amplitude δ Sct (HADS) stars.

The distribution of the frequency of the highest amplitude pulsation mode is shown by the black region in Fig. 4.10, which demonstrates that the dominant pulsation mode frequency typically lies below $\nu \lesssim 40$ d^{-1} for most δ Sct stars. This agrees with the analysis by Balona and Dziembowski (2011). However, the bias introduced by the amplitude visibility function means that stars with pulsation modes at or near the *Kepler* sampling frequency are unlikely to have been included, which explains the dearth of δ Sct stars with frequencies $\nu \gtrsim 40$ d^{-1} in the *Kepler* data set.

4.7.1 Pulsation and Effective Temperature

A semi-empirical relationship exists between the effective temperature and the observed pulsation mode frequencies in a δ Sct star. As discussed in Sect. 1.2.3,

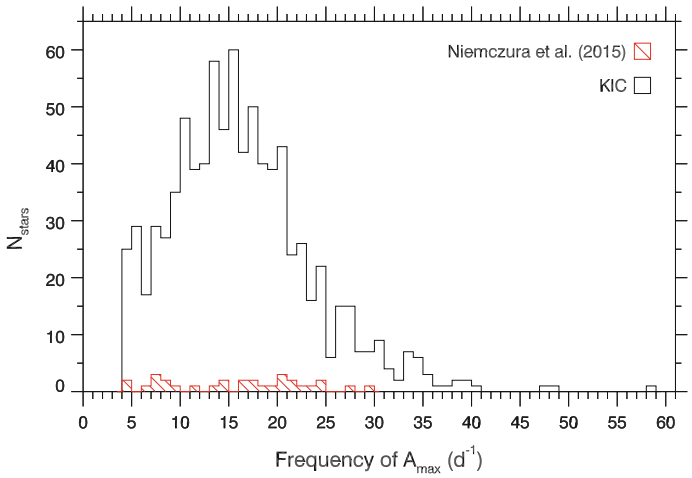

Fig. 4.10 The distribution of the frequency of maximum amplitude for the ensemble of 983 δ Sct stars. The frequency of maximum amplitude is extracted from the frequency range of $4 \leq \nu \leq 98\ \mathrm{d}^{-1}$, and is optimised using non-linear least-squares fit to the data set for each star. The subgroup of bright A and F stars studied by Niemczura et al. (2015) is also plotted in *red* for comparison

the depth of the He II ionisation zone is a function of T_{eff} in the stellar envelope. A hot δ Sct star near the blue edge will typically pulsate in higher radial overtone modes, resulting in higher pulsation mode frequencies (Pamyatnykh 1999, 2000; Christensen-Dalsgaard 2000; Dupret et al. 2004, 2005). Thus, hotter δ Sct stars typically have higher pulsation mode frequencies, a relationship that has been observed from the ground (see e.g., Breger and Bregman 1975; Breger 2000a).

Theoretically, there are predictions of where the δ Sct instability region is located in the HR diagram (Pamyatnykh 1999; Dupret et al. 2004, 2005; Grigahcène et al. 2010a), but the predictions depend on the numerical treatment of convection used in stellar models, especially for determining the red edge of the classical instability strip (see e.g., Dupret et al. 2004, 2005). Observationally, the blue and red edges are well-constrained using ground-based data (Rodríguez and Breger 2001), but with less accuracy when using space-based observations primarily because of the lower levels of noise revealing many more significant pulsation modes in δ Sct stars (Grigahcène et al. 2010a; Uytterhoeven et al. 2011; Balona and Dziembowski 2011; Bowman et al. 2016).

The frequency of the highest amplitude pulsation mode is plotted against T_{eff} using the KIC parameters for the ensemble of 983 δ Sct stars in Fig. 4.11. A linear regression of these two parameters, shown as a black line in Fig. 4.11, and a Pearson coefficient of $R = 0.282$ indicate a weak correlation between the frequency of the highest amplitude pulsation mode and effective temperature in δ Sct stars observed by the *Kepler* Space Telescope. The subsample of bright A and F stars from Niemczura et al. (2015) are also plotted in Fig. 4.11 as filled red circles for comparison, for which a separate linear regression is plotted as a red line.

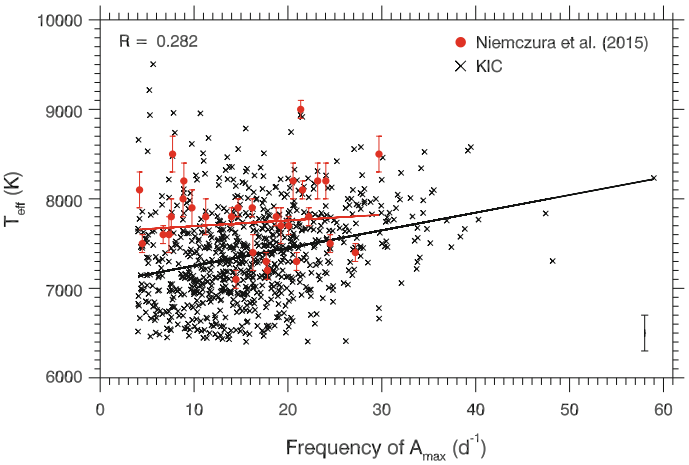

Fig. 4.11 A linear regression of the frequency of maximum amplitude against $T_{\rm eff}$ using the KIC parameters for the ensemble of 983 δ Sct stars is shown as a *black line*. The Pearson coefficient is shown in the *top-left corner* of the plot indicating a weak correlation, and a typical *error bar* for each data point is shown in the *bottom-right corner* of the plot. The subsample of δ Sct stars for which accurate spectroscopic values of $T_{\rm eff}$ obtained from Niemczura et al. (2015) are plotted as *filled red circles*, with a separate linear regression of these values plotted as the *red line*

The amplitude suppression of high frequency pulsation modes in LC *Kepler* data may explain why only a weak correlation was found between pulsation and effective temperature as very few δ Sct stars with pulsation mode frequencies above 40 d^{-1} are included in the ensemble of 983 δ Sct stars. For example, the δ Sct KIC 10977859 discussed in Sect. 4.5.1 has an effective temperature of $T_{\rm eff} = 8180 \pm 170$ K (Huber et al. 2014) and pulsates with pulsation mode frequencies between $50 \leq \nu \leq 60$ d^{-1}, so clearly at least one hot, high-frequency δ Sct star has not been included in the ensemble, which would improve the correlation in Fig. 4.11. Despite this, the observed correlation is in agreement with the expectation that hotter δ Sct stars have higher pulsation mode frequencies (Breger and Bregman 1975; Breger 2000a).

4.7.2 Pulsation and Surface Gravity

Another semi-empirical relationship exists between the evolutionary state and the observed pulsation mode frequencies in a δ Sct star. As discussed previously in Sect. 1.1.1, the evolutionary state of a star influences its pulsations with post-main sequence stars exhibiting mixed modes (Osaki 1975), which are the result of the coupling of the g- and p-mode pulsation cavities (e.g., Lenz et al. 2010). The δ Sct stars are interesting as they include main sequence and post-main sequence stars, with models of δ Sct stars predicting that mixed modes can be excited in these stars (Dziembowski et al. 1995; Christensen-Dalsgaard 2000).

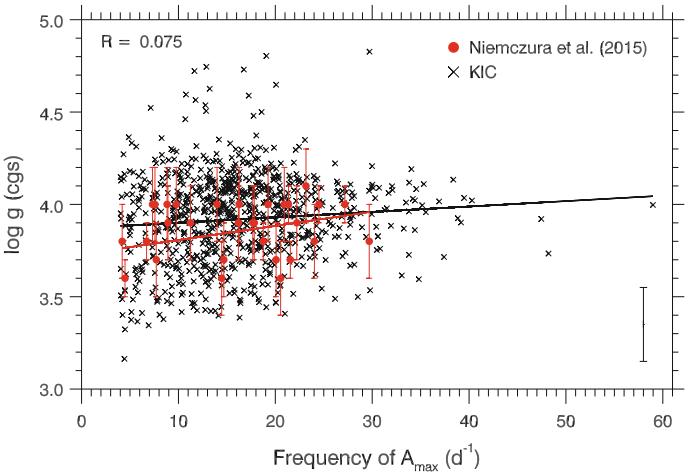

Fig. 4.12 A linear regression of the frequency of maximum amplitude against log g using the KIC parameters for the ensemble of 983 δ Sct stars is shown as a *black line*. The Pearson coefficient is shown in the *top-left corner* of the plot indicating no correlation, and a typical *error bar* for each of the data points is shown in the *bottom-right corner* of the plot. The subsample of δ Sct stars for which accurate spectroscopic values of log g obtained from Niemczura et al. (2015) are plotted as *filled red circles*, with a separate linear regression of these values plotted as the *red line*

The evolutionary state of a star can be inferred from its log g value, with the more evolved stars having lower log g values. This is caused by the increase in radius after a star has evolved beyond the TAMS. Therefore, a more-evolved δ Sct star in a post-main sequence stage of stellar evolution will generally have lower pulsation mode frequencies than its ZAMS counterpart for a given effective temperature.

The frequency of the highest amplitude pulsation mode is plotted against log g using the KIC parameters for the ensemble of 983 δ Sct stars in Fig. 4.12. A linear regression of these two parameters, shown as a black line in Fig. 4.12, and a Pearson coefficient of $R = 0.075$ indicate no correlation between the frequency of the highest amplitude pulsation mode and surface gravity in δ Sct stars observed by the *Kepler* Space Telescope. The subsample of bright A and F stars from Niemczura et al. (2015) are also plotted in Fig. 4.12 as filled red circles for comparison, for which a separate linear regression is plotted as a red line. The lack of correlation in Fig. 4.12 is likely because of the previously discussed bias towards lower frequencies resulting in only a narrow range of extracted frequencies. Furthermore, there is degeneracy in the observed pulsation mode frequencies between evolved stars and cool main sequence stars, with both groups of δ Sct stars typically having lower pulsation mode frequencies.

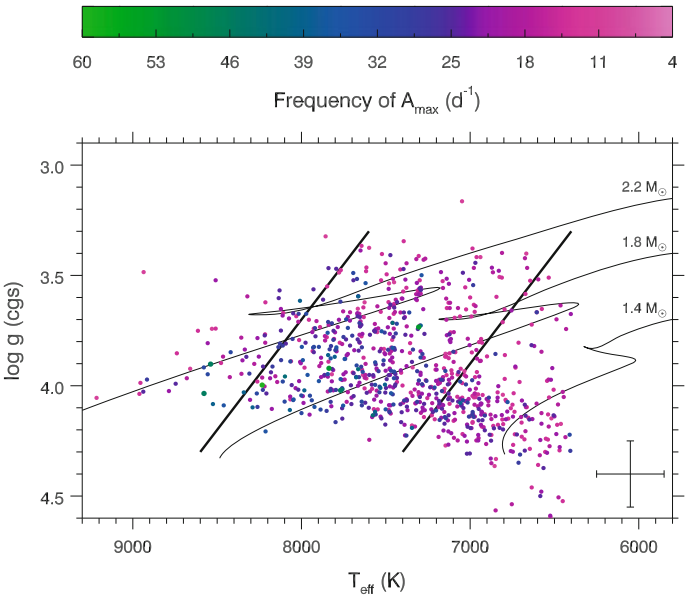

Fig. 4.13 Pulsation across the $T_{\rm eff}$ – log g diagram. This figure is the same as Fig. 4.7, but each *filled circle* has been coloured by the frequency of its highest amplitude pulsation mode. High densities of δ Sct stars with low-frequency pulsations ($\nu \leq 25$ d^{-1}) are found near the ZAMS *red edge* and the TAMS, whereas δ Sct stars with high-frequency pulsations ($\nu > 25$ d^{-1}) are found closer to the *blue edge*

4.7.3 *Pulsation Across the* $T_{\rm eff}$ – log g *Diagram*

The relationships between pulsation and effective temperature, and pulsation and surface gravity are degenerate, making it difficult to distinguish cool main sequence and evolved δ Sct stars. Therefore, using a $T_{\rm eff}$ – log g diagram is a sensible way to investigate these correlations further. The ensemble of 983 δ Sct stars observed by *Kepler* are plotted in a $T_{\rm eff}$ – log g in Fig. 4.13, which is colour-coded to denote the frequency of the highest amplitude pulsation mode. As expected, the δ Sct stars with higher pulsation mode frequencies ($\nu \geq 40$ d^{-1}) typically lie at higher effective temperatures in Fig. 4.13.

The ensemble of 983 δ Sct stars shown in Fig. 4.13 are divided into three populations and plotted separately in Fig. 4.14 for comparison. In this figure, the top, middle and bottom panels correspond to the stars with low-frequency pulsations ($4 < \nu < 18$ d^{-1}), mid-range pulsation frequencies ($18 < \nu < 32$ d^{-1}), and high-frequency pulsations ($32 < \nu < 60$ d^{-1}), respectively. Although, there is a dearth of high-frequency δ Sct stars, a shift from lower log g and $T_{\rm eff}$ to higher values of log g and $T_{\rm eff}$ can be seen from the top to bottom panels in Fig. 4.14.

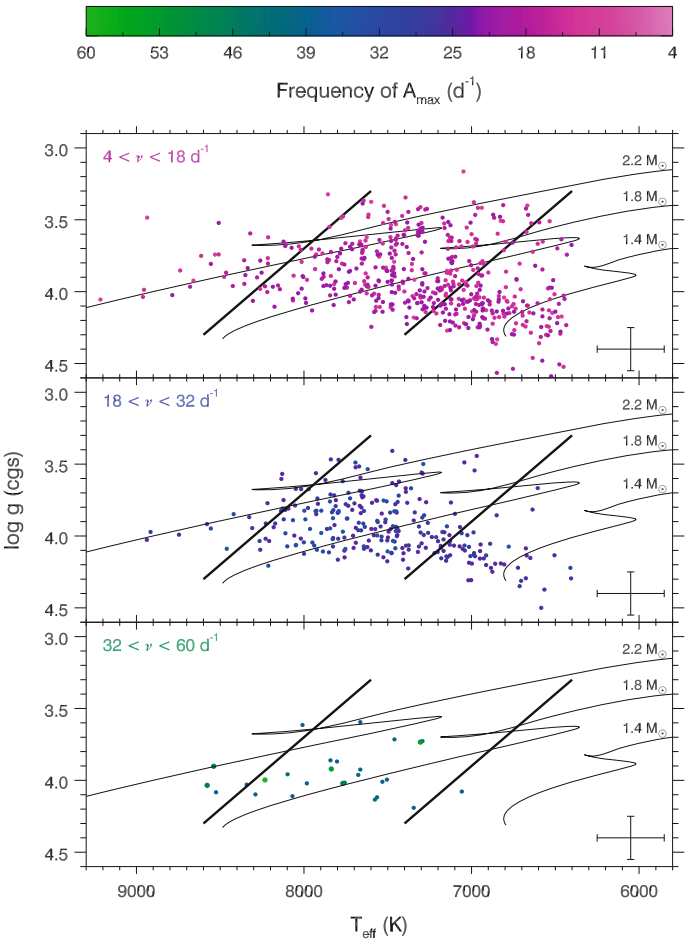

Fig. 4.14 Distribution of pulsation across the $T_{\rm eff} - \log\ g$ diagram. This figure is similar to Fig. 4.13, but the ensemble of 983 δ Sct stars has been split into three populations based on the frequency of the highest amplitude pulsation mode. The *top*, *middle* and *bottom panels* show the $4 < \nu < 18\ {\rm d}^{-1}$, $18 < \nu < 32\ {\rm d}^{-1}$ and $32 < \nu < 60\ {\rm d}^{-1}$ populations, respectively

The relationships between the frequency of the highest amplitude pulsation mode and the stellar parameters $T_{\rm eff}$ and $\log\ g$ presented in this monograph may not be completely representative of δ Sct stars, as only a single pulsation mode frequency was used for each star. Many δ Sct stars have a large range of pulsation mode frequencies, which is not taken into account in Figs. 4.10, 4.11, 4.12, 4.13 and 4.14. Moreover, the degeneracy between evolved and cool main sequence δ Sct stars complicates the method for determining general properties of an ensemble of δ Sct stars. Nonetheless, the high-frequency δ Sct stars are typically located nearer the blue edge of the instability strip and the ZAMS as shown in Figs. 4.13 and 4.14. This relationship has been predicted by theoretical models (Pamyatnykh 1999, 2000; Christensen-Dalsgaard

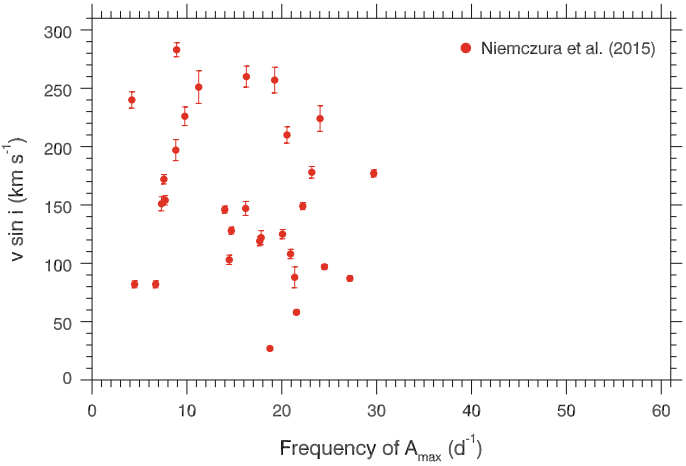

Fig. 4.15 The frequency of the highest amplitude pulsation mode plotted against v sin i using the subsample of δ Sct stars from Niemczura et al. (2015), which reveals no correlation between these two parameters

2000; Dupret et al. 2004, 2005) and studied using ground-based observations of δ Sct stars (Breger and Bregman 1975; Breger 2000a), and so the results presented here are consistent with previous analyses.

4.7.4 Pulsation and Rotation

The frequency of the highest amplitude pulsation mode is plotted against v sin i using the subsample of δ Sct stars from Niemczura et al. (2015) in Fig. 4.15, for which accurate values of v sin i were obtained from high-resolution spectroscopy. The effects of rotation modify the pulsation mode frequencies of a star by lifting the degeneracy of non-radial modes into their $2\ell + 1$ components, but there is no expectation for either slow or fast rotating δ Sct stars to have dominant high or low pulsation mode frequencies, or vice versa. As shown in Fig. 4.15, there is no correlation between the rotational velocity of a δ Sct star and the frequency of the highest amplitude pulsation mode, although there are not many stars included here.

4.8 Discussion

From ground-based observations, the δ Sct stars are found on or near the main sequence within the classical instability strip, and are well-defined by the observational blue and red edges from Rodríguez and Breger (2001). The γ Dor stars are

located in a nearby and overlapping region in the HR diagram (Dupret et al. 2004), but only a small minority of stars were predicted to be simultaneously unstable to both δ Sct and γ Dor excitation mechanisms (Dupret et al. 2005). However, *Kepler* observations have revealed that many pulsating A and F stars are hybrid stars pulsating in both p and g modes (Grigahcène et al. 2010a; Uytterhoeven et al. 2011; Balona and Dziembowski 2011), which is shown in Fig. 4.1.

From the in-depth studies of individual hybrid stars, it has been shown that p modes from the κ mechanism and g modes from the flux blocking mechanism can be simultaneously excited and be intrinsic to a single star (see e.g., Chapellier et al. 2012 and Kurtz et al. 2014). Also, it has been shown that hybrid stars can exist in binary systems, with all pulsations originating in the primary (see e.g., Van Reeth et al. 2015). Therefore, binarity does not offer a ubiquitous solution for why many δ Sct stars are hybrid pulsators. It has been suggested that all δ Sct stars are hybrid stars (Balona 2014; Balona et al. 2015), but stars pulsating in purely p modes with no statistically significant peaks in the g-mode frequency regime do exist. This was demonstrated using KIC 5617488 in Sect. 4.2.2.

In Sect. 4.3, it was discussed how a diverse range of as yet unexplained phenomena can exist in δ Sct stars, including the incidence of low-frequency peaks in δ Sct stars. These so-called organ pipe stars have a series of low-frequency peaks in their amplitude spectra that are highly variable in amplitude and phase throughout the *Kepler* data set, and it has been claimed that these low-frequency peaks are caused by rotation (Balona 2011, 2013). The δ Sct star KIC 10407873 was shown to contain a rotationally-split dipole mode, which was used to calculate a rotational velocity of $v_{\rm eq} \simeq 70\,{\rm km\,s^{-1}}$ for this star. This value is not consistent with the rotational velocity of $v_{\rm eq} \simeq 100\,{\rm km\,s^{-1}}$ calculated using the low-frequency peaks. Therefore, rotational modulation from starspots is not always the cause of low-frequency peaks in δ Sct stars. Further work is clearly needed to investigate the cause of these low-frequency peaks in δ Sct stars.

In this chapter, 4 yr of continuous *Kepler* data have been used to create an ensemble of 983 δ Sct stars to study the statistical properties of these stars, including the correlations between the fundamental stellar parameters and the frequency of the highest amplitude pulsation mode in each star. The majority of the 983 δ Sct stars are located inside the classical instability strip, as shown in Fig. 4.7, especially if the uncertainties in $T_{\rm eff}$ and $\log\ g$, and the 200 K systematic underestimation of KIC effective temperatures (Pinsonneault et al. 2012; Huber et al. 2014; Niemczura et al. 2015) are taken into account. However, a small fraction of stars are located outside the classical instability strip, and if the effective temperatures and surface gravities of these stars are accurate, then the observational blue and red edges from Rodríguez and Breger (2001) may need to be revised.

The correlations between the frequency of the highest amplitude pulsation mode and effective temperatures and surface gravities were investigated using the ensemble of 983 δ Sct stars in Sect. 4.7. For a hot δ Sct star near the blue edge of the classical instability strip, a high effective temperature facilitates the excitation of higher overtone modes because the κ mechanism operating in the He II ionisation zone is closer to the surface of the star (Pamyatnykh 1999; Christensen-Dalsgaard

2000; Dupret et al. 2004, 2005). The linear regression of the frequency of the highest amplitude pulsation mode against effective temperature shown in Fig. 4.11 indicates a weak correlation between these two parameters. This relationship was also found in ground-based observations of δ Sct stars (Breger and Bregman 1975; Breger 2000a).

Similarly, there is an expectation for post-main sequence δ Sct stars to exhibit lower pulsation mode frequencies from the presence of mixed modes (Osaki 1975) and the increase in radius caused by stellar evolution. A linear regression of the frequency of the highest amplitude pulsation mode against surface gravity is shown in Fig. 4.12, which reveals no significant correlation between these parameters. However, the degeneracy in pulsation mode frequencies for cool main sequence and evolved stars makes finding any correlation difficult.

In Figs. 4.7, 4.9, 4.10, 4.11 and 4.12, a subsample of δ Sct stars from Niemczura et al. (2015) are also shown, for which accurate $T_{\rm eff}$ and log g values obtained from high-resolution spectroscopy are known. The spectroscopic observations of v sin i for the subsample of δ Sct stars from Niemczura et al. (2015) are plotted against the frequency of the maximum amplitude pulsation mode in Fig. 4.15, which shows no correlation between the frequency of the highest amplitude pulsation mode and rotational velocity in this subsample of δ Sct stars.

References

Abt, H. A. 2009, AJ, 138, 28
Aerts, C., Christensen-Dalsgaard, J., & Kurtz, D. W. 2010, Asteroseismology(Springer)
Balona, L. A. 2011, MNRAS, 415, 1691
Balona, L. A. 2013, MNRAS, 431, 2240
Balona, L. A. 2014, MNRAS, 437, 1476
Balona, L. A. & Dziembowski, W. A. 2011, MNRAS, 417, 591
Balona, L. A., Pigulski, A., Cat, P. D., et al. 2011, MNRAS, 413, 2403
Balona, L. A., Daszyńska-Daszkiewicz, J., & Pamyatnykh, A. A. 2015, MNRAS, 452, 3073
Bowman, D. M. & Kurtz, D. W. 2014, MNRAS, 444, 1909
Bowman, D. M., Kurtz, D. W., Breger, M., Murphy, S. J., & Holdsworth, D. L. 2016, MNRAS, 460, 1970
Breger, M. 2000a, in Astronomical Society of the Pacific Conference Series, Vol. 210, Delta Scuti and Related Stars, ed. M. Breger & M. Montgomery, 3
Breger, M. 2000b, MNRAS, 313, 129
Breger, M. 2016, A&A, 592, A97
Breger, M. & Bregman, J. N. 1975, ApJ, 200, 343
Breger, M., Stich, J., Garrido, R., et al. 1993, A&A, 271, 482
Brown, T. M., Latham, D. W., Everett, M. E., & Esquerdo, G. A. 2011, AJ, 142, 112
Chapellier, E., Mathias, P., Weiss, W. W., Le Contel, D., & Debosscher, J. 2012, A&A, 540, A117
Christensen-Dalsgaard, J. 2000, in Astronomical Society of the Pacific Conference Series, Vol. 210, Delta Scuti and Related Stars, ed. M. Breger & M. Montgomery, 187
Duchêne, G. & Kraus, A. 2013, ARA&A, 51, 269
Dupret, M. A., Grigahcène, A., Garrido, R., Gabriel, M., & Scuflaire, R. 2004, A&A, 414, L17
Dupret, M. A., Grigahcène, A., Garrido, R., Gabriel, M., & Scuflaire, R. 2005, A&A, 435, 927

Dziembowski, W. A., Goode, P. R., Pamyatnykh, A. A., & Sienkiewicz, R. 1995, in Astronomical Society of the Pacific Conference Series, Vol. 76, GONG 1994. Helio- and Astro-Seismology from the Earth and Space, ed. R. K. Ulrich, E. J. Rhodes, Jr., & W. Dappen, 124
Grigahcène, A., Antoci, V., Balona, L., et al. 2010a, ApJL, 713, L192
Grigahcène, A., Uytterhoeven, K., Antoci, V., et al. 2010b, Astronomische Nachrichten, 331, 989
Guzik, J. A., Kaye, A. B., Bradley, P. A., Cox, A. N., & Neuforge, C. 2000, ApJL, 542, L57
Handler, G. 2009, MNRAS, 398, 1339
Handler, G. & Shobbrook, R. R. 2002a, in Astronomical Society of the Pacific Conference Series, Vol. 256, Observational Aspects of Pulsating B- and A Stars, ed. C. Sterken & D. W. Kurtz, 117
Handler, G. & Shobbrook, R. R. 2002b, MNRAS, 333, 251
Handler, G., Balona, L. A., Shobbrook, R. R., et al. 2002, MNRAS, 333, 262
Holdsworth, D. L., Smalley, B., Gillon, M., et al. 2014, MNRAS, 439, 2078
Huber, D., Silva Aguirre, V., Matthews, J. M., et al. 2014, ApJS, 211, 2
Keen, M. A., Bedding, T. R., Murphy, S. J., et al. 2015, MNRAS, 454, 1792
Kurtz, D. W., Saio, H., Takata, M., et al. 2014, MNRAS, 444, 102
Kurtz, D. W., Shibahashi, H., Murphy, S. J., Bedding, T. R., & Bowman, D. M. 2015, MNRAS, 450, 3015
Lenz, P., Pamyatnykh, A. A., Zdravkov, T., & Breger, M. 2010, A&A, 509, A90
McNamara, B. J., Jackiewicz, J., & McKeever, J. 2012, AJ, 143, 101
Moe, M. & Di Stefano, R. 2017, Mind Your Ps and Qs: The Interrelation between Period (P) and Mass-ratio (Q) Distributions of Binary Stars, APJS, 230, 15
Murphy, S. J., Shibahashi, H., & Kurtz, D. W. 2013, MNRAS, 430, 2986
Murphy, S. J., Fossati, L., Bedding, T. R., et al. 2016, MNRAS, 459, 1201
Niemczura, E., Murphy, S. J., Smalley, B., et al. 2015, MNRAS, 450, 2764
Osaki, J. 1975, PASJ, 27, 237
Pamyatnykh, A. A. 1999, Acta Astronomica, 49, 119
Pamyatnykh, A. A. 2000, in Astronomical Society of the Pacific Conference Series, Vol. 210, Delta Scuti and Related Stars, ed. M. Breger & M. Montgomery, 215
Pinsonneault, M. H., An, D., Molenda-Żakowicz, J., et al. 2012, ApJS, 199, 30
Raskin, G., van Winckel, H., Hensberge, H., et al. 2011, A&A, 526, A69
Rodríguez, E. & Breger, M. 2001, A&A, 366, 178
Saio, H., Kurtz, D. W., Takata, M., et al. 2015, MNRAS, 447, 3264
Schmid, V. S. & Aerts, C. 2016, A&A, 592, A116
Triana, S. A., Moravveji, E., Pápics, P. I., et al. 2015, ApJ, 810, 16
Uytterhoeven, K., Moya, A., Grigahcène, A., et al. 2011, A&A, 534, A125
Van Reeth, T., Tkachenko, A., Aerts, C., et al. 2015, ApJS, 218, 27

Chapter 5
Amplitude Modulation in *Kepler* Delta Scuti Stars

5.1 Introductory Remarks

The various causes of why δ Sct stars exhibit variable pulsation mode amplitudes (and/or frequencies) can be loosely grouped as intrinsic and extrinsic, i.e., those physical and interior to the star and those caused by external effects, respectively. The statistical search for amplitude modulation in a large number of δ Sct stars, which is presented in this chapter, is primarily motivated by studies of the δ Sct star KIC 7106205 discussed in Chap. 3. The *Kepler* data set offers the opportunity to test if this phenomenon is common among a large number of δ Sct stars. Further motivation comes from well-studied δ Sct stars observed from the ground. The δ Sct star 4 CVn, which was discussed in Sect. 1.5, epitomises the diversity among all δ Sct stars, because it has been shown to be part of a binary system (Schmid et al. 2014), has beating of close-frequency pulsation modes (Breger and Bischof 2002), has a mode coupling mechanism (Breger 2000), and exhibits amplitude modulation from an unknown mechanism (Breger 2016).

In this chapter, inspired by the extensive literature on the δ Sct star 4 CVn and the previous analyses of KIC 7106205, the following research questions are tested using the ensemble of 983 δ Sct stars discussed in Chap. 4, which are:

(i) Is amplitude modulation common among δ Sct stars?
(ii) How can one distinguish the various causes of amplitude modulation?
(iii) Is the pulsational energy budget of a δ Sct star conserved over 4 yr?

5.2 Searching for Significant Amplitude Modulation

In this section, the method used by Bowman et al. (2016) to conduct a statistical search for amplitude modulation in approximately 1000 δ Sct stars is discussed.

D.M. Bowman, *Amplitude Modulation of Pulsation Modes in Delta Scuti Stars*,
Springer Theses, DOI 10.1007/978-3-319-66649-5_5

5.2.1 Identifying Pulsation Modes with Variable Amplitudes

For their study of amplitude modulation in δ Sct stars, Bowman et al. (2016) used the ensemble of 983 stars discussed in Chap. 4. An amplitude and phase tracking method similar to that used to study the δ Sct star KIC 7106205 by Bowman and Kurtz (2014) was automated for all 983 δ Sct stars and was used to measure amplitude and phase (at fixed frequency) for the 12 highest-amplitude peaks in the amplitude spectrum of each star throughout the 4-yr *Kepler* data set. Bowman et al. (2016) comment how extracting and tracking a maximum of 12 peaks for each star is somewhat arbitrary, since their goal was to identify the changes in the dominant pulsation modes for a large ensemble of δ Sct stars. Some δ Sct stars only pulsate in only a few modes so extracting up to 12 peaks was sufficient. On the other hand, some δ Sct stars pulsate in dozens of modes and have possibly hundreds of combination frequencies in their amplitude spectra, so extracting up to 12 frequencies may not fully disentangle the star but provides information on the most dominant behaviour. A commonly used criterion for whether a peak in an amplitude spectrum is statistically significant is if it has a signal-to-noise ratio in amplitude of $S/N \geq 4$ (Breger et al. 1993). Note, however, that only peaks with amplitudes greater than $A \geq 0.10$ mmag were extracted in the analysis of Bowman et al. (2016), which is much higher than the typical noise level in *Kepler* data, so fewer than 12 frequencies can be listed for a star.

The frequencies for each star were extracted by iteratively pre-whitening the amplitude spectrum and subsequently optimised using a simultaneous multifrequency non-linear least-squares fit to the 4-yr data set, which ensured that the highest frequency resolution and amplitude precision were obtained (Bowman et al. 2016). The data set for each star was then divided into 30 time bins, each 100 d in length (except the last bin) with a 50-d overlap, and values of amplitude and phase were optimised at fixed frequency using linear least-squares in each bin for each frequency (Bowman et al. 2016). The amplitudes and phases of each time bin for the frequencies were plotted against time in what Bowman et al. (2016) term tracking plots, which allowed amplitude and phase modulation to be studied in each star.

5.2.2 Defining Significant Amplitude Modulation

Identifying significant amplitude modulation in a star's pulsation modes by visual inspection of its tracking plot is straightforward but time consuming for all 983 δ Sct stars, so this process was automated by Bowman et al. (2016) using the following methodology. A mean amplitude for each peak was calculated excluding the last time bin as it contained fewer data points, and any bins that were more than $\pm 5\sigma$ in amplitude away from the mean were flagged. An example of this definition of significant amplitude modulation is shown graphically in Fig. 5.1 where solid and dashed lines represent the mean amplitude and the $\pm 5\sigma$ significance interval, respectively,

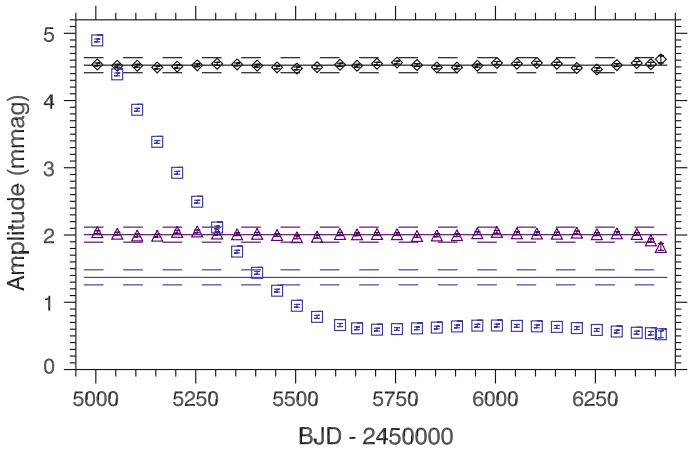

Fig. 5.1 Amplitude tracking plot for KIC 7106205 showing pulsation mode frequencies $\nu_1 = 10.0323662\ \mathrm{d}^{-1}$, $\nu_2 = 10.7273166\ \mathrm{d}^{-1}$ and $\nu_3 = 13.3941749\ \mathrm{d}^{-1}$ as *black diamonds*, *purple triangles* and *blue squares*, respectively. The *solid line* for each frequency is the mean of 30 time bins and the *dashed lines* represent the $\pm 5\sigma$ amplitude significance interval from the mean. Figure from Bowman et al. (2016), their Fig. 1

for the three highest amplitude pulsation modes in KIC 7106205. If at least 15 (i.e., half) of the amplitude bins were more than $\pm 5\sigma$ from the mean value, then a peak was labelled as exhibiting significant amplitude modulation. For example, only $\nu_3 \equiv \nu_{\mathrm{mod}} = 13.3941749\ \mathrm{d}^{-1}$ in KIC 7106205 satisfied this definition as shown in Fig. 5.1, with all other peaks in this star flagged as constant amplitudes.

This method for identifying significant amplitude modulation was applied to all 983 δ Sct stars, with the abbreviation AMod (**A**mplitude **Mod**ulated) to identify stars with at least a single pulsation mode that is variable in amplitude over the 4-yr *Kepler* data set, and the abbreviation NoMod (**No Mod**ulation) for those that do not (Bowman et al. 2016). It should also be noted that the threshold of more than half of the bins being greater than $\pm 5\sigma$ is a choice made by Bowman et al. (2016), and that choosing a threshold of, for example, more than a third of the bins being greater $\pm 3\sigma$ would yield different fractions of stars being identified as AMod and NoMod.

5.2.3 *Phase Adjustment*

Similarly to the analysis of the δ Sct star KIC 7106205 discussed in Sect. 3.2, values of frequencies, amplitudes and phases were optimised using a least-squares fit using the cosinusoid function $\Delta m = A\cos(2\pi\nu(t - t_0) + \phi)$. The zero-point of the time scale was $t_0 = 2\,455\,688.770$ BJD with phase defined within the interval of $-\pi \leq \phi \leq \pi$ rad for each star so comparisons could be made (Bowman et al. 2016). Thus, the phase of a pulsation mode could be adjusted by adding or subtracting

integer values of 2π rad. Bowman et al. (2016) comment that if the difference between consecutive phase bins for in a tracking exceeded 5 rad, then $\pm 2\pi$ rad phase adjustments were made. This phase adjustment did not remove any beating signals between pulsation mode frequencies since the phase change caused by beating at the epoch of minimum amplitude in a beat cycle cannot exceed π rad (Bowman et al. 2016).

5.3 Amplitude Modulation Catalogue Case Studies

In their analysis of 983 δ Sct stars, Bowman et al. (2016) collated all the amplitude spectra and tracking plots into a single catalogue.[1] A table of stellar parameters from Huber et al. (2014), the number of AMod and NoMod frequencies, and the pulsator type as either δ Sct or hybrid based on its frequencies was also included as an appendix in Bowman et al. (2016), with an abridged version given in Table 5.1.

In the following subsections, individual stars are used as case studies to demonstrate the diversity of pulsational behaviour in δ Sct stars and the different causes of amplitude modulation, although Bowman et al. (2016) gave more examples for each of the following scenarios.

5.3.1 Phase Modulation Caused by Super-Nyquist Peaks

It was discussed in Sect. 2.3.1 and shown graphically in Fig. 2.3 how a super-Nyquist alias peak is split into a multiplet in an amplitude spectrum because of the variable *Kepler* LC Nyquist frequency. In the amplitude and phase tracking method employed by Bowman et al. (2016), the HADS star KIC 5950759 is used to demonstrate how phase modulation can also be used to identify alias peaks in an amplitude spectrum. The amplitude and phase tracking plot in Fig. 5.2 shows the results of the tracking method applied to the real and alias peaks for the harmonic of the fundamental radial mode frequency in the HADS star KIC 5950759. The alias peak shown as blue crosses experiences phase modulation with a peak-to-peak amplitude of approximately $\pi/2$ rad and a period equal to the *Kepler* satellite orbital period (372.5 d) caused by the variable LC *Kepler* Nyquist frequency (Murphy et al. 2013; Bowman et al. 2016). This example demonstrates how super-Nyquist aliases of real frequencies can be easily identified from the 372.5-d periodic phase modulation (see also Murphy et al. 2014, their Fig. 2). Frequencies identified as super-Nyquist aliases are labelled as sNa in figure captions and in Table 1 of Bowman et al. (2016).

[1] The amplitude modulation catalogue containing the amplitude spectra and tracking plots of all 983 δ Sct stars can be obtained from http://uclandata.uclan.ac.uk/id/eprint/42 as a PDF.

Table 5.1 Stellar parameters from Huber et al. (2014) for the NoMod and AMod δ Sct case study stars discussed in Sect. 5.3 of this monograph. For each star, the number of constant-amplitude and variable-amplitude pulsation mode frequencies, N_ν, above the amplitude extraction threshold of $A \geq 0.10$ mmag are listed under the columns NoMod and AMod, respectively. An unabridged version of this table is available from Bowman et al. (2016) and a machine-readable version is available through CDS[†]

KIC ID	$T_{\rm eff}$ (K)	log g (cgs)	[Fe/H] (dex)	N_ν		Comments
				NoMod	AMod	
NoMod:						
2304168	7220 ± 270	3.67 ± 0.19	-0.06 ± 0.30	11	0	
AMod caused by beating:						
4641555	7170 ± 250	4.22 ± 0.25	-0.12 ± 0.32	8	1	$P_{\rm beat} = 1166 \pm 1$ d
8246833	7330 ± 270	3.96 ± 0.22	-0.32 ± 0.30	9	3	$P_{\rm beat} = 1002 \pm 1$ d
Pure AMod:						
8453431	7180 ± 270	3.63 ± 0.19	-0.06 ± 0.29	2	1	
Binarity:						
9651065	7010 ± 150	3.83 ± 0.13	-0.10 ± 0.15	12	0	$P_{\rm orb} = 272.7 \pm 0.8$ d

[†]http://cdsarc.u-strasbg.fr/viz-bin/Cat?J/MNRAS/460/1970

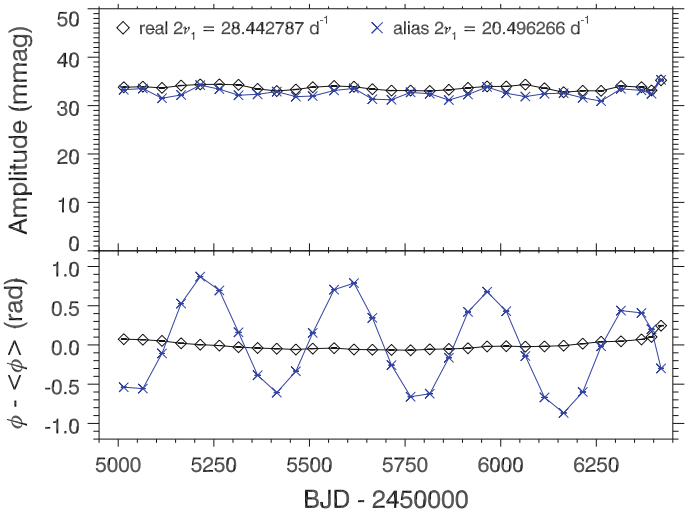

Fig. 5.2 The amplitude and phase tracking plot for the real and super-Nyquist alias of the harmonic of the fundamental radial mode in the HADS star KIC 5950759 shows how the alias peak experiences periodic phase modulation, which is caused by the Barycentric time-stamp corrections made to *Kepler* data. Whereas the real peak has approximately constant phase and thus can be easily identified. Figure from Bowman et al. (2016), their Fig. 2

5.3.2 Constant Amplitudes and Phases: NoMod Stars

Using their methodology for identifying significant amplitude modulation, Bowman et al. (2016) found 380 NoMod δ Sct stars within the ensemble of 983 stars, thus many δ Sct stars exhibit little or no change in their pulsation mode amplitudes over time scales of order a few years. This subset supports the view that δ Sct stars are typically coherent and periodic pulsators. A good example of a NoMod δ Sct star that exhibits constant-amplitude and constant-phase pulsation modes over the 4-yr *Kepler* data set is KIC 2304168, which is shown in Fig. 5.3. The stellar parameters of KIC 2304168 from Huber et al. (2014) and the number of NoMod and AMod peaks are given in Table 5.1.

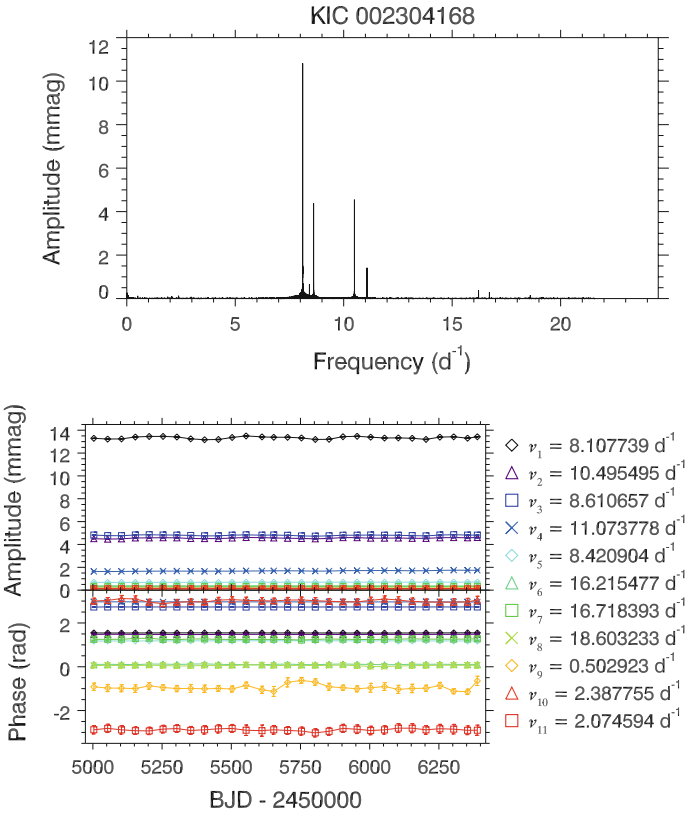

Fig. 5.3 An example of an NoMod δ Sct star, KIC 2304168, in the KIC range $6400 \leq T_{\rm eff} \leq 10\,000$ K that shows no significant variability in its pulsation mode amplitudes or phases over the 4-yr *Kepler* data set. The *top panel* shows the 4-yr amplitude spectrum calculated out to the LC Nyquist frequency, and the *bottom panel* shows the amplitude and phase tracking plot for the 11 significant pulsation modes. Figure from Bowman et al. (2016), their Fig. 3

The δ Sct star KIC 2304168 was also studied by Balona and Dziembowski (2011), who used *Kepler* observations and asteroseismic modelling to identify its two high-amplitude pulsation modes (which they term $f_1 = 8.1055\,\mathrm{d}^{-1}$ and $f_2 = 10.4931\,\mathrm{d}^{-1}$) as the fundamental and first overtone radial p modes, respectively. With a much longer data set available, Bowman et al. (2016) re-analysed this star and calculated that the period ratio from 4 yr of *Kepler* data for $\nu_1 = 8.107739\,\mathrm{d}^{-1}$ and $\nu_2 = 10.495495\,\mathrm{d}^{-1}$ is 0.7725, which is typical for the ratio of the first overtone and fundamental radial modes. Bowman et al. (2016) also calculated pulsation constants for ν_1 and ν_2 as 0.028 and 0.022, respectively, which are consistent with the mode identification by Balona and Dziembowski (2011) considering the typical uncertainties in this calculation (Breger 1990). The harmonic of ν_1 also has a relatively high amplitude in KIC 2304168, which is labelled as ν_6 in Fig. 5.3. Bowman et al. (2016) comment that this star is an excellent example of a NoMod δ Sct star, since it has low mode density in its amplitude spectrum and mode identification is possible, but most importantly, all its pulsation modes are very stable over 4 yr. In contrast to the δ Sct star KIC 7106205 discussed in Chap. 3, it is certainly interesting how δ Sct stars of similar T_{eff}, $\log g$ and [Fe/H] can be AMod or NoMod — what mechanism is causing amplitude modulation in some δ Sct stars, yet is absent in others?

5.3.3 *Amplitude and Phase Modulation Caused by Beating of Close-Frequency Modes*

In their statistical study of amplitude modulation in 983 δ Sct stars, Bowman et al. (2016) found two stars, KIC 4641555 and KIC 8246833, that are AMod from the beating of pulsation modes spaced closer than $0.001\,\mathrm{d}^{-1}$. This is perhaps one of the strongest examples that demonstrates the superiority of *Kepler* data purely because of the length: 4 yr is only just long enough to resolve the closely-spaced pairs of pulsation mode frequencies in these two stars. The amplitude spectra and a zoom-in of the close-frequency pulsation modes in KIC 4641555 and KIC 8246833 are shown in Figs. 5.4 and 5.5, respectively. The stellar parameters of KIC 4641555 and KIC 8246833 from Huber et al. (2014) and the number of NoMod and AMod peaks are given in Table 5.1. The observed amplitude modulation caused by the beating in these two stars is discussed in more detail in Sect. 5.7.2.

5.3.4 *Pure Amplitude Modulation with No Phase Variability*

Although they were not studied separately in detail, the subgroup of stars denoted as pure AMod stars by Bowman et al. (2016) are perhaps the most interesting in terms of their pulsational properties. This pure form of amplitude modulation is unlikely to be caused by beating of unresolved pulsation modes or mode coupling because no phase modulation is observed, which is required by both mechanisms.

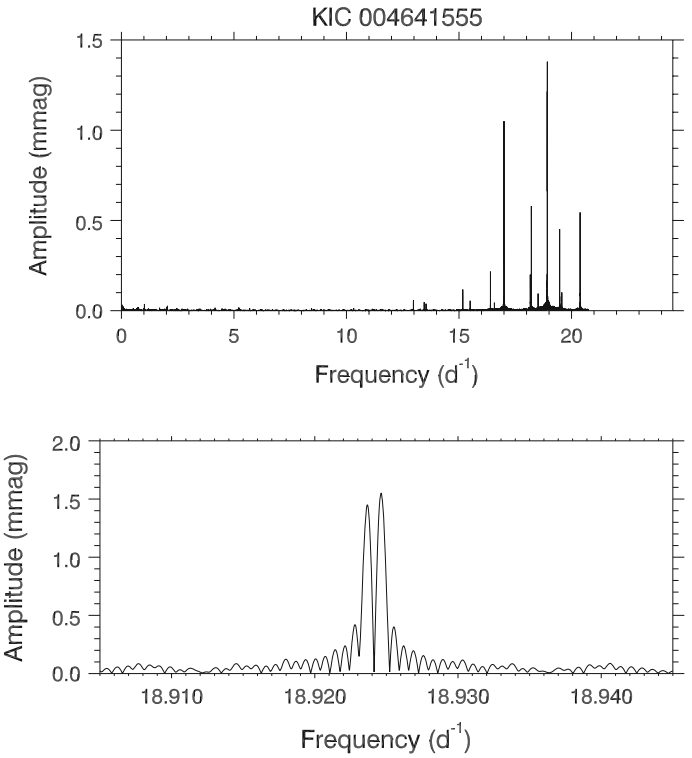

Fig. 5.4 An example of an AMod δ Sct star, KIC 4641555, in the KIC range $6400 \leq T_{\rm eff} \leq 10\,000$ K that shows variable pulsation amplitudes and phases over the 4-yr *Kepler* data set caused by beating of extremely close-frequency modes. The top panel shows the 4-yr amplitude spectrum calculated out to the LC Nyquist frequency, and the bottom panel shows a zoom-in of the pair of close-frequency modes in the amplitude spectrum that lie closer than 0.001 d^{-1} in frequency. Figure from Bowman et al. (2016), their Fig. 4

This subgroup contains perhaps the most interesting δ Sct stars, with no obvious selection effect that determines why some stars do this and others do not. Bowman et al. (2016) conjecture that pure amplitude modulation could be caused by variable driving and/or damping within a star. Therefore, it remains an unsolved problem why this occurs. An example of a pure AMod δ Sct star is KIC 8453431 with its amplitude spectrum and tracking plot shown in Fig. 5.6. The stellar parameters of KIC 8453431 from Huber et al. (2014) and the number of NoMod and AMod peaks are given in Table 5.1.

KIC 8453431 is one of the four examples of pure AMod stars presented in Bowman et al. (2016), but it is perhaps the best example since its amplitude spectrum only contains three pulsation modes with amplitudes greater than $A \geq 0.10$ mmag, labelled as $\nu_1 = 13.859080\ \mathrm{d}^{-1}$, $\nu_2 = 22.154964\ \mathrm{d}^{-1}$ and $\nu_3 = 10.380567\ \mathrm{d}^{-1}$ in Fig. 5.6. The period ratio of ν_2 and ν_1 is 0.6256 and the period ratio of ν_3 and ν_1 is

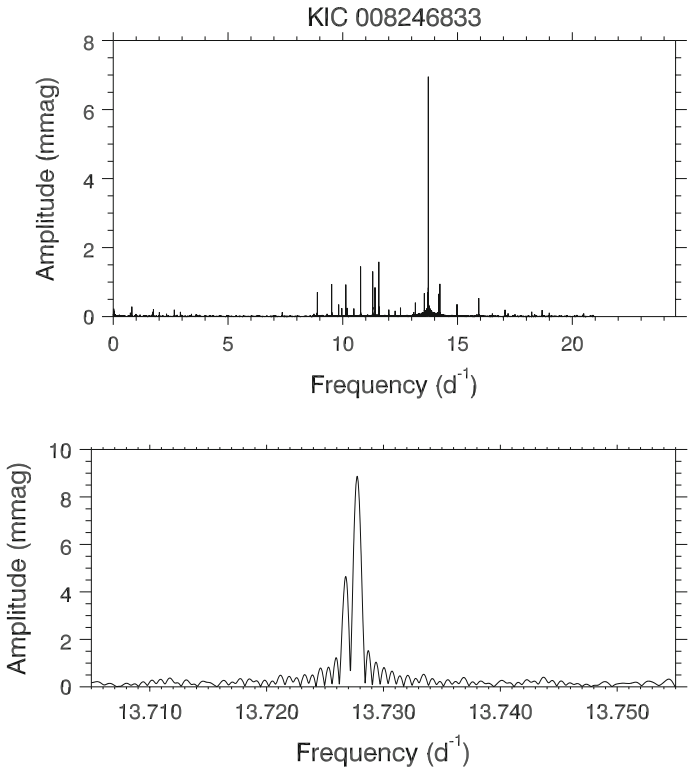

Fig. 5.5 An example of an AMod δ Sct star, KIC 8246833, in the KIC range $6400 \leq T_{\rm eff} \leq 10\,000$ K that shows variable pulsation amplitudes and phases over the 4-yr *Kepler* data set caused by beating of extremely close-frequency modes. The *top panel* shows the 4-yr amplitude spectrum calculated out to the LC Nyquist frequency, and the *bottom panel* shows a zoom-in of the pair of close-frequency modes in the amplitude spectrum that lie closer than 0.001 d^{-1} in frequency. Figure from Bowman et al. (2016), their Fig. 4

0.7490, but pulsation constants indicate that neither ν_3 or ν_1 is the fundamental radial mode (Bowman et al. 2016). Therefore, it can only be concluded that the three modes are low-overtone radial modes considering the typical uncertainties associated with calculating Q values (Breger 1990). Regardless of the method for mode identification, only a single pulsation mode frequency, ν_2, slowly increases in amplitude whilst staying at constant phase.

KIC 8453431 is a counterpoint example of the δ Sct star KIC 7106205 discussed in Sect. 3.2, where KIC 8453431 contains a single pulsation mode that *increases* in amplitude whilst all other pulsation modes stay constant in amplitude and phase. Within the ensemble of 983 δ Sct stars, approximately the same number of increasing pure AMod stars as decreasing pure AMod stars were found, suggesting that this behaviour is intrinsic to the pulsation excitation mechanism in δ Sct stars (Bowman et al. 2016).

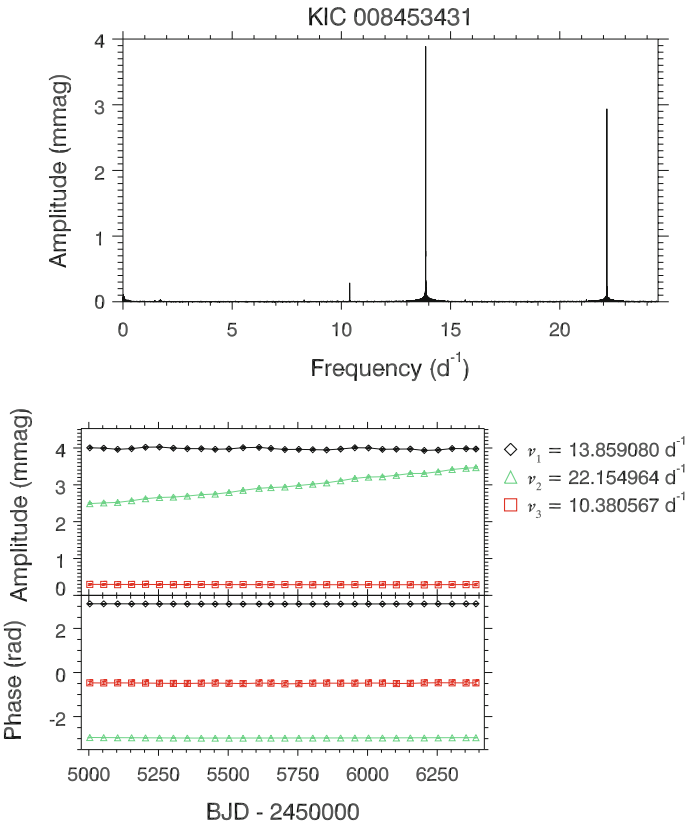

Fig. 5.6 An example of a pure AMod δ Sct star, KIC 8453431, in the KIC range $6400 \leq T_{\rm eff} \leq 10\,000$ K that shows variable pulsation mode amplitudes with constant phases over the 4-yr *Kepler* data set. The *top panel* shows the 4-yr amplitude spectrum calculated out to the LC Nyquist frequency, and the *bottom panel* shows the amplitude and phase tracking plot for the three significant pulsation modes. Figure from Bowman et al. (2016), their Fig. 5

5.3.5 *Phase Modulation Due to Binarity*

Using recent novel methods, binarity in a stellar system can be tested using photometric data by applying the Frequency Modulation technique (FM; Shibahashi and Kurtz 2012; Shibahashi et al. 2015) and/or the Phase Modulation technique (PM; Murphy et al. 2014; Murphy and Shibahashi 2015). The FM technique exploits the fact that the motion of a pulsating star about the Barycentre of a binary (or multiple) system will introduce a small frequency shift to a pulsation mode frequency throughout the orbit. If the observations are longer than the orbital period of the system, then

this perturbation will be resolved and produce sidelobes on either side of a pulsation mode frequency in the amplitude spectrum (Shibahashi and Kurtz 2012). The orbital period of the system can then be directly measured as the inverse of the separation in frequency between the central peak of a multiplet and its sidelobes in the amplitude spectrum.

Similarly, the PM technique exploits the difference in light travel time of a star across the orbit in a binary system, thus the phases of pulsation modes will vary periodically throughout the orbit (Murphy et al. 2014). The peak-to-peak amplitude of the observed phase modulation in the PM technique is a function of frequency when expressed as light travel time delays (see Eq. (3) from Murphy et al. 2014). If all the pulsation modes in a star vary in phase with the same period, this can be explained by the Doppler effect modulating the pulsation signal throughout the orbital period (Murphy et al. 2014). The significance of the FM and PM techniques is made evident as the orbital parameters $P_{\rm orb}$, e, $a \sin i$, $f(m)$ and argument of periastron can be determined without necessarily obtaining radial velocity measurements (Kurtz et al. 2015).

The binary fraction of δ Sct stars is not significantly different to the binary fraction of all A stars, as was discussed in Sect. 4.2.1. Therefore, a non-negligible fraction of binary δ Sct stars are expected amongst the 983 in the ensemble studied by Bowman et al. (2016). A previously confirmed binary δ Sct star included in the ensemble study was KIC 9651065, which was also analysed using the PM technique by Murphy et al. (2014), who calculated an orbital period of $P_{\rm orb} = 272.7 \pm 0.8$ d. Later using the FM technique, Shibahashi et al. (2015) found pulsation mode frequencies with first, second and third FM sidelobes in the amplitude spectrum of KIC 9651065, indicating that the orbit of this binary system is highly eccentric. An eccentricity of $e = 0.569 \pm 0.030$ was calculated from the amplitude ratio of the FM sidelobes (Shibahashi et al. 2015).

To show compatibility with the PM technique, KIC 9651065 was included as an example of a δ Sct star in a binary system in the study by Bowman et al. (2016), with its stellar parameters from Huber et al. (2014) and the number of NoMod and AMod peaks given in Table 5.1. Binarity within a stellar system causes all the pulsation modes to exhibit phase modulation with a period equal to the orbital period of the star. Figure 5.7 shows the amplitude spectrum and the tracking plot of KIC 9651065, in which the period of the phase modulation can be seen and is $P_{\rm orb} = 272.7 \pm 0.8$ d (Murphy et al. 2014; Bowman et al. 2016). Note that ν_4 in Fig. 5.7 is a super-Nyquist alias frequency so does does not directly follow the same phase modulation behaviour. The amplitude modulation in KIC 9651065 appears unrelated to the phase modulation caused by the presence of a companion object, demonstrating the diverse range of pulsation properties in δ Sct stars for both single and multiple stellar systems.

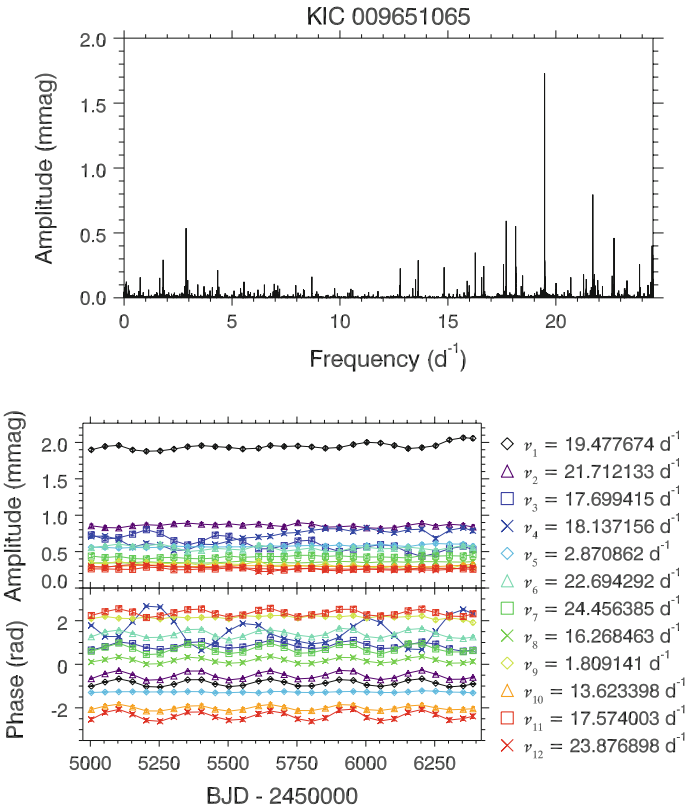

Fig. 5.7 An example of an AMod δ Sct star, KIC 9651065, in the KIC range $6400 \leq T_{\rm eff} \leq 10\,000$ K that shows phase modulation in its pulsation modes over the 4-yr *Kepler* data set because of binarity. The *top panel* shows the 4-yr amplitude spectrum calculated out to the LC Nyquist frequency, and the *bottom panel* shows the amplitude and phase tracking plot for the 12 highest-amplitude peaks in the amplitude spectrum. Note that ν_4 is a super-Nyquist alias frequency. The orbital period of 272.7 ± 0.8 d is calculated from the period of the phase modulation in the tracking plot, and is consistent with the result from the PM and FM techniques (Murphy et al. 2014; Shibahashi et al. 2015). Figure from Bowman et al. (2016), their Fig. 6

5.4 Statistics from an Ensemble Study of Amplitude Modulation

The ensemble of 983 δ Sct stars studied by Bowman et al. (2016) comprised all stars between $6400 \leq T_{\rm eff} \leq 10\,000$ K in the KIC (Brown et al. 2011), that were found to pulsate in p-mode frequencies between $4 \leq \nu \leq 24$ d^{-1} and that were observed continuously by the *Kepler* Space Telescope for 4 yr. From each star's amplitude spectrum, the number of peaks with amplitudes larger than $A \geq 0.10$ mmag (up to a maximum of 12) were flagged and identified as exhibiting constant or significant modulation in amplitude by tracking how the amplitude of each peak changed

throughout the *Kepler* data set. The criterion of significant amplitude modulation chosen by Bowman et al. (2016) was that if 15 time bins for a peak were greater than $\pm 5\sigma$ in amplitude from the mean then the star was identified as an AMod star, which is shown graphically in Fig. 5.1. If none of the extracted peaks satisfied this criterion, then a star was labelled as NoMod.

From a total of 983 stars, 380 stars (38.7%) were classified as NoMod and 603 stars (61.3%) were classified as AMod (Bowman et al. 2016). The distribution of the number of stars against the number of AMod peaks is shown in the top-left panel of Fig. 5.8. Thus, one of the main conclusions of the search for amplitude modulation by Bowman et al. (2016) is that this behaviour is common among δ Sct stars since the majority of stars were classified as AMod using their criteria. A subset of 201 stars were found to have only a single AMod pulsation mode whilst all other peaks remained constant in amplitude (Bowman et al. 2016). The discovery that this behaviour is common among δ Sct stars is a new result from Bowman et al. (2016).

Various distributions of stellar parameters are also shown in Fig. 5.8 for both the original KIC values (Brown et al. 2011) and the revised values given in Huber et al. (2014) in the left- and right-hand columns, respectively. In Fig. 5.8, the unhatched black region represents all 983 stars in the ensemble and the blue and red hatched regions show the NoMod and AMod stars, respectively. The distributions of $T_{\rm eff}$, $\log\, g$, [Fe/H] and Kp magnitude for the NoMod and AMod stars are similar, demonstrating that amplitude modulation is common and widespread amongst δ Sct stars (Bowman et al. 2016). The physical causes of amplitude modulation must not solely depend on a star's parameters but on other physics.

It might be expected that evolved δ Sct stars (i.e., stars with lower $\log\, g$ values) to be AMod stars, because they are more likely to contain mixed modes, or because the structure of such a star is changing in a relatively short period of time. Even whilst on the main sequence the convective core of a star can increase or decrease in mass depending on the initial mass (see Fig. 3.6 from Aerts et al. 2010). However, the $\log\, g$ distributions for NoMod and AMod in Fig. 5.8 are centred on approximately the same value, but there is a stronger bimodality in the $\log\, g$ distribution of AMod stars compared to the NoMod stars using values from Huber et al. (2014). This supports the expectation that evolved δ Sct stars are more likely to be AMod, but the bimodality was not seen in the KIC $\log\, g$ values so it may be an artefact of the Huber et al. (2014) method.

To investigate the location of AMod and NoMod stars within the classical instability strip, Bowman et al. (2016) created $T_{\rm eff} - \log\, g$ diagrams using the original and revised KIC values, which are shown in Fig. 5.9. The observational blue and red edges of the classical instability strip from Rodríguez and Breger (2001) are also plotted as solid black lines in Fig. 5.9, with NoMod and AMod stars plotted as blue diamonds and red squares, respectively. There is no obvious correlation between amplitude modulation and the stellar parameters $T_{\rm eff}$ or $\log\, g$, thus with a star's location within the classical instability strip (Bowman et al. 2016). An important inference from this work is that amplitude modulation is not directly dependent on the fundamental stellar parameters of a δ Sct star, but appears related to the pulsation excitation mechanism itself (Bowman et al. 2016).

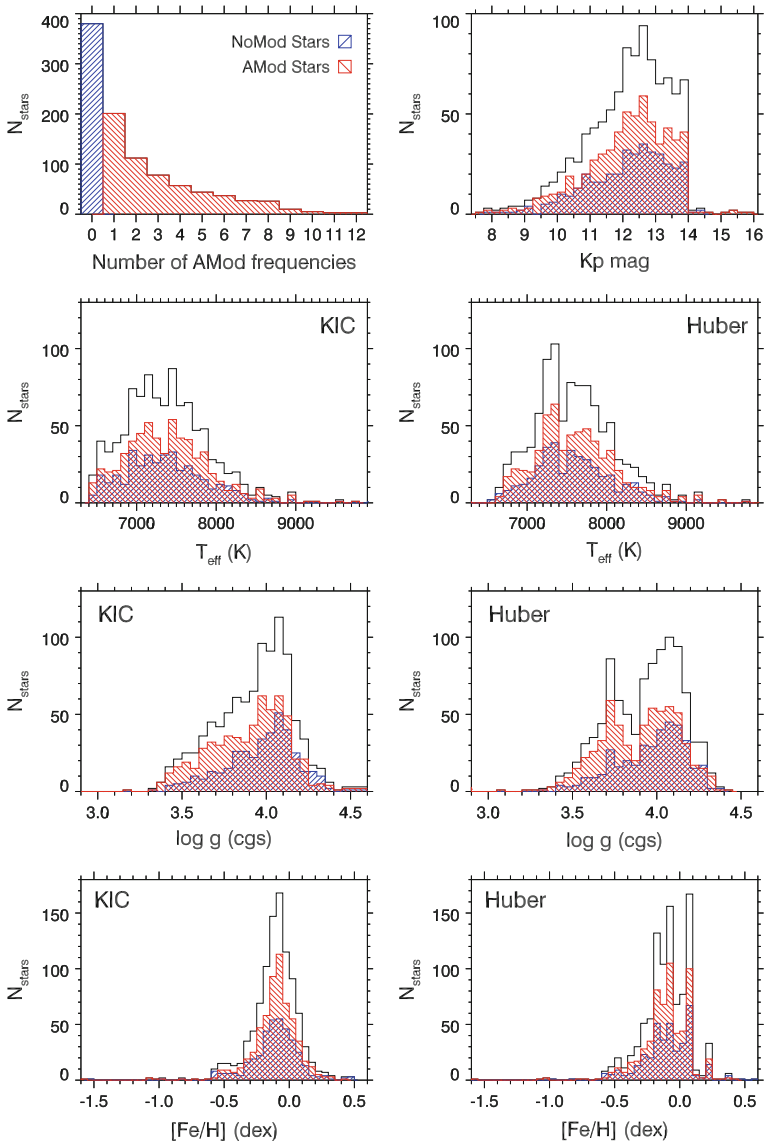

Fig. 5.8 The distribution of the number of stars against the number of AMod peaks in the ensemble is shown in the *top-left panel*. The distribution of the number stars against $T_{\rm eff}$, log g, [Fe/H] and Kp mag, in which the unhatched *black region* represents all 983 stars in the ensemble, the hatched *blue region* represents the 380 NoMod stars and the hatched red region represents the 603 AMod stars. Distributions of $T_{\rm eff}$, log g, [Fe/H] using the original KIC values are shown in the *left-hand panels*, and the revised values from Huber et al. (2014) are shown in the *right-hand panels*. Figure from Bowman et al. (2016), their Fig. 11

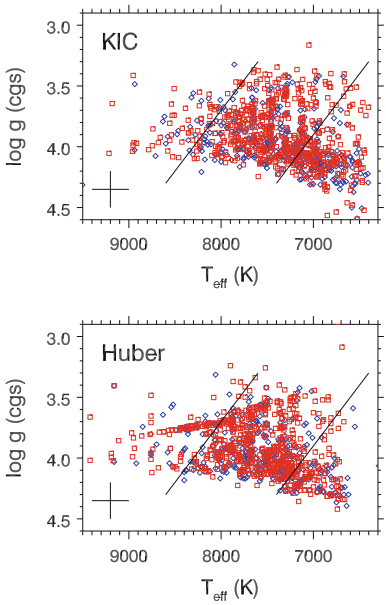

Fig. 5.9 $T_{\rm eff} - \log\, g$ diagrams for the stellar parameters listed in the KIC (*top panel*) and the revised values given by Huber et al. (2014) (*bottom panel*). The diamonds represent the 380 NoMod stars and the squares represent the 603 AMod stars. The *solid lines* are the observational blue and red edges of the classical instability strip from Rodríguez and Breger (2001), and the cross represents the typical uncertainty for each point. Figure from Bowman et al. (2016), their Fig. 12

5.5 Amplitude Modulation Catalogue Extract

Using a similar approach to the *Kepler* data catalogues discussed in Sect. 2.4, an amplitude modulation catalogue[2] was created for the ensemble of 983 δ Sct stars (Bowman et al. 2016). However, in the amplitude modulation catalogue there is only a single page per star, which lists a star's unique KIC number and the stellar parameters listed in the KIC at the top of the page. Figure 5.10 is an extract from the automated amplitude modulation catalogue for the δ Sct star KIC 7106205. The top panel is the amplitude spectrum using 4 yr of LC *Kepler* data calculated out to the LC Nyquist frequency. The amplitude and phase tracking plot is shown in the bottom panel, in which nine peaks (out of a maximum of 12) that have amplitudes greater than $A \geq 0.10$ mmag are tracked in 100-d bins with a 50-d overlap.

This amplitude modulation catalogue, and especially the example of KIC 7106205, clearly demonstrates how δ Sct stars can be aperiodic and can have dramatic variability in pulsation mode amplitudes and phases. This catalogue will remain of great use to the research community for years to come as the length of the 4-yr *Kepler* data set will not be surpassed for some time.

[2]The published amplitude modulation catalogue for all 983 δ Sct stars can be obtained in PDF format from http://uclandata.uclan.ac.uk/42/.

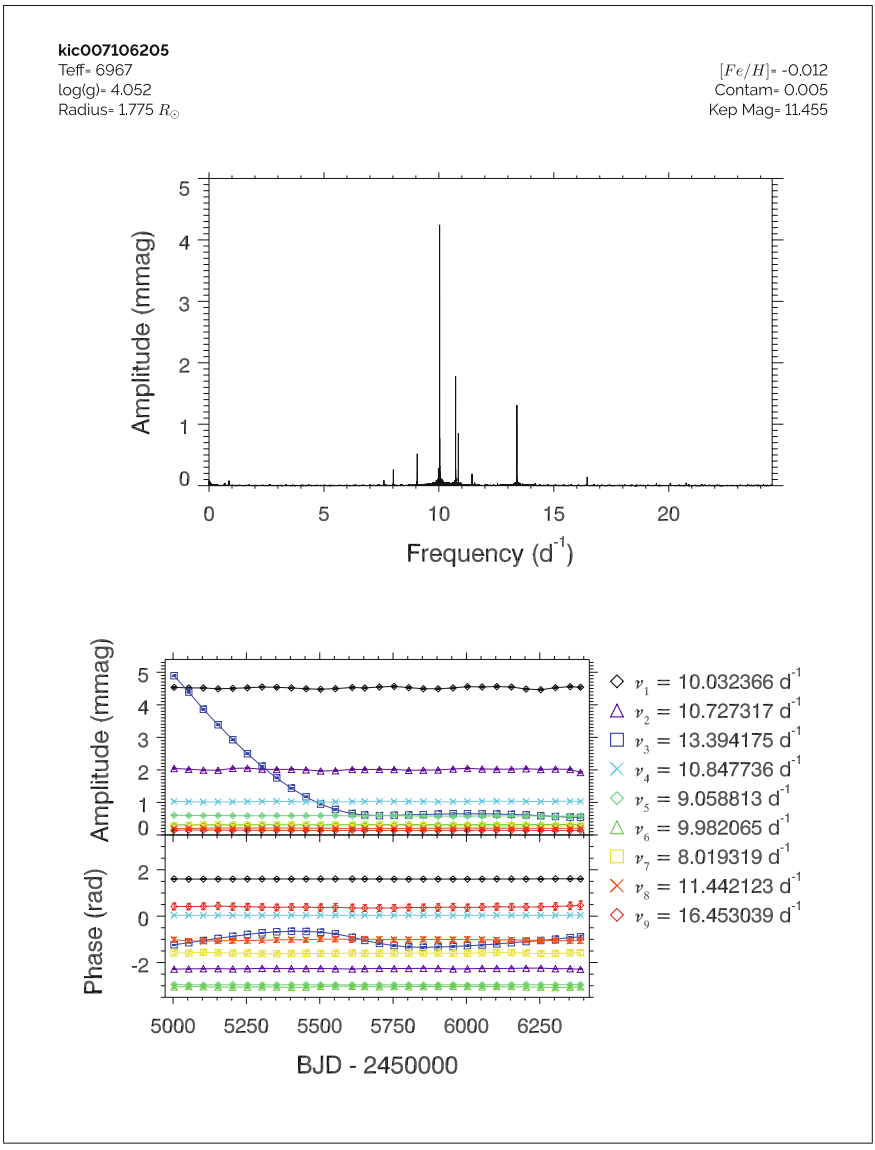

Fig. 5.10 An example page from the amplitude modulation catalogue page for the δ Sct star KIC 7106205

5.6 Ruling Out Rotation as the Ubiquitous Cause of Amplitude Modulation

There is no obvious correlation between a star being classified as AMod and the rotational velocity of a star. This is investigated using the subsample of δ Sct stars studied by Niemczura et al. (2015), for which accurate values of $v \sin i$ determined from high-resolution spectroscopy are available. The distribution of the frequency of the highest amplitude pulsation mode against $v \sin i$ from Fig. 4.15 has been regenerated in Fig. 5.11, but with each star denoted as a blue diamond or a red square to represent if it is NoMod or AMod, respectively. AMod and NoMod stars are found amongst the slow and fast rotators in the subsample of δ Sct stars studied by Niemczura et al. (2015), so it is unlikely to be related to the amplitude modulation in δ Sct stars. Note that the ordinate and abscissa axes have been plotted using the same scale as in Fig. 4.15 for comparison.

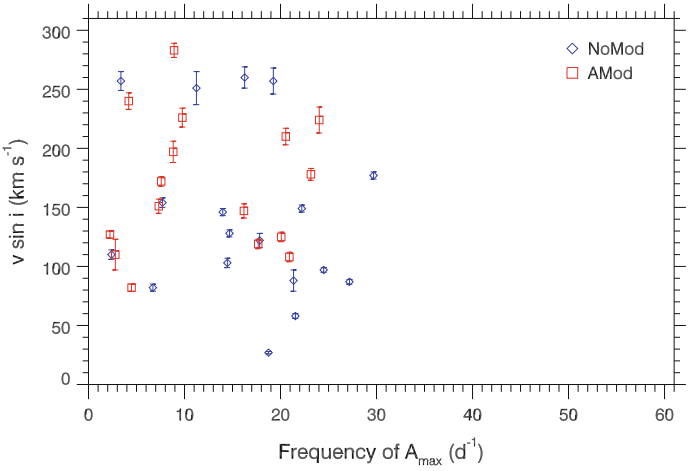

Fig. 5.11 Relationship between rotation, pulsation and amplitude modulation. The same subsample of δ Sct stars studied by Niemczura et al. (2015) as shown in Fig. 4.15 are given here, but each star is now denoted as a *blue diamond* or *red square* if it is NoMod or AMod, respectively. For the few stars in this figure, there is no obvious correlation between rotational velocity and amplitude modulation

5.7 Differentiating Beating and Pure Amplitude Modulation

A study of seven δ Sct stars by Breger and Bischof (2002) established that pairs of close-frequency pulsation modes, which were separated by less than 0.01 d^{-1}, were not uncommon and often found near the expected frequencies of radial modes (Breger and Bischof 2002). It was concluded that these close-frequency pulsation modes were unlikely to be caused by rotation since most δ Sct stars are fast rotators, which produce much larger rotational splittings than the observed separation in frequency of 0.01 d^{-1}. For example, the slowly rotating δ Sct star 44 Tau (HD 26322) has a measured rotational velocity of $v \sin i = 3 \pm 2$ km s^{-1} (Zima et al. 2006), which was calculated to produce a rotational splitting of approximately 0.02 d^{-1} (Breger et al. 2009).

Another more recent example is the δ Sct star KIC 11145123 that was determined to have a surface rotation period of approximately 100 d, which can be converted into a rotational velocity of $v_{eq} \simeq 1$ km s^{-1} (Kurtz et al. 2014). This measured rotation period is *extremely* slow compared to the vast majority of A and F stars (Zorec and Royer 2012; Murphy 2014), but is capable of producing a rotational splitting of less than 0.01 d^{-1}. Thus for pairs or groups of pulsation mode frequencies to be separated by less than 0.01 d^{-1}, then the host δ Sct star must be an very slow rotator like the δ Sct star KIC 11145123.

Breger et al. (2009) showed that pulsation mode frequencies in δ Sct stars are not distributed at random and that many non-radial modes had frequencies near radial mode frequencies (Breger et al. 2009). These regularities in the amplitude spectra were explained by mode trapping in the stellar envelope (Dziembowski and Krolikowska 1990), which was clearly demonstrated as the cause of regularities in the amplitude spectrum of the δ Sct star FG Vir (HD 106384) by Breger et al. (2009).

Clearly the beating effects of close-frequency pulsation modes, using the definition from Breger and Bischof (2002) of a separation of less than 0.01 d^{-1}, are important to consider when studying δ Sct stars. Without studying the changes in amplitude and frequency (i.e., phase at fixed frequency) of pulsation modes, it is difficult to establish if amplitude modulation is caused by beating of two stable and independent pulsation modes, or has an astrophysical cause. This distinction cannot be achieved from simple inspection of the light curve or amplitude spectrum of a pulsating star, even with such an excellent data set such as from *Kepler* because the convolved amplitude and frequency modulation signals cannot be disentangled.

The beating pattern of two close-frequency and resolved pulsation modes produces periodic amplitude modulation, with a characteristic change in phase at the epoch of minimum amplitude (Breger and Pamyatnykh 2006; Bowman et al. 2016). The simplest example is for two cosinusoids with equal amplitude, each of the form

$y = A\ \cos\,(2\pi\nu t + \phi)$, where A is the amplitude, ν is the frequency and ϕ is the phase. Using the sum rule in trigonometry for two equal-amplitude cosinusoids with frequencies ν_1 and ν_2, each with a phase of 0.0 rad, the summation is given by

$$\begin{aligned} y_1 + y_2 &= A\ \cos\ 2\pi\,\nu_1 t + A\ \cos 2\pi\,\nu_2 t \\ &= 2A\ \cos 2\pi\ \tfrac{\nu_1+\nu_2}{2}\ t\ \cos 2\pi\ \tfrac{\nu_1-\nu_2}{2}\ t\ , \end{aligned} \tag{5.1}$$

from which, the beat frequency is defined by

$$\nu_{\rm beat} = |\nu_1 - \nu_2|\ , \tag{5.2}$$

which is the absolute difference of the frequencies of the two cosinusoids.

Beating is most easily recognised with two cosinusoids of equal amplitude because the assumed single visible frequency (if they are unresolved) varies sinusoidally in amplitude between $2A$ and 0 with a period equal to the beat period, but also varies in phase: a π rad phase change occurs at the epoch of minimum amplitude (Breger and Pamyatnykh 2006; Bowman et al. 2016). For cosinusoids with increasingly different amplitudes, the amplitude and phase changes get smaller. However, the amplitude and phase always varies synchronously with a phase lag close to $\pi/2$ rad, with the amplitude minimum in the beat cycle occurring at the time of most rapid change in phase (Breger and Pamyatnykh 2006; Bowman et al. 2016).

5.7.1 Modelling Pure Amplitude Modulation

From theoretical studies of non-linearity in δ Sct stars, pure amplitude modulation of a single pulsation mode may appear as an unresolved group of close-frequency peaks in an amplitude spectrum (Buchler et al. 1997), thus the presence of multiple peaks does not prove the existence of multiple independent pulsation modes. Pure amplitude modulation of a single pulsation mode also excludes phase variability, which is required when two unresolved frequencies are beating against each other (Breger and Pamyatnykh 2006). This means that it is only by studying amplitude and frequency (i.e., phase at fixed frequency) modulation of peaks in an amplitude spectrum that differentiates variability caused by pure amplitude modulation of a single mode, or the beating pattern of multiple close-frequency pulsation modes (Breger and Bischof 2002; Bowman et al. 2016).

This concept was tested and demonstrated by Breger and Bischof (2002) using ground-based data, and later by Bowman et al. (2016) using synthetic data, specifically 4-yr of *Kepler* time stamps with calculated magnitudesusing $\Delta m = A\ e^{-t/\tau}$ cos $(2\pi\,\nu(t - t_0) + \phi)$, where τ is an exponential decay time of 300 d, A is an amplitude

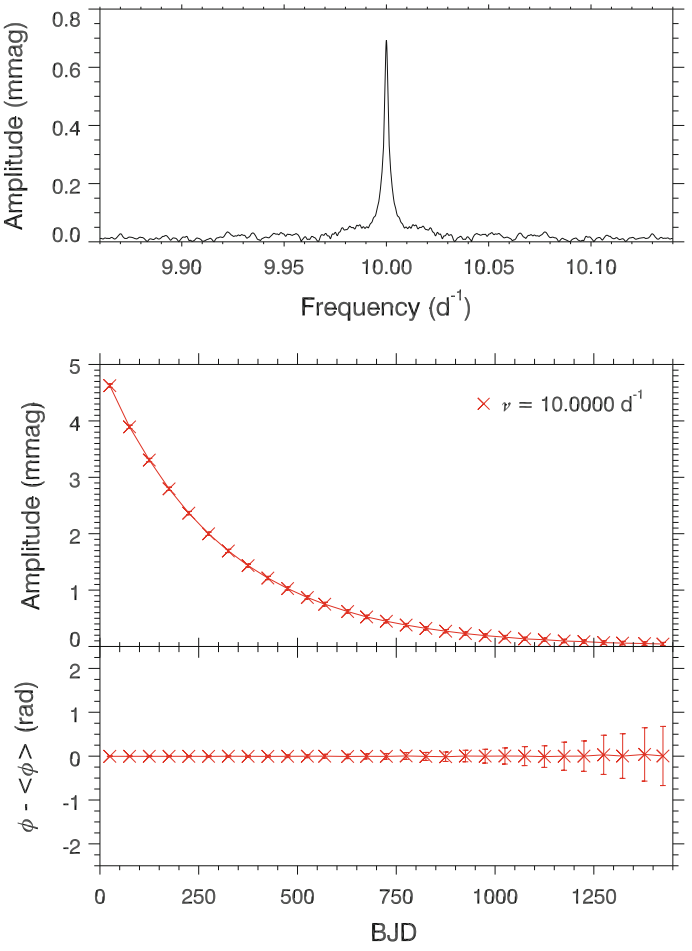

Fig. 5.12 Pure amplitude modulation for an exponentially decaying amplitude and fixed frequency and phase cosinusoid using a synthetic *Kepler* data set. The *top panel* shows the Lorentzian profile peak in the amplitude spectrum and the *bottom panel* is the amplitude and phase tracking plot for pure amplitude modulation with no associated phase variation. Figure from Bowman et al. (2016), their Fig. 9

of 5.0 mmag, ν is a frequency of 10.0 d^{-1} and ϕ is a phase of 0.0 rad relative to the centre of the data set (i.e., $t_0 = 2\,455\,688.770$ BJD). The amplitude spectrum of this exponentially decaying signal produced a Lorentzian profile peak in the Fourier domain as expected, which is shown in the top panel of Fig. 5.12.

Bowman et al. (2016) applied the same amplitude and phase tracking method to the synthetic *Kepler* data set at a frequency of $\nu = 10.0\,\mathrm{d}^{-1}$ using linear least-squares with the results shown in the bottom panel of Fig. 5.12. The cosinusoidal signal has a constant phase at fixed frequency but a decaying amplitude, thus produces a pure form of amplitude modulation with no concomitant phase modulation, which is shown in the bottom panel of Fig. 5.12. A similar result was also obtained if a tanh $(-t/\tau)$ factor is used instead of $e^{-t/\tau}$ as an amplitude modulation factor (Bowman et al. 2016). Therefore, as expected, if only the amplitude of a cosinusoidal signal is modified, this does not affect the frequency or phase.

5.7.2 Modelling Beating in KIC 4641555 and KIC 8246833

As previously discussed, the difference in amplitude and frequency of two (or more) pulsation modes govern the beating signal and consequently the observed amplitude and phase modulation. In previous observations of δ Sct stars, close-frequency pulsation modes cannot always be explained by rotation or pure amplitude modulation of a single pulsation mode, as this leads to a more complex structure in the amplitude spectrum and not two resolved peaks.

The δ Sct stars KIC 4641555 and KIC 8246833, which were first discussed in Sect. 5.3.3, each contain pairs of pulsation modes separated in frequency by less than $0.001\ \mathrm{d}^{-1}$ and are excellent case studies to further investigate the beating of a pair of close-frequency pulsation modes that are barely resolved using 4 yr of *Kepler* observations. To that end, Bowman et al. (2016) constructed beating models of a pair of close-frequency pulsation modes were made using synthetic *Kepler* data for each star. Specifically, 4-yr of *Kepler* time stamps were used to create a synthetic light curve from white noise and the two cosinusoids with the necessary mode parameters required to reproduce the observed beating pattern.

These beating models were successfully matched to observations of amplitude modulation in KIC 4641555 and KIC 8246833, yielding beat periods of 1166 ± 1 d and 1002 ± 1 d, respectively (Bowman et al. 2016). The observed amplitude modulation of the highest-amplitude pulsation mode frequency is shown as black diamonds and the best-fitting beating model is shown as red crosses in the bottom panels of Figs. 5.13 and 5.14 for KIC 4641555 and KIC 8246833, respectively. These two case studies demonstrate that it is possible for δ Sct stars to pulsate with low-degree p-mode frequencies that lie very close to the Rayleigh resolution criterion in frequency for the 4-yr *Kepler* data set and yet maintain their independent identities (Bowman et al. 2016).

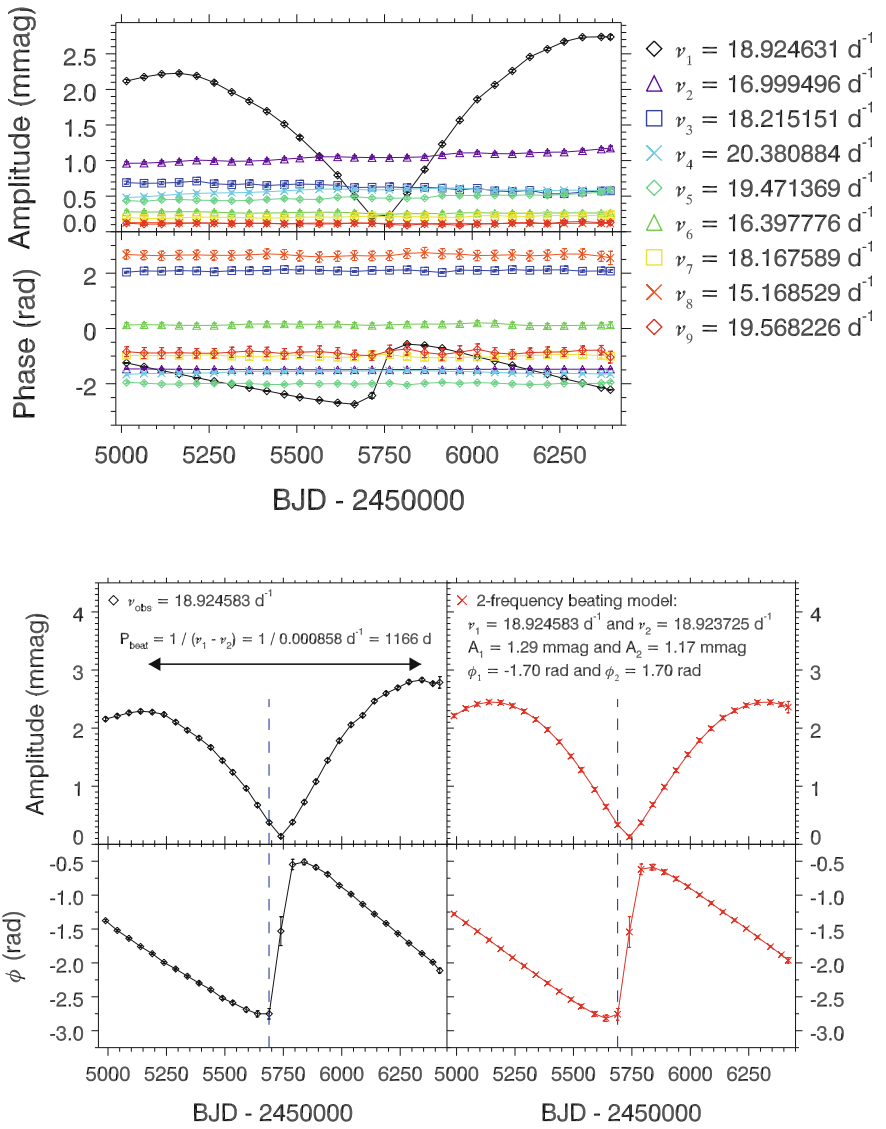

Fig. 5.13 Modelling beating in the δ Sct star KIC 4641555. The *top panel* shows the observed amplitude and phase modulation in the nine highest-amplitude p modes. In the *bottom panel*, the *left-* and *right-hand* columns show the observed and predicted amplitude (*top*) and phase (*bottom*) modulation in KIC 4641555, respectively. The *dashed vertical line* indicates the centre of the *Kepler* data set that has been chosen as the zero-point in time, specifically $t_0 = 2\,455\,688.770$ BJD. The beating model (shown as *red crosses*) represents the summation of two cosinusoid functions that accurately reproduce the observed amplitude and phase modulation. Thus, KIC 4641555 has a pair of high-amplitude pulsation mode frequencies lie closer than 0.001 d^{-1} in frequency, resulting in a beat period of 1166 ± 1 d. Figure from Bowman et al. (2016), their Fig. 4

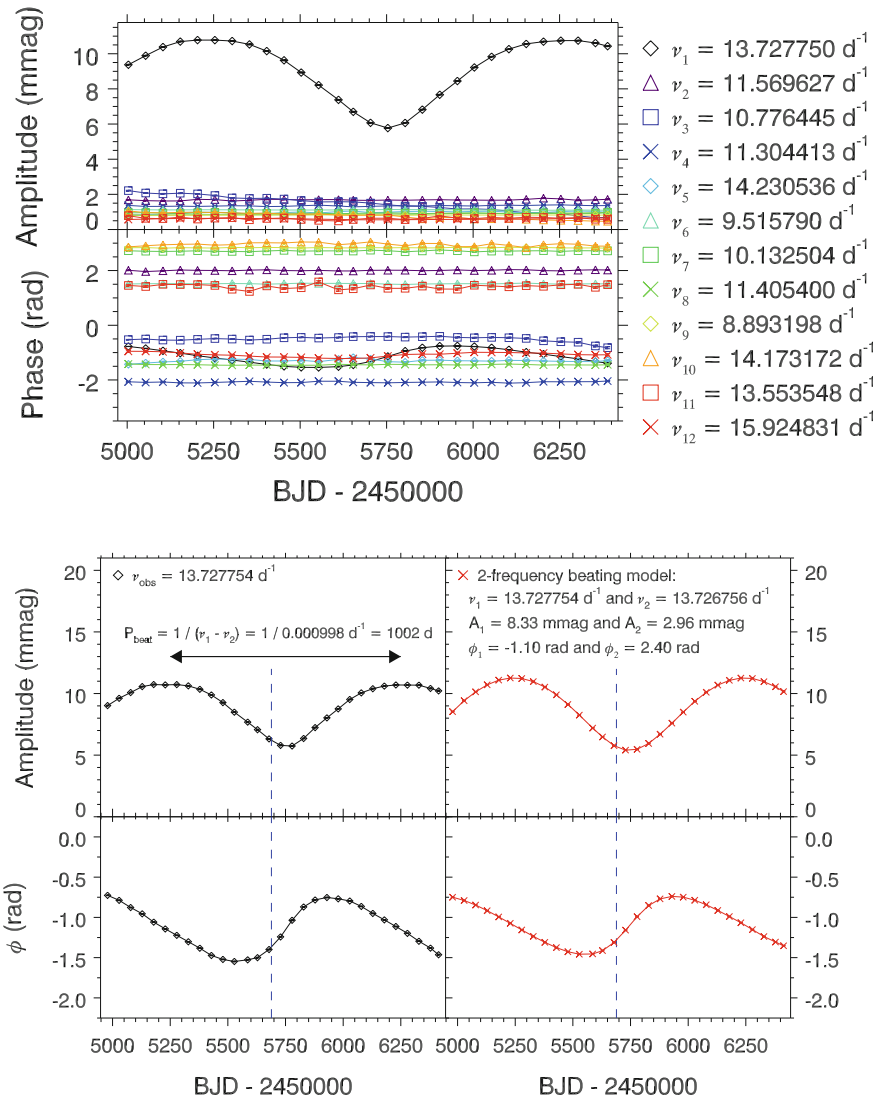

Fig. 5.14 Modelling beating in the δ Sct star KIC 4641555. The *top panel* shows the observed amplitude and phase modulation in the 12 highest-amplitude p modes. In the *bottom panel*, the *left-* and *right-hand* columns show the observed and predicted amplitude (*top*) and phase (*bottom*) modulation in KIC 4641555, respectively. The *dashed vertical line* indicates the centre of the *Kepler* data set that has been chosen as the zero-point in time, specifically $t_0 = 2\,455\,688.770$ BJD. The beating model (shown as *red crosses*) represents the summation of two cosinusoid functions that accurately reproduce the observed amplitude and phase modulation. Thus, KIC 8246833 has a pair of high-amplitude pulsation mode frequencies lie closer than 0.001 d^{-1} in frequency, resulting in a beat period of 1002 ± 1 d. Figure from Bowman et al. (2016), their Fig. 4

5.8 Investigating the Unresolved Close-Frequency Mode Hypothesis

It is certainly plausible that many AMod δ Sct stars can be explained by the beating of unresolved close-frequency pulsation modes. Using a similar method to that discussed in Sect. 5.7.2 for resolved pulsation mode frequencies, beating models of multiple unresolved frequencies could be constructed to explain amplitude modulation in many δ Sct stars, but this requires the number of frequencies to be known *a priori*. Theoretically, it is possible for many non-radial pulsation mode frequencies to exist closer than the 4-yr *Kepler* resolution limit of 0.00068 d^{-1}, and maintain their independent identity over several years (H. Saio, *private communication*), but this has not been confirmed observationally. If this is the case for many of the AMod δ Sct stars discussed in the present chapter, it would explain the non-sinusoidal modulation cycles because of the complicated beating pattern of multiple unresolved close-frequency pulsation modes (Bowman et al. 2016).

To test this hypothesis, synthetic *Kepler* data with appropriate white noise and three unresolved pulsation modes were generated using 4 yr of *Kepler* time stamps and the frequencies, amplitudes and phases given in Table 5.2. The properties of these three hypothetical pulsation modes were chosen to emulate the observed amplitude modulation in the δ Sct star KIC 7106205, which was discussed in Chap. 3. The resultant light curve and a zoom-in of the unresolved peak in the amplitude spectrum are shown in the top and middle panels of Fig. 5.15, respectively.

The amplitude and phase tracking routine was applied to the synthetic data set, such that frequency, amplitude and phase values were extracted and optimised using a non-linear least-squares fit. Subsequently, amplitude and phase were tracked in 100-d bins with a 50-d overlap at fixed frequency using linear least-squares throughout the 1500-d synthetic data set. Note that only a single frequency was extracted from the amplitude spectrum because the other two lie within the 4-yr *Kepler* resolution limit and are not resolved. The amplitude and phase tracking plot for the extracted frequency, $\nu = 13.393998\ d^{-1}$, is shown in the bottom panel of Fig. 5.15.

The amplitude and phase modulation for this synthetic data set is qualitatively similar to the observed amplitude and phase modulation in KIC 7106205 studied by Bowman and Kurtz (2014) and discussed in Chap. 3. For example, the extracted peak at $\nu = 13.393998\ d^{-1}$ experiences an approximately linear decrease in amplitude and then stays approximately constant in amplitude over 4 yr, whilst a quasi-sinusoidal phase modulation is observed. The cause of the amplitude modulation in

Table 5.2 Parameters of three hypothetical pulsation modes used to demonstrate amplitude and phase modulation caused by the beating of unresolved frequencies in a synthetic *Kepler* data set

	Frequency (d^{-1})	Amplitude (mmag)	Phase (rad)
ν_1	13.393837	5.00	−3.00
ν_2	13.394177	10.00	−1.00
ν_3	13.394517	5.00	2.00

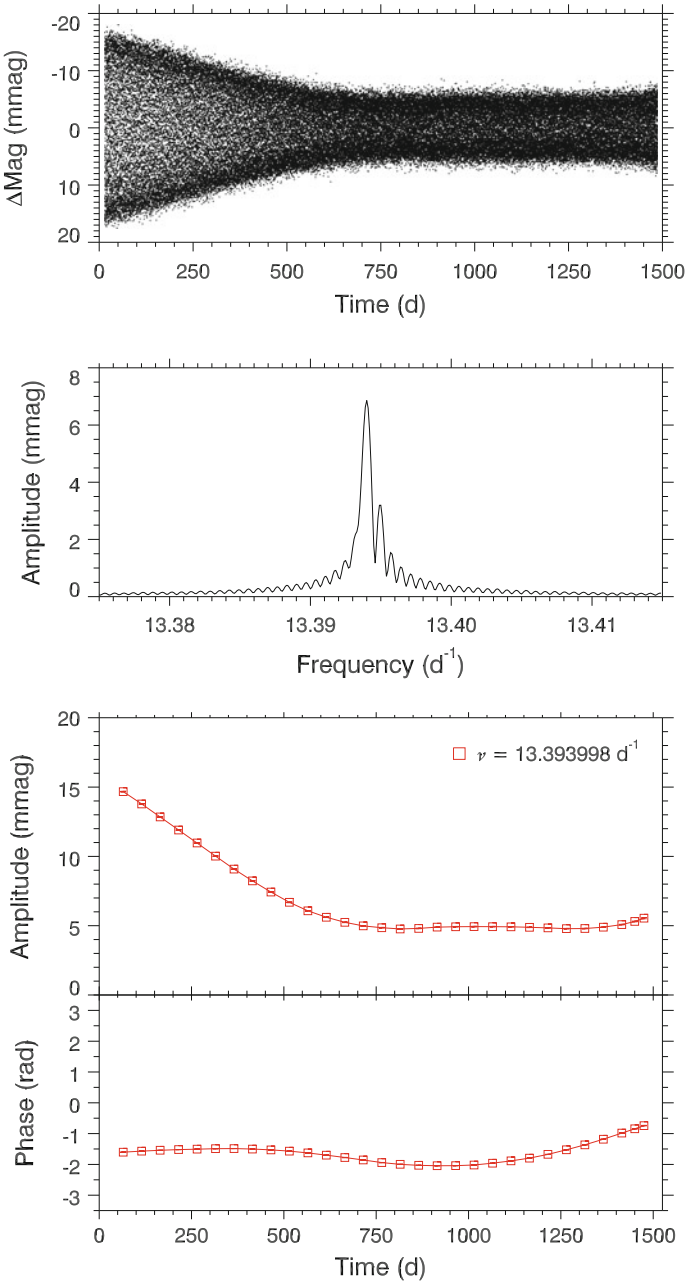

Fig. 5.15 Analysis of synthetic *Kepler* data with three hypothetical unresolved pulsation modes. The *top panel* is the 1500-d light curve. The *middle panel* is a zoom-in of the unresolved peaks in the amplitude spectrum. The *bottom panel* is the resultant amplitude and phase tracking plot for the extracted frequency of $\nu = 13.393998\ \mathrm{d}^{-1}$

KIC 7106205 was not definitively established by Bowman and Kurtz (2014), who were unable to conclude if beating, mode coupling to invisible pulsation modes or variable driving/damping in the star was the cause. The similar characteristic amplitude modulation observed using this hypothetical case study demonstrates that beating of unresolved close-frequency pulsation modes is a viable solution, not only for the observed amplitude modulation in KIC 7106205 but in other δ Sct stars as well.

For beating from multiple unresolved close-frequency pulsation modes, the number of unresolved pulsation modes and their frequencies, amplitudes and phases determine the observed amplitude modulation. It was concluded by Bowman et al. (2016) that the functional form of the curves in an amplitude and phase tracking plot can be used to estimate the number of input modes needed, but a reliable method is needed to determine the frequencies, amplitudes and phases of these modes. One such method is discussed next in Sect. 5.8.1.

5.8.1 A Bayesian MCMC Approach to Extracting Unresolved Frequencies

In this section, a discussion of the feasibility of using a Bayesian Markov-chain Monte-Carlo (MCMC) simulation for investigating if amplitude modulation is caused by the beating of close-frequency pulsation modes is provided. This method is computationally expensive compared to frequency extraction by iterative pre-whitening and optimisation by least-squares, but may offer a solution to extracting unresolved pulsation mode frequencies. The EMCEE software used to carry out this simulation was first implemented by Foreman-Mackey et al. (2013) and was extensively discussed by Hambleton (2016) in the context of studying eccentric binary stars. In the following paragraphs, a brief outline of how the MCMC simulation works is provided; we refer the reader to Hambleton (2016) for full details.

A Monte Carlo simulation is the random sampling of variables to obtain a distribution of possible results. A Markov chain is a stochastic chain of events that changes state in discrete steps, which has the special property that the transition between steps only depends on the current state and not on a previous state. These two principles were first combined by Metropolis et al. (1953) who proposed using a series of chains to perform a random walk using the following prescription. The walkers are given a range of inputs for each variable (i.e., priors), which are used to perform a computation and calculate a probability. The result of the next step is compared to the result of the previous step and only results that improve the value of the probability are accepted.

The initial period of a MCMC simulation is called the burn-in period, which is when the chains are still converging to the optimum solution. After a sufficiently large enough number of iterations, which depends on the problem being solved, each chain will have sampled the parameter space where the probability density is highest and

converged to the best-fitting solution. From the posterior distributions of each model parameter, such as the amplitude, frequency and phase of a cosinusoid, an optimum value and its uncertainty can be determined by fitting a Gaussian to the 1D posterior distribution of a parameter and extracting its mean and standard deviation.

5.8.1.1 Implementation for a Single Pulsation Mode

To demonstrate using a MCMC simulation for mode extraction from a pulsating star's light curve, a single pulsation mode with frequency $\nu = 10.0\ \mathrm{d}^{-1}$, amplitude $A = 10.0$ mmag and phase $\phi = 0.0$ rad was injected into a synthetic *Kepler* time series. A MCMC simulation was carried out using uniform priors to search for the optimum cosinusoid solution. Specifically, the priors for each parameter were $9.5 \leq \nu \leq 10.5\ \mathrm{d}^{-1}$, $0.1 \leq A \leq 50$ mmag and $-\pi \leq \phi \leq \pi$ rad, respectively, which were chosen to be consistent with observations of δ Sct stars.

The results from the search for a pulsation mode using a MCMC simulation are shown in Fig. 5.16, which contains the 1D distributions and 2D contour plots showing the maximum in the log-likelihood probability, thus indicating convergence to the correct solution. The frequency, amplitude and phase solutions and their 1σ uncertainties are given above each column in Fig. 5.16, with the values and uncertainties calculated from the centroids and standard deviations, respectively, of the Gaussian fits to the 1D distribution in each column.

The successful implementation of a Bayesian MCMC simulation to find a single pulsation mode using synthetic *Kepler* data is a proof of concept exercise. It has been demonstrated that this method is able to converge to the correct multiparameter solution using this hypothetical scenario. In the following section, a MCMC simulation is used to find three unresolved pulsation modes that lie closer together than the 4-yr *Kepler* frequency resolution.

5.8.1.2 Implementation for Three Unresolved Pulsation Modes

Using a similar method to that discussed in the previous section for a single pulsation mode, a MCMC simulation was used to search for three pulsation modes in a synthetic *Kepler* data set created using the parameters given in Table 5.2. The priors in amplitude, frequency and phase used were $13.0 \leq \nu \leq 13.8\ \mathrm{d}^{-1}$, $0.1 \leq A \leq 50$ mmag and $-\pi \leq \phi \leq \pi$ rad, respectively. The results from the search for these three pulsation modes using a MCMC simulation are shown in Fig. 5.17, which has a similar layout to Fig. 5.16 but instead shows a grid with nine rows and columns for the three pulsation modes and their respective frequencies, amplitudes and phases. Similarly to the previous hypothetical example using synthetic *Kepler* data, the MCMC simulation has successfully converged to the correct solution, with the parameters and their respective errors given above plot in Fig. 5.17, which are within 1σ of the input parameters given in Table 5.2.

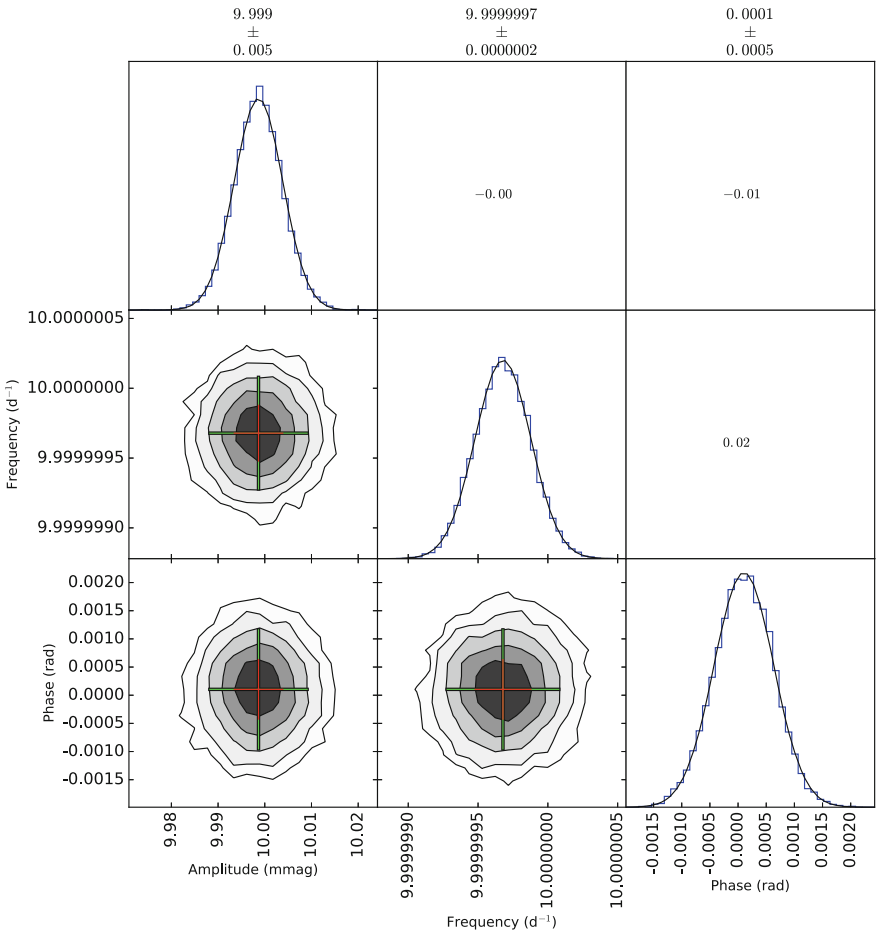

Fig. 5.16 Results from a successful MCMC simulation to find the parameters of a single pulsation mode using synthetic *Kepler* data. The contour plots in the lower-left sub-plots show cross-sections of the posterior probability distribution functions for the amplitude, frequency and phase, with the *red* and *green crosses* showing the 1σ and 2σ uncertainties, respectively. The sub-plots on the diagonal from *top-left* to *bottom-right* show the probability distribution for each parameter, with a mean value and its 1σ uncertainty obtained from a Gaussian fit given above each column of the plot. The numbers in the *top-right* sub-plots give the correlation between two parameters with 1 indicating direct correlation and -1 indicating direct anti-correlation

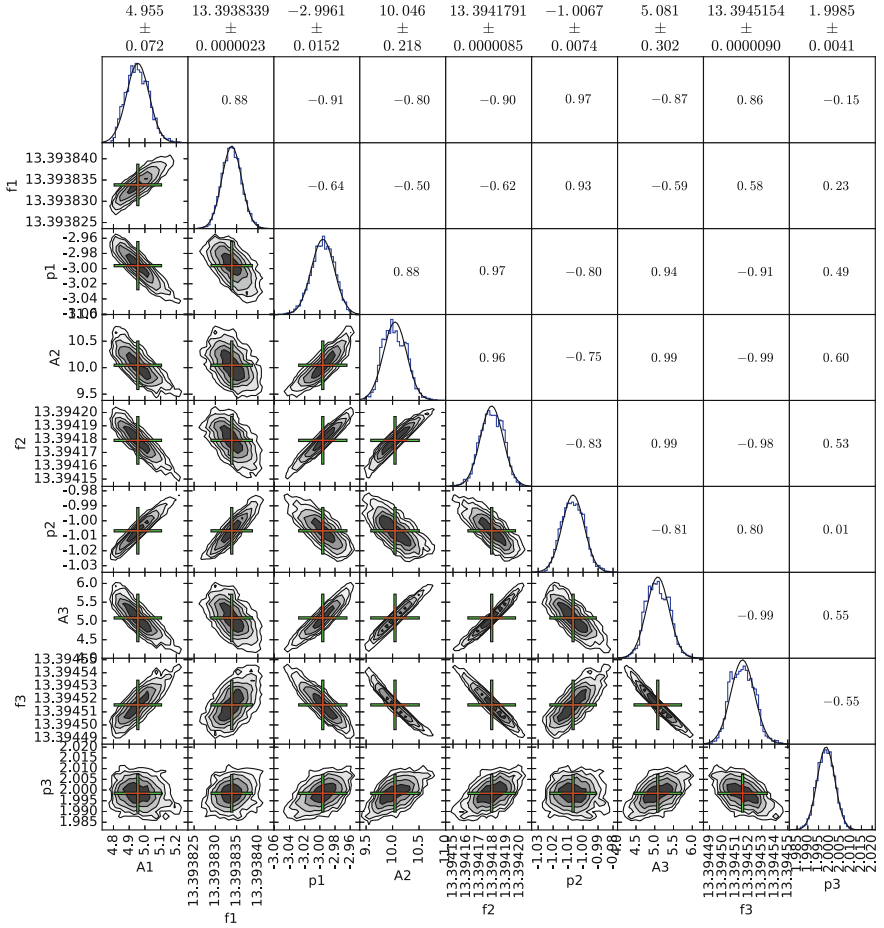

Fig. 5.17 Results from a successful MCMC simulation to find the parameters of three pulsation modes that lie closer than the 4-yr *Kepler* frequency resolution using synthetic data. The layout of this figure is similar to that of Fig. 5.16, but has three frequencies, amplitudes and phases instead

This MCMC simulation is also another useful proof of concept exercise that demonstrates that it is possible to determine the parameters of unresolved pulsation modes in a δ Sct star in the *Kepler* data set. It should be noted that the synthetic data used in this and the previous example do not contain any other pulsation modes, thus these simulations should be considered idealistic scenarios. Most importantly, the *number* of pulsation modes is known in these hypothetical scenarios, which is certainly not true when applying this technique to real observations of δ Sct stars in the *Kepler* data set.

In a similar way, a multifrequency solution could be found that accurately describes the observed amplitude modulation in at least a few of the AMod δ Sct

stars discussed by Bowman et al. (2016). However, such a simulation is computationally expensive to run, and is therefore inefficient for frequency extraction compared to, for example, Fourier analysis and iterative pre-whitening techniques. In the next section, the implementation of using MCMC simulations is discussed for the δ Sct star KIC 7106205, which was studied by Bowman and Kurtz (2014) and was discussed in Chap. 3.

5.8.1.3 Application to KIC 7106205

It was shown by Bowman et al. (2016) that the beating of two cosinusoidal signals produces periodic amplitude modulation and a phase change at the epoch of minimum amplitude. The observed amplitude modulation in KIC 7106205 was not periodic over the 4-yr *Kepler* data set, indicating that if beating of unresolved close-frequency pulsation modes is responsible, a minimum of three pulsation modes are required. Multiple MCMC simulations using two, three and four pulsation modes were implemented for the *Kepler* data set for the δ Sct star KIC 7106205 covering a variety of prior distributions, but none of these simulations converged to a meaningful solution, thus did not produce meaningful posterior probability distributions.

Since in the previous section it was demonstrated that an MCMC simulation was able to converge to the correct solution and extract the parameters of three unresolved pulsation modes using synthetic *Kepler* data, it can be inferred that the beating of two, three of four pulsation modes is not responsible for the observed amplitude modulation in KIC 7106205. It is highly unlikely that five or more independent pulsation modes can lie closer together than the 4-yr *Kepler* frequency resolution of 0.00068 d^{-1} (8 nHz) in a star with a low mode density such as KIC 7106205. Therefore, the exact cause of the amplitude modulation in the δ Sct star KIC 7106205 remains an unsolved problem.

5.9 Discussion

In this chapter, the results of a thorough search for amplitude modulation in 983 δ Sct stars that were continuously observed by the *Kepler* Space Telescope for 4 yr have been presented. The *Kepler* data set provides extremely high frequency resolution and amplitude precision, which were used to track amplitude and phase at fixed frequency in 100-d bins with a 50-d overlap for a maximum number of 12 peaks with amplitudes greater that $A \geq 0.10$ mmag for each star in an ensemble of 983 δ Sct stars, with the results collated into an amplitude modulation catalogue published by Bowman et al. (2016). Various case studies of stars were used by Bowman et al. (2016) to demonstrate the diversity in pulsational behaviour of δ Sct stars including binarity, beating and non-linearity, which were discussed in Sect. 5.2. An extract of

the amplitude modulation catalogue[3] from Bowman et al. (2016) was also presented in Sect. 5.5, which will remain of great use to the research community for some time.

The main conclusion from the study by Bowman et al. (2016) is that 603 of the 983 δ Sct stars in the ensemble (61.3%) exhibit at least one pulsation mode that varies significantly in amplitude over 4 yr, and so amplitude modulation is common among δ Sct stars. The causes of variable pulsation amplitudes in δ Sct stars, which were termed AMod stars by Bowman et al. (2016), can be categorised into those that are caused by extrinsic or intrinsic causes. The extrinsic causes of phase variability include binarity (or multiplicity) in the stellar system which acts as a perturbation to the observed pulsation mode frequencies (Shibahashi and Kurtz 2012; Shibahashi et al. 2015). A pulsating star can also be easily recognised as being part of a multiple system as all its pulsation modes will be phase modulated by the orbital period of the stellar system (Murphy et al. 2014). Similarly, super-Nyquist aliases are easily identifiable because they are periodically phase modulated by a variable Nyquist frequency with the orbital period of the *Kepler* Space Telescope (Murphy et al. 2013; Bowman et al. 2016).

It is important to note that the method employed by Bowman et al. (2016) for studying amplitude modulation in δ Sct stars does not automatically determine if an extracted frequency is a pulsation mode, a combination frequency or a super-Nyquist alias frequency. Furthermore, it does not automatically determine the cause of the observed amplitude modulation if present, such as beating or non-linearity, but does provide a quantitative insight into the problem of mode stability in δ Sct stars. Also, the fractions of AMod and NoMod stars obtained by Bowman et al. (2016) from an ensemble of 983 δ Sct stars would change if different criteria for defining significant amplitude modulation were used.

Intrinsic causes of amplitude modulation include beating and non-linearity, the latter of which is discussed in more detail in Chap. 6. The δ Sct stars that exhibit amplitude modulation with no phase change are particularly interesting. In these stars, the amplitude change is typically monotonic over the 4-yr *Kepler* data set. Approximately the same number of δ Sct stars with linearly increasing and decreasing amplitudes were found, but also similar numbers of stars with non-linearly increasing and decreasing amplitudes (Bowman et al. 2016). These pure AMod stars remain a challenge to understand, so one can only speculate until further investigation is carried out.

Amplitude modulation caused by beating of pairs (or groups) of close-frequency pulsation modes are not uncommon in δ Sct stars (Breger and Bischof 2002; Breger and Pamyatnykh 2006). A resolved beating pattern is most recognisable for two cosinusoidal signals from the periodic change in amplitude, but most importantly, from the phase change at the epoch of minimum amplitude. This phase change is π rad for two equal-amplitude cosinusoids, and tends to zero as the amplitudes get significantly different from each other. Beating models for a pair of close-frequency pulsation modes separated by less than 0.001 d^{-1} in KIC 4641555 and KIC 8246833

[3]The published amplitude modulation catalogue for all 983 δ Sct stars can be obtained in PDF format from http://uclandata.uclan.ac.uk/42/.

were successfully matched to observations by Bowman et al. (2016) and are shown in Figs. 5.13 and 5.14, respectively. The beat periods in KIC 4641555 and KIC 8246833 were determined to be 1166 ± 1 d and 1002 ± 1 d, respectively, which means that these independent pulsation modes are barely resolved using 4 yr of *Kepler* observations.

Beating of unresolved close-frequency pulsation modes is a plausible explanation for the amplitude modulation observed in many δ Sct stars, but it is yet to be established how and why this could occur in stars with such low mode densities in their amplitude spectra (e.g., KIC 7106205). To test this hypothesis, a Bayesian MCMC simulation was successfully able to extract pulsation mode parameters from a synthetic data set containing three unresolved pulsation modes. This technique may be computationally expensive and time-consuming compared to frequency extraction by iterative pre-whitening, but it was a useful proof of concept exercise. However, the implementation of this technique for the δ Sct star KIC 7106205 yielded no conclusive results. Thus, the cause of the observed amplitude modulation remains unexplained in this δ Sct star.

The 380 δ Sct stars classified as NoMod by Bowman et al. (2016) comprise 38.7% of the ensemble of 983 δ Sct stars and represent the stars for which the highest precision measurements of amplitude and frequency are possible. This is important in the search for planets orbiting these stars when using the FM method (Shibahashi and Kurtz 2012; Shibahashi et al. 2015). These NoMod stars are also excellent targets for determining precise frequencies and amplitudes for asteroseismic modelling (Bowman et al. 2016), and warrant further study.

Note that from an observational point of view, the cause of the amplitude modulation in δ Sct stars is interesting, but not necessarily important. What is important to realise is that short term observations of the order a few years provide an *average* amplitude of a pulsation mode, if it is varying on time-scales of the order a few decades or longer. Naturally, it is interesting to determine the mechanism that causes amplitude modulation, as it has implications for our understanding of non-linearity, driving and damping processes in these stars, which is discussed in further detail Chap. 6.

The catalogue of 983 δ Sct stars published by Bowman et al. (2016) demonstrates that observations spanning years (and longer) are often needed to study and resolve pulsational behaviour in these stars. The published amplitude modulation catalogue will be useful for comparison purposes when studying δ Sct stars observed by K2 (Howell et al. 2014), TESS (Ricker et al. 2015) and in the not so distant future PLATO (Rauer et al. 2014). Eventually, these missions will observe a large area of the sky, but for only a relatively short length of time compared to the *Kepler* data set. Therefore, *Kepler* may represent the best data set for studying δ Sct stars as its 4-yr length of continuous observations will not be surpassed in the foreseeable future.

References

Aerts, C., Christensen-Dalsgaard, J., & Kurtz, D. W. 2010, Asteroseismology (Springer)
Balona, L. A. & Dziembowski, W. A. 2011, MNRAS, 417, 591

Bowman, D. M. & Kurtz, D. W. 2014, MNRAS, 444, 1909
Bowman, D. M., Kurtz, D. W., Breger, M., Murphy, S. J., & Holdsworth, D. L. 2016, MNRAS, 460, 1970
Breger, M. & Bischof, K. M. 2002, A&A, 385, 537
Breger, M. & Pamyatnykh, A. A. 2006, MNRAS, 368, 571
Breger, M., Lenz, P., & Pamyatnykh, A. A. 2009, MNRAS, 396, 291
Breger, M., Stich, J., Garrido, R., et al. 1993, A&A, 271, 482
Breger, M. 1990, A&A, 240, 308
Breger, M. 1990, Delta Scuti Star Newsletter, 2, 13
Breger, M. 2000, MNRAS, 313, 129
Breger, M. 2016, A&A, 592, A97
Brown, T. M., Latham, D. W., Everett, M. E., & Esquerdo, G. A. 2011, AJ, 142, 112
Buchler, J. R., Goupil, M.-J., & Hansen, C. J. 1997, A&A, 321, 159
Dziembowski, W. & Krolikowska, M. 1990, Acta Astronomica, 40, 19
Foreman-Mackey, D., Hogg, D. W., Lang, D., & Goodman, J. 2013, PASP, 125, 306
Hambleton, K. M. 2016, PhD thesis, Jeremiah Horrocks Institute, University of Central Lancashire, UK
Howell, S. B., Sobeck, C., Haas, M., et al. 2014, PASP, 126, 398
Huber, D., Silva Aguirre, V., Matthews, J. M., et al. 2014, ApJS, 211, 2
Kurtz, D. W., Hambleton, K. M., Shibahashi, H., Murphy, S. J., & Prša, A. 2015, MNRAS, 446, 1223
Kurtz, D. W., Saio, H., Takata, M., et al. 2014, MNRAS, 444, 102
Metropolis, N., Rosenbluth, A. W., Rosenbluth, M. N., Teller, A. H., & Teller, E. 1953, Journal of Chemical Physics, 21, 1087
Murphy, S. J. & Shibahashi, H. 2015, MNRAS, 450, 4475
Murphy, S. J., Bedding, T. R., Shibahashi, H., Kurtz, D. W., & Kjeldsen, H. 2014, MNRAS, 441, 2515
Murphy, S. J., Shibahashi, H., & Kurtz, D. W. 2013, MNRAS, 430, 2986
Murphy, S. J. 2014, PhD thesis, Jeremiah Horrocks Institute, University of Central Lancashire, UK
Niemczura, E., Murphy, S. J., Smalley, B., et al. 2015, MNRAS, 450, 2764
Rauer, H., Catala, C., Aerts, C., et al. 2014, Experimental Astronomy, 38, 249
Ricker, G. R., Winn, J. N., Vanderspek, R., et al. 2015, Journal of Astronomical Telescopes, Instruments, and Systems, 1, 014003
Rodríguez, E. & Breger, M. 2001, A&A, 366, 178
Schmid, V. S., Themeßl, N., Breger, M., et al. 2014, A&A, 570, A33
Shibahashi, H. & Kurtz, D. W. 2012, MNRAS, 422, 738
Shibahashi, H., Kurtz, D. W., & Murphy, S. J. 2015, MNRAS, 450, 3999
Zima, W., Wright, D., Bentley, J., et al. 2006, A&A, 455, 235
Zorec, J. & Royer, F. 2012, A&A, 537, A120

Chapter 6
Characterising Pulsational Non-linearity

6.1 Introductory Remarks

It has been known for some time that non-linear stellar pulsation models are needed to accurately reproduce observations of δ Sct stars (Cox 1980; Stellingwerf 1980; Saio and Cox 1980), with linear models providing no predictive power of pulsation mode amplitudes. The observed temporal variability in pulsation mode frequencies, amplitudes and phases demonstrated for the majority of δ Sct stars in Chap. 5 is beyond the linear theory of non-radial stellar pulsation given by Unno et al. (1989). Furthermore, non-linear theoretical models of δ Sct stars often predict much larger pulsation mode amplitudes than are observed, which suggests that an amplitude limitation mechanism or limit cycle is required to stop the exponential growth of pulsation mode amplitudes (Breger 2000; Aerts et al. 2010).

In this chapter, the non-linearity of pulsations in δ Sct and γ Dor stars is investigated. It is only recently that high-quality observations, such as those provided by the *Kepler* Space Telescope, have allowed theoretical predictions of non-linearity to be investigated in δ Sct stars. Using models of mode coupling discussed by Breger and Montgomery (2014) and Bowman et al. (2016), the strength of non-linearity can be investigated in pulsating stars. In Sect. 6.2, the distinction between combination frequencies and mode coupling of pulsation modes is discussed, with the application of the mode coupling hypothesis to case studies of δ Sct and γ Dor stars presented in Sects. 6.3 and 6.4, respectively. In Sect. 6.5 the pulsational energy budget is discussed in the context of amplitude modulation in δ Sct stars.

6.2 Coupling Versus Combination Frequencies?

Fourier analysis is the preferred method for analysing pulsating stars and extracting pulsation mode frequencies, with a stellar time series being represented as a series of sinusoids or cosinusoids, but harmonics and combination frequencies are

D.M. Bowman, *Amplitude Modulation of Pulsation Modes in Delta Scuti Stars*,
Springer Theses, DOI 10.1007/978-3-319-66649-5_6

mathematically required to describe non-linearity in the frequency domain. This is analogous to a non-sinusoidal light curve describing non-linearity of pulsations in the time domain. One form of non-linearity is quicker rise times than fall times over the pulsation cycle in the light curves of high amplitude pulsators, which is commonly observed in type I Cepheids and RRab stars (see Sect. 1.4.4). These stars have asymmetric light curves that are often characterised as 'upwards' light curves, but it has also been shown that non-linearity can be responsible for the 'downwards' asymmetry seen in the light curves of γ Dor and SPB stars (Kurtz et al. 2015) and RV Tauri stars (see Fig. 2.37 from Aerts et al. 2010).

Therefore, one of the important tasks when studying a pulsating star is to identify which peaks in the amplitude spectrum are pulsation mode frequencies and which peaks are combination frequencies and harmonics. Not only can this greatly simplify an amplitude spectrum, but the pulsation mode frequencies are the main parameters used for asteroseismic modelling. This task can be difficult for stars with high pulsation mode densities in their amplitude spectra — for example, see Pápics (2012), Breger and Montgomery (2014) and Kurtz et al. (2015).

From an observational perspective, there is a subtle difference between coupled modes and combinations frequencies in an amplitude spectrum, with each arising from different physical mechanisms. Combination frequencies and harmonics occur due to the mathematical representation of the summation of sine and cosine terms for a non-linear signal when calculating the Fourier transform. Physically, this effect differs to what is known as a 'family' of pulsation modes, which contain parent modes that are able to interact and resonantly excite a child mode in a star (e.g., Breger and Montgomery 2014).

The study of non-linearity in pulsating stars is further complicated because it was shown mathematically and observationally by Kurtz et al. (2015) that combination frequencies can have higher amplitudes than the parent pulsation modes that create them. Often in the literature, peaks suspected of being combination frequencies in an amplitude spectrum are extracted and removed based solely on their frequency and because they have smaller amplitudes than the assumed parent pulsation modes, but this is not a prudent nor scientific approach when studying stars with combination frequencies. Therefore, one must distinguish real pulsation mode frequencies and combination frequencies using a reliable method, and not simply exclude combination frequencies because they provide physical insight of non-linearity within a star.

In this section, a method for identifying combination frequencies and the strength of non-linearity in a star is discussed, with a specific case study from the literature of the δ Sct star KIC 8054146 studied by Breger and Montgomery (2014) included in Sect. 6.2.4.

6.2.1 Combination Frequencies

Combination frequencies and harmonics are common amongst pulsating stars across the HR diagram, which include δ Sct stars (see e.g., Breger et al. 2012; Murphy et al. 2013; Breger and Montgomery 2014), β Cep stars (see e.g., Handler et al. 2004;

Degroote et al. 2009, SPB stars (see e.g., Pápics 2012, 2013; Pápics et al. 2017), γ Dor stars (see e.g., Kurtz et al. 2015; Van Reeth et al. 2015) and pulsating white dwarf stars (see e.g., Wu and Goldreich 2001; Wu 2001). Combination frequencies are mathematical sum and difference frequencies of pulsation mode frequencies, $\nu_{\rm i}$ and $\nu_{\rm j}$, that have the form $n\nu_{\rm i} \pm m\nu_{\rm j}$, in which n and m are integers. Combination frequencies have been extensively studied in pulsating DA and DB white dwarf stars, and therefore a significant fraction of the literature on studying the physics of combination frequencies is based on g mode pulsators with thin convective envelopes (see e.g., Brickhill 1983, 1990, 1991a, b, 1992a, b; Brassard et al. 1993; Wu and Goldreich 2001; Wu 2001; Montgomery 2005).

Possible mechanisms to explain combination frequencies in variable DA and DB white dwarfs are that the stellar medium does not respond linearly to the pulsation wave, or that the dependence of emergent flux variation is not a linear transformation from the temperature variation in the Stefan–Boltzmann law $F = \sigma T^4$. These mechanisms are often grouped into what is termed the non-linear distortion model (e.g., Degroote et al. 2009). The assumptions and predictions made from these studies of variable white dwarfs may not apply to all types of pulsator, but act as a useful starting point for an investigation of non-linearity in main sequence stars.

In the case of the β Cep star HD 180642, Degroote et al. (2009) found that the sum and difference combination frequencies had similar amplitudes, but that there were significantly more sum combination frequencies in the star's amplitude spectrum. The comparable amplitudes of three peaks, which were related in frequency and phase and formed a family of modes, did not distinguish between non-linearity in the form of a non-linear distortion model and non-linearity in the form of resonant mode coupling (Degroote et al. 2009).

The simplest and lowest order non-linear combination signal, $y_{\rm c}(t)$, that can be produced from the mixing of

$$y_1(t) = A_1 \cos\left(2\pi\nu_1 t + \phi_1\right)$$

and

$$y_2(t) = A_2 \cos\left(2\pi\nu_2 t + \phi_2\right)$$

is given by

$$\begin{aligned} y_{\rm c}(t) &\propto y_1\, y_2 \\ &\propto A_1 \cos\left(2\pi\nu_1 t + \phi_1\right) A_2 \cos\left(2\pi\nu_2 t + \phi_2\right) \\ &\equiv A_{\rm c} \cos\left(2\pi\nu_{\rm c+} t + \phi_{\rm c+}\right) + A_{\rm c} \cos\left(2\pi\nu_{\rm c-} t + \phi_{\rm c-}\right) \ , \end{aligned}$$

where

$$\begin{aligned} A_{\rm c} &= \frac{1}{2} A_1 A_2 \\ \nu_{\rm c\pm} &= \nu_1 \pm \nu_2 \\ \phi_{\rm c\pm} &= \phi_1 \pm \phi_2 \ . \end{aligned}$$

This was discussed in detail by Brickhill (1992b) and Wu (2001), who stated that since combination frequencies are not intrinsic stellar pulsation mode frequencies but are in fact caused by non-linearities within a star, thus the amplitudes and phases of combination frequencies must mimic the parent pulsations, $y_1(t)$ and $y_2(t)$, that create them. However, it was shown by Kurtz et al. (2015) that it is possible for combination frequencies to have larger observed amplitudes than the parent modes. This demonstrates that our understanding of combination frequencies, specifically how they are formed, is far from complete.

One method of identifying combination frequencies is to mathematically generate all the possible combination terms from a small number of parent mode frequencies, optimise them by least-squares and remove them by pre-whitening (e.g., Kurtz et al. 2015). Using this method, any variance that remains after calculating the amplitude spectrum of the residuals is not caused by the parent mode frequencies and their associated combination frequencies. Alternatively, iterative pre-whitening can be used to extract all statistically-significant frequencies and then exclude those that satisfy a combination frequency relation (e.g., Van Reeth et al. 2015). However, the physical mechanism that causes combination frequencies is not immediately obvious using either of these methods.

In Fig. 6.1, synthetic data are used to demonstrate how triplets of exactly equally-split frequencies can be made from two intrinsic pulsation modes, ν_1 and ν_2, in an amplitude spectrum. The two pulsation mode frequencies, the harmonics of ν_1 and ν_2, the combination frequencies $\nu_1 + \nu_2$, $\nu_2 - \nu_1$ and $2\nu_1 - \nu_2$ are labelled in Fig. 6.1, showing how regularities in the amplitude spectrum of a pulsating star can be created from only two pulsation mode frequencies and their associated combination frequencies. It is important to note that the combination frequency, $2\nu_1 - \nu_2$, and the second pulsation mode frequency, ν_2, could be misinterpreted as part of an equally split

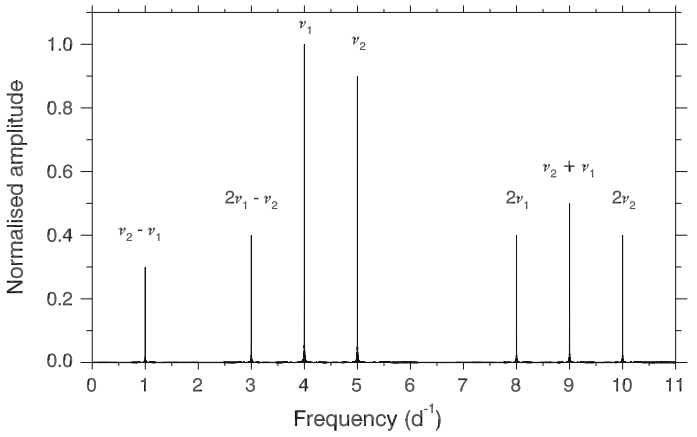

Fig. 6.1 Schematic demonstrating how two non-linear pulsation frequencies, ν_1 and ν_2, can create combination frequency triplets, for example, $2\nu_1$, $\nu_2 + \nu_1$ and $2\nu_2$, and apparent regularities in an amplitude spectrum. Figure inspired by Breger and Kolenberg (2006), their Fig. 1

triplet around ν_1, which was also demonstrated and discussed by Breger and Kolenberg (2006). Mathematically, combination frequencies produce *exactly* equally-split multiplets, whereas the second-order effects of rotation perturb the symmetry of frequencies in a rotationally split multiplet (Goupil et al. 2000; Pamyatnykh 2003; Aerts et al. 2010). This is especially true for stars that are moderate and fast rotators, such as the δ Sct star KIC 8054146 (Breger et al. 2013; Breger and Montgomery 2014) discussed in Sect. 6.2.4.

6.2.2 The Role of Resonances in Pulsating Stars

The role of non-linearity and resonances within pulsators driven by the heat engine driving mechanism is clearly non-trivial, and has been extensively studied in the literature (Dziembowski 1982; Buchler and Goupil 1984; Dziembowski and Krolikowska 1985; Moskalik 1985; Dziembowski et al. 1988; Dziembowski and Krolikowska 1990; Dziembowski and Goode 1992; Goupil and Buchler 1994; Van Hoolst 1994; Buchler et al. 1995, 1997; Goupil et al. 1998; Wu and Goldreich 2001; Wu 2001; Nowakowski 2005). In this section, an overview of the main forms of resonances in pulsating stars is given.

Direct Resonances: Parents and Children

An example of how non-linearity can act as an amplitude limitation mechanism in δ Sct stars is resonant mode coupling between a child mode and two parent modes (Dziembowski 1982). This form of pulsational non-linearity gives rise to variable frequencies and amplitudes in pulsation modes over time, which appear as a cluster of unresolved peaks in the amplitude spectrum. Resonant mode coupling has been suggested as the amplitude limitation mechanism operating in δ Sct stars but not in HADS stars, which explains the large difference in pulsation mode amplitudes between the two subgroups (Dziembowski and Krolikowska 1985). This form of resonance is commonly referred to as a direct resonance (Dziembowski 1982) or parent-child mode coupling (Breger and Montgomery 2014; Bowman et al. 2016), and is discussed further in Sect. 6.2.3.

Rotationally Induced Resonance

For a slowly rotating star, a non-radial pulsation mode will be split into its $2\ell + 1$ components. Taking a particular case of a dipole mode, a nearly equally split triplet of frequencies will be formed with a central frequency, ν_0, that corresponds to the $m = 0$ component and frequencies ν_- and ν_+ that correspond to the $m = -1$ and $m = +1$ components, respectively. It was first discussed by Buchler et al. (1995, 1997) and later by Goupil et al. (1998) how a resonance condition that satisfies $2\nu_0 \simeq \nu_+ + \nu_-$ exists, and causes variable pulsation mode amplitudes. This form of resonant mode coupling can be separated into three regimes governed by the rotational velocity of the star.

The first regime is the case of non-linear frequency locking for the cases of slow rotation. In this regime the triplet of frequencies is exactly equally split, which produces constant amplitudes and thus no amplitude modulation. The second, so-called intermediate regime is when the frequency splitting of the triplet is no longer symmetric, which causes periodic amplitude modulation amongst the components of the triplet on a characteristic time-scale of $P_{\rm mod} \sim \frac{1}{\delta\nu}$, where $\delta\nu$ is the asymmetry of the triplet (Goupil et al. 1998). When the frequency splitting is significantly asymmetric, for example in the presence of rapid rotation, the resonance condition is no longer satisfied because the non-linear frequency perturbations are very small, such that the observed frequencies are closer to the linear values (Buchler et al. 1995, 1997; Goupil et al. 1998). This is the case for the third regime.

Resonant mode coupling induced by rotation has been studied in pulsating white dwarf stars (Vauclair 2013; Zong et al. 2016b) and pulsating sdB stars (Zong et al. 2016a). For example, the DBV star KIC 8626021 was studied by Østensen et al. (2011) and later by Zong et al. (2016b), who used approximately 684 d of SC *Kepler* data to discover several rotationally-split dipole modes that exhibit amplitude modulation. From the asymmetry of the frequency splitting in the triplets and the variable pulsation mode amplitudes, Zong et al. (2016b) were able to study the hyperfine structure of the component frequencies in various triplets of rotationally-split pulsation modes and conclude that non-linearity in the form of resonant mode coupling was responsible for the observed amplitude modulation.

Parametric Resonance Instability

The parametric resonance instability, which is also called a decay instability, was discussed by Dziembowski (1982) who demonstrated that two linearly damped low-frequency modes are able to damp a linearly driven high frequency pulsation mode when it has reached a critical amplitude. In his study, Dziembowski (1982) concluded that the most likely scenario is an unstable p mode coupling with two linearly damped g modes, which would cause the growth and decay of the p and g modes in anti-correlation because energy is being exchanged amongst them (Dziembowski 1982; Dziembowski and Krolikowska 1985). Furthermore, the g modes may not have observable surface amplitudes – in this case, the modes are referred to as internal g modes (Dziembowski and Krolikowska 1985) – making the testing of this theoretical prediction difficult (see e.g., Bowman and Kurtz 2014). To first order, the modulation time-scale is the inverse of the growth rate of the child mode involved in the resonance, which can produce modulation time-scales between days and several decades in δ Sct stars (Nowakowski 2005).

6.2.3 Mode Coupling

In this section, the direct resonance form of mode coupling among pulsation modes is discussed. Coupled pulsation modes are grouped into families of child and parent

modes (e.g., Breger and Montgomery 2014), which can lead to amplitude modulation and the exchange of energy amongst different members of the family (Dziembowski 1982; Buchler et al. 1997; Nowakowski 2005). In a direct resonance, a child mode must have a frequency very close to the sum, or difference, of the frequencies of two linearly-driven (unstable) parent modes, thus satisfy

$$\nu_1 \simeq \nu_2 \pm \nu_3 \ , \tag{6.1}$$

where ν_1 is the frequency of the child mode, and ν_2 and ν_3 are the frequencies of the parent modes. However, the frequency resonance criterion given in Eq. (6.1) does not solely distinguish which frequency within a family is a combination or coupled mode frequency of the other two, as demonstrated by Fig. 6.1.

To make this distinction, the amplitude of a child mode can be modelled as a product of the two parent modes' amplitudes using

$$A_1 = \mu_{\rm c} A_2 A_3 \ , \tag{6.2}$$

and the linear combination of the parent modes' phases

$$\phi_1 = \phi_2 \pm \phi_3 \ , \tag{6.3}$$

where A and ϕ represent amplitude and phase for the corresponding child and parent modes, and $\mu_{\rm c}$ is defined as the coupling factor. For combination frequencies arising from a non-linear distortion model, small values of $\mu_{\rm c}$ are expected and thus the amplitude and/or phase variability in combination frequencies will mimic the parent modes that produce them (Brickhill 1992b; Wu 2001; Breger and Lenz 2008b). However, for the case of resonant mode coupling, one expects the amplitudes of the three modes to be comparable with larger values of $\mu_{\rm c}$ because mode energy is physically being exchanged between the child and parent modes.

In the steady state solution described by Dziembowski (1982), the coupling coefficient, $\mu_{\rm c}$, in Eq. (6.2) is a measure of the damping rate, γ_1, and mode inertia, I_1 of the child mode in the form

$$\mu_{\rm c} = \frac{H}{2\sigma_1 \gamma_1 I_1} \ , \tag{6.4}$$

where H is a coefficient that determines the strength of the coupling between the child mode ν_1 and the parent modes ν_2 and ν_3, and σ_1 is the dimensionless frequency of the child mode. The coupling coefficient $\mu_{\rm c}$ was introduced by Breger and Montgomery (2014) because the quantities σ_1, γ_1 and I_1 cannot be determined observationally from an amplitude spectrum, such that by using Eq. (6.2) the authors were able to measure the *strength* of coupling between pulsation modes in the δ Sct star KIC 8054146. This is discussed further in Sect. 6.2.4.

The method described here to is similar to the approach devised by van Kerkwijk et al. (2000) to study non-linearity in pulsating sdB stars. They defined the parameter R as

$$R = \frac{A_1}{A_2 A_3} \,, \tag{6.5}$$

where A_1, A_2 and A_3 are the amplitudes of pulsation modes with corresponding frequencies ν_1, ν_2 and ν_3 involved in a resonance. The value of the parameter R was found to be less than 10 for combination frequencies from a non-linear distortion model (van Kerkwijk et al. 2000), whereas for families of frequencies that have R values greater than 10, the amplitude of a coupled (child) mode is being strengthened by being in resonance with the parent pulsation modes giving rise to larger values. The relation given in Eq. (6.5), however, is purely empirical and should only be used as an indicator of which frequencies represent combinations, since it has been shown that combination frequencies are able to have larger amplitudes than their parent pulsation modes (Kurtz et al. 2015).

6.2.4 *Resonant Mode Coupling in the Delta Scuti Star KIC 8054146*

The fast rotating ($v \sin i \simeq 300\,\mathrm{km\,s^{-1}}$) δ Sct star KIC 8054146 contains 349 statistically significant frequencies between $0 < \nu \leq 200\,\mathrm{d^{-1}}$ including two high-amplitude triplets. The labelled amplitude spectrum from Breger and Montgomery (2014) is shown in Fig. 6.2. The interactions between low- and high-frequency families of pulsation modes were found to create regularities in its amplitude spectrum (Breger et al. 2012), so this star acts as a useful example of how the g- and p-mode frequency regimes are not independent of one another in a δ Sct star. For example, Breger et al. (2013) found that peaks in the high frequency regime contained p modes and high-degree g modes, specifically high-degree prograde sectoral modes.

KIC 8054146 was recently analysed by Breger and Montgomery (2014), who investigated the incidence of resonant mode coupling between two parent modes and a single child mode, as predicted by the direct resonance criterion (Dziembowski 1982). The 928-d SC *Kepler* data set (spanning Q5 – Q14) was divided into 45-d bins as a compromise between temporal and frequency resolution, and the amplitudes and phases of different peaks were tracked over time. The observed amplitude modulation in ten dominant pulsation modes is shown in Fig. 6.3. Breger and Montgomery (2014) found three separate families of frequencies in which the amplitude modulation of the low-frequency peaks correlated with the high-frequency peaks.

The amplitude of a coupled (child) pulsation mode is predicted to be proportional to the product of the amplitudes of the two parent modes, as given by Eq. (6.2), so the child and parent modes in a family can be identified by determining the value of the coupling coefficient, μ_c. In the case of KIC 8054146, the value of μ_c was of the order 1000 for coupled modes in families with parent mode amplitudes of order

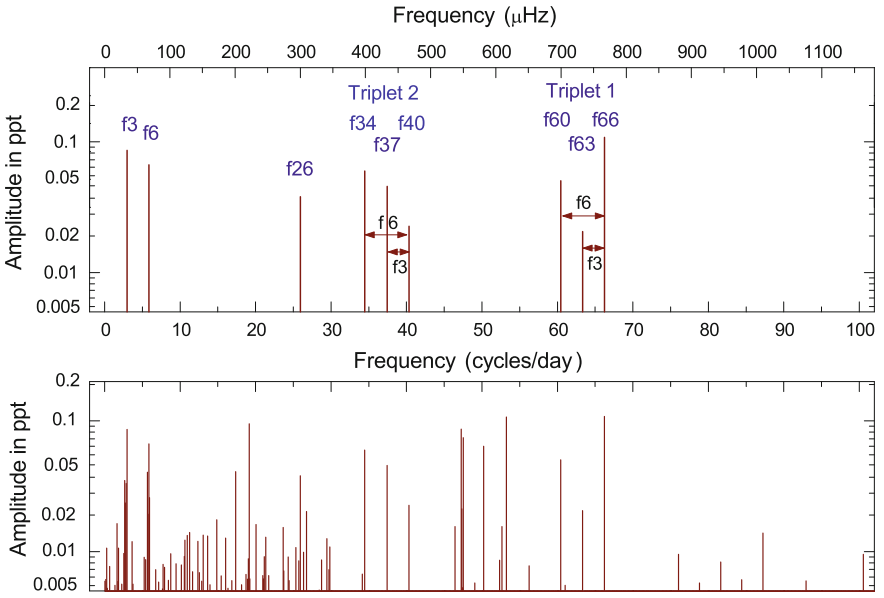

Fig. 6.2 The amplitude spectrum for the δ Sct star KIC 8054146. The *top panel* shows only the nine dominant peaks, labelled as the "T family" by Breger and Montgomery (2014), which contain two triplets, T1 and T2. The *bottom panel* shows all the peaks in the amplitude spectrum of KIC 8054146 below $\nu \leq 100$ d^{-1}. Note the logarithmic ordinate scale. Figure from Breger and Montgomery (2014), their Fig. 1. © AAS; reproduced with permission from author and AAS

0.1 mmag (Breger and Montgomery 2014). It was concluded that the amplitudes of coupled modes were larger than expected because they were being strengthened by resonant mode coupling (Breger and Montgomery 2014).

The observed phase variability of an individual frequency family in the δ Sct star KIC 8054146 is given by the $O - C$ diagram shown in Fig. 6.4, which contains the high-frequency component of triplets T1 and T2, and $\nu = 25.9509$ d^{-1} (labelled as f 26 in Fig. 6.2). Breger and Montgomery (2014) used the phase relation predicted by the mode coupling model in Eq. (6.3) to predict the phase variability for the coupled mode in T2, which accurately matched the observations. Thus, the visible energy associated with the observed amplitude modulation was conserved in KIC 8054146 (Breger and Montgomery 2014).

In their analysis of KIC 8054146, Breger et al. (2012) stated that even if three frequencies within a family obey the frequency, amplitude and phase relations given in Eqs. (6.1)–(6.3), respectively, it does not *prove* that they are combination frequencies, but merely behave like combination frequencies, thus variable pulsation mode amplitudes can be interpreted as being caused by either non-linearity from a non-linear distortion model or resonant mode coupling.

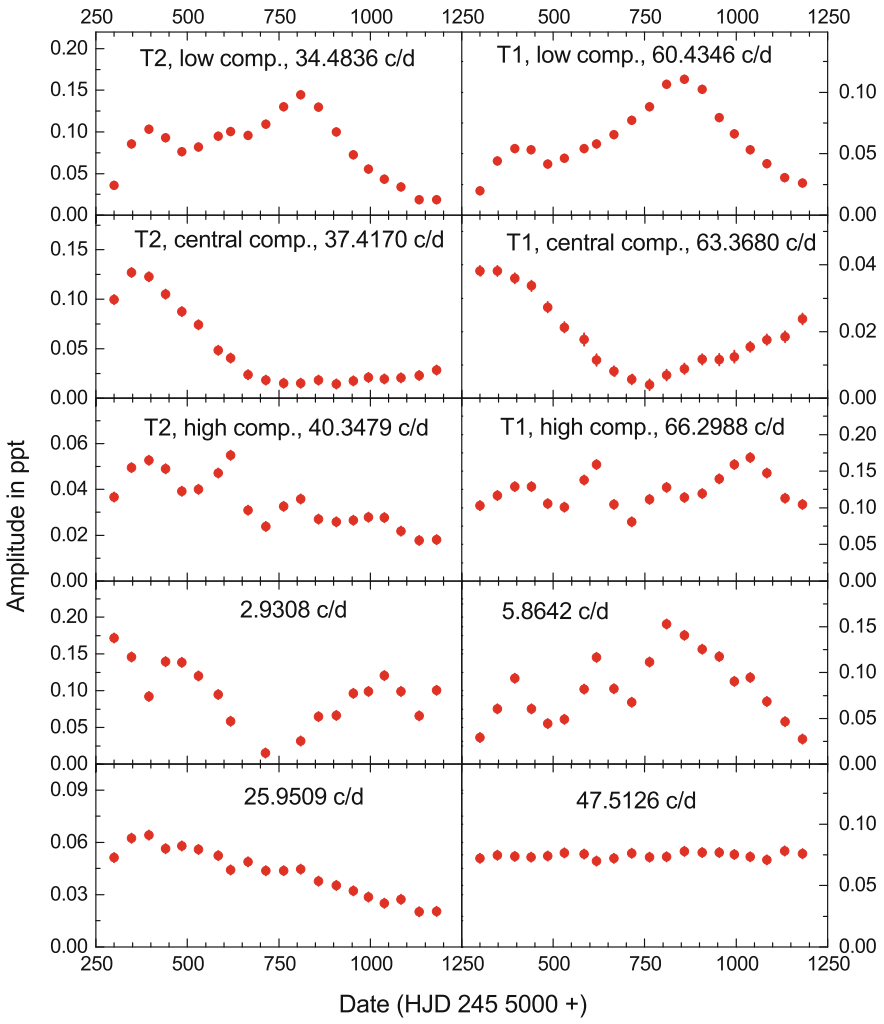

Fig. 6.3 Amplitude modulation caused by mode coupling for various pulsation modes in the δ Sct star KIC 8054146. The observed amplitude modulation in each component frequency in each triplet, T1 and T2, is correlated, which can be seen by comparing the *left* and *right* columns for each row. Figure from Breger and Montgomery (2014), their Fig. 2. © AAS; reproduced with permission from author and AAS

Therefore, the testable prediction for resonant mode coupling between a child and two parent modes in δ Sct stars is significant amplitude modulation in three similar amplitude modes with large values of μ_c (Breger and Montgomery 2014; Bowman et al. 2016). From the study of pulsation mode variability discussed in Chap. 5, it is clear that it is not a simple task to distinguish physically coupled modes from combination frequencies, emphasising the need to study the frequency, amplitude and phase variability of each of the members within each family.

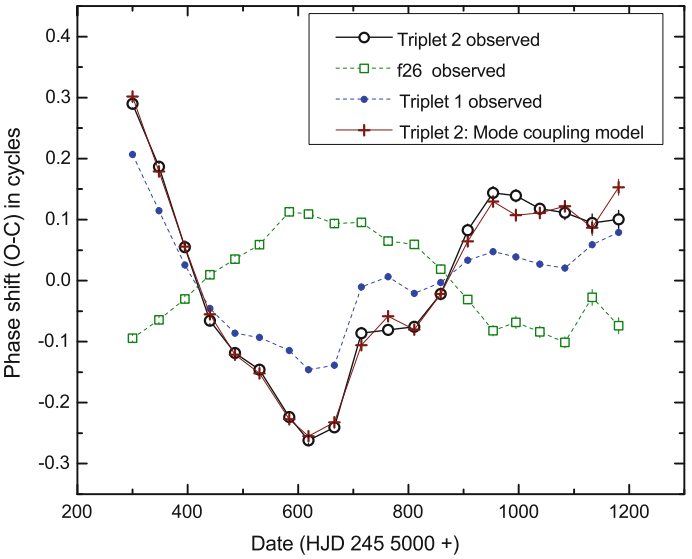

Fig. 6.4 An $O - C$ diagram for the observed phase variability in the high-frequency component of T1 and T2, of $\nu = 25.9509\ \mathrm{d}^{-1}$ (labelled as f26), and the predicted phase variability of T2 by a mode coupling model. The agreement between the predicted and observed phase variability indicates mode coupling between parent pulsation modes, f26 and T1, and the coupled mode in T2. Figure from Breger and Montgomery (2014), their Fig. 5. © AAS; reproduced with permission from author and AAS

6.3 Non-linearity in Delta Scuti Stars

In Sect. 6.2.3, it was discussed how a family of pulsation modes must satisfy the frequency criterion given in Eq. (6.1) and the phase criterion given in Eq. (6.3). To test the mode coupling hypothesis, all three members of a family must be variable in amplitude so that the child and parent modes can be identified and a model predicting the observed amplitude modulation can be constructed using Eq. (6.2). By optimising the value of the coupling coefficient μ_c to match the observed amplitude modulation, the strength of coupling and non-linearity amongst pulsation modes can be estimated. In this way, non-linearity within a family can be distinguished as coupling between a child and two parent modes or combination frequencies. Small values of μ_c imply weak-coupling and favour the non-linear distortion model producing combination frequencies, whereas large values of μ_c imply strong coupling and favour resonant mode coupling (Breger and Montgomery 2014; Bowman et al. 2016).

Note that a large value of μ_c is defined by the amplitudes of the parent modes and thus is specific to each family. For example using Eq. (6.2), if $A_2 = A_3 = 2$ mmag, then to achieve a similar child mode amplitude of $A_1 \simeq 2$ mmag a value of $\mu_c \simeq 0.25$ is required. Using the same parent mode amplitudes, a small value of $\mu_c \simeq 0.01$ would produce a child mode amplitude of $A_1 \simeq 0.04$ mmag. Therefore, in this hypothetical

example, $\mu_c \gtrsim 0.1$ is considered strong coupling and $\mu_c \lesssim 0.01$ is considered weak coupling.

It is also important to emphasise that when studying the possible energy exchange between pulsation modes, the peak in the amplitude spectrum which potentially represents a coupled mode, ν_c, is extracted from an amplitude spectrum and optimised using a non-linear least-squares fit to the data set. The difference in the observed frequency, ν_c, from the expected combination frequency value from the two parent modes does not necessarily prove or disprove that ν_c is a combination frequency or a coupled mode if the difference is smaller than the frequency resolution of the 4-yr *Kepler* data set (0.00068 d^{-1}).

Using this approach, the strength of non-linearity was investigated in the δ Sct stars KIC 4733344 by Bowman et al. (2016) and KIC 5857714 by Bowman (2016), which are discussed in Sects. 6.3.1 and 6.3.2, respectively.

6.3.1 KIC 4733344

The δ Sct star KIC 4733344 was among the ensemble of 983 δ Sct stars discussed in Chap. 5, such that the amplitudes and phases of its twelve dominant pulsation modes were tracked throughout the 4-yr *Kepler* data set. The amplitude spectrum of KIC 473344 and the corresponding tracking plot for the twelve most dominant peaks are shown in the top and bottom panels of Fig. 6.5, respectively. The pulsation mode frequencies $\nu_2 = 7.226764\ d^{-1}$ and $\nu_3 = 9.412445\ d^{-1}$ have a period ratio of 0.7678, which is indicative of the fundamental and first overtone radial modes. Pulsation constants were also calculated using Eq. (1.2) for ν_2 and ν_3, which also suggest they are likely the fundamental and the first overtone radial modes, respectively, considering the typical uncertainties associated with calculating Q values (Breger 1990). The highest-amplitude pulsation mode frequency, $\nu_1 = 8.462183\ d^{-1}$, could not be identified as it lies between ν_2 and ν_3, thus suggesting it is likely a non-radial mode (Bowman et al. 2016). This is a plausible inference since non-radial modes can have higher amplitudes than radial modes (see Fig. 1.5 from Aerts et al. 2010). These three pulsation modes were discovered to be variable in amplitude and phase, so KIC 4733344 was classified as an AMod star by Bowman et al. (2016).

The stellar parameters of KIC 4733344 from the KIC and Huber et al. (2014) are given in Table 6.1, which characterise it as an evolved early-F star. Previously in Sect. 5.3, the NoMod δ Sct star KIC 2304168 was discussed, which has similar $T_{\rm eff}$, log g and [Fe/H] values to the AMod δ Sct star KIC 4733344. Both of these δ Sct stars were shown to pulsate in low-overtone radial modes, specifically the fundamental and first overtone radial mode by Bowman et al. (2016). It is interesting to ponder the possible differences in the driving and damping mechanisms at work within these two δ Sct stars considering the observed differences in the variability in their pulsation modes.

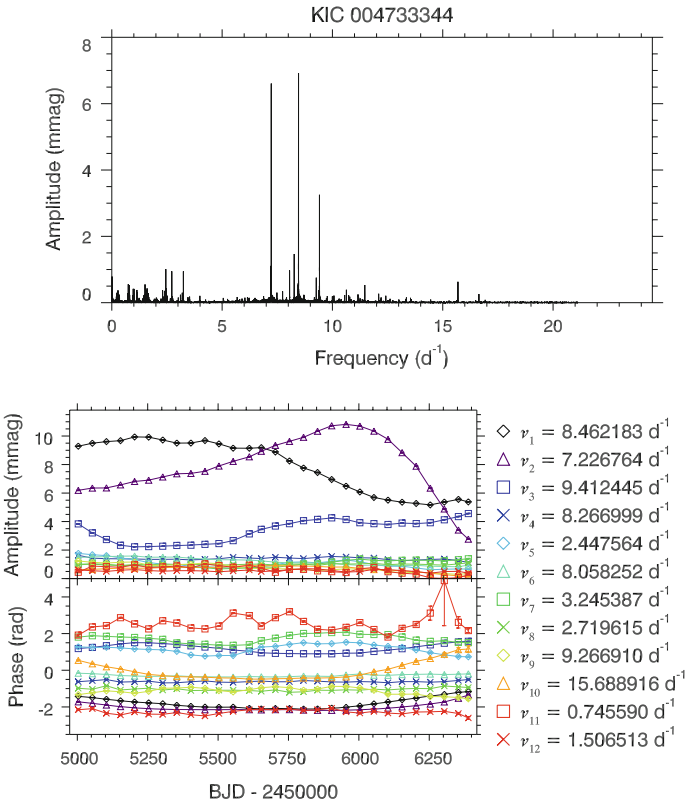

Fig. 6.5 The AMod δ Sct (hybrid) star KIC 4733344 has variable pulsation amplitudes and phases over the 4-yr *Kepler* data set, which can be explained by non-linearity. The *top panel* is the 4-yr amplitude spectrum calculated out to the LC Nyquist frequency and the *bottom panel* shows the amplitude and phase tracking plot which demonstrates the variability in pulsation amplitudes and phases over 4 yr. Figure from Bowman et al. (2016), their Fig. 10

Table 6.1 Stellar parameters of the δ Sct star KIC 4733344 from the KIC (Brown et al. 2011) and the revised values from Huber et al. (2014)

	$T_{\rm eff}$ (K)	log g (cgs)	[Fe/H] (dex)
KIC	6990 ± 200	3.38 ± 0.20	-0.12 ± 0.20
Huber et al. (2014)	7210 ± 260	3.50 ± 0.23	-0.28 ± 0.28

Using Eq. (6.2), coupling models for two families of frequencies in KIC 4733344 were calculated by Bowman et al. (2016), with the results shown in Fig. 6.6. The two families in this star were found to have similar small values for the coupling coefficient $\mu_{\rm c} \simeq 0.01$, which imply non-linearity in the form of combination frequencies from the non-linear distortion model (Bowman et al. 2016). For example, as shown in the top-left panel of Fig. 6.6, the parent modes ν_2 and ν_1 have amplitudes

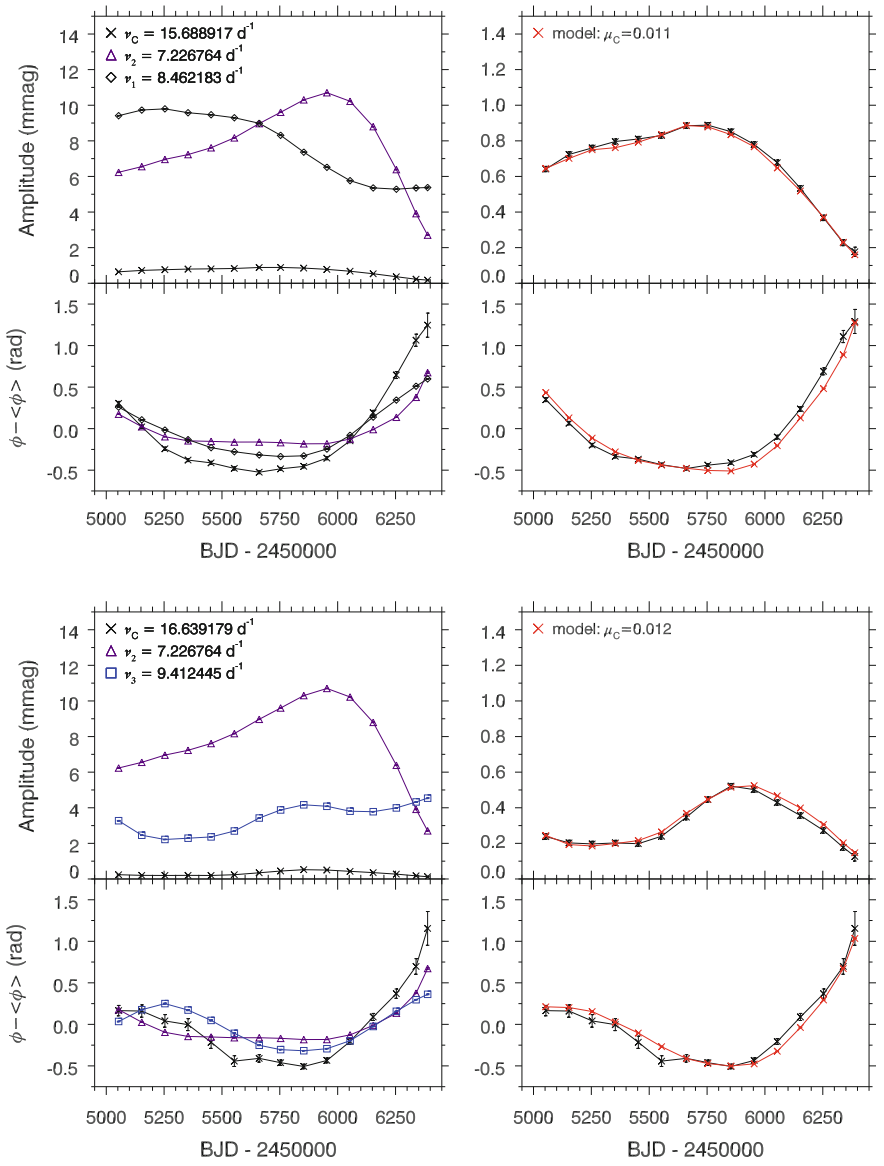

Fig. 6.6 Coupling models for two families of frequencies in KIC 4733344. In each panel, the amplitude and phase changes of the two parent frequencies with the corresponding frequencies $\nu_1 + \nu_2$ shown in the *top panel* and $\nu_2 + \nu_3$ in the *bottom panel*. The colours and frequency labels have been chosen to be consistent with the amplitude and tracking plot given in Fig. 6.5. The coupling model is plotted in *red* on the *right hand side* for both amplitude and phase variability for each chosen value of the coupling coefficient μ_c. The amplitude ordinate scales have been kept the same in each panel for comparison. Figure from Bowman et al. (2016), their Fig. 10

of $A_2 \simeq 6$ mmag and $A_1 \simeq 9$ mmag, respectively, at the start of the *Kepler* observations. From a hypothetical coupling coefficient of $\mu_c \simeq 0.1$, one would expect a child mode amplitude of $A_c \simeq 5$ mmag, which is approximately an order of magnitude larger than the observed amplitude of the child mode of $A_c \simeq 0.6$ mmag. Therefore, Bowman et al. (2016) concluded that resonant mode coupling is unlikely to be the cause of non-linearity and amplitude modulation in KIC 4733344, and that ν_c is a combination frequency of the parent modes ν_1 and ν_2.

6.3.2 KIC 5857714

In this section, the study of non-linearity and mode coupling is extended to the δ Sct KIC 5857714. Note that this star, however, is not a member of the ensemble of 983 stars discussed in Chaps. 4 and 5 because it is a module 3 star, which were not observed by *Kepler* during every fourth LC quarter because of a technical failure of the CCD module. KIC 5857714 acts as a useful example here because it has high amplitude pulsations with significant amplitude modulation, and because it has a low mode density in its amplitude spectrum. The stellar parameters of KIC 5857714 from the KIC and Huber et al. (2014) are given in Table 6.2, which characterise it as an evolved early-F star.

The light curve of KIC 5857714 is shown in the top-left panel of Fig. 6.7, in which the gaps caused by the failure of CCD module 3 can clearly be seen. The amplitude spectrum of KIC 5857714 is shown in the bottom-left panel of Fig. 6.7, in which the two highest amplitude pulsation mode frequencies, $\nu_1 = 12.227331$ d^{-1} and $\nu_2 = 10.273765$ d^{-1}, and their first-order sum and difference frequencies are labelled. A zoom-in of ν_1 in the amplitude spectrum is given in the right panel of Fig. 6.7, in which a more-complicated spectral window pattern can be seen because KIC 5857714 is a module 3 star. KIC 5857714 pulsates with two high-amplitude parent p modes, ν_1 and ν_2, which are non-linearly interacting to form frequencies at $\nu_1 + \nu_2 = 22.501101$ d^{-1} and $\nu_1 - \nu_2 = 1.953569$ d^{-1}, and other higher order combination frequencies and harmonics which are not labelled in Fig. 6.7.

Using the method employed by Bowman et al. (2016), the strength of the non-linearity in these sum and difference combination frequencies was tested by constructing mode coupling models and determining the optimum value of the coupling coefficient, μ_c, with the results shown in Fig. 6.8. The two parent modes vary

Table 6.2 Stellar parameters of the δ Sct star KIC 5857714 from the KIC (Brown et al. 2011) and the revised values from Huber et al. (2014)

	T_{eff} (K)	log g (cgs)	[Fe/H] (dex)
KIC	6710 ± 200	3.80 ± 0.20	-0.23 ± 0.20
Huber et al. (2014)	7050 ± 220	3.81 ± 0.22	0.24 ± 0.30

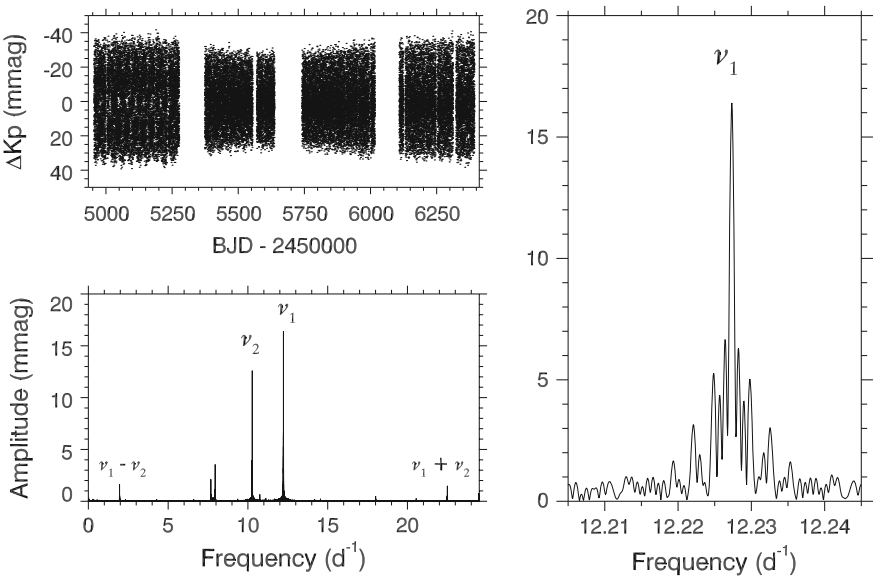

Fig. 6.7 The *top-left panel* is the 4-yr LC light curve for the δ Sct star KIC 5857714, which falls on module 3 of the *Kepler* CCD resulting in the large gaps. The *bottom-left panel* is the amplitude spectrum for the δ Sct star KIC 5857714 calculated out to the LC *Kepler* Nyquist frequency. The two parent p-mode frequencies, labelled as $\nu_1 = 12.227331\ \mathrm{d}^{-1}$ and $\nu_2 = 10.273765\ \mathrm{d}^{-1}$, non-linearly interact to form frequencies at $\nu_1 + \nu_2 = 22.501101\ \mathrm{d}^{-1}$ and $\nu_1 - \nu_2 = 1.953569\ \mathrm{d}^{-1}$, respectively. The *right panel* is a zoom-in of the highest amplitude parent mode, ν_1, which has a complicated window pattern from the gaps in the data set

considerably in amplitude over the 4-yr *Kepler* data set, and the peaks at $\nu_1 + \nu_2$ and $\nu_2 - \nu_1$ mimic the behaviour of the amplitude modulation in the parent modes. The small values of $\mu_c \simeq 0.008$ in KIC 5857714 indicate that the sum and difference frequencies are combination frequencies from a non-linear distortion model and not coupled modes involved in a direct resonance.

Similarly to KIC 4733344 discussed in Sect. 6.3.1, the observed amplitude modulation in KIC 5857714 raises the following question: where does the energy associated with these parent pulsation modes go to and come from if not the other visible pulsation modes? Do these results indicate that the sum and difference combination frequencies in these case studies are in fact physical modes that are involved in a weakly-coupled direct resonance or are they combination frequencies? The method of measuring the strength of mode coupling employed by Bowman et al. (2016) implies the latter, but our understanding of the physics responsible for combination frequencies in δ Sct stars is far from complete.

It is clear from the discussion in Chap. 5 that many δ Sct stars exhibit significant amplitude modulation, and furthermore, also do not conserve their visible pulsation energy budget over 4 yr of *Kepler* observations. The conservation of visible pulsation mode energy is explored further in Sect. 6.5.

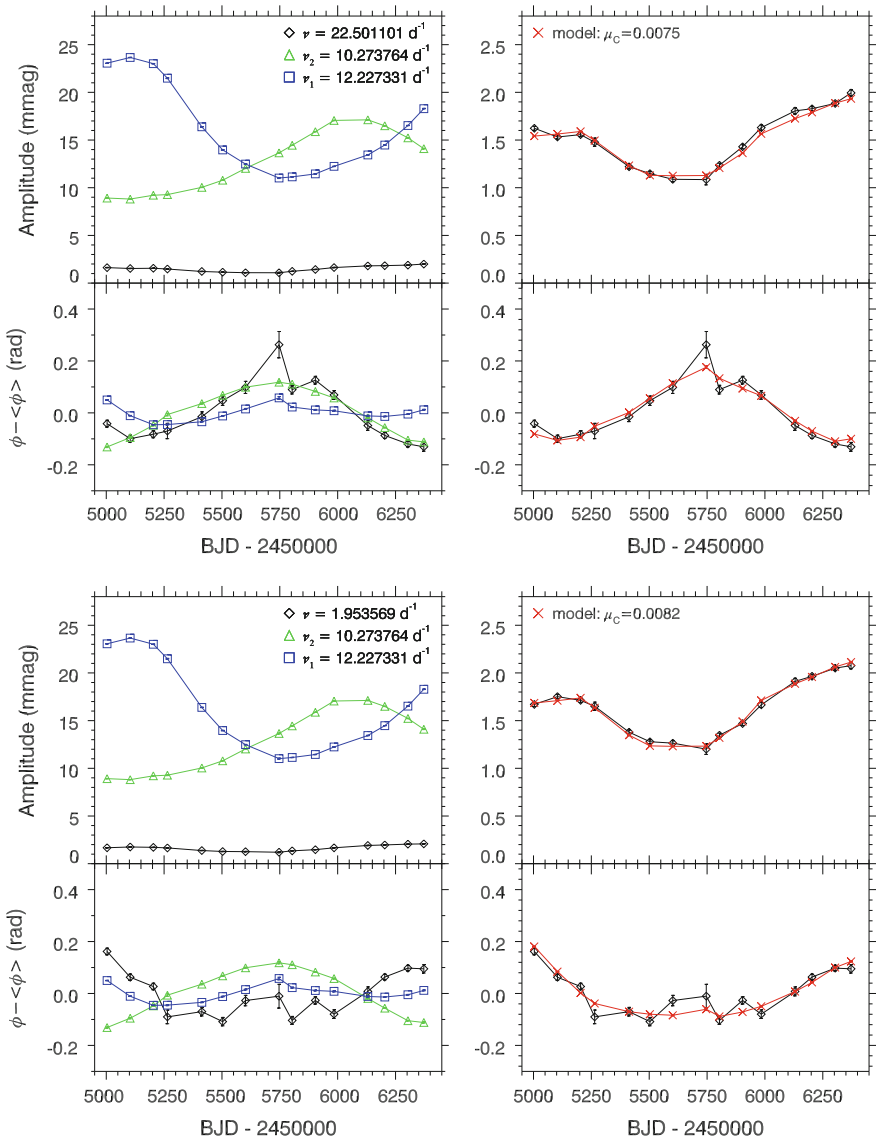

Fig. 6.8 Coupling models for two families of frequencies in KIC 5857714. In both panels, the amplitude and phase changes of the two parent frequencies $\nu_1 = 12.227331\ \mathrm{d}^{-1}$ and $\nu_2 = 10.273765\ \mathrm{d}^{-1}$ are shown in *blue* and *green*, with the corresponding frequencies, $\nu_1 + \nu_2$ (*top panel*) and $\nu_1 - \nu_2$ (*bottom panel*) are shown in *black*. The coupling model is plotted in *red* on the *right hand side* for both amplitude and phase variability for each chosen value of the coupling coefficient μ_c. The amplitude ordinate scales have been kept the same in each panel for comparison

6.4 Non-linearity in Gamma Doradus Stars

Non-linearity is certainly important in γ Dor stars. This was demonstrated by Kurtz et al. (2015), who found that the asymmetry of SPB and γ Dor light curves can be explained by the relative phases of combination frequencies to the parent pulsation modes. It was also shown that the 'frequency groups' in these stars were a result of non-linearity in the form of high-order combination frequencies — once identified and removed, the amplitude spectra were noticeably simplified (Kurtz et al. 2015). Non-linearity is often associated with high-amplitude pulsations with the high-order combinations observed in some γ Dor and SPB stars indicating extremely high amplitude g-mode pulsations in the cores of these stars (Kurtz et al. 2015).

Although rarer and more difficult to study because of the high mode densities in the amplitude spectra of γ Dor stars, amplitude modulation is also found among these stars. In the following subsections, two unique examples of γ Dor stars are presented. The first is KIC 4731916, in which the combination frequencies do not mimic the variability of the parent g mode frequencies — this is unexpected and cannot be unexplained by our current understanding of combination frequencies. The second is KIC 4358571, in which there are no peaks in the amplitude spectrum, neither combination frequencies nor coupled pulsation modes, that can explain the amplitude modulation observed in the parent g modes.

6.4.1 KIC 4731916

In Sect. 6.2.1 and in Fig. 6.1, it is demonstrated how multiplets of equally-spaced frequencies can be present from the non-linear interaction of parent frequencies and produce combination frequencies and regularity in an amplitude spectrum. For a multiplet of combination frequencies, the splitting of the multiplet must be exact since combination frequencies are sum and difference frequencies. Therefore, if a small number of parent pulsation mode frequencies can be identified, it is sensible to generate all the possible combination terms, optimise the amplitudes and phases using linear least-squares at fixed frequency and calculate the amplitude spectrum of the residuals. Using this method, the γ Dor star KIC 4731916 was identified to contain a triplet of combination frequencies that do not mimic the amplitude modulation in the two parent g modes.

The 4-yr *Kepler* light curve and amplitude spectrum of the γ Dor star KIC 4731916 are shown in the top-left and bottom panels of Fig. 6.9, respectively. The stellar parameters listed in the KIC and the revised values from Huber et al. (2014) for KIC 4731916 are given in Table 6.3, which characterise it as an early-F star and place it inside the γ Dor instability region. Note that KIC 4731916 is closer to the TAMS than the ZAMS from its log g value, which is not uncommon considering the quoted uncertainties and that typically log $g \simeq 4$ for γ Dor stars observed by *Kepler*

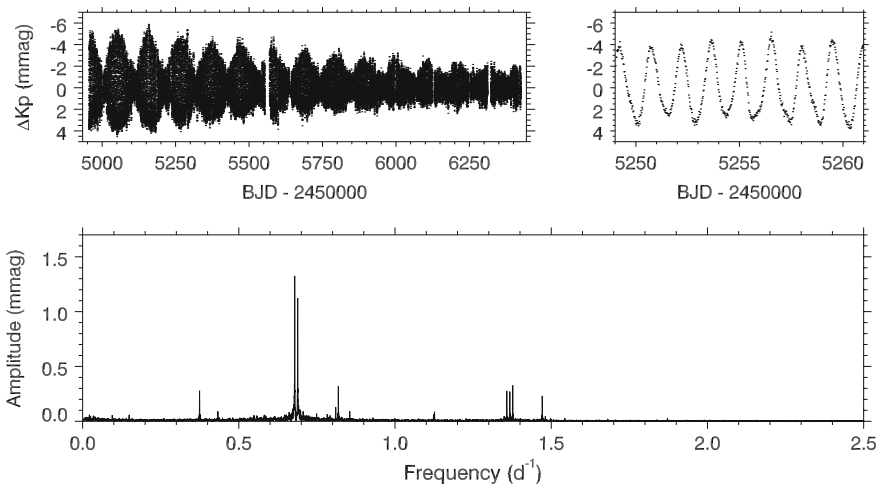

Fig. 6.9 The 4-yr LC *Kepler* light curve, in which a ∼105-d beat period and amplitude modulation envelope can be seen, is shown in the *top-left panel* and a 12-d insert of the LC light curve is shown in the *top-right panel*. The *bottom panel* is the LC amplitude spectrum between $0 \leq \nu \leq 2.5$ d^{-1}. KIC 4731916 is a γ Dor star with only g modes and combination frequencies

Table 6.3 Stellar parameters of the γ Dor star KIC 4731916 from the KIC (Brown et al. 2011) and the revised values from Huber et al. (2014)

	$T_{\rm eff}$ (K)	log g (cgs)	[Fe/H] (dex)
KIC	6640 ± 200	3.85 ± 0.20	-0.14 ± 0.20
Huber et al. (2014)	6910 ± 240	3.87 ± 0.23	-0.14 ± 0.29

and confirmed using spectroscopy (Tkachenko et al. 2013; Van Reeth et al. 2015). Its current state of evolution may shed light on the unusual pulsational behaviour in KIC 4731916, which is discussed in later sections.

Light Curve Asymmetry

Upon first inspection of the 4-yr light curve, shown in the top-left panel of Fig. 6.9, two forms of variability that modulate the intrinsic pulsations are evident. The first is a regular beat period of approximately 105 d resulting from two closely-spaced frequencies. The second form of variability is an envelope of decreasing amplitude which modulates the light curve excursions.

The light curve is asymmetric with larger upward than downward excursions about the mean, which has been set to zero. This can also be seen in the 12-d insert of the light curve shown in the top-right panel of Fig. 6.9. The phases of combination frequencies relative to the parent mode frequencies govern the asymmetry of a light curve (Kurtz et al. 2015). Combination frequencies with relative phases near 0 (or 2π) to the parent mode phases produce an upwards light curve, whereas combination frequencies with

relative phases near π to the parent mode phases produce a downwards light curve (Kurtz et al. 2015). This effect is not very strong in KIC 4731916, resulting in only a slightly upwards light curve.

Frequency Analysis

In the amplitude spectrum of KIC 4731916, two relatively high amplitude peaks at $\nu_1 = 0.6788739$ d^{-1} and $\nu_2 = 0.6883655$ d^{-1} can be seen. A zoom-in of the amplitude spectrum for ν_1 and ν_2 is shown in the left panel of Fig. 6.10. These peaks lie within the typical frequency range for a γ Dor star ($0.3 < \nu < 3$ d^{-1}), and are likely g-mode pulsation frequencies. There are no p mode frequencies ($4 < \nu < 100$ d^{-1}) associated with δ Sct pulsations, but there are other low-amplitude g-mode pulsation frequencies in the expected g-mode frequency range. A triplet of equally-spaced frequencies is also present, a zoom-in of which is shown in the right panel of Fig. 6.10.

To find combination frequencies present within KIC 4731916, a non-linear least-squares fit using the cosine function, $\Delta m = A\cos(2\pi\nu(t-t_0)+\phi)$, of the two parent mode frequencies was used. All possible combination frequencies up to order 3ν with amplitudes greater than 0.012 mmag (i.e., 3σ of the error in amplitude) yielded 12 combination terms, which are given in Table 6.4. Higher order terms may exist in the amplitude spectrum, but only those with amplitudes greater than the amplitude cut-off are included in Table 6.4, along with their respective amplitudes and phases.

Subsequently, a multifrequency fit of these 14 frequencies using linear least-squares was performed and the data set was pre-whitened to find any remaining variance. The amplitude spectrum of the residuals was re-calculated and the triplet of frequencies was almost completely removed, with before and after pre-whitening shown

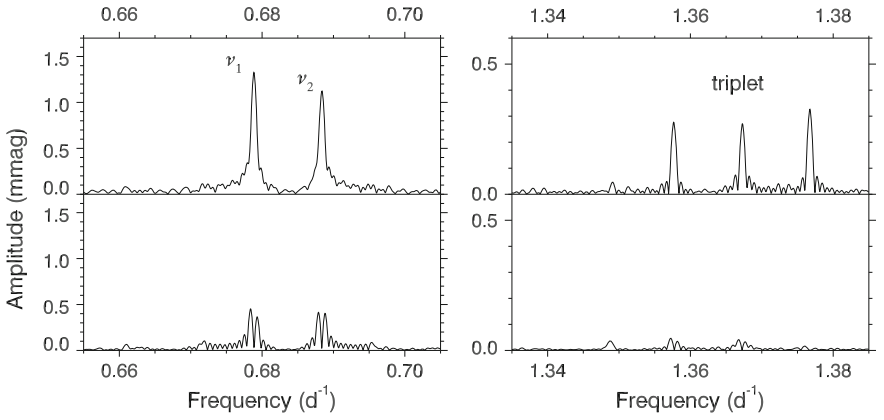

Fig. 6.10 An zoom-in of the LC amplitude spectrum of the γ Dor star KIC 4731916, for the two parent g modes (*left panel*) and the combination frequency triplet (*right panel*). Note the difference in ordinate scales between the two panels. The amplitude spectrum is shown before and after pre-whitening the data using a multifrequency least-squares fit as *top* and *bottom*, respectively. The combination triplet is removed but the two parent g modes are not because of their intrinsic amplitude modulation

Table 6.4 A non-linear least-squares fit of the two parent pulsation mode frequencies of KIC 4731916, plus a linear least-squares fit of 12 additional combination frequencies up to order 3ν with amplitudes greater than 0.012 mmag. The zero point of the time scale is $t_0 = 2\,455\,688.77$ BJD

	Frequency (d^{-1})	Amplitude ± 0.004 (mmag)	Phase (rad)
ν_1	0.6788739 ± 0.0000013	1.337	-0.287 ± 0.003
ν_2	0.6883655 ± 0.0000015	1.142	-0.193 ± 0.004
$-\nu_1 + \nu_2$	0.0094916	0.015	-1.607 ± 0.273
$-2\nu_1 + 2\nu_2$	0.0189832	0.046	1.866 ± 0.088
$-3\nu_1 + 3\nu_2$	0.0284748	0.019	0.163 ± 0.216
$2\nu_1 - \nu_2$	0.6693823	0.069	0.913 ± 0.059
$-\nu_1 + 2\nu_2$	0.6978571	0.072	2.176 ± 0.057
$-2\nu_1 + 3\nu_2$	0.7073487	0.017	-1.029 ± 0.242
$3\nu_1 - \nu_2$	1.3482562	0.014	1.042 ± 0.299
$2\nu_1$	1.3577478	0.278	2.995 ± 0.015
$\nu_1 + \nu_2$	1.3672394	0.273	2.052 ± 0.015
$2\nu_2$	1.3767310	0.325	-2.345 ± 0.013
$-\nu_1 + 3\nu_2$	1.3862226	0.016	0.185 ± 0.264
$3\nu_1 + \nu_2$	2.7249872	0.025	2.821 ± 0.163

in the top and bottom panels of Fig. 6.10, respectively. This clearly demonstrates that the triplet is comprised of harmonics and a combination frequency of the two parent frequencies, specifically $2\nu_1 = 1.3577478\ d^{-1}$, $\nu_1 + \nu_2 = 1.3672394\ d^{-1}$ and $2\nu_2 = 1.3767309\ d^{-1}$. It is important to emphasise that the combination frequency hypothesis requires a multiplet in an amplitude spectrum to be *exactly* equally-split, since harmonics and combination terms are a mathematical representation of the non-linearity and non-sinusoidal shape of the light curve. This is the case for the triplet found in KIC 4731916.

There are other peaks in the amplitude spectrum (e.g., a peak lies to the left of the triplet in the right panel of Fig. 6.10), which were not removed after pre-whitening the multifrequency linear least-squares fit demonstrating that these peaks are not combination frequencies of the two parent g-modes. The triplet contains the only combination frequencies with relatively high amplitudes in the amplitude spectrum of KIC 4731916.

Discounting a Spot Model

Inhomogeneities or spots on the surface of a star do not produce combination frequencies in an amplitude spectrum of a pulsating star (Kurtz et al. 2015). The presence of the $\nu_1 + \nu_2$ combination frequency cannot be explained in a spot model. Furthermore, there are many peaks over a large frequency range shown in Fig. 6.9, which are likely other g-mode pulsation frequencies. A spot model would have to conjecture

differential rotation greater than a factor of three in rotation frequency to explain *all* frequencies observed in KIC 4731916, when no star has ever been observed or modelled to have such behaviour.

No regular period spacing pattern is detected in the amplitude spectrum of KIC 4731916, which is also true for many γ Dor stars. However, the period spacing between ν_1 and ν_2 of 0.0203 d ($\simeq$ 1754 s) is consistent with consecutive dipole modes of the same azimuthal order, supporting the inference that these frequencies are g modes and not rotational modulation caused by spots. It has been shown that a cool γ Dor star with essentially no rotation can have period spacings of $\simeq$ 0.0203 d — see Fig. 8 of Kurtz et al. (2014) to see how the period spacings change with age for stars in the $1.6 - 2.2$ $M_\odot$ mass range; 0.0203 d is not surprising. This, coupled with the impossibility of explaining the combination frequency with spots, completely rules out any spot model for KIC 4731916.

Variable Pulsation Mode Amplitudes

To study the variability in amplitude and phase of ν_1, ν_2 and the combination frequency triplet, the 4-yr *Kepler* data set for KIC 4731916 was divided into 300-d bins using a 150-d overlap for consecutive bins, and values of amplitude and phase were optimised at fixed frequency in each bin using linear least-squares. The difference in the two parent frequencies, $\nu_2 - \nu_1 = 0.0094916$ d^{-1}, produces a beat period of $P_{\rm beat} = 105.36 \pm 0.02$ d. Therefore a bin size of 300 d with 150-d overlap was large enough to resolve the beating of this pair of close-frequency pulsation modes. Using a 150-d overlap also smoothed variation in amplitude and phase between bins, similar to the tracking method used by Bowman et al. (2016).

The resultant tracking plots are shown in Fig. 6.11, in which the phases of all frequencies have been normalised to be zero in the mean so that any relative phase variability is clear. Note that a constant amplitude, frequency and phase cosinusoid would appear as a perfectly flat horizontal line in both amplitude and phase panels. The two parent mode frequencies steadily decrease in amplitude over the 4-yr *Kepler* observations. Specifically, ν_1 decreases from 2.06 ± 0.01 to 0.57 ± 0.02 mmag, and ν_2 decreases from 1.90 ± 0.01 to 0.40 ± 0.02 mmag, with neither frequency exhibiting any significant change in phase. The lack of significant phase modulation suggests that ν_1 and ν_2 exhibit a pure form of amplitude modulation, rather than amplitude modulation caused by mode coupling or beating from close-frequency pulsation modes (see Fig. 9 and associated discussion from Bowman et al. 2016). The amplitude variability can also be seen in the zoom-in of the parent mode frequencies in the amplitude spectrum in Fig. 6.10. Neither peak is a sinc function, thus the behaviour is unresolved. The mode energy associated with this decrease in amplitude is not transferred to any new or existing mode frequency visible in the amplitude spectrum.

The most remarkable result from the variability analysis of KIC 4731916 is that the members of the combination frequency triplet do not mirror the two parent frequencies that create it. This is unexpected. Since harmonics and combination frequencies describe the non-linearity and non-sinusoidal shape of the light curve, any changes in the amplitude and/or phase of the parent mode frequencies should cause similar

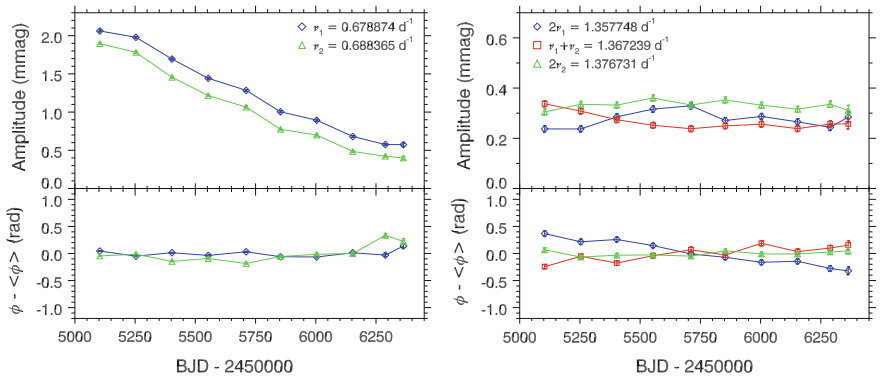

Fig. 6.11 Tracking plots for the two parent g modes and combination frequency triplet in the γ Dor star KIC 4731916. Amplitude and phase are calculated at a fixed frequency using least-squares in a series of 300-d bins with 150-d overlap. The *left panel* shows the two parent g-mode frequencies $\nu_1 = 0.678874$ d^{-1} and $\nu_2 = 0.688365$ d^{-1} as *blue diamonds* and *green triangles*, respectively. The *right panel* shows the harmonics $2\nu_1 = 1.357748$ d^{-1}, $2\nu_2 = 1.376731$ d^{-1} as *blue diamonds* and *green triangles*, respectively, and the combination frequency $\nu_1 + \nu_2 = 1.367239$ d^{-1} as *red squares*, which together form an equally split frequency triplet. Note the difference in ordinate scale between the two panels

variability in any combination frequencies. The amplitudes and phases of combination frequencies in white dwarf stars are a function of the parent mode frequencies (Brickhill 1992b; Wu 2001), and combination frequencies are observed to mirror variability in the parent frequencies in δ Sct stars (Breger and Lenz 2008b; Bowman et al. 2016). This is not the case for the γ Dor star KIC 4731916, which is evident by comparing the two panels in Fig. 6.11.

As discussed by Kurtz et al. (2015), the strong non-linear interactions of g modes visible at the surface of a γ Dor star imply high pulsation mode amplitudes near the cores of these stars. In the case of KIC 4731916 and its decreasing parent mode amplitudes, at some point the non-linearity should change, because it may disappear at low amplitudes. Since the combination frequency is observed to remain at a constant amplitude whilst the parent modes decrease implies that the strength of the non-linearity is *increasing* with decreasing amplitude. This is even more unexpected and remains a challenge to theoretical expectations of combination frequencies.

6.4.2 KIC 4358571

In this section, another unique example of amplitude modulation in a γ Dor star is presented, specifically KIC 4358571. The stellar parameters of this star from the KIC and from Huber et al. (2014) are given in Table 6.5, which characterise it as an early-F star inside the γ Dor instability region. The 4-yr *Kepler* light curve and amplitude spectrum of KIC 4358571 are shown in the top- and bottom-left panels of

Table 6.5 Stellar parameters of the γ Dor star KIC 4358571 from the KIC (Brown et al. 2011) and the revised values from Huber et al. (2014)

	T_{eff} (K)	log g (cgs)	[Fe/H] (dex)
KIC	6870 ± 200	4.01 ± 0.20	-0.17 ± 0.02
Huber et al. (2014)	7150 ± 230	3.99 ± 0.23	-0.16 ± 0.31

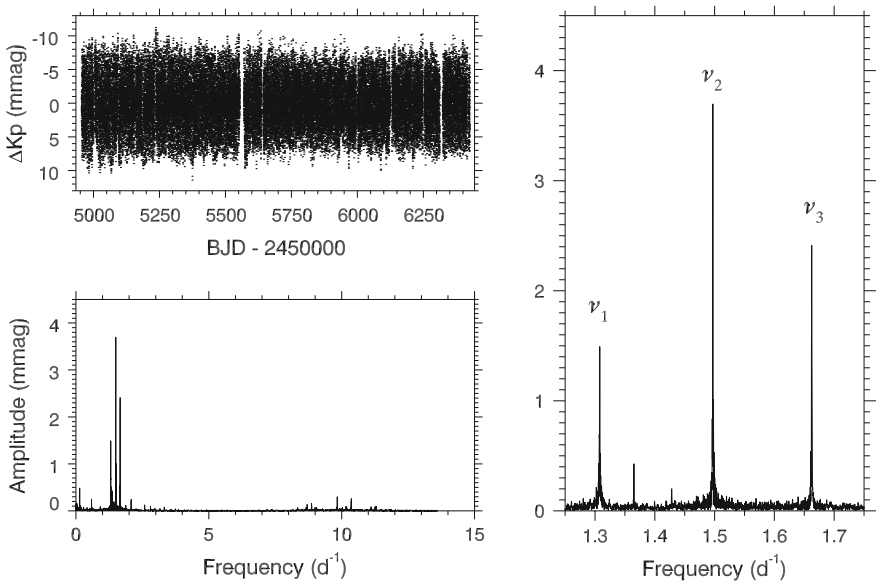

Fig. 6.12 The *top-left panel* shows the 4 yr light curve using LC data for KIC 4358571. The amplitude spectrum calculated out to the LC Nyquist frequency is given in the *bottom-left panel* and a zoom-in of the three parent g-mode frequencies is shown in the *right panel*

Fig. 6.12, respectively. An zoom-in of the amplitude spectrum is shown in the right panel of Fig. 6.12, in which the three highest amplitude peaks are labelled and are typical of high-amplitude g modes for such a star.

The same amplitude and phase tracking method by Bowman et al. (2016) was used to study amplitude modulation of the three principal pulsation mode frequencies, specifically $\nu_1 = 1.307952$ d^{-1}, $\nu_2 = 1.497101$ d^{-1}, and $\nu_3 = 1.662438$ d^{-1}, with the results shown in Fig. 6.13. Similarly to KIC 4731916, the parent g modes in KIC 4358571 are variable in amplitude over the 4 yr *Kepler* data set. Higher frequency peaks are present in the amplitude spectrum, but no combination frequencies with significant amplitude of the three parent g-modes could be identified. Therefore, the mode energy associated with the variable parent g modes is not transferred to any of the other visible pulsation modes in this star.

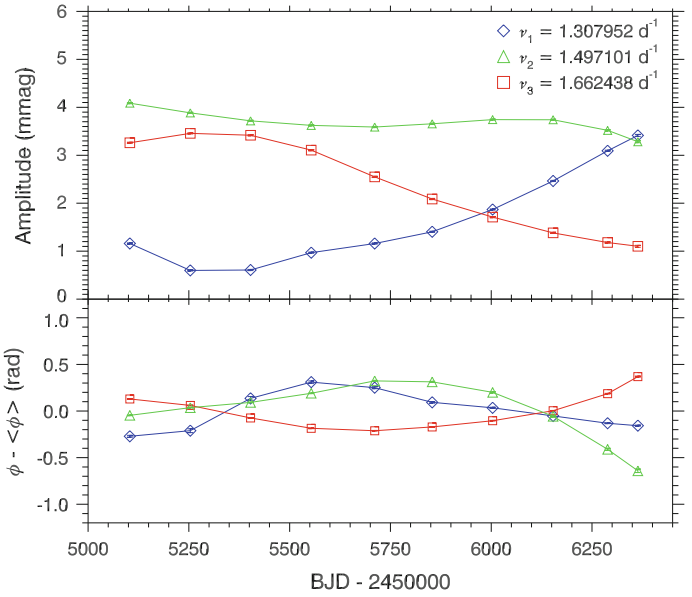

Fig. 6.13 Tracking plot showing amplitude and phase modulation at fixed frequency in KIC 4358571 of the three high-amplitude parent g mode frequencies, using 300 d bins with 150-d overlap. There are no significant combination frequencies of these three parent pulsation mode frequencies

In the current and previous sections, two γ Dor stars have been presented, KIC 4731916 and KIC 4358571, which demonstrate that amplitude modulation is also found among g-mode pulsators. Mode coupling models using Eq. (6.2) could not be used to study KIC 4731916 because the combination frequencies did not mimic the variability in the parent g modes, whereas no combination frequencies could be found in KIC 4358571. Therefore, it is also possible for γ Dor stars to not conserve their visible pulsational energy budget in a similar way to many δ Sct stars observed over 4 yr by the *Kepler* Space Telescope.

6.5 Energy Conservation of Pulsation Modes

The Sun is the only star for which the total pulsational energy budget can be measured, because pulsation modes over many radial orders covering a large range in angular degree are observable. The pulsation mode energy in the Sun and stars with solar-like oscillations is determined by the physics of the convective envelope, with the connection between convection and pulsation in the Sun having been studied extensively in the literature (Goldreich and Keeley 1977a, b; Libbrecht and Woodard 1991; Goldreich et al. 1994).

An observational measurement of the energy contained within the radial modes of the Sun was achieved by Chaplin et al. (1998) using data from the Birmingham Solar-Oscillations Network (BiSON).[1] It was calculated that the solar mode energy peaks at a frequency of approximately 3200 μHz with a value of $E \sim 10^{28}$ erg (Chaplin et al. 1998). Independently, Komm et al. (2000) used data from the Global Oscillation Network Group (GONG)[2] to measure the total energy for modes with angular degrees of $9 \leq \ell \leq 150$, and found a consistent value of the energy per mode as $E \simeq 2.2 \times 10^{28}$ erg. The mode energy is a function of frequency and if extrapolated to cover the frequency range between $400 \leq \nu \leq 5000$ μHz (i.e., $\ell \lesssim 1000$), then the total energy contained in the Sun's acoustic waves was calculated to be $E_{\rm Tot} \simeq 4.2 \times 10^{34}$ erg (Komm et al. 2000).

Although it is not directly responsible for the pulsations, convection is undoubtedly important in intermediate-mass γ Dor and δ Sct stars – see Houdek and Dupret (2015) for a recent thorough review – since it may be responsible for the non-linearity that creates harmonics and combination frequencies. For early-A stars that are near the blue edge of the classical instability strip, models have indicated that granulation produces of order 10 ppm μHz^{-1}, which is non-negligible (Kallinger and Matthews 2010). The interaction between convection and pulsation is also important, especially near the red edge of the classical instability strip at which the δ Sct pulsation modes are returned to stability (Houdek et al. 1999; Houdek 2000; Xiong and Deng 2001; Dupret et al. 2005; Grigahcène et al. 2005).

Using *Kepler* observations, one is unable to measure the total pulsational energy budget of a star, but proxies such as pulsation mode amplitudes can be used instead to test variable driving/damping over time. Nowakowski (2005) defines a general formula for mode energy, E, as

$$E = \frac{1}{2} I \left| \nu^2 A^2 \right| \ , \tag{6.6}$$

where I is the mode inertia, ν is the frequency, and A is the amplitude. If this is normalised using units of $\frac{1}{2} I_0 \nu_0^2$ (see Eq. (19) of Nowakowski 2005), then the energy of a pulsation mode can be simplified to

$$E = \left| A^2 \right| \ . \tag{6.7}$$

In the next section, Eq. (6.7) is used to study energy conservation of pulsation modes in δ Sct stars that exhibit amplitude modulation.

[1] BiSON website: http://bison.ph.bham.ac.uk.

[2] GONG website: http://www.gong.noao.edu.

6.5.1 Application to Case Studies of Delta Scuti and Gamma Dor Stars

In this section, an observable called "energy" using Eq. (6.7) is introduced to study energy conservation of pulsation modes over time in δ Sct and γ Dor stars. The amplitude tracking routine is adapted to plot the total visible pulsation energy in a star, E_T, as a function of time using

$$E_T(t) = \sum_{i}^{N} A_i^2(t) \, , \tag{6.8}$$

where N is the number of pulsation mode amplitudes, A_i, at a given time step.

The total visible pulsation energy for the δ Sct and γ Dor stars discussed in this chapter, specifically KIC 4733344, KIC 5857714, KIC 4731916 and KIC 4358571 along with KIC 7106205, is plotted in Fig. 6.14. Clearly, these case study stars do not conserve their visible pulsation energy budget over time, such that the decay in amplitude of one pulsation mode does not coincide with a comparable increase in amplitude of another, or vice versa. This is best demonstrated using the δ Sct star KIC 7106205, discussed in Chap. 3, in which a single pulsation mode was responsible for the observed amplitude modulation whilst all other pulsation modes remained constant in amplitude over the 4-yr *Kepler* data set. Many other δ Sct stars observed by the *Kepler* Space Telescope also do not conserve their visible energy budget — simply put, where does the mode energy go or come from if not the other pulsation modes?

There are several astrophysical possibilities that may explain the unconserved pulsation mode energy in δ Sct stars. First, resonant mode coupling to high-degree pulsation modes or internal g modes, which are invisible in broad-band photometric observations (Dziembowski 1977), can explain observations of amplitude modulation (Dziembowski 1982; Dziembowski and Krolikowska 1985; Nowakowski 2005). For the δ Sct stars this is a convincing and realistic possibility but is difficult to test. One must also explain why this is not observed in all δ Sct stars, since the analysis of 983 δ Sct stars by Bowman et al. (2016) demonstrated that approximately 40 per cent of δ Sct stars do not show variable pulsation mode amplitudes. Therefore, if mode coupling is the solution, why is it not ubiquitous?

A second solution is that the interplay between pulsation and convection facilitates the exchange of mode energy with the stellar medium on time-scales of order a few years. Models of δ Sct stars near the red edge of the instability strip show that, for example, turbulent pressure is important in returning a star to stability (Houdek 2008), but also that turbulent pressure is able to excite high-frequency pulsation modes in δ Sct stars in the centre of the classical instability strip (Antoci et al. 2014). Further work on modelling individual δ Sct stars is clearly needed to explain the diverse range of pulsation behaviour observed in all δ Sct stars.

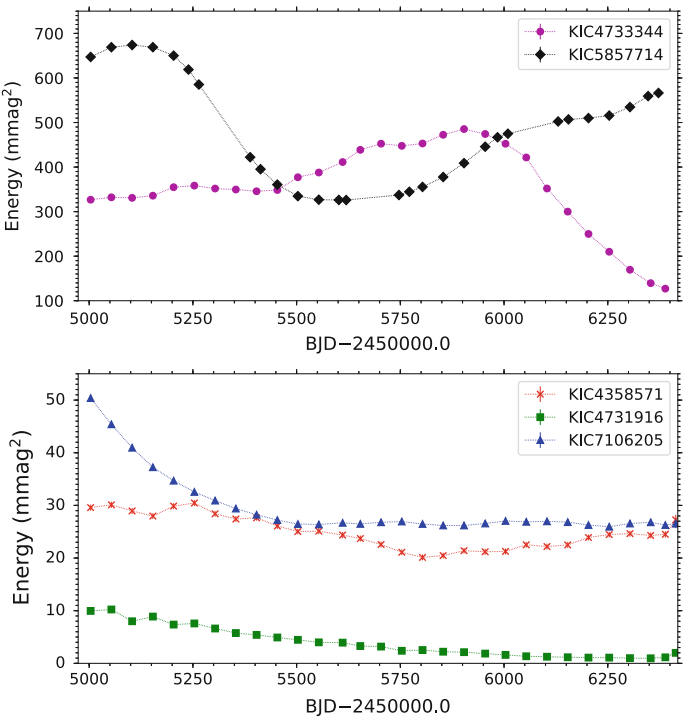

Fig. 6.14 The observable "energy" ($=A^2$) is used to study energy conservation of visible pulsation modes in a selection of case study δ Sct and γ Dor stars discussed in this chapter. The *top panel* shows the high amplitude (module 3) δ Sct star KIC 5857714 as *black diamonds* and the δ Sct star KIC 4733344 as *purple circles*. The *bottom panel* shows the δ Sct star KIC 7106205 and the γ Dor stars KIC 4731916 and KIC 4358571 as *blue triangles*, *green squares* and *red crosses*, respectively

6.6 Discussion

Stars that exhibit non-linearity are evident from the non-sinusoidal shape of the light curve and the presence of harmonics and combination frequencies in their amplitude spectra. The frequency, amplitude and phase of a coupled mode or combination frequency are a function of the two parent modes, and so a coupling coefficient, μ_c, can be used to distinguish between these two forms of non-linearity within a star. Small values of μ_c imply combination frequencies from a non-linear distortion model that mimic any variability in the parent modes (Brickhill 1992b; Wu 2001; Breger and Lenz 2008b), whereas large values of μ_c imply resonant mode coupling with mode energy being exchanged among family members (van Kerkwijk et al. 2000; Breger and Montgomery 2014; Bowman et al. 2016).

In Sects. 6.3.1 and 6.3.2, the application of the mode coupling hypothesis using Eq. (6.2) was discussed for the δ Sct stars KIC 4733344 (Bowman et al. 2016) and KIC 5857714 (Bowman 2016), respectively. For two families of frequencies

in KIC 4733344, values of $\mu_c \lesssim 0.01$ were found, which indicated the sum and difference frequencies were combination frequencies caused by the non-linear distortion model and were not strongly-coupled modes (Bowman et al. 2016). Similar values of μ_c were also found in the δ Sct star KIC 5857714, thus yielded similar results (Bowman 2016). Many δ Sct stars contain combination frequencies but the physical cause of this form of non-linearity in δ Sct stars is as yet understood (see e.g., Breger and Lenz 2008a; Pápics 2012; Balona 2012, 2016).

For many δ Sct stars, the total visible pulsation mode energy is not conserved in 4 yr of *Kepler* observations (Bowman et al. 2016). This was demonstrated in Fig. 6.14 using the δ Sct stars KIC 7106205, KIC 4733344 and KIC 5857714, but also for the γ Dor stars KIC 4731916 and KIC 4358571. The unconserved mode energy in many δ Sct stars may be caused by mode coupling to invisible high-degree modes, or internal g modes (Dziembowski 1982; Dziembowski and Krolikowska 1985), or intrinsic variability in driving and/or damping rates within a star. Photometry from the *Kepler* Space Telescope is insensitive to high-degree modes from geometric cancellation (Dziembowski 1977), and so it is difficult to determine if the amplitude modulation in a low-degree child p-mode is caused by high-degree parent modes, or internal g modes.

The intermediate-mass stars have thin surface convective envelopes, which in γ Dor stars are responsible for exciting g modes (Guzik et al. 2000; Dupret et al. 2005). Similarly, the turbulent pressure in the surface convection zone has also been shown to excite high overtone p modes in δ Sct stars (Antoci et al. 2014). The convective envelopes of these stars could also mix the pulsation eigenmode signals, distort the light curve and produce combination frequencies and harmonics in δ Sct stars, which has been extensively discussed for variable white dwarf stars (Brickhill 1992b; Brassard et al. 1993; Wu and Goldreich 2001; Wu 2001; Montgomery 2005).

In this chapter, the unique γ Dor star KIC 4731916 has been presented. The only significant harmonics and combination frequencies in this star comprise an equally-split triplet, whose amplitudes and phases do *not* mirror the variability of the two parent pulsation modes. There is little chance that these peaks are not combination frequencies, because of the *exact* values of the frequency splitting. This is a significant advantage of generating the combination frequencies mathematically (see e.g., Kurtz et al. 2015), as the likelihood of finding false combination terms is greatly reduced compared to frequency extraction by iterative pre-whitening. The lack of expected variability in combination frequencies created from intrinsically variable parent mode frequencies has implications for future work on γ Dor stars, both observationally and theoretically. Physically, how can combination frequencies act independently? The γ Dor star KIC 4731916 is an important example for expanding our understanding of intrinsically variable pulsation modes and how combination frequencies are generated in pulsating stars, especially in γ Dor stars.

It is clear that non-linearity is at work within many, if not all, δ Sct stars, and also in a few γ Dor stars, which can appear as amplitude modulation caused by resonant mode coupling and/or combination frequencies and harmonics from a non-linear distortion model. Modelling studies of individual δ Sct stars using the stellar evolutionary code `MESA` (Paxton et al. 2011, 2013, 2015) and the stellar oscillation code

GYRE (Townsend and Teitler 2013) are needed to test the hypothesis that variable driving and/or damping could be cause of the observed amplitude modulation on time-scales of order years, and the nature of the mechanism that causes combination frequencies and harmonics in γ Dor and δ Sct stars.

References

Aerts, C., Christensen-Dalsgaard, J., & Kurtz, D. W. 2010, Asteroseismology (Springer)
Antoci, V., Cunha, M., Houdek, G., et al. 2014, ApJ, 796, 118
Balona, L. A. 2012, MNRAS, 422, 1092
Balona, L. A. 2016, MNRAS, 459, 1097
Bowman, D. M. & Kurtz, D. W. 2014, MNRAS, 444, 1909
Bowman, D. M., Kurtz, D. W., Breger, M., Murphy, S. J., & Holdsworth, D. L. 2016, MNRAS, 460, 1970
Bowman, D. M. 2016, PhD thesis, Jeremiah Horrocks Institute, University of Central Lancashire, UK
Brassard, P., Fontaine, G., Wesemael, F., & Talon, A. 1993, in NATO Advanced Science Institutes (ASI) Series C, Vol. 403, NATO Advanced Science Institutes (ASI) Series C, ed. M. A. Barstow, 485
Breger, M. & Kolenberg, K. 2006, A&A, 460, 167
Breger, M. & Lenz, P. 2008a, Communications in Asteroseismology, 157, 292
Breger, M. & Lenz, P. 2008b, A&A, 488, 643
Breger, M. & Montgomery, M. H. 2014, ApJ, 783, 89
Breger, M., Fossati, L., Balona, L., et al. 2012, ApJ, 759, 62
Breger, M., Lenz, P., & Pamyatnykh, A. A. 2013, ApJ, 773, 56
Breger, M. 1990, Delta Scuti Star Newsletter, 2, 13
Breger, M. 2000, in Astronomical Society of the Pacific Conference Series, Vol. 210, Delta Scuti and Related Stars, ed. M. Breger & M. Montgomery, 3
Brickhill, A. J. 1983, MNRAS, 204, 537
Brickhill, A. J. 1990, MNRAS, 246, 510
Brickhill, A. J. 1991a, MNRAS, 251, 673
Brickhill, A. J. 1991b, MNRAS, 252, 334
Brickhill, A. J. 1992a, MNRAS, 259, 529
Brickhill, A. J. 1992b, MNRAS, 259, 519
Brown, T. M., Latham, D. W., Everett, M. E., & Esquerdo, G. A. 2011, AJ, 142, 112
Buchler, J. R. & Goupil, M.-J. 1984, ApJ, 279, 394
Buchler, J. R., Goupil, M.-J., & Hansen, C. J. 1997, A&A, 321, 159
Buchler, J. R., Goupil, M. J., & Serre, T. 1995, A&A, 296, 405
Chaplin, W. J., Elsworth, Y., Isaak, G. R., et al. 1998, MNRAS, 298, L7
Cox, J. P. 1980, Theory of stellar pulsation (Princeton Series in Astrophysics)
Degroote, P., Briquet, M., Catala, C., et al. 2009, A&A, 506, 111
Dupret, M. A., Grigahcène, A., Garrido, R., Gabriel, M., & Scuflaire, R. 2005, A&A, 435, 927
Dziembowski, W. A. & Goode, P. R. 1992, ApJ, 394, 670
Dziembowski, W. & Krolikowska, M. 1985, Acta Astronomica, 35, 5
Dziembowski, W. & Krolikowska, M. 1990, Acta Astronomica, 40, 19
Dziembowski, W., Krolikowska, M., & Kosovichev, A. 1988, Acta Astronomica, 38, 61
Dziembowski, W. 1977, Acta Astronomica, 27, 203
Dziembowski, W. 1982, Acta Astronomica, 32, 147
Goldreich, P. & Keeley, D. A. 1977a, ApJ, 211, 934
Goldreich, P. & Keeley, D. A. 1977b, ApJ, 212, 243
Goldreich, P., Murray, N., & Kumar, P. 1994, ApJ, 424, 466

Goupil, M.-J. & Buchler, J. R. 1994, A&A, 291, 481
Goupil, M. J., Dziembowski, W. A., & Fontaine, G. 1998, Baltic Astronomy, 7, 21
Goupil, M.-J., Dziembowski, W. A., Pamyatnykh, A. A., & Talon, S. 2000, in Astronomical Society of the Pacific Conference Series, Vol. 210, Delta Scuti and Related Stars, ed. M. Breger & M. Montgomery, 267
Grigahcène, A., Dupret, M.-A., Gabriel, M., Garrido, R., & Scuflaire, R. 2005, A&A, 434, 1055
Guzik, J. A., Kaye, A. B., Bradley, P. A., Cox, A. N., & Neuforge, C. 2000, ApJL, 542, L57
Handler, G., Shobbrook, R. R., Jerzykiewicz, M., et al. 2004, MNRAS, 347, 454
Houdek, G. & Dupret, M.-A. 2015, Living Reviews in Solar Physics, 12
Houdek, G., Balmforth, N. J., Christensen-Dalsgaard, J., & Gough, D. O. 1999, in Astronomical Society of the Pacific Conference Series, Vol. 173, Stellar Structure: Theory and Test of Connective Energy Transport, ed. A. Gimenez, E. F. Guinan, & B. Montesinos, 317
Houdek, G. 2000, in Astronomical Society of the Pacific Conference Series, Vol. 210, Delta Scuti and Related Stars, ed. M. Breger & M. Montgomery, 454
Houdek, G. 2008, Communications in Asteroseismology, 157, 137
Huber, D., Silva Aguirre, V., Matthews, J. M., et al. 2014, ApJS, 211, 2
Kallinger, T. & Matthews, J. M. 2010, ApJL, 711, L35
Komm, R. W., Howe, R., & Hill, F. 2000, ApJ, 543, 472
Kurtz, D. W., Saio, H., Takata, M., et al. 2014, MNRAS, 444, 102.
Kurtz, D. W., Shibahashi, H., Murphy, S. J., Bedding, T. R., & Bowman, D. M. 2015, MNRAS, 450, 3015
Libbrecht, K. G. & Woodard, M. F. 1991, Science, 253, 152
Montgomery, M. H. 2005, ApJ, 633, 1142
Moskalik, P. 1985, Acta Astronomica, 35, 229
Murphy, S. J., Pigulski, A., Kurtz, D. W., et al. 2013, MNRAS, 432, 2284
Nowakowski, R. M. 2005, Acta Astronomica, 55, 1
Østensen, R. H., Bloemen, S., Vučković, M., et al. 2011, ApJL, 736, L39
Pamyatnykh, A. A. 2003, Ap&SS, 284, 97
Pápics, P. I., Tkachenko, A., Van Reeth, T., et al. 2017, A&A, 598, A74
Pápics, P. I. 2012, Astronomische Nachrichten, 333, 1053
Pápics, P. I. 2013, PhD thesis, Instituut voor Sterrenkunde, KU Leuven, Celestijnenlaan 200D, B-3001 Leuven, Belgium.
Paxton, B., Bildsten, L., Dotter, A., et al. 2011, ApJS, 192, 3
Paxton, B., Cantiello, M., Arras, P., et al. 2013, ApJS, 208, 4
Paxton, B., Marchant, P., Schwab, J., et al. 2015, ApJS, 220, 15
Saio, H. & Cox, J. P. 1980, ApJ, 236, 549
Stellingwerf, R. F. 1980, in Lecture Notes in Physics, Berlin Springer Verlag, Vol. 125, Nonradial and Nonlinear Stellar Pulsation, ed. H. A. Hill & W. A. Dziembowski, 50–54
Tkachenko, A., Lehmann, H., Smalley, B., & Uytterhoeven, K. 2013, MNRAS, 431, 3685
Townsend, R. H. D. & Teitler, S. A. 2013, MNRAS, 435, 3406
Unno, W., Osaki, Y., Ando, H., Saio, H., & Shibahashi, H. 1989, Nonradial oscillations of stars, Tokyo: University of Tokyo Press, 2nd ed. (University of Tokyo Press)
Van Hoolst, T. 1994, A&A, 292, 471
van Kerkwijk, M. H., Clemens, J. C., & Wu, Y. 2000, MNRAS, 314, 209
Van Reeth, T., Tkachenko, A., Aerts, C., et al. 2015, ApJS, 218, 27
Vauclair, G. 2013, in Astronomical Society of the Pacific Conference Series, Vol. 479, Progress in Physics of the Sun and Stars: A New Era in Helio- and Asteroseismology, ed. H. Shibahashi & A. E. Lynas-Gray, 223
Wu, Y. & Goldreich, P. 2001, ApJ, 546, 469
Wu, Y. 2001, MNRAS, 323, 248
Xiong, D. R. & Deng, L. 2001, MNRAS, 324, 243
Zong, W., Charpinet, S., & Vauclair, G. 2016a, A&A, 594, A46
Zong, W., Charpinet, S., Vauclair, G., Giammichele, N., & Van Grootel, V. 2016b, A&A, 585, A22

Chapter 7
Investigating the HADS Stars with *Kepler* Data

7.1 Introductory Remarks

The high-amplitude δ Sct (HADS) stars are a subgroup of δ Sct stars that are typically slow rotators and predominantly pulsate in the fundamental and/or first overtone radial mode (Petersen and Christensen-Dalsgaard 1996; Breger 2000; McNamara 2000; Rodríguez et al. 2000). As discussed in Sect. 1.2.6, the HADS stars were originally defined by McNamara (2000) as δ Sct stars with peak-to-peak light amplitudes exceeding 0.3 mag with pulsation periods between 1 and 6 hr. These stars are rare, making up less than one per cent of pulsating stars within the classical instability strip (Lee et al. 2008), and exhibit similarities to evolved pulsators such as Cepheids in the classical instability strip (Soszyński et al. 2008; Poleski et al. 2010).

There have been several detailed studies of HADS stars in the literature, which aimed to determine if these stars are distinct from δ Sct stars. For example, Petersen and Christensen-Dalsgaard (1996) claimed that HADS stars are able to pulsate at significantly higher amplitudes because they are in a post-main sequence stage of evolution. On the other hand, Breger (2000) conjectured that the slow rotation in these stars, which is typically $v \sin i \lesssim 40$ km s^{-1} (McNamara 2000; Rodríguez et al. 2000), facilitates the high amplitude pulsations. If HADS stars are in a post-main sequence stage of evolution, then these stars represent a subsample of δ Sct stars to investigate possible period changes in radial pulsation modes caused by stellar evolution.

In this chapter, a review of studying stellar evolution from observations of changes in pulsation periods is given in Sect. 7.2 for δ Sct stars and SX Phe stars. In Sect. 7.3, a case study from the literature of possible stellar evolution in the ρ Pup star KIC 3429637 is revisited using 4 yr of *Kepler* observations. In Sects. 7.5 and 7.6, the only two HADS stars observed by the *Kepler* Space Telescope are analysed to determine if any observed period changes are caused by stellar evolution.

D.M. Bowman, *Amplitude Modulation of Pulsation Modes in Delta Scuti Stars*,
Springer Theses, DOI 10.1007/978-3-319-66649-5_7

7.2 Pulsation Period Changes Caused by Stellar Evolution

One of the goals of astrophysics is to improve the models of stellar evolution by using observations, which as a consequence has widespread implications throughout astronomy — for example, the study of the Milky Way Galaxy using galactic archaeology (see e.g., Miglio et al. 2013; Casagrande et al. 2014, 2016). The evolutionary path of an intermediate-mass star ($M \simeq 2\ \mathrm{M}_{\odot}$) from the main sequence to the red giant branch was extensively discussed by Iben (1966, 1967a, b, c, 2013a, b), with the main-sequence lifetime lasting approximately 1 Gyr. Stellar evolution theory predicts that when the hydrogen in the core of a $2\ \mathrm{M}_{\odot}$ star has been exhausted at the TAMS, the star ignites hydrogen shell burning around the degenerate helium core to prevent collapse and maintain hydrostatic equilibrium. The star's core contracts, raising its temperature as the hydrogen shell moves outwards and more helium is added to the inert core, which causes the star's radius and luminosity to increase and its surface temperature to decrease.

The consequence of stellar evolution on the structure of a star is that an increase in stellar radius causes the period of the fundamental radial mode to increase (Breger and Pamyatnykh 1998). Clearly, the main sequence lifetime of a star is extremely long when compared to even the longest observations available of such stars, but a higher chance of observing evolutionary changes exists for stars in a post-main sequence state of evolution because the subgiant expansion phase of a 2-$\mathrm{M}_{\odot}$ δ Sct star is approximately between 20–100 Myr (Breger and Pamyatnykh 1998).

One of the traditional methods for inferring changes to the structure of a pulsating star is to measure the change in period of its oscillations. However, Percy et al. (1980) caution *"the study of period changes has had a long and sometimes dubious history"* and *"in most cases is a source of confusion and frustration"*.[1] Since the time of Percy et al. (1980), some authors have had success in observing changes in pulsation periods, yet it is not clear if the observed changes are caused by stellar evolution; for example, in Chap. 6 it was discussed how non-linearity causes pulsation modes to change in period (i.e., change in phase at fixed frequency) over time and so it can be difficult to disentangle these signals.

Based on the work of Percy et al. (1980) and later developed by Breger and Pamyatnykh (1998), period changes in pulsation modes can be determined from

$$(O - C) = \frac{1}{2}\left(\frac{1}{P}\frac{dP}{dt}\right)t^2\ , \tag{7.1}$$

where $(O-C)$ is the difference between the observed and calculated times of maxima in units of days, t is the length of the observations in days, and P is the period of the signal in d such that a factor of 365.25 is needed to convert the fractional period change, $\left(\frac{1}{P}\frac{dP}{dt}\right)$, into the conventional units of yr^{-1}. Thus, according to Eq. 7.1 a quadratic change in phase or $O - C$, is expected for a uniformly changing period. For a star on the main sequence, stellar evolution predicts an increasing period, which

[1] This quote remains as true today!

would produce a concave upwards parabola with a local minima (Percy et al. 1980; Breger and Pamyatnykh 1998).

The technique of studying period changes has been employed in a variety of pulsators with differing levels of success — for example, δ Sct stars (Breger 1990; Rodríguez et al. 1995; Breger and Pamyatnykh 1998; Walraven et al. 1992), β Cep stars (Neilson and Ignace 2015), sdBV stars (Kilkenny 2010) and variable white dwarf stars (Fontaine and Brassard 2008; Hermes et al. 2013). In the following sections, a review of studying period changes in δ Sct and SX Phe stars is given.

7.2.1 Period Changes in Delta Scuti Stars

Contrary to stellar evolution theory, many δ Sct stars have been observed to exhibit decreasing periods (e.g., Breger 1990 and Guzik and Cox 1991). Breger and Pamyatnykh (1998) found that approximately an equal number of Population I δ Sct stars had increasing periods as decreasing periods in their radial modes, with typical period changes of $\left|\frac{1}{P}\frac{dP}{dt}\right| \simeq 10^{-7}$ yr^{-1}, which are an order of magnitude larger than those predicted by evolutionary models. For radial pulsation modes, stellar models predict a decreasing period throughout the pre-main sequence and contraction phase just before the TAMS, and an increasing period throughout the main sequence and post-main sequence, with the rate of the period change governed by the rate of stellar evolution (Breger and Pamyatnykh 1998; Walraven et al. 1992).

An important case study of amplitude modulation and period changes in the HADS star AI Velorum is given by Walraven et al. (1992). The authors discovered that this HADS star pulsates in the fundamental and first-overtone radial modes and possibly also a non-radial mode (Walraven et al. 1992). The discovery of the period increase of the first overtone radial mode was unlikely to be caused by an evolutionary change in radius as no concomitant period change was observed in the fundamental radial mode (Walraven et al. 1992), since the periods of radial modes are dependent on the average stellar density, and thus the stellar radius as given by Eq. 1.1. The studies of δ Sct stars, including AI Velorum, have revealed that observed period changes often cannot be attributed to stellar evolution, because the magnitudes of the observed period changes were significantly larger than those predicted by evolutionary models (Walraven et al. 1992; Rodríguez et al. 1995; Breger and Pamyatnykh 1998). Furthermore, it is difficult to extract reliable period changes in δ Sct stars because many of these stars exhibit amplitude and phase modulation caused by non-linearity or beating from close-frequency pulsation modes in their dense amplitude spectra (Bowman et al. 2016).

7.2.2 Period Changes in SX Phe Stars

The history of studying period changes in the Population II SX Phe stars is somewhat different to that of δ Sct stars. Similarly to the δ Sct stars, stellar evolution theory

cannot explain the decreasing periods of radial modes observed in many SX Phe stars (Rodríguez et al. 1995). However, the SX Phe stars present another layer of complexity because sudden jumps in the observed periods are common between observations, rather than smooth variation over time (see, for example, Rodríguez et al. 1995 and references therein). An example of such an SX Phe star is SX Phe itself, with sudden jumps in the pulsation periods of its fundamental and first overtone radial modes noted by Coates et al. (1982) and Thompson and Coates (1991). Without a gradual change in the observed pulsation periods over time, it is difficult to draw any significant conclusions from these stars other than changes in the structure of a star caused by stellar evolution may not be a smooth process.

7.3 The ρ Pup Star KIC 3429637

In this section, the ρ Pup star KIC 3429637 (HD 178875) is discussed in the context of detecting changes in pulsation modes caused by stellar evolution. KIC 3429637 was studied by Murphy et al. (2012) using 2 yr of *Kepler* data and was found to exhibit amplitude and phase modulation, which was conjectured to be caused by stellar evolution. The ρ Pup stars are evolved Am stars (Gray and Garrison 1989), many of which pulsate and are also δ Sct stars (Kurtz 1976). Pulsating Am stars observed by *Kepler* were discussed by Balona et al. (2011) and those observed from the ground using the WASP project were discussed by Smalley et al. (2011, 2017), who found that approximately 14 per cent of Am stars have δ Sct pulsations.

As part of a spectroscopic survey of bright stars within the classical instability strip by Catanzaro et al. (2011), KIC 3429637 was classified with the spectral type F0 III m, which is consistent with the original classification of KIC 3429637 being an Am star by Abt (1984). High-resolution spectroscopy of KIC 3429637 obtained by Murphy et al. (2012) allowed accurate $T_{\rm eff}$, log g and metallicity to be determined and classify the star as a ρ Pup star. A comparison of the stellar parameters obtained by Catanzaro et al. (2011) and Murphy et al. (2012) is given in Table 7.1, as well as the stellar parameters from the KIC and from Huber et al. (2014).

Table 7.1 Stellar parameters of the ρ Pup star KIC 3429637 from the KIC, the revised values from Huber et al. (2014), and from spectroscopic observations from Catanzaro et al. (2011) and Murphy et al. (2012)

	$T_{\rm eff}$ (K)	log g (cgs)	v sin i (km s^{-1})
KIC	6960 ± 150	3.42 ± 0.20	
Huber et al. (2014)	7210 ± 150	3.99 ± 0.15	
Catanzaro et al. (2011)	7100 ± 150	3.0 ± 0.2	50 ± 5
Murphy et al. (2012)	7300 ± 100	3.0 ± 0.1	51 ± 1

7.3.1 Asteroseismic Analysis of KIC 3429637

The ρ Pup star KIC 3429637 was observed by the *Kepler* Space Telescope between Q1 – Q17 in LC and Q7 – Q10 in SC, and is the ninth brightest star among all the δ Sct stars observed with a magnitude of Kp = 7.71 in the *Kepler* passband. Using 670 d (Q1 – Q8) of LC data, Murphy et al. (2012) discovered that KIC 3429637 exhibits amplitude modulation with a linear increase in the amplitude of the two dominant pulsation modes and a linear decrease in a third pulsation mode occurring throughout the initial 2 yr of the *Kepler* mission. Each pulsation mode required different functional forms to fit the amplitude variability, which demonstrated that this was not an instrumental effect, as all modes would decrease or increase with the same functional form if the modulation was instrumental (Murphy et al. 2012). The amplitude modulation observed by Murphy et al. (2012) in the three highest-amplitude pulsation modes, denoted $f_1 = 10.337$ d^{-1}, $f_2 = 12.427$ d^{-1} and $f_3 = 10.936$ d^{-1}, is shown in Fig. 7.1.

From asteroseismic modelling using the Code Liégeois d'Évolution Stellaire (CLES; Scuflaire et al. 2008), the mode frequencies f_1 and f_2 were identified as the third and fourth radial overtone modes (Murphy et al. 2012). The location of KIC 3429637 in the HR diagram is shown in Fig. 7.2, which contains the best-fitting evolutionary model with $M = 2.178$ M$_\odot$, $T_{\rm eff} = 7452$ K, log $L = 1.570$ L$_\odot$, log $g = 3.648$, $R = 3.666$ R$_\odot$, and an age of 898.2 Myr (Murphy et al. 2012).

The discovery that KIC 3429637 is located near the TAMS inspired Murphy et al. (2012) to speculate that the amplitude modulation may be caused by stellar evolution. As the star evolves, the structural changes in the relative depths of different pulsation cavities, and particularly the location of the He II ionisation zone, could be modulating the observed pulsation amplitudes and causing the observed amplitude modulation (Murphy et al. 2012).

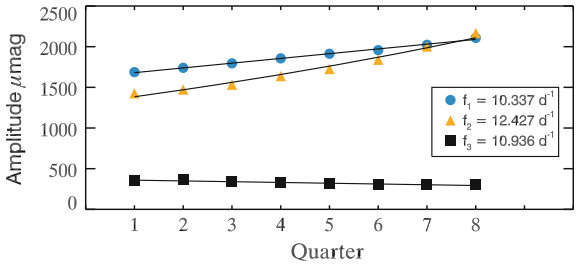

Fig. 7.1 Amplitude modulation of the three highest-amplitude pulsation modes using approximately 670 d (Q1 – Q8) of LC *Kepler* data. Figure from Murphy et al. (2012), their Fig. 3 Reproduced with permission from author and OUP on behalf of MNRAS

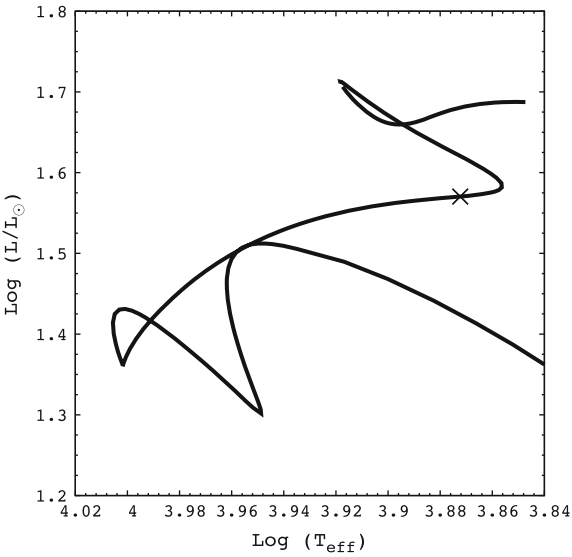

Fig. 7.2 The location of the ρ Pup star KIC 3429637 in the HR diagram is shown by the cross, which places it near the TAMS. The *solid line* represents the best-fitting evolutionary model to the spectroscopic stellar parameters. Figure from Murphy et al. (2012), their Fig. 6 Reproduced with permission from author and OUP on behalf of MNRAS

7.3.2 Revisiting the Analysis of KIC 3429637

Since the study of KIC 3429637 by Murphy et al. (2012), an additional 2 yr of *Kepler* observations have been made available. If the entire 4-yr data set of KIC 3429637 is analysed using the amplitude and phase tracking routine discussed in Chap. 5, the same functions to describe the observed amplitude modulation used by Murphy et al. (2012) are no longer valid. Specifically, the linear increase in the mode amplitude for $\nu_2 = 12.471494\ \mathrm{d}^{-1}$ is not maintained over 4 yr, which is shown in the bottom panel of Fig. 7.3. Specifically, after $t \simeq 5800$ (BJD – 2 450 000), the amplitude reaches a maximum and turns over, with a significant change in phase occurring at the epoch of minimum amplitude. The non-linear amplitude modulation in this mode suggests beating or a mode coupling mechanism is at work in this star.

If stellar evolution is the cause of the observed amplitude modulation in the ρ Pup star KIC 3429637, then phase modulation of its pulsation modes following the quadratic function given in Eq. 7.1 is also expected. However, this is not the case as can be seen in Fig. 7.3. Although the discussion of structural changes driven by stellar evolution from Murphy et al. (2012) is still valid because KIC 3429637 is near the TAMS, this star is yet another example of a δ Sct star with non-linear and non-periodic amplitude modulation. KIC 3429637 was classified as an AMod star by Bowman et al. (2016) and is one of the 603 δ Sct stars with significant amplitude modulation in the *Kepler* data set discussed in Chap. 5.

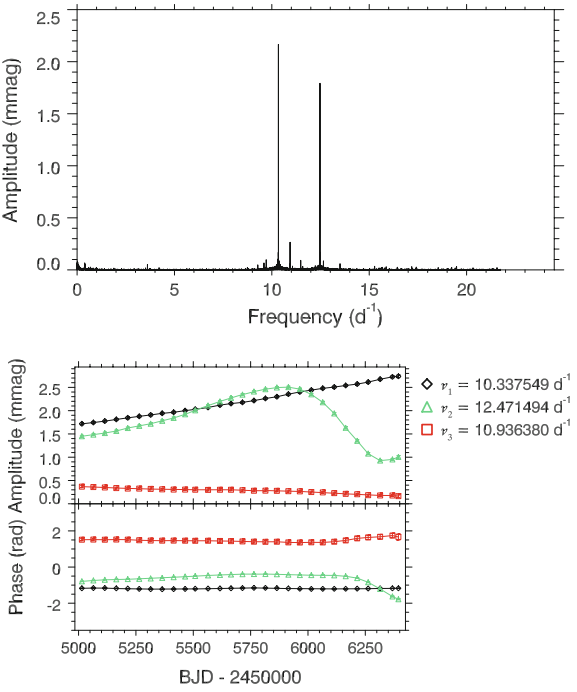

Fig. 7.3 Amplitude modulation in KIC 3429637. The *top* panel is the amplitude spectrum using 4 yr of *Kepler* data. The *bottom* panel is the tracking plot, showing the changes in the amplitudes and phases between the first and second halves of the *Kepler* mission

7.4 The Scarcity of HADS Stars Observed by *Kepler*

Using the definition of a HADS star as a δ Sct star with a peak-to-peak light amplitude variations greater than 0.3 mag (McNamara 2000), only two HADS were observed by *Kepler*, specifically KIC 5950759 and KIC 9408694 (Bowman et al. 2016). The stellar parameters of KIC 5950759 and KIC 9408694 are given in Table 7.2. Some δ Sct stars were only observed for limited subsets of LC data and consequently were not included in the ensemble of 983 stars by Bowman et al. (2016). Fortuitously, the two HADS stars were observed by *Kepler* continuously for 4 yr and were included in the ensemble (Bowman et al. 2016). Since there are several thousand A and F stars in the *Kepler* data set, the classical instability strip is well-sampled near the TAMS, for example see Niemczura et al. (2015), thus the implication from Bowman et al. (2016) is that HADS stars are rare.

Although the criterion of 0.3 mag is somewhat arbitrary, it is non-trivial as it clearly demonstrates the rarity of high-amplitude pulsators on or near the main sequence in the classical instability strip. The scarcity of high-amplitude pulsations in δ Sct stars is most evident in Fig. 4.9, in which only a few stars have pulsation mode amplitudes greater than 0.1 mag. Therefore, the implication from finding few HADS stars in a large and complete data set such as *Kepler*, is that HADS stars are rare (Lee et al. 2008; Bowman et al. 2016).

The HADS stars observed by *Kepler* were also studied by Balona (2016), who did not restrict his sample to only stars that were observed continuously for 4 yr. Balona (2016) concurs that only two *conventional* HADS stars using the definition from McNamara (2000) exist in the *Kepler* data set. If, however, the definition is relaxed to peak-to-peak light excursions exceeding 0.1 mag, three more δ Sct stars are included as (possible) HADS stars (Balona 2016).

In his study of HADS stars observed by *Kepler*, Balona (2016) compared the location of the five (possible) HADS stars in the HR diagram to the large catalogues of δ Sct stars by Rodríguez et al. (2000) and Poleski et al. (2010), which contain approximately 600 and 1200 stars, respectively. However, five stars were not enough to infer any significant conclusions. Balona (2016) found that the number and relative amplitudes of harmonics and combination frequencies were not viable criteria to distinguish δ Sct and HADS stars because non-linearity is also common among δ Sct stars — a result that has been previously demonstrated in Chaps. 5 and 6 of this monograph.

The prospect of determining a significant physical distinction between HADS stars and their low-amplitude δ Sct counterparts remains to be established and warrants further study. In particular, it has not be definitively established why the HADS stars are so rare, or whether these stars are in a post-main sequence stage of evolution as conjectured by Petersen and Christensen-Dalsgaard (1996). The nature of non-linearity in the high amplitude pulsations of these stars, and if this is related to their slow rotational velocities of $v \sin i \lesssim 40$ km s^{-1}, has also not been established (Breger 2000; McNamara 2000; Rodríguez et al. 2000).

In the next two sections, the only two traditional HADS stars observed by *Kepler*, KIC 5950759 and KIC 9408694, are discussed in greater detail with a particular focus of studying non-linearity and possible period changes caused by stellar evolution.

7.5 The Unique HADS Star KIC 5950759

The first of the two HADS stars observed by *Kepler* is KIC 5950759, with its stellar parameters from the KIC and from Huber et al. (2014) given in Table 7.2. This δ Sct star is clear example of a HADS star with large peak-to-peak light excursions

Table 7.2 Stellar parameters of the two HADS stars observed by *Kepler*, KIC 5950579 and KIC 9408694, from the KIC (Brown et al. 2011) and the revised values from Huber et al. (2014). The results of a spectroscopic analysis of KIC 9408694 by Balona et al. (2012) are also included

	$T_{\rm eff}$ (K)	log g (cgs)	[Fe/H] (dex)	
KIC 5950759	7840 ± 300	4.03 ± 0.25	-0.07 ± 0.25	KIC
	8040 ± 270	4.05 ± 0.22	-0.10 ± 0.33	Huber et al. (2014)
KIC 9408694	7480 ± 200	3.62 ± 0.20	-0.43 ± 0.20	KIC
	6810 ± 140	3.78 ± 0.11	-0.08 ± 0.15	Huber et al. (2014)
	7300 ± 150	3.50 ± 0.10		Balona et al. (2012)

exceeding 0.5 mag in the time domain and pulsation mode amplitudes exceeding 0.1 mag in its amplitude spectrum.

7.5.1 Frequency Analysis

The amplitude spectrum calculated using 4 yr of LC *Kepler* data for KIC 5950759, and the amplitude and phase tracking plot from Bowman et al. (2016) are shown in the top and bottom panels of Fig. 7.4, respectively. KIC 5950759 has two dominant pulsation mode frequencies, ν_1 and ν_2, which are given in Table 7.3 and have a period ratio of 0.7755, thus identifying them as fundamental and first overtone radial modes, respectively (Bowman et al. 2016).

As discussed in Sect. 2.3.1 and shown graphically in Fig. 2.3, there are super-Nyquist alias (sNa) peaks in the LC amplitude spectrum of KIC 5950759. These sNa peaks can be easily identified from the periodic phase modulation in the tracking plot in the bottom panel of Fig. 7.4. Fortunately, KIC 5950759 was also observed in SC (M1 from Q04) consisting of 45449 data points spanning 31.1 d, and has an effective Nyquist frequency of 686.3 d^{-1}. The much larger Nyquist frequency when using SC compared to LC *Kepler* data removes the super-Nyquist aliasing problem and simplifies the frequency analysis, but does not allow the temporal properties of a star's pulsation modes to be studied because of its short time span of approximately 1 month.

The amplitude spectrum of KIC 5950759 using the only available month of SC is shown in the top panel of Fig. 7.5, which has been calculated out to 75 d^{-1}. Many of the significant peaks in the SC amplitude spectrum have been identified and labelled, which include ν_1 and ν_2 (i.e., the two dominant radial pulsation modes) and their harmonics and combination frequencies. It should be noted that the harmonic $5\nu_1$ is the highest-order combination frequency labelled on the far right of the top panel in Fig. 7.5, but much higher-order combination frequencies exist in KIC 5950759. For example, the harmonic $20\nu_1$ is detectable in the SC data with an amplitude of approximately 10 μmag. Thus, the HADS star KIC 5950759 is demonstrably a non-linear pulsator with many combination frequencies and harmonics associated with the non-linear distortion model.

Table 7.3 Frequency, amplitude, and phase of the two principal pulsation modes, ν_1 and ν_2, for the HADS star KIC 5950759 obtained using a non-linear least-squares fit to the 4-yr LC *Kepler* data set. Phases were calculated with respect to the time zero-point $t_0 = 2\,455\,688.77$ BJD

	Frequency (d^{-1})	Amplitude (mmag)	Phase (rad)
ν_1	$14.22139376 \pm 0.00000093$	167.714 ± 0.287	1.685 ± 0.002
ν_2	$18.33729387 \pm 0.00000147$	74.066 ± 0.287	1.178 ± 0.004

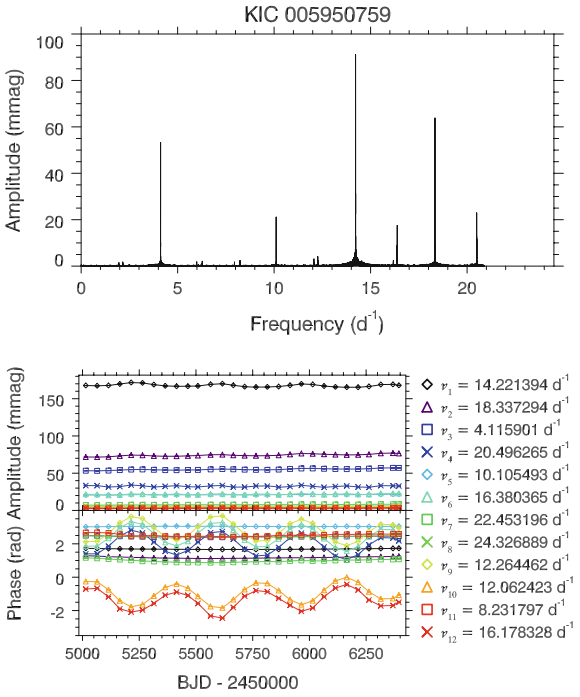

Fig. 7.4 The *top* panel is the 4-yr amplitude spectrum calculated using 4 yr of LC out to the Nyquist frequency for the HADS star KIC 5950759 (ν_4, ν_6, ν_9, ν_{10} and ν_{12} are super-Nyquist aliases). The *bottom* panel shows the amplitude and phase tracking plot, in which there is little or no variability in the amplitudes and phases of the radial pulsation mode frequencies, if instrumental modulation caused by the *Kepler* satellite is removed. Figure from Bowman et al. (2016), their Fig. 7

To find the remaining variance in the light curve of KIC 5950759, and ultimately identify additional pulsation modes other than ν_1 and ν_2, a non-linear least-squares fit using the cosine function, $\Delta m = A\cos(2\pi\nu(t-t_0)+\phi)$, of the two radial pulsation modes frequencies was calculated using the available SC data. Possible combination frequencies up to order 5ν with amplitudes greater than 0.09 mmag (i.e., 3σ of the error in amplitude) were calculated and are listed in Table 7.4. Higher order terms do exist in the amplitude spectrum beyond 75 d^{-1}, for example, higher order harmonics of ν_1 and ν_2, but only combination frequencies up to order 5ν are listed in Table 7.4.

In the bottom panel of Fig. 7.5, the amplitude spectrum of the residuals of a simultaneous multifrequency fit to the SC light curve of KIC 5950759 using all the frequencies in Table 7.4 is given. The corresponding location of the two dominant pulsation modes, ν_1 and ν_2, in the top panel of Fig. 7.5 are shown by vertical grey lines in the bottom panel. Clearly, there is significant remaining variance in the amplitude spectrum of the residuals, which cannot be associated with being combination frequencies and harmonics of the two radial pulsation modes ν_1 and ν_2. The residual amplitude spectrum is similar to a typical δ Sct star with a forest of peaks almost randomly distributed between $10 \leq \nu \leq 70$ d^{-1}, many of which could be interpreted as independent pulsation modes. Thus, KIC 5950759 likely contains additional pulsation modes other than ν_1 and ν_2 identified as the fundamental and first-overtone radial modes, respectively, by Bowman et al. (2016).

Table 7.4 The harmonics and combination frequencies of $\nu_1 = 14.22139376\ \mathrm{d}^{-1}$ and $\nu_2 = 18.33729387\ \mathrm{d}^{-1}$ up to order 5ν that have amplitudes greater than 3σ in amplitude for the HADS star KIC 5950759. Phases were calculated with respect to the time zero-point $t_0 = 2\,455\,688.77$ BJD

	Frequency (d^{-1})	Amplitude ± 0.030 (mmag)	Phase (rad)
$4\nu_1 - 3\nu_2$	1.87369343	0.338	2.360 ± 0.089
$-5\nu_1 + 4\nu_2$	2.24220668	0.229	-2.529 ± 0.131
$-\nu_1 + \nu_2$	4.11590011	55.000	2.433 ± 0.001
$3\nu_1 - 2\nu_2$	5.98959354	1.938	-0.587 ± 0.016
$-2\nu_1 + 2\nu_2$	8.23180022	2.804	2.530 ± 0.011
$2\nu_1 - \nu_2$	10.10549365	21.114	3.040 ± 0.001
$-3\nu_1 + 3\nu_2$	12.34770033	0.333	-2.005 ± 0.090
$5\nu_1 - 3\nu_2$	16.09508719	0.591	0.426 ± 0.051
$4\nu_1 - 2\nu_2$	20.21098730	1.265	-1.804 ± 0.024
$-\nu_1 + 2\nu_2$	22.45319398	7.637	0.985 ± 0.004
$3\nu_1 - \nu_2$	24.32688741	5.805	2.443 ± 0.005
$-2\nu_1 + 3\nu_2$	26.56909409	0.816	1.452 ± 0.037
$2\nu_1$	28.44278752	33.562	1.030 ± 0.001
$6\nu_1 - 3\nu_2$	30.31648095	0.121	-0.740 ± 0.248
$-3\nu_1 + 4\nu_2$	30.68499420	0.091	1.132 ± 0.330
$\nu_1 + \nu_2$	32.55868763	22.375	0.517 ± 0.001
$5\nu_1 - 2\nu_2$	34.43238106	0.200	-2.721 ± 0.150
$2\nu_2$	36.67458774	5.004	0.192 ± 0.006
$4\nu_1 - \nu_2$	38.54828117	0.939	2.329 ± 0.032
$-\nu_1 + 3\nu_2$	40.79048785	0.413	0.439 ± 0.073
$3\nu_1$	42.66418128	2.714	1.043 ± 0.011
$2\nu_1 + \nu_2$	46.78008139	2.176	1.497 ± 0.014
$-3\nu_1 + 5\nu_2$	49.02228807	0.099	1.821 ± 0.303
$\nu_1 + 2\nu_2$	50.89598150	1.941	1.782 ± 0.016
$5\nu_1 - \nu_2$	52.76967493	0.292	-2.379 ± 0.103
$3\nu_2$	55.01188161	0.795	1.687 ± 0.038
$4\nu_1$	56.88557504	2.089	2.648 ± 0.014
$-\nu_1 + 4\nu_2$	59.12778172	0.158	1.743 ± 0.190
$3\nu_1 + \nu_2$	61.00147515	4.008	2.041 ± 0.008
$2\nu_1 + 2\nu_2$	65.11737526	3.049	1.600 ± 0.010
$6\nu_1 - \nu_2$	66.99106869	0.147	-2.079 ± 0.205
$\nu_1 + 3\nu_2$	69.23327537	1.173	1.278 ± 0.026
$5\nu_1$	71.10696880	1.133	2.415 ± 0.027
$4\nu_2$	73.34917548	0.276	0.992 ± 0.109

(continued)

Table 7.4 (continued)

	Frequency (d^{-1})	Amplitude ±0.030 (mmag)	Phase (rad)
$4\nu_1 + \nu_2$	75.22286891	2.081	1.659 ± 0.014
$3\nu_1 + 2\nu_2$	79.33876902	1.556	1.177 ± 0.019
$2\nu_1 + 3\nu_2$	83.45466913	0.639	0.933 ± 0.047
$\nu_1 + 4\nu_2$	87.57056924	0.158	0.883 ± 0.190
$5\nu_1 + \nu_2$	89.44426267	0.467	1.640 ± 0.064
$4\nu_1 + 2\nu_2$	93.56016278	0.297	1.447 ± 0.101
$3\nu_1 + 3\nu 2$	97.67606289	0.189	1.990 ± 0.159
$2\nu_1 + 4\nu_2$	101.79196300	0.116	2.098 ± 0.257
$5\nu_1 + 2\nu_2$	107.78155654	0.477	2.752 ± 0.063
$4\nu_1 + 3\nu_2$	111.89745665	0.399	2.327 ± 0.075
$3\nu_1 + 4\nu_2$	116.01335676	0.221	2.039 ± 0.135
$2\nu_1 + 5\nu_2$	120.12925687	0.091	1.904 ± 0.327
$5\nu_1 + 3\nu_2$	126.11885041	0.326	1.898 ± 0.092

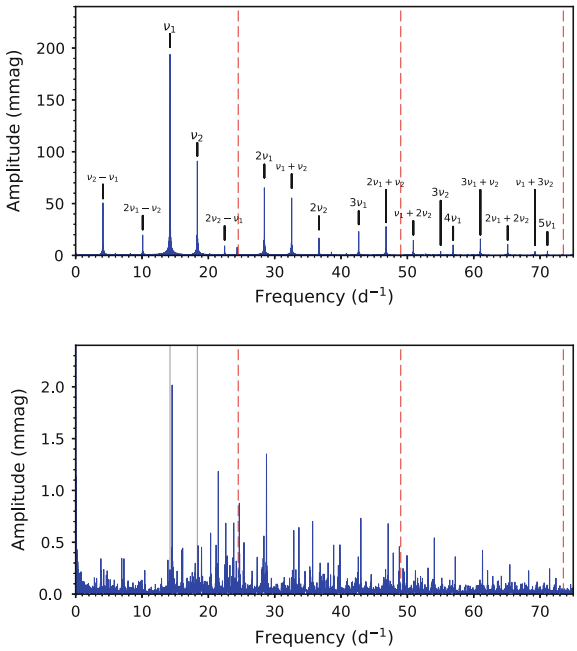

Fig. 7.5 The *top* panel shows the amplitude spectrum calculated using the only available month of SC data (M1 from Q04) for the HADS star KIC 5950759, in which the dominant pulsation modes ν_1 and ν_2 and their significant harmonics and combination frequencies are labelled. The *bottom* panel shows the amplitude spectrum of the residuals of pre-whitening ν_1 and ν_2 and their harmonics and combination frequencies, in which the *vertical grey lines* indicate the location of ν_1 and ν_2 in the *top* panel. Note that the abscissa scale has been kept the same in both panels, but the ordinate scale has not. The *vertical dashed red lines* show integer multiples of the LC *Kepler* Nyquist frequency

7.5.2 Amplitude and Phase Modulation

The amplitude and phase variability of the fundamental and first overtone radial modes, ν_1 and ν_2, are shown in the top and bottom panels of Fig. 7.6, respectively. However, the observed quasi-periodic amplitude modulation in Fig. 7.6 is instrumental in origin and is caused by the changing pixel mask as the *Kepler* Space Telescope rotated 90 degrees every ∼93 d. When the $P_{\rm Kep} \simeq 372.5$-d amplitude modulation is removed, only a slight linear decrease in the fundamental radial mode, and increase in the first overtone radial mode are observed.

The observed phase modulation in the fundamental and first overtone radial modes shown in Fig. 7.6, however, is not instrumental — could this be evidence of stellar evolution altering the structure of the star? Pulsation mode frequencies change with the evolution of stellar structure, and the concomitant changes in the cavities of individual pulsation modes. Could these changes be observable over the 4-yr *Kepler* data set? KIC 5950759 is an example of a δ Sct star in which there is variability in the non-sinusoidal light variations over the 4-yr *Kepler* data set, a form of non-linearity that is observed as phase modulation in the fundamental and first overtone radial pulsation modes.

As discussed by Percy et al. (1980) and Breger and Pamyatnykh (1998), and given in Eq. 7.1, a quadratic change in phase is expected for a uniformly changing pulsation period. Note that a linear change in phase means that an incorrect frequency has been used to calculate phase. The shape of the observed phase modulation in the fundamental and first overtone radial modes in KIC 5950759 shown in the top and bottom panels of Fig. 7.6, respectively, is not only parabolic, but is also indicative of an increasing period. The periods of radial modes are predicted to increase throughout the majority of a δ Sct star's main sequence lifetime (Percy et al. 1980; Breger 1990; Rodríguez et al. 1995; Breger and Pamyatnykh 1998). This raises an interesting question: can a time-scale as short as 4 yr be considered significant in terms of the structural evolution of a star?

The phase modulation of the fundamental and first overtone radial modes in KIC 5950759 shown in the top and bottom panels of Fig. 7.6, respectively, was converted into time delays ($O - C$) using

$$O - C = \frac{\phi(t)}{2\pi\,\nu}\,, \tag{7.2}$$

where $\phi(t)$ is the phase of a pulsation mode at a given time in units of rad, which has a known and assumed fixed frequency of ν in units of d^{-1}. The $O - C$ values were normalised to the reference time $t_0 = 2\,455\,688.770$ BJD and were plotted for the fundamental and first overtone radial modes in the top and bottom panels of Fig. 7.7, respectively. The quadratic change in each $O - C$ diagram was fitted using Eq. 7.1 with the term $\left(\frac{1}{P}\frac{dP}{dt}\right)$ as a free parameter. The optimum parabolic fit is shown as the solid black lines in Fig. 7.7, with the free parameter $\left(\frac{1}{P}\frac{dP}{dt}\right)$ representing the fractional rate of change in period in units of d^{-1} since t and $O - C$ are in units of d.

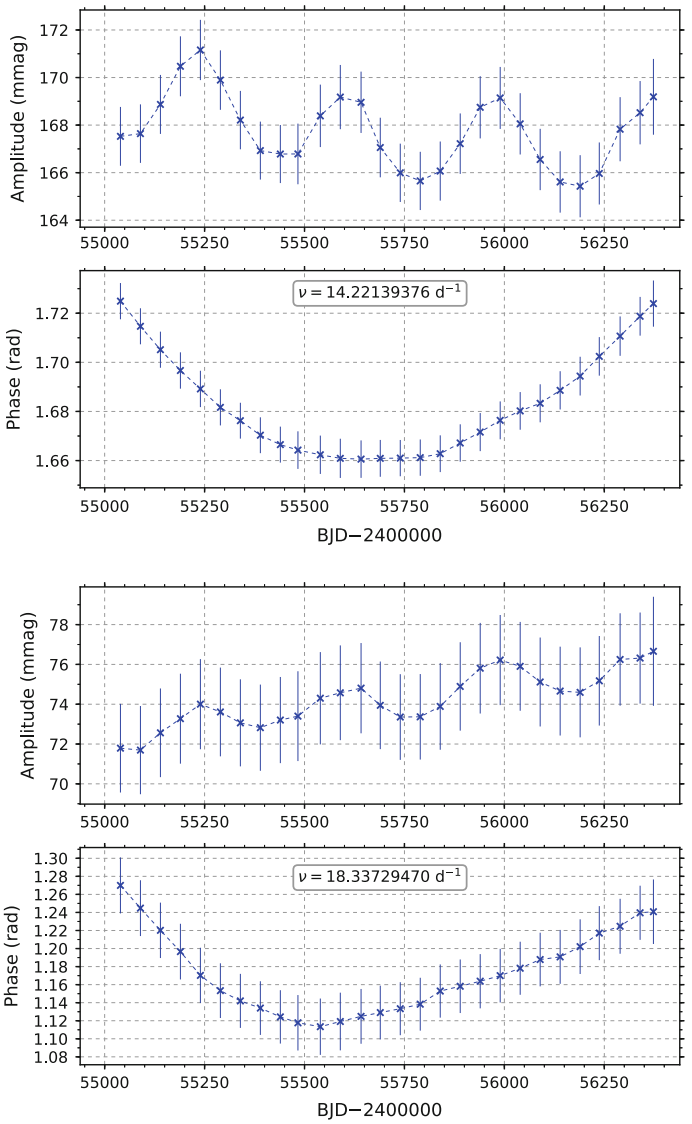

Fig. 7.6 Amplitude and phase modulation in the HADS star KIC 5950759. The *top* and *bottom* panels are the amplitude and phase tracking plots for the fundamental and first overtone radial modes, respectively, using 150-d bins and a 100-d overlap. Note the difference in ordinate scales when comparing the two panels

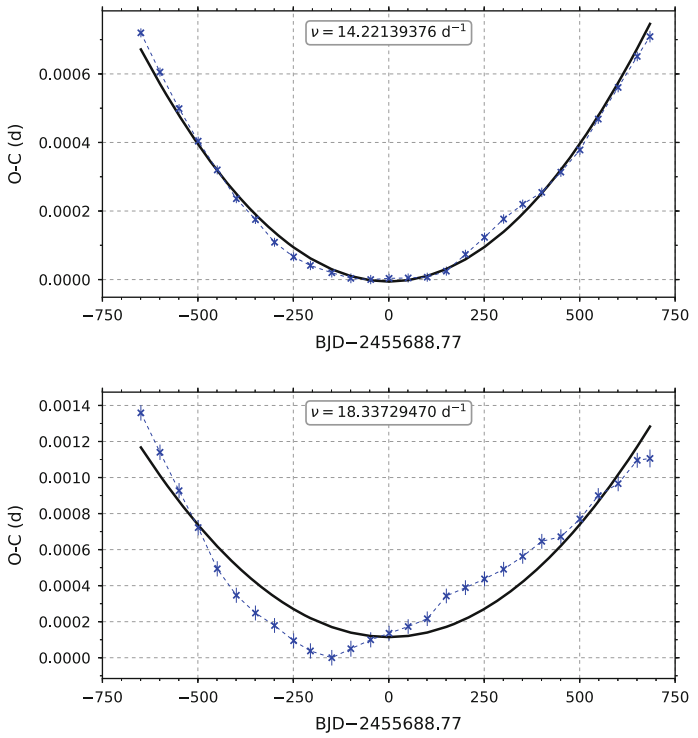

Fig. 7.7 $O - C$ diagram for the HADS star KIC 5950759. *Top* and *bottom* panels are the observed period changes for the fundamental and first overtone radial modes, respectively. The *solid black line* represents the parabolic fit to the observations with $\left(\frac{1}{P}\frac{dP}{dt}\right)$ as a free parameter, which represents the fractional rate of change in the period of the pulsation mode

Thus, the best fit value was converted into units of yr^{-1} by being multiplied by 365.25, which resulted in best-fitting values of 1.18×10^{-6} yr^{-1} and 1.82×10^{-6} yr^{-1} for the fundamental and first overtone radial modes, respectively.

Stellar evolution theory predicts positive values of $\left(\frac{1}{P}\frac{dP}{dt}\right) \sim 1 \times 10^{-8}$ yr^{-1} for radial pulsation modes in δ Sct stars (Percy et al. 1980; Breger 1990; Rodríguez et al. 1995; Breger and Pamyatnykh 1998). The observed values in KIC 5950759 are the correct sign for an increasing period, but are much larger than those predicted by stellar evolution theory. It is not clear if the observed phase modulation in KIC 5950759 is caused by stellar evolution driving structural changes in this HADS star, as the period changes may not be uniform during the main sequence — for example, larger period changes may be expected for a star near or beyond the TAMS compared to the ZAMS. Historically, observations covering decades have been needed to infer evolutionary changes to the pulsation modes in HADS stars and δ Sct stars (Percy et al. 1980; Breger 1990; Rodríguez et al. 1995; Breger and Pamyatnykh 1998).

On the other hand, it could be concluded that the observed phase modulation in KIC 5950759 is evolutionary, since the period of the fundamental and first overtone radial modes are increasing over time. In β Cep stars studied by Neilson and Ignace (2015), period changes of order $\sim 10^{-5}$ yr^{-1} were observed in several stars, including β Cep itself. Perhaps stellar evolutionary models underestimate the rate of period change for δ Sct stars near the TAMS, and that values of $\left(\frac{1}{P}\frac{dP}{dt}\right)$ could be significantly larger than $\sim 1 \times 10^{-8}$ yr^{-1} for short or intermittent epochs throughout the main sequence lifetime of an intermediate-mass star. The analysis of KIC 5950759 clearly shows that the pulsation periods of the fundamental and first overtone radial modes are increasing over the 4-yr data set. Further work, including modelling the period changes in this HADS star, is needed to understand these observations.

7.6 The HADS Star KIC 9408694

The second HADS star observed by the *Kepler* Space Telescope is KIC 9408694 with the amplitude spectrum and tracking plot from Bowman et al. (2016) shown in the top and bottom panels of Fig. 7.8, respectively. This HADS star pulsates with mode frequencies $\nu_1 = 5.661057$ d^{-1} and $\nu_3 = 7.148953$ d^{-1} that have a period ratio of 0.7919, which is outside the expected range for the fundamental and first overtone

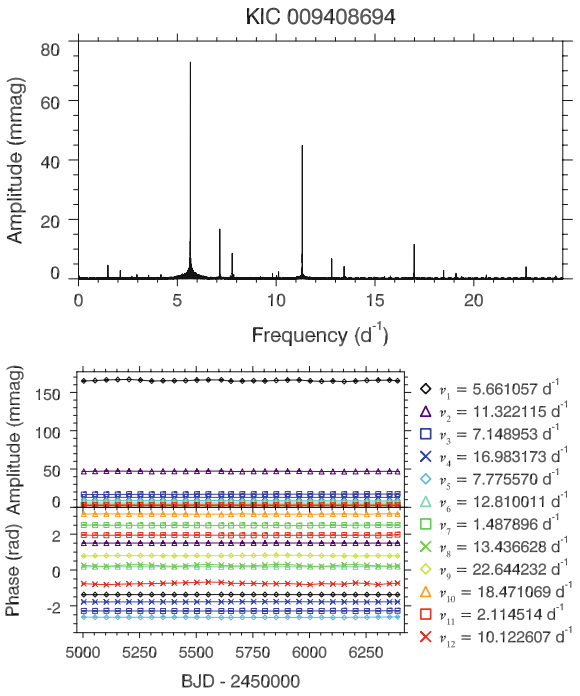

Fig. 7.8 The *top* panel is the 4-yr amplitude spectrum calculated out to the LC Nyquist frequency for the HADS star KIC 9408694. The *bottom* panel shows the amplitude and phase tracking plot, in which there is little or no variability in the amplitudes and phases of the radial pulsation mode frequencies, if instrumental modulation caused by the *Kepler* satellite is removed. Figure from Bowman et al. (2016), their Fig. 7

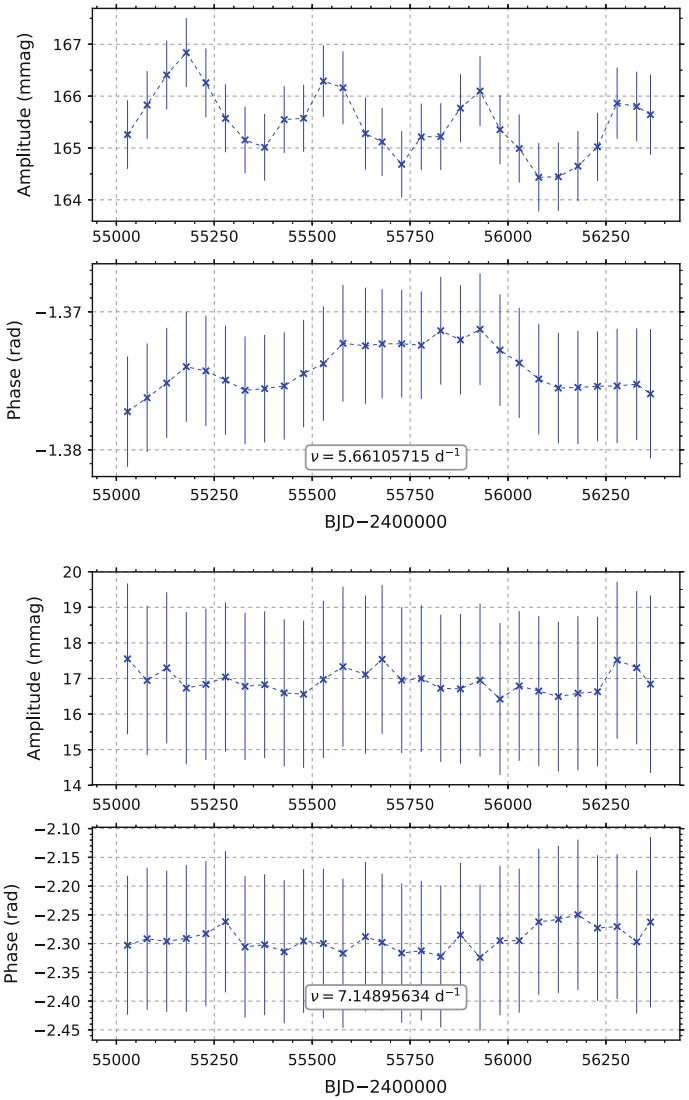

Fig. 7.9 Amplitude and phase modulation in the HADS star KIC 9408694. *Top* and *bottom* panels are the amplitude and phase tracking plots for the fundamental and first overtone radial modes, respectively, using 150-d bins with 100-d overlaps. Note the difference in ordinate scales when comparing the two panels

radial modes (Stellingwerf 1979). KIC 9408694 was analysed spectroscopically by Balona et al. (2012) who determined an effective temperature and surface gravity for KIC 9408694, which are included in Table 7.2 for comparison. From the spectroscopic analysis, Balona et al. (2012) discovered that KIC 9408694 had a rotational

velocity of $v \sin i = 100 \pm 10\,\mathrm{km\,s^{-1}}$, which is unusually high for HADS stars with typical rotational velocities being $v \sin i \lesssim 40\,\mathrm{km\,s^{-1}}$ (Breger 2000; McNamara 2000; Rodríguez et al. 2000). The high rotation rate of KIC 9408694 was determined to perturb the observed pulsation mode frequencies and explain the atypical period ratio in this star, with a model including fast rotation successfully identifying ν_1 and ν_3 as the fundamental and first overtone radial modes, respectively (Balona et al. 2012).

Similarly to KIC 5950759, the HADS star KIC 9408694 also exhibits instrumental periodic amplitude modulation in its fundamental radial mode, which can be seen in the top panel of Fig. 7.9. However, the amplitude modulation is clearly instrumental in origin and if removed then there is little or no variability in the amplitudes of the radial modes, which was also concluded by Balona et al. (2012) for KIC 9408694.

On the other hand, unlike the previous HADS star, KIC 9408694 does not exhibit significant quadratic phase modulation in either of its radial pulsation modes, which can be seen in Fig. 7.9. Thus, a calculation of the observed period changes cannot be performed for KIC 9408694. This raises the question: can these two HADS stars be considered at similar stages of stellar evolution, since their stellar parameters given in Table 7.2 are significantly different? Moreover, the analysis of the amplitude and phase modulation in their fundamental and first overtone radial pulsation modes yielded significantly different results, with only KIC 5950759 exhibiting increasing pulsation periods over time as predicted by stellar evolutionary models. Since there are only two HADS to study in the *Kepler* data set, it is difficult to draw any meaningful conclusions about the general statistical properties of the HADS stars, but the analysis of stars presented in this chapter provides motivation for further investigation.

7.7 Discussion

Many studies over the last few decades have attempted to measure the period changes in pulsation modes caused by evolutionary changes in stellar structure of δ Sct stars (Percy et al. 1980; Breger 1990; Rodríguez et al. 1995; Breger and Pamyatnykh 1998). All stars are evolving with time, but the question remains whether the observable parameters of a star, specifically pulsation mode frequencies, amplitudes and phases, are influenced on time-scales as short as the 4-yr *Kepler* data set. Although it remains small, the likelihood of observing evolutionary changes in a star is increased for a star near the TAMS or in a post-main sequence stage of evolution, as the structure of the star is changing on much shorter time-scales relative to its main sequence lifetime. For example, the post-main sequence expansion phase of a 2-$M_\odot$ δ Sct star is approximately between 20–100 Myr (Breger and Pamyatnykh 1998), but this is still several orders of magnitude larger than the longest-studied δ Sct stars (e.g., Breger et al. 1990; Breger 2000, 2016).

The ρ Pup star KIC 3429637 remains a useful case study of amplitude modulation, because a study using high-resolution spectroscopy, *Kepler* photometry and accurate asteroseismic modelling was performed by Murphy et al. (2012). This star

was determined to be near the TAMS and its amplitude modulation was conjectured to be caused by structural changes driven by stellar evolution (Murphy et al. 2012). Few δ Sct stars have been observed using high-resolution spectroscopy and even fewer have been modelled asteroseismically. However, it was shown in Sect. 7.3 that KIC 3429637 exhibits amplitude and phase modulation that is typical of many δ Sct stars in the 4-yr *Kepler* data set. Further work is needed to perform similar analyses of other AMod stars, which were discussed in Chaps. 5 and 6, to determine if the observed amplitude and phase modulation is related to stellar evolution.

The HADS stars offer the opportunity to study non-linearity and possible structural changes caused by stellar evolution in a subgroup of high-amplitude, slowly-rotating δ Sct stars (Petersen and Christensen-Dalsgaard 1996; Breger 2000; McNamara 2000; Rodríguez et al. 2000). Only two HADS stars were observed by *Kepler*, specifically KIC 5950759 and KIC 9408694, which exhibit fractional amplitude variability of order 1 per cent with a period equal to the *Kepler* orbital period, and thus the observed amplitude modulation is instrumental in origin (Bowman et al. 2016). From only two HADS stars no significant conclusions can be made about the location of HADS stars in the HR diagram (see e.g., Balona 2016).

The same amplitude limitation mechanism predicted for the low-amplitude δ Sct stars is not at work within HADS stars, which pulsate at much higher amplitudes (Breger 2000). It is interesting to note that high amplitude pulsations are typically associated with non-linearity in the form of harmonics and combination terms, which are found in KIC 5950759 and KIC 9408694, but the lack of significant amplitude modulation in these HADS stars suggests that non-linearity in the form of resonant mode coupling is not significant in these stars (Bowman et al. 2016). This result is interesting since it has been suggested that resonant mode coupling is the amplitude limitation mechanism that operates in δ Sct stars but not in HADS stars, thus explaining the large difference in pulsation mode amplitudes between the two subgroups (Dziembowski and Krolikowska 1985).

Furthermore, HADS stars have similarities to Cepheid variables (Eggen 1976; Breger 2000; McNamara 2000; Soszyński et al. 2008; Poleski et al. 2010). It was suggested by Dziembowski (1977) that radiative damping is stronger in more massive stars, leading to fewer non-radial pulsation modes, which may explain why the so-called transitionary δ Sct stars, i.e., the HADS and ρ Pup stars, pulsate in mainly radial pulsation modes and evolved stars such as Cepheids pulsate exclusively in radial modes.

On the other hand, HADS stars also share similarities to δ Sct stars. For example, HADS stars have been confirmed to contain low-amplitude non-radial modes in addition to high-amplitude radial modes (Mathias et al. 1997; Poretti 2003; Balona et al. 2012). Although significant amplitude modulation was not found in KIC 5950759 and KIC 9408694, Poretti et al. (2011) discovered quasi-periodic amplitude modulation – similar to the Blazhko effect in RR Lyr stars – in the fundamental radial mode of the CoRoT HADS star ID 101155310. Also, amplitude modulation in the second overtone radial mode in the triple-mode HADS star GSC 03144-595 was recently discovered by Mow et al. (2016), whilst the fundamental and first overtone radial

modes had constant amplitudes. These studies support the view that HADS stars are transitionary objects within the classical instability strip, and are in a post-main sequence stage of stellar evolution (Poretti et al. 2011; Mow et al. 2016), but a larger sample size of stars is needed to make more significant conclusions.

In Sect. 7.5 it was discussed how one of the two HADS stars, KIC 5950759, showed parabolic phase modulation in its fundamental and first overtone radial modes, whereas KIC 9408694 showed constant pulsation mode phases. The parabolic phase modulation observed in KIC 5950759 was fitted using Eq. 7.1 and yielded fractional period changes, $\left(\frac{1}{P}\frac{dP}{dt}\right)$, of 1.18×10^{-6} yr^{-1} and 1.82×10^{-6} yr^{-1} for the fundamental and first overtone radial modes, respectively, which is two orders of magnitude larger than predicted by stellar evolutionary models (Percy et al. 1980; Breger 1990; Rodríguez et al. 1995; Breger and Pamyatnykh 1998). Therefore, assuming that the period changes predicted by stellar evolutionary models are accurate, the observed period changes in KIC 5950759 are too large to be caused by stellar evolution and represent shorter time-scale changes to the pulsation cavities, and therefore average stellar density, in KIC 5950759. On the other hand, the predictions from evolutionary models may be inaccurate, or may not be applicable for stars near the TAMS that evolve at a faster rate compared to the majority of the main sequence, so further work is needed to address this as clearly the periods of the radial modes in KIC 5950759 are increasing in time.

Note that in Chap. 5, it was demonstrated that the majority of δ Sct stars have variable pulsation amplitudes, many also with associated phase modulation over the 4-yr *Kepler* data set. It was also demonstrated in Chaps. 5 and 6 that frequency and amplitude modulation of pulsation modes can be caused by beating or non-linearity, with either of these mechanisms causing a larger magnitude of phase variability than is expected from stellar evolution. Thus, it becomes difficult to disentangle modulation caused by non-linearity and possible phase modulation caused by stellar evolution.

The HADS stars are certainly interesting stars to study, with each one being unique for a different reason. Large-number studies of δ Sct stars in the LMC (Poleski et al. 2010) and the Milky Way galaxy (Lee et al. 2008) have established that HADS stars are rare, making up less than 1 per cent of pulsating main sequence stars inside the classical instability strip. There are two possible inferences to consider when studying HADS stars, which are not necessarily mutually exclusive: the HADS stars are transitionary δ Sct stars in a post-main sequence stage of evolution (Petersen and Christensen-Dalsgaard 1996); or, slow rotation is a prerequisite for large pulsation amplitudes (Breger 2000; Rodríguez et al. 2000). The small number of HADS stars observed by *Kepler* means one must be cautious when defining the characteristics of a group of stars (e.g., Balona 2016). In the future, it will be interesting to create large catalogue of HADS stars and build on the methods developed in this monograph to study non-linearity, and the effects of slow rotation and stellar evolution in these stars.

References

Abt, H. A. 1984, ApJ, 285, 247
Balona, L. A., Lenz, P., Antoci, V., et al. 2012, MNRAS, 419, 3028
Balona, L. A., Ripepi, V., Catanzaro, G., et al. 2011, MNRAS, 414, 792
Balona, L. A. 2016, MNRAS, 459, 1097
Bowman, D. M., Kurtz, D. W., Breger, M., Murphy, S. J., & Holdsworth, D. L. 2016, MNRAS, 460, 1970
Breger, M. & Pamyatnykh, A. A. 1998, A&A, 332, 958
Breger, M., McNamara, B. J., Kerschbaum, F., et al. 1990, A&A, 231, 56
Breger, M. 1990, in Astronomical Society of the Pacific Conference Series, Vol. 11, Confrontation Between Stellar Pulsation and Evolution, ed. C. Cacciari & G. Clementini, 263–273
Breger, M. 2000, in Astronomical Society of the Pacific Conference Series, Vol. 210, Delta Scuti and Related Stars, ed. M. Breger & M. Montgomery, 3
Breger, M. 2000, MNRAS, 313, 129
Breger, M. 2016, A&A, 592, A97
Brown, T. M., Latham, D. W., Everett, M. E., & Esquerdo, G. A. 2011, AJ, 142, 112
Casagrande, L., Silva Aguirre, V., Schlesinger, K. J., et al. 2016, MNRAS, 455, 987
Casagrande, L., Silva Aguirre, V., Stello, D., et al. 2014, ApJ, 787, 110
Catanzaro, G., Ripepi, V., Bernabei, S., et al. 2011, MNRAS, 411, 1167
Coates, D. W., Halprin, L., & Thompson, K. 1982, MNRAS, 199, 135
Dziembowski, W. & Krolikowska, M. 1985, Acta Astronomica, 35, 5
Dziembowski, W. 1977, Acta Astronomica, 27, 95
Eggen, O. J. 1976, PASP, 88, 402
Fontaine, G. & Brassard, P. 2008, PASP, 120, 1043
Gray, R. O. & Garrison, R. F. 1989, ApJS, 69, 301
Guzik, J. A. & Cox, A. N. 1991, Delta Scuti Star Newsletter, 3, 6
Hermes, J. J., Montgomery, M. H., Mullally, F., Winget, D. E., & Bischoff-Kim, A. 2013, ApJ, 766, 42
Huber, D., Silva Aguirre, V., Matthews, J. M., et al. 2014, ApJS, 211, 2
Iben, Jr., I. 1966, ApJ, 143, 483
Iben, Jr., I. 1967a, ApJ, 147, 624
Iben, Jr., I. 1967b, ARA&A, 5, 571
Iben, Jr., I. 1967c, ApJ, 147, 650
Iben, Jr., I. 2013a, Stellar Evolution Physics, Volume 1: Physical Processes in Stellar Interiors (Cambridge University Press)
Iben, Jr., I. 2013b, Stellar Evolution Physics, Volume 2: Advanced Evolution of Single Stars (Cambridge University Press)
Kilkenny, D. 2010, Ap&SS, 329, 175
Kurtz, D. W. 1976, ApJS, 32, 651
Lee, Y.-H., Kim, S. S., Shin, J., Lee, J., & Jin, H. 2008, PASJ, 60, 551
Mathias, P., Gillet, D., Aerts, C., & Breitfellner, M. G. 1997, A&A, 327, 1077
McNamara, D. H. 2000, in Astronomical Society of the Pacific Conference Series, Vol. 210, Delta Scuti and Related Stars, ed. M. Breger & M. Montgomery, 373
Miglio, A., Chiappini, C., Morel, T., et al. 2013, MNRAS, 429, 423
Mow, B., Reinhart, E., Nhim, S., & Watkins, R. 2016, AJ, 152, 17
Murphy, S. J., Grigahcène, A., Niemczura, E., Kurtz, D. W., & Uytterhoeven, K. 2012, MNRAS, 427, 1418
Neilson, H. R. & Ignace, R. 2015, A&A, 584, A58
Niemczura, E., Murphy, S. J., Smalley, B., et al. 2015, MNRAS, 450, 2764
Percy, J. R., Matthews, J. M., & Wade, J. D. 1980, A&A, 82, 172
Petersen, J. O. & Christensen-Dalsgaard, J. 1996, A&A, 312, 463
Poleski, R., Soszyński, I., Udalski, A., et al. 2010, Acta Astronomica, 60, 1

Poretti, E., Rainer, M., Weiss, W. W., et al. 2011, A&A, 528, A147
Poretti, E. 2003, A&A, 409, 1031
Rodríguez, E., López de Coca, P., Costa, V., & Martín, S. 1995, A&A, 299, 108
Rodríguez, E., López-González, M. J., & López de Coca, P. 2000, A&AS, 144, 469
Scuflaire, R., Théado, S., Montalbán, J., et al. 2008, Ap&SS, 316, 83
Smalley, B., Antoci, V., Holdsworth, D. L., et al. 2017, MNRAS, 465, 2662
Smalley, B., Kurtz, D. W., Smith, A. M. S., et al. 2011, A&A, 535, A3
Soszyński, I., Poleski, R., Udalski, A., et al. 2008, Acta Astronomica, 58, 163
Stellingwerf, R. F. 1979, ApJ, 227, 935
Thompson, K. & Coates, D. W. 1991, Proceedings of the Astronomical Society of Australia, 9, 281
Walraven, T., Walraven, J., & Balona, L. A. 1992, MNRAS, 254, 59

Chapter 8
Conclusions and Future Work

8.1 Conclusions

The δ Sct stars represent a diverse group of pulsating stars, in which many aspects of physics, such as rotation, binarity, magnetism and chemical peculiarities, play important roles. In this monograph, an ensemble of 983 δ Sct stars that were observed continuously by the *Kepler* Space Telescope over 4 yr was created and used to study the pulsational properties of these stars, and primarily the incidence of amplitude modulation of their pulsation modes.

It was discussed in Chap. 2, how the *Kepler* Space Telescope provided continuous observations of approximately 150 000 stars for 4 yr with a photometric precision of order a few μmag (Borucki et al. 2010; Koch et al. 2010; Gilliland et al. 2010). The advent of space telescopes created a photometry revolution and has allowed different aspects of physics to be probed in detail for the first time in a large number of δ Sct stars, which could not be achieved from ground-based observations. In Chap. 2, it was demonstrated how the amplitude visibility function when using LC data causes amplitude suppression for, on average, high-frequency signals, which biases *Kepler* LC observations of pulsating stars to low frequency pulsation modes. However, few δ Sct stars were observed for long periods of time with SC, so LC observations represent a more complete data set with increased frequency resolution for studying δ Sct stars.

The δ Sct star KIC 7106205 studied by Bowman and Kurtz (2014) and discussed in Chap. 3 is an archetypal example of amplitude modulation in δ Sct stars, as it contains few pulsation modes in its amplitude spectrum with only a single p mode that changed significantly in amplitude over 4 yr. A further study of KIC 7106205 by Bowman et al. (2015) using ground-based photometry from the Wide Angle Search for Planets (WASP; Pollacco et al. 2006) project was also discussed in Chap. 3, in which WASP data were used to extend the study of amplitude modulation in KIC 7106205 2 yr prior to the launch of the *Kepler* Space Telescope. It was shown that a single pulsation mode decreased in amplitude from 11.70 ± 0.05 mmag in 2007, to 5.87 ± 0.03 mmag in 2009, and to 0.58 ± 0.06 mmag in 2013 (Bowman

D.M. Bowman, *Amplitude Modulation of Pulsation Modes in Delta Scuti Stars*,
Springer Theses, DOI 10.1007/978-3-319-66649-5_8

et al. 2015). Time spans of years and decades are clearly important in δ Sct stars, with the study of KIC 7106205 demonstrating that different pulsation mode amplitudes would be obtained if only short and intermittent observations of this star were studied. The analysis of the KIC 7106205 provided clear and strong evidence that a physical mechanism within the star is causing the observed amplitude modulation. Furthermore, the visible pulsation energy budget in this star was not conserved over 6 yr of combined WASP and *Kepler* observations (Bowman and Kurtz 2014; Bowman et al. 2015). Spectroscopic observations of KIC 7106205 revealed that this star is not a classical Am star, but does have some relatively strong metal lines for its Ca K line strength and can be considered a marginal Am star. However, the metallic line strengths are unrelated to the observed amplitude modulation.

From the study of radial pulsation modes in δ Sct stars from the ground, it was established that hotter δ Sct stars typically have higher pulsation mode frequencies (Breger and Bregman 1975; Breger 2000). Hotter δ Sct stars have the He II ionisation zone located closer to the stellar surface, which facilitates higher overtone and therefore higher frequency modes to be excited (Pamyatnykh 1999, 2000; Christensen-Dalsgaard 2000; Dupret et al. 2004, 2005). In Chap. 4, an ensemble of 983 δ Sct stars that were observed continuously by *Kepler* for 4 yr was presented, and the statistical properties of these stars were investigated, including relationships between stellar parameters and the frequency of the highest amplitude pulsation mode. It was found that the hotter δ Sct stars typically have higher pulsation mode frequencies, as shown by Fig. 4.11 and the $T_{\rm eff} - \log\, g$ diagrams in Figs. 4.13 and 4.14. However, the bias towards low frequency pulsation modes caused by the LC amplitude visibility function resulted in few hot δ Sct stars to be included in the ensemble. Consequently, the correlation found between the frequency of the highest amplitude pulsation mode and effective temperature is a lower bound of the true correlation as there are few δ Sct stars included in the ensemble of 983 stars with frequencies above $\nu \gtrsim 40\ \mathrm{d}^{-1}$. Another outcome from the statistical study of δ Sct stars discussed in Sect. 4.7 was that a small yet significant fraction of δ Sct and γ Dor stars are found outside of their respective instability regions, such that the observational edges of the classical instability strip need to be updated.

A statistical study of amplitude modulation in all 983 δ Sct stars by Bowman et al. (2016) was presented in Chap. 5. The results of this study provide strong evidence that variable pulsation amplitudes are common in δ Sct stars, with 61.3% of the 983 δ Sct stars exhibiting significant amplitude modulation in at least one pulsation mode over the 4-yr *Kepler* data set. Similarly to KIC 7106205, the most remarkable result from this analysis is that many δ Sct stars to do not conserve their visible pulsation energy budget over 4 yr (Bowman et al. 2016). Moreover, the 38.7% of NoMod δ Sct stars that exhibit constant pulsation mode amplitudes and phases, were found across the classical instability strip in the HR diagram, thus the mechanisms that cause variable pulsation amplitudes are not restricted to a small region in the HR diagram (Bowman et al. 2016). The published amplitude modulation catalogue of 983 δ Sct stars utilising 4 yr of continuous *Kepler* observations will be a valuable resource for comparison to observations of similar stars with K2 (Howell et al. 2014), TESS (Ricker et al. 2015) and PLATO (Rauer et al. 2014). Eventually, these missions will

observe a large area of the sky, but for only a relatively short length of time compared to the 4-yr *Kepler* data set. Therefore, *Kepler* data will remain the best data set for studying δ Sct stars as its length will not be surpassed for some time.

It was demonstrated by Bowman et al. (2016) how a pair of close-frequency pulsation modes produce amplitude modulation, with a characteristic beat period as the inverse of the difference in pulsation mode frequencies. Amplitude modulation caused by beating is most easily recognised because a phase change occurs at the epoch of minimum amplitude, which is equal to π rad for two equal-amplitude cosinusoids. For increasingly different amplitudes, this phase change gets progressively smaller. It was shown in Chap. 5 that some of the stars classified as AMod by Bowman et al. (2016) are the result of beating from close-frequency pulsation modes. Specifically, two pairs of close-frequency modes separated by less than 0.001 d^{-1} in the δ Sct stars KIC 4641555 and KIC 8246833, were used to construct beating models that accurately reproduced observations. These stars demonstrate that it is possible for δ Sct stars to contain pulsation mode frequencies that are barely resolved using the 4-yr *Kepler* data set (Bowman et al. 2016).

Therefore, it is possible that other AMod δ Sct stars are the result of beating from unresolved close-frequency pulsation modes. In Chap. 5, a Bayesian MCMC simulation was used to extract the parameters of three hypothetical pulsation modes using a synthetic *Kepler* data set. The simulation was able to accurately extract the frequencies, amplitudes and phases of these modes, which were chosen to emulate the observed amplitude modulation in the δ Sct star KIC 7106205. However, the implementation of two-, three- and four-mode MCMC simulations to the *Kepler* observations of KIC 7106205 did not converge to a meaningful solution. This supports the conclusions from Bowman and Kurtz (2014) that the observed amplitude modulation in KIC 7106205 is caused by a mode coupling mechanism to high-degree p modes or internal g modes; or energy lost to an unknown damping/driving region; and is not caused by beating.

The observation of concomitant amplitude and phase modulation can be used to distinguish between cases of intrinsic amplitude modulation of a single pulsation mode or beating from unresolved close-frequency pulsation modes (Breger and Pamyatnykh 2006; Bowman et al. 2016). A subgroup of pure AMod stars was defined by Bowman et al. (2016), which contained stars with pulsation modes that were variable in amplitude but constant in phase. This pure form of amplitude modulation cannot be explained by beating or a mode coupling mechanism. These pure AMod stars are arguably the most interesting of all the AMod stars, since they were an unexpected discovery and are as yet unexplained. It was conjectured by Bowman et al. (2016) that pure AMod δ Sct stars are caused by slow changes in the relative driving and damping in these stars, but further work is needed to address this.

In Chaps. 5 and 6, the mathematical relationships in frequency, amplitude and phase between two parent modes and a child mode were discussed. Models of mode coupling were also used to distinguish between different forms of non-linearity in δ Sct stars, particularly combination frequencies arising from a non-linear distortion model or coupled modes from resonant mode coupling. If a child mode is resonantly excited from a mode coupling mechanism, it will have a larger amplitude than a

combination frequency from a non-linear distortion model (van Kerkwijk et al. 2000; Breger and Montgomery 2014; Bowman et al. 2016). Moreover, the observed amplitude modulation in the parent modes allowed the strength of non-linearity between a child and parent modes to be quantified. The coupling strength was tested for a selection of δ Sct stars with amplitude modulation, specifically KIC 4733344 and KIC 5857714 in Chap. 6, which distinguished whether a child mode was excited by resonant mode coupling or was a combination frequency from a non-linear distortion model (Bowman et al. 2016).

Non-linearity in the form of harmonics and combination frequencies are ubiquitous in all types of pulsators driven by the κ mechanism. The frequencies and phases of combination frequencies are predicted to be locked to the parent pulsation modes, with any variability in the parent pulsation modes being mirrored by the combination frequencies (Brickhill 1992; Wu and Goldreich 2001; Wu 2001), which is commonly found for different types of pulsator including δ Sct stars (see e.g., KIC 4733344 and KIC 5857714, or Breger and Lenz 2008). However, in Chap. 6 it was shown that this was not the case for the γ Dor star KIC 4731916. The amplitude variability of a triplet of combination frequencies ($2\nu_1$, $\nu_1+\nu_2$ and $2\nu_2$) did not mirror the amplitude variability of the two parent g modes, ν_1 and ν_2. This is an unexpected result and the γ Dor star KIC 4731916 demonstrates that we lack a complete physical description of combination frequencies, and how they are generated. Clearly, non-linearity is at work in this star, but the interplay between the mechanism that generates the combination frequencies and the mechanism that causes the amplitude modulation requires further investigation.

In Chap. 7, the concept of measuring period changes in pulsation modes was investigated for the ρ Pup star KIC 3429637 and the HADS stars KIC 5950759 and KIC 9408694. The ρ Pup and HADS stars are considered evolved stars (Petersen and Christensen-Dalsgaard 1996; Breger 2000; Murphy et al. 2012), so there is a greater likelihood of observing real-time stellar evolutionary changes in their observed pulsation modes. However, from ground-based observations, similar numbers of increasing and decreasing pulsation periods of radial modes have been observed in δ Sct stars (Breger 1990; Guzik and Cox 1991; Rodríguez and Breger 2001). This cannot be explained by stellar evolution since pulsation periods should predominantly increase throughout the main sequence and post-main sequence (Percy et al. 1980; Breger 1990; Rodríguez et al. 1995; Breger and Pamyatnykh 1998).

Most importantly, it was demonstrated in Chaps. 5, 6 and 7 that the observed phase modulation in δ Sct stars is often much larger than the quadratic change in phase predicted by stellar evolution models, with fractional changes in pulsation periods of $\left(\frac{1}{P}\frac{dP}{dt}\right) \sim 10^{-8}$ yr^{-1} predicted by stellar evolutionary models (Percy et al. 1980; Breger 1990; Rodríguez et al. 1995; Breger and Pamyatnykh 1998). The parabolic phase modulation observed in the HADS star KIC 5950759 yielded fractional period changes, $\left(\frac{1}{P}\frac{dP}{dt}\right)$, of 1.18×10^{-6} yr^{-1} and 1.82×10^{-6} yr^{-1} for the fundamental and first overtone radial modes, respectively. Thus, it was concluded that 4 yr is sufficient to observe period changes in a δ Sct star, but these may not necessarily be caused by stellar evolution, because modulation signals from non-linearity typically dominate observations on this time-scale. On the other hand, it was clearly demonstrated that the

pulsation periods of the radial modes are increasing in KIC 5950759, and evolutionary models may underestimate period changes for stars near the TAMS.

HADS stars also offer the opportunity to study non-linearity in the form of harmonics and combination frequencies from a non-linear distortion model, typically in the absence of amplitude modulation and non-linearity in the form of resonant mode coupling. It remains to be established if HADS stars are demonstrably separate from their low-amplitude δ Sct counterparts. With so few HADS stars available to study with high-quality observations, further observations and theoretical work on modelling non-linearity in HADS stars and their low-amplitude δ Sct counterparts is needed.

8.2 Future Work

Much of the work discussed in this monograph has demonstrated that δ Sct stars commonly exhibit amplitude modulation on time-scales of order years and longer, but that there is also a large range in the diversity of the temporal behaviour observed. In Sects. 1.4.3 and 1.4.4 it was discussed how pulsating main sequence B stars and evolved stars, such as RR Lyr, sdBV and variable white dwarfs, all show amplitude modulation of their respective pulsation modes if the length of observations is long enough to resolve the behaviour. A question resulting from this work is: are the δ Sct stars similar to other pulsating stars driven by the κ mechanism in terms of the mechanism(s) that causes non-linearity in the form of amplitude modulation and combination frequencies? This is an interesting question as most types of stars do show some form of amplitude modulation.

There are various theoretical and observational synergies between pulsating A and B stars, such that β Cep stars can be considered analogues of δ Sct stars, from the similar pulsation mode frequencies observed. The κ mechanism operating in the Z bump in opacity causes low-order p modes to become unstable (Dziembowski and Pamyatnykh 1993). Hybrid B stars pulsating in both g- and p-mode frequencies have also been observed (Handler 2009; Degroote et al. 2012), which can be explained by increasing opacity in the Z bump (Pamyatnykh et al. 2004). Further similarity exists, as Degroote et al. (2009) found evidence for resonant mode coupling in the β Cep star HD 180642 using CoRoT photometry. The authors found that the sum and difference combination frequencies had similar amplitudes, but a greater number of sum combination frequencies (Degroote et al. 2009). It would be interesting to investigate the synergy in mode coupling within hybrid stars, between A and B stars, both observationally and theoretically.

To achieve this, modelling of individual stars using stellar evolution codes such as `MESA` (Paxton et al. 2011, 2013, 2015) and pulsation codes such as `GYRE` (Townsend and Teitler 2013), is needed to fully understand the observed behaviour. The following questions need to be tested: why do only some and not all of the δ Sct stars, and by extension different pulsators driven by the κ mechanism, show variable pulsation mode amplitudes over time-scales of years and longer? Is this behaviour governed

by stellar evolution, or the pulsation excitation mechanism or both? A starting point for such a project is to study stars for which mode identification is relatively simple; for example, the HADS stars. The HADS stars have large pulsation amplitudes and exhibit non-linearity in the form of harmonics and combination frequencies, but non-linearity in the form of amplitude modulation and resonant mode coupling is absent in these stars (Bowman et al. 2016). Resonant mode coupling has been suggested as the amplitude limitation mechanism operating in δ Sct stars to explain the large difference in pulsation mode amplitudes between HADS stars and their low-amplitude δ Sct counterparts (Dziembowski and Krolikowska 1985). Further work is needed to establish why the HADS stars are rare and the possible physical differences between them and the δ Sct stars, especially if they are transitionary objects in a post-main sequence stage of stellar evolution.

Recent work by Fuller et al. (2015) and Stello et al. (2016) has shown that many red giant stars have suppressed dipole modes, which could possibly be explained by the scattering of mode energy into high-degree modes as the modes interact with a magnetic field in a star's core. This effect, termed the Magnetic Greenhouse Effect (Fuller et al. 2015), essentially traps the mode energy in the magnetised core of a red giant star resulting in low surface amplitudes for the dipole modes. Stello et al. (2016) demonstrated that not all red giant stars exhibit suppressed dipole modes and that it is a strong function of stellar mass.

Among other pulsating stars, Cantiello et al. (2016) modelled a 1.6-$M_{\odot}$ main sequence γ Dor star and suggested that it is possible for a dynamo-generated magnetic field to be induced near the core in such a star. This could alter the pulsational behaviour of a star and redistribute mode energy into higher degrees, hence dramatically reduce their visible amplitudes (Cantiello et al. 2016). Could a similar mechanism be the cause for a number of the AMod δ Sct stars in the ensemble of δ Sct stars studied by Bowman et al. (2016)? The A and F stars have convective cores on the main sequence and if a magnetic field is sustained throughout the transition from post-main sequence to the red giant branch, it is reasonable to assume that the progenitors of red giant stars with suppressed dipole modes also had magnetic fields near their cores on the main sequence. The evolutionary progenitors of the suppressed dipole mode red giant stars from Fuller et al. (2015) and Stello et al. (2016) are within the ensemble of 983 δ Sct stars.

8.2.1 Spectroscopic Follow-Up of Delta Scuti Stars

As previously discussed in Sect. 3.4, spectroscopic follow-up observations of 23 δ Sct stars were made with the Intermediate dispersion Spectrograph and Imaging System (ISIS) on the William Herschel Telescope (WHT). Details of these stars, including their positions and apparent visual magnitudes, were given in Table 3.3. All of these stars were observed spectroscopically because they are relatively bright targets for *Kepler* stars, with a mixture of δ Sct stars that exhibit amplitude modulation and others that do not.

It was shown in Sect. 3.4, that the spectrum of the δ Sct star KIC 7106205 indicated that this star has signatures of being a marginal Am star. In the future, it is intended to supplement this study with the analysis of other δ Sct stars, to determine if amplitude modulation is more commonly found in chemically normal or peculiar stars, fast or slowly-rotating stars, or a combination of these parameters. It is known that there is a physical relationship between pulsation and chemical peculiarities in the Am stars (Smalley et al. 2011, 2017). Ultimately, the aim is to understand if chemical peculiarity is related to amplitude modulation in δ Sct stars.

8.2.2 Future Missions

The future of asteroseismology is bright with ongoing projects such as WASP, K2 and BRITE continuing to produce many interesting and exciting results. In the near future, the NASA TESS mission (Ricker et al. 2015) and the ESA PLATO 2.0 mission (Rauer et al. 2014) will be launched in 2018 and 2024, respectively, which will vastly increase the number of stars studied in the Milky Way galaxy.

The TESS Mission

The Transiting Exoplanet Survey Satellite (TESS; Ricker et al. 2015) will be launched in 2018, with a primary goal of finding exoplanets around late-type stars. To achieve this it will have a passband of 600–1000 nm, which is redder than the passband of 420–900 nm of the *Kepler* Space Telescope (Koch et al. 2010). For an early-F star with $T_{\rm eff} = 7000$ K star, pulsation mode amplitudes will be approximately 47% that of *Kepler* from the difference in passband, which is shown graphically in the top panel of Fig. 8.1. For an early-A star with $T_{\rm eff} = 10\,000$ K star, pulsation mode amplitudes will be approximately 39% that of *Kepler* from the difference in passband, which is shown graphically in the bottom panel of Fig. 8.1.

Eventually, TESS will observe a large fraction of the sky, with observing runs that last from 27 d up to 1 yr in the continuous viewing zones near the ecliptic polar regions (Ricker et al. 2015). After data downlinks, TESS will start re-observing at a random phase, which will create a variable Nyquist frequency and successfully allow the sNa technique to be implemented for pulsation mode frequencies that lie above the TESS Nyquist frequency (Murphy 2015). Although TESS is optimised to study cool stars, asteroseismology of many different types of stars will be possible.

The GAIA Mission

GAIA will change everything. Astrometric results from the GAIA mission (Perryman et al. 2001) will soon be available to the scientific community, which will allow almost all *Kepler* targets to be accurately placed in the HR diagram — see Lindegren et al. (2008, 2012) for more details. GAIA is currently measuring parallaxes for many stars in the Milky Way and will provide distances for more than 150 000 stars that

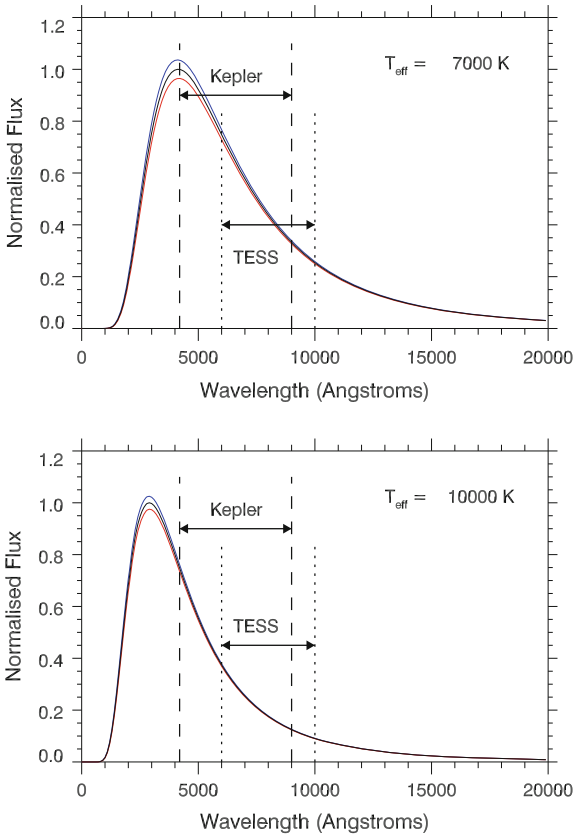

Fig. 8.1 The Planck blackbody functions for a $T_{\rm eff} = 7000$ K and a $T_{\rm eff} = 10\,000$ K star are shown in the *top* and *bottom panels*, respectively, as *black solid curves*. The *red* and *blue curves* show the change in the Planck function for ± 50 K change in temperature in each star. Approximate *Kepler* and TESS passbands are plotted as *dashed* and *dotted lines*, respectively

are accurate to 0.1%, and distances for more than a million stars that are accurate to 1%. This will be a phenomenal improvement to current estimates of luminosity for practically all previously observed stars in the Milky Way and will constrain future observations and in turn models of stellar structure and evolution.

8.3 Final Remarks

It has been a privilege and a pleasure to work within the *Kepler* Asteroseismic Science Consortium (KASC) on the analysis of δ Sct stars. I trust that this monograph and the research work it contains is of use to others. We are currently in a golden age of astronomy, a Space Photometry Revolution, and I hope that the success of asteroseismology will continue to grow exponentially, and improve our understanding of stellar structure and evolution for intermediate-mass stars.

References

Borucki, W. J., Koch, D., Basri, G., et al. 2010, Science, 327, 977
Bowman, D. M. & Kurtz, D. W. 2014, MNRAS, 444, 1909
Bowman, D. M., Holdsworth, D. L., & Kurtz, D. W. 2015, MNRAS, 449, 1004
Bowman, D. M., Kurtz, D. W., Breger, M., Murphy, S. J., & Holdsworth, D. L. 2016, MNRAS, 460, 1970
Breger, M. 1990, in Astronomical Society of the Pacific Conference Series, Vol. 11, Confrontation Between Stellar Pulsation and Evolution, ed. C. Cacciari & G. Clementini, 263–273
Breger, M. 2000, in Astronomical Society of the Pacific Conference Series, Vol. 210, Delta Scuti and Related Stars, ed. M. Breger & M. Montgomery, 3
Breger, M. & Bregman, J. N. 1975, ApJ, 200, 343
Breger, M. & Lenz, P. 2008, A&A, 488, 643
Breger, M. & Montgomery, M. H. 2014, ApJ, 783, 89
Breger, M. & Pamyatnykh, A. A. 1998, A&A, 332, 958
Breger, M. & Pamyatnykh, A. A. 2006, MNRAS, 368, 571
Brickhill, A. J. 1992, MNRAS, 259, 519
Cantiello, M., Fuller, J., & Bildsten, L. 2016, ApJ, 824, 14
Christensen-Dalsgaard, J. 2000, in Astronomical Society of the Pacific Conference Series, Vol. 210, Delta Scuti and Related Stars, ed. M. Breger & M. Montgomery, 187
Degroote, P., Briquet, M., Catala, C., et al. 2009, A&A, 506, 111
Degroote, P., Aerts, C., Michel, E., et al. 2012, A&A, 542, A88
Dupret, M. A., Grigahcène, A., Garrido, R., Gabriel, M., & Scuflaire, R. 2004, A&A, 414, L17
Dupret, M. A., Grigahcène, A., Garrido, R., Gabriel, M., & Scuflaire, R. 2005, A&A, 435, 927
Dziembowski, W. & Krolikowska, M. 1985, Acta Astronomica, 35, 5
Dziembowski, W. A. & Pamyatnykh, A. A. 1993, in Astronomical Society of the Pacific Conference Series, Vol. 40, IAU Colloq. 137: Inside the Stars, ed. W. W. Weiss & A. Baglin, 721
Fuller, J., Cantiello, M., Stello, D., Garcia, R. A., & Bildsten, L. 2015, Science, 350, 423
Gilliland, R. L., Brown, T. M., Christensen-Dalsgaard, J., et al. 2010, PASP, 122, 131
Guzik, J. A. & Cox, A. N. 1991, Delta Scuti Star Newsletter, 3, 6
Handler, G. 2009, MNRAS, 398, 1339
Howell, S. B., Sobeck, C., Haas, M., et al. 2014, PASP, 126, 398
Koch, D. G., Borucki, W. J., Basri, G., et al. 2010, ApJL, 713, L79
Lindegren, L., Babusiaux, C., Bailer-Jones, C., et al. 2008, in IAU Symposium, Vol. 248, A Giant Step: from Milli- to Micro-arcsecond Astrometry, ed. W. J. Jin, I. Platais, & M. A. C. Perryman, 217–223
Lindegren, L., Lammers, U., Hobbs, D., et al. 2012, A&A, 538, A78
Murphy, S. J. 2015, MNRAS, 453, 2569
Murphy, S. J., Grigahcène, A., Niemczura, E., Kurtz, D. W., & Uytterhoeven, K. 2012, MNRAS, 427, 1418
Pamyatnykh, A. A. 1999, Acta Astronomica, 49, 119
Pamyatnykh, A. A. 2000, in Astronomical Society of the Pacific Conference Series, Vol. 210, Delta Scuti and Related Stars, ed. M. Breger & M. Montgomery, 215
Pamyatnykh, A. A., Handler, G., & Dziembowski, W. A. 2004, MNRAS, 350, 1022
Paxton, B., Bildsten, L., Dotter, A., et al. 2011, ApJS, 192, 3
Paxton, B., Cantiello, M., Arras, P., et al. 2013, ApJS, 208, 4
Paxton, B., Marchant, P., Schwab, J., et al. 2015, ApJS, 220, 15
Percy, J. R., Matthews, J. M., & Wade, J. D. 1980, A&A, 82, 172
Perryman, M. A. C., de Boer, K. S., Gilmore, G., et al. 2001, A&A, 369, 339
Petersen, J. O. & Christensen-Dalsgaard, J. 1996, A&A, 312, 463
Pollacco, D. L., Skillen, I., Collier Cameron, A., et al. 2006, PASP, 118, 1407
Rauer, H., Catala, C., Aerts, C., et al. 2014, Experimental Astronomy, 38, 249

Ricker, G. R., Winn, J. N., Vanderspek, R., et al. 2015, Journal of Astronomical Telescopes, Instruments, and Systems, 1, 014003
Rodríguez, E. & Breger, M. 2001, A&A, 366, 178
Rodríguez, E., López de Coca, P., Costa, V., & Martín, S. 1995, A&A, 299, 108
Smalley, B., Kurtz, D. W., Smith, A. M. S., et al. 2011, A&A, 535, A3
Smalley, B., Antoci, V., Holdsworth, D. L., et al. 2017, MNRAS, 465, 2662
Stello, D., Cantiello, M., Fuller, J., et al. 2016, Nature, 529, 364
Townsend, R. H. D. & Teitler, S. A. 2013, MNRAS, 435, 3406
van Kerkwijk, M. H., Kaspi, V. M., Klemola, A. R., et al. 2000, ApJ, 529, 428
Wu, Y. 2001, MNRAS, 323, 248
Wu, Y. & Goldreich, P. 2001, ApJ, 546, 469

Correction to: Amplitude Modulation of Pulsation Modes in Delta Scuti Stars

Correction to:
D. M. Bowman, *Amplitude Modulation of Pulsation Modes in Delta Scuti Stars*, Springer Theses,
https://doi.org/10.1007/978-3-319-66649-5

In the original version of the book, the Book author's family name and given name have been updated in all the Chapters 1 to 8. The book and the chapters have been updated with the changes.

The updated version of the book can be found at
https://doi.org/10.1007/978-3-319-66649-5

D. M. Bowman, *Amplitude Modulation of Pulsation Modes in Delta Scuti Stars*,
Springer Theses, https://doi.org/10.1007/978-3-319-66649-5_9